Characterisation of a Novel Transmembrane Protein in Primary Human CD4+ T-cells

Katherine Louise Crossland

Doctor of Philosophy

Institute of Cellular Medicine

December 2013

Abstract

There are two main mechanisms of tolerance, one in the thymus and one in the periphery. Anergy, a peripheral mechanism, is a state of hypo-responsiveness where T-cells fail to respond to antigenic stimulus. A breakdown in immunological self-tolerance leads to autoimmunity and so provides an exciting research area for therapeutic intervention in autoimmune disease.

Differential display studies comparing anergic and activated CD4+ T-cells identified claudin domain containing protein 1 (CLDND1) to be differentially expressed between these two states. In addition, preliminary experiments performed in our lab identified CLDND1 as a potential negative regulator of CD4+ T-cell activation.

The aim of this study was to identify the role of CLDND1 in CD4+ T-cells. Antibodies against CLDND1 were raised and validated before use to determine CLDND1 expression in immune cell subsets and during T-cell activation. The function of CLDND1 in T-cells was investigated using gene silencing or over-expression techniques. CLDND1 expression was also sought in the autoimmune disease, rheumatoid arthritis (RA), to identify whether CLDND1 may be involved in disease pathogenesis.

Antibodies were successfully raised against CLDND1 and CLDND1 was found to be transiently up-regulated during CD4+ T-cell activation. CLDND1 gene silencing attempts, while successful at the RNA level, did not translate to a reduction in CLDND1 protein, suggesting CLDND1 may be regulated independently of gene transcription. Over-expression studies were consistent with CLDND1 being a negative regulator of T-cell proliferation or an inducer of cell death, depending on the activating stimulus used. CLDND1 expression was found to correlate with rheumatoid factor (RF) status in early RA patients and may suggest a role for CLDND1 in the disease setting. Some findings identify similarities between CLDND1 and other proteins, providing links for functional pathways and a plethora of further avenues of research.

Acknowledgments

I would like to acknowledge my supervisors, firstly John Isaacs for help in the planning and execution of the project, his ambitious ideas and his input during the writing of the thesis. In addition I would like to thank Amy Anderson who helped with day to day queries in the lab and for reading every chapter of this thesis. I would like to thank all my supervisors, including David Young and Catharien Hilkens for their valuable input to the project.

A major part of this work was supported by employees at UCB Celltech and co-ordinated through Tim Bourne, Louise Healy and Gillian McCluskey and so I would like to thank them for their willingness to help and drive the project forward. I also appreciate the work that Helene Finney, Kerry Tyson and Terry Baker performed in generating peptides, performing the immunisations for antibody generation and advice on molecular cloning.

Many members of the MRG, in particular Rachel Harry, Julie Diboll and Matt Barter, provided invaluable advice and some were also willing and regular blood donors.

I would also like to say a massive thanks to my partner, Adam, who cheered me up and pulled me through the rough times and celebrated with me during the highs. I would also like to acknowledge my parents who continue to support me in my aspirations.

Finally, thanks to the biotechnology and biological sciences research council (BBSRC) and UCB Celltech for providing funding for this CASE Studentship, for without this, the research would not have been possible.

Declaration

The candidate confirms that the work submitted is her own work and that appropriate credit has been given where reference has been made to the work of others. The work in this thesis was performed from September 2010 to September 2013. All work was performed in either the Musculoskeletal Research Group, Institute of Cellular Medicine, Newcastle University or at UCB Celltech, Slough. No part of this thesis has been submitted for the award of any other degree.

Table of Contents

List of Figures and Tables

List of Abbreviations

^{3}HTdR	Tritiated thymidine
[Ca]i	Intracellular Ca^{2+}
AFP	Autofluorescent protein
AICD	Activation induced cell death
AMPA	2-amino-3-(3-hydroxy-5-methyl-isoxazol-4-yl)propanoic acid
AP-1	Activator protein 1
APC	Antigen presenting cells
ATP	Adenosine-5'-triphosphate
BBSRC	Biotechnology and biological sciences research council
Bcl-6	B-cell lymphoma-6 protein
BLAST	Basic local alignment search tool
BSA	Albumin from bovine serum
CACNG	Voltage dependent calcium gamma subunit
cAMP	Cyclic adenosine monophosphate
CCP	α-citrillunated antibody
CCR	C-C chemokine receptor
cDNA	Copy deoxyribonucleic acid
CDR	Complementary determining regions
CFSE	5(6)-Carboxyfluorescein diacetate N-succinimidyl ester
CLDND1	Claudin domain containing protein 1
CLDND1(V)	Transfected CLDND1 (UCB) transcript
CMT1A	Charcot–Marie–Tooth 1A
CPM	Counts per minute
CTLA-4	Cytotoxic T-lymphocyte antigen-4
CXCR	C-X-C chemokine receptor type
DAG	Diacylglycerol
DAPI	4',6-diamidino-2-phenylindole

DC	Dendritic cell
DGK	DAG kinase
DMEM	Dulbecco's modified eagle medium
DMSO	Dimethyl sulfoxide
dsRNA	Double stranded RNA
EA	Early arthritis
EDTA	Ethylenediaminetetraacetic acid
ELISA	Enzyme linked immunosorbent assay
EMP	Epithelial membrane protein
ER	Endoplasmic reticulum
ERK	Extracellular-signal-regulated kinases
FBS	Fetal bovine serum
FCA	Freund’s complete adjuvant
FHHNC	Familial hypomagnesemia with hypercalciurea and nephroclacinosis
FIA	Freund’s imcomplete adjuvant
FLS	Fibroblast-like synoviocytes
FMO	Fluorescence minus one
Foxp3	Forkhead box P3
FT	Flowthrough
Fyn	Proto-oncogene tyrosine-protein kinase
GATA	GATA-binding factor
GFP	Green fluorescent protein
GlcNAc	N-Acetylglucosamine
GM-CSF	Granulocyte macrophage colony-stimulating factor
GMFI	Geometric mean fluorescence intensity
GPI	Glycosylphosphatidylinositol
Grb	Growth factor receptor-bound protein 2
GTP	Guanosine triphosphate

H_2L_2	Intact antibody
HBSS	Hanks Balanced salt solution
HL	Heavy and light chain monomer
HLA	Human leukocyte antigen
HNPP	Hereditary neuropathy with liability to pressure palsies
HSA	Human serum albumin
ICOS	Inducible T-cell co-stimulator
IFN	Interferon
IKK	IκB kinase
IL	Interleukin
IP	Immunoprecipitation
IP_3	Inositol 1-4-5-trisphosphate
IP39	Integral plasma membrane protein 39
IRES	Internal ribosome entry site
IS	Immunological synapse
ITAMs	Immunoreceptor tyrosine-based activation motifs
iTreg	Inducible regulatory T-cells
JAK	Janus kinase
KLH	Keyhole limpet hemocyanin
LAT	Linker for activation of T-cell
LB	Luria Bertani
Lck	Lymphocyte-specific protein tyrosine kinase
LMIP	Lens intrinsic membrane protein
LPS	Lipopolysaccharide
mAb	Monoclonal antibody
MAPK	Mitogen-activated protein kinase
matDC	Mature dendritic cell
methylol	Hydroxyl methyl

MHC	Major histocompatability complex
MLR	Mixed lymphocyte reaction
MMP	Matrix metalloproteinase
MP	Movement protein
mRNA	Messenger RNA
mTECs	Medullary thymic epithelial cells
mTOR	Mammalian target of rapamycin
NAIRD	Newcastle autoimmune inflammatory rheumatic diseases research biobank
NFAT	Nuclear factor of activated T-cells
NFκB	Nuclear factor kappa-light-chain-enhancer of activated B-cells
NK	Natural killer
NMDA	N-methyl-D-aspartate activated receptors
NMR	Nuclear magnetic resonance
NT	Non-targeting
nTreg	Natural regulatory T-cells
OPD	*o*-Phenylenediamine dihydrochloride
Orai	Calcium release-activated calcium channel protein
ORF	Open reading frame
OVA	Ovalbumin
P2X	ATP-responsive purinergic P2 receptors
pAbs	Polyclonal antibodies
PBMC	Peripheral blood mononuclear cells
PBS	Phosphate buffered saline
PCR	Polymerase chain reaction
PD-1	Programmed cell death protein-1
PI_3K	Phosphoinositide 3-kinase
PIP_2	Phosphatidylinositol bisphosphate

PKC	Protein kinase C
PLC	Phospholipase C
PMP-22	Peripheral myelin protein 22-growth arrest specific protein
PPP	Platelet poor plasma
PRP	Platelet rich plasma
PRR	Pathogen recognition receptors
PVDF	Polyvinylidene fluoride
qRT-PCR	Quantitative real-time PCR
RA	Rheumatoid arthritis
RF	Rheumatoid factor
RISC	RNA induced silencing complex
RNAi	RNA interference
RORγ	RAR-related orphan receptor gamma
RPMI	Roswell park memorial institute medium
RT	Room temperature
SA	Streptavidin
SDS	Sodium dodecyl sulphate
SDS-PAGE	Sodium dodecyl sulphate polyacrylamide gel electrophoresis
SH_2	Src homology 2
siRNA	Short interfering RNA
SLAP	Src-like adaptor protein
SMAD	Mothers against decapentaplegic homologue
SMURFS	SMAD specific E3 ubiquitin protein ligases
STAT	Signal transducer and activator of transcription
STIM	Stromal interaction molecule
TAE	Tris-acetate-ethlenediamine tetraacetic acid
TARP	Transmembrane AMPA receptor regulatory proteins

TCR	T-cell receptor
Teff	Effector T-cells
Tfh	Follicular helper T-cells
TGF	Transforming growth factor
Th	T-helper
TJ	Tight junction
TLR	Toll-like receptors
TNF	Tumour necrosis factor
TolDC	Tolerogenic dendritic cell
Tr1	IL-10 producing Treg
Treg	Regulatory T-cells
USH3	Usher syndrome type 3
UTR	Untranslated region
v/v	Volume to volume
v/w	Volume to weight
VCAM	Vascular cell adhesion protein
VDCC	Voltage dependent calcium channels
Xv15	X-vivo 15
ZAP	Zeta-chain-associated protein kinase
ZO	Zona occludens

Chapter 1. Introduction

CD4+ T-cells are a population of mononuclear cells that underpin key elements of the adaptive immune response. Diverse responses can be induced, which depend on the context of T-cell activation. Full activation is a critical step in mounting an effective immune response. Given the pivotal role of T-cells, tight regulation of their activity is essential, starting in the thymus and continuing into the periphery, to control for aberrant T-cell activation. Failure in these regulatory mechanisms plays a major role in the pathogenesis of autoimmune diseases.

1.1 T-cell Selection in the Thymus

Following development from a common lymphoid progenitor in the bone marrow, T-cell precursors migrate to the thymus where a small proportion of these cells differentiate into mature CD3 α:β CD4+ T-cells. A small portion of precursor cells also develop into CD3 γ:δ T-cells, but these cells will not be covered here. Several steps are involved in the generation of mature CD4+ T-cells; from double negative precursor cells, which express neither CD3 T-cell receptor (TCR) nor CD4/CD8 co-receptor upon entry into the thymus, through to double positive thymocytes, which express a pre-TCR, CD4 and CD8, to single positive CD4 thymocytes, which retain TCR expression and CD4 expression.

Two selection processes occur during this transition to single positive CD4 thymocytes to prevent the selection of non-responsive or highly self-reactive TCR, which are dependent on interactions between the TCR and the major histocompatibility complex (MHC) class II molecules present on a range of cell types. CD4/CD8 double positive thymocytes initially express low levels of a specific TCR, of which most do not recognize self-MHC class II molecules. These cells fail the positive selection process and die by neglect. CD4/CD8 double positive cells that recognize self-MHC class II go on to mature into single positive thymocytes and express high levels of a specific TCR. CD4 single positive thymocytes then undergo negative selection, which eliminates those cells capable of strongly responding to self-antigens presented by medullary dendritic cells (mDC) and medullary thymic epithelial cells (mTECs), thus preventing the formation of self-reactive T-cells. The remaining single positive T-cells make up approximately 2 % of the starting population and are exported from the thymus to form the peripheral T-cell repertoire. The survival of newly

formed T-cells is determined by sustained and repeated contact with MHC: self-peptide complexes, similar or identical to those that originally positively selected them, in combination with signals through the interleukin-7 (IL-7) cytokine receptor (Janeway et al., 2001).

1.2 T-cell Activation

Upon initiation of an immune response, antigen presenting cells (APC) process and present on MHC class II molecules peptides derived from antigenic proteins. These cells are then capable of activating CD4+ T-cells provided the three criteria for stimulation are provided. Recognition of the antigen presented on MHC class II molecules of professional APC is required by the TCR. This event is accompanied by co-stimulatory molecule interaction from APC, such as CD28 expressed on T-cells interacting with the B7 molecules, CD80 and CD86, on APC (Kalergis, 2003). The third signal required to elicit T-cell activation is an appropriate cytokine milieu (Curtsinger and Mescher, 2010).

Recognition of antigen bound to MHC class II molecules by the TCR in the presence of a pro-inflammatory environment leads to the formation of the immunological synapse (IS) and initiates a complex signalling pathway in the T-cell, mediated not only by the TCR, but also through co-stimulatory and adhesion molecules found within the synapse. The importance of the IS function has been the centre of much discussion (Dustin et al., 2010). One of the first steps in this signalling cascade involves phosphorylation of the immunoreceptor tyrosine-based activation motifs (ITAMs) of the TCR complex, mediated by the src family of tyrosine kinases (e.g. lymphocyte-specific protein tyrosine kinase (lck) and fyn) (Palacios and Weiss, 2004). The syk family kinase, zeta-chain-associated protein kinase (zap)-70, is recruited to the phosphorylated ITAMs through src homology 2 (SH_2) domains, where it is phosphorylated and activated (Visco et al., 2000). Ultimately, linker for activation of T-cell (LAT) molecules are activated which leads to the initiation of multiple pathways such as the ras/extracellular-signal-regulated kinases (ERK)/mitogen-activated protein kinase (MAPK), and the calcium/calcineurin and the phosphoinositide 3-kinase (PI_3K)/protein kinase C (PKC) pathway. These pathways up-regulate the transcription factors activator protein-1 (AP-1), nuclear factor of activated T-cells (NFAT) and nuclear factor kappa-light-chain-enhancer of activated B-cells (NFκB), which positively regulate the induction of T-cell proliferation genes

(Wonerow and Watson, 2001, Oh-hora and Rao, 2008) (Figure 1). Of these genes activated, IL-2 is considered to be an important factor for both auto- and paracrine activating signalling.

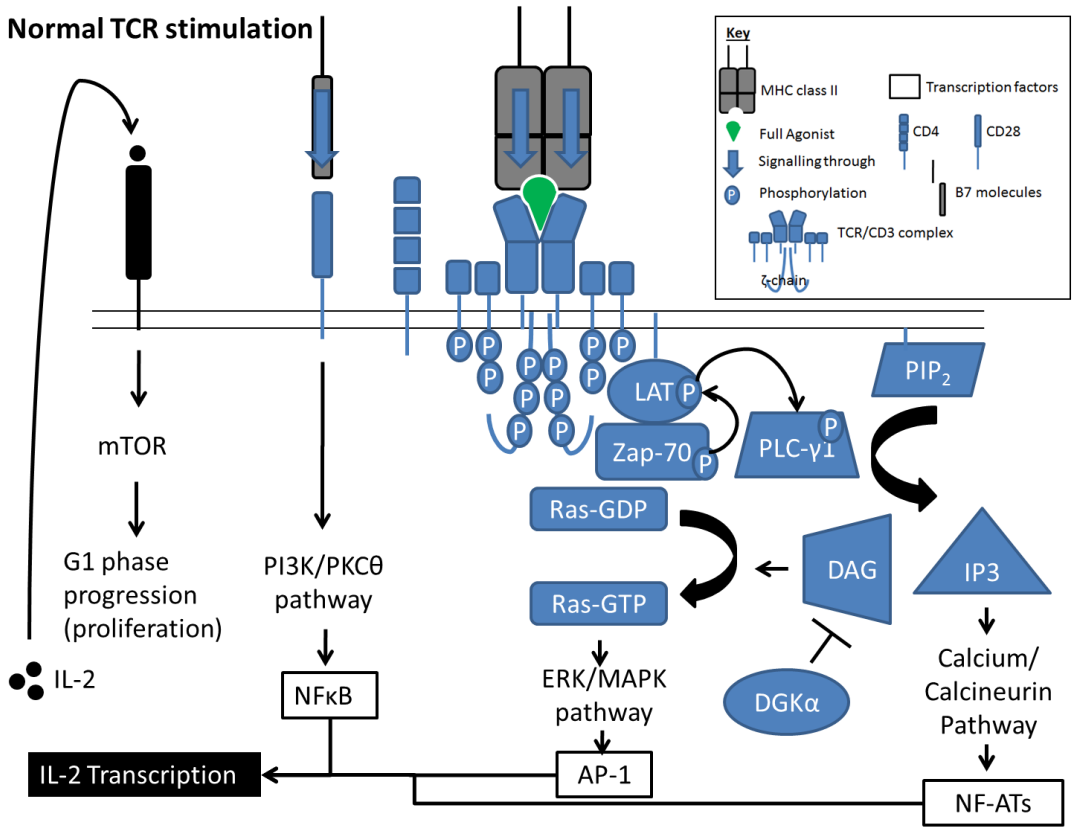

Figure 1. T-cell signalling events during full T-cell activation

Full triggering through the TCR and co-stimulatory molecules results in the activation of the three main pathways: PI_3K/PKC, ERK/MAPK and the calcium/calcineurin pathway to activate the transcription factors NFkB, AP-1 and NFATs. Co-operation between these transcription factors results in IL-2 production, which through positive feedback mechanisms, activates mTOR and leads to the progression of the cell cycle.

1.2.1 Importance of IL-2 signalling

IL-2 binds to a heterotrimeric IL-2 receptor comprised of non-covalently associated α (CD25), β (CD122) and γ (CD132) subunits. IL-2 binds to the α and β chains, while the γ-and β subunits initiate signal transduction. IL-2/IL-2 receptor signalling initiates the janus kinase (JAK)/ signal transducer and activator of transcription (STAT) signalling pathway and induce a positive feedback loop through the activation of MAPK and PI_3K pathways (Lan et al. 2008). IL-2 signalling also leads to the activation of the serine/threonine protein kinase, mammalian target of rapamycin (mTOR); shown to be an important activator of cell cycle progression (Figure 1) (Morice et al., 1993, Nourse et al., 1994).

The expression of IL-2 is controlled at multiple levels. The IL-2 promoter sequence contains binding sites for the NFAT family of proteins, AP-1 and NFκB, all of which require occupation for the transcription of IL-2 (Rooney et al., 1995, Choi et al., 2009, Shapiro et al., 1997). Co-stimulatory signalling via CD28 during T-cell activation is a major pathway to activate NFkB, and so this pathway is crucial for IL-2 transcription. CD28 activates PKCθ through PI_3K or by growth factor receptor-bound protein (Grb)-2. These signalling pathways lead to the degradation of the inhibitory IκB kinase (IKK) subunit of the NFkB complex and lead to the activation of genes containing NFkB binding elements (Tuosto, 2011), such as IL-2.

1.2.2 Calcium signalling

TCR triggering activates phospholipase C (PLC)-γ, which cleaves phosphatidylinositol bisphosphate (PIP_2) into inositol 1-4-5-trisphosphate (IP_3) and diacylglycerol (DAG) and initiates intracellular Ca^{2+} ([Ca]i) signalling pathways (Figure 1). The original paradigm involves IP_3 binding to IP_3 receptors expressed on the membrane of the endoplasmic reticulum (ER). [Ca]i stores are released which induce a conformational change in stromal interaction molecule (STIM)-1, an ER Ca^{2+} sensor, which ultimately activates calcium release-activated calcium channel protein (Orai)-1 at the plasma membrane, resulting in [Ca]i influx. The increase in [Ca]i may activate the calcium-calmodulin kinase pathways, and calcineurin, a Ca^{2+}-dependent phosphatase, which dephosphorylates members of the NFAT family, allowing their nuclear localization and transcription of target genes (Robert et al., 2011). This

paradigm however, would not explain how differences in [Ca]i signal intensity can govern T-cell activation, tolerance or anergy (Qu et al., 2011), or differences in the [Ca]i regulation between T-cell subsets, where the rise of [Ca]i elicited by TCR engagement is lower in T-helper (Th)2 cells compared to Th1 or Th17 cells (Weber et al., 2008). More recently, additional types of calcium channels have been identified on T-cells, including adenosine-5'-triphosphate (ATP)-responsive purinergic P2 receptors (P2X), which are ATP-gated ion channels that permit the influx of extracellular cations; N-methyl-D-aspartate activated receptors (NMDA), a class of ligand-gated glutamate receptors originally found in the nervous system to play a crucial role in neuronal cell function; and the voltage-dependent Ca^{2+} channels, which are typically activated in excitable cells such as nerve or muscle cells in response to membrane polarisation. Emerging roles for these receptors in T-cells are becoming elucidated, yet specific mechanisms of how they fit with the current paradigm are still under investigation (Omilusik et al., 2013).

1.3 Types of T-Effector Cells

Differentiation of activated naïve CD4+ T-cells into functionally distinct helper T subsets is crucial for proper host defence and normal immunoregulation (Figure 2). Originally, CD4+ T-cells were viewed as having two major fates: Th1 cells, which express T-bet, selectively produce interferon (IFN)-γ and target intracellular pathogens; and Th2 cells, which express GATA-binding factor (GATA)-3, produce IL-4 and IL-5, and target extracellular pathogens. More recently, newer lineages have been added. Regulatory T (Treg) cells express the transcription factor forkhead box P3 (Foxp3), a range of inhibitory receptors, secrete anti-inflammatory cytokines such as TGF-β and IL-10, and are important in the regulation of T-cell and APC immune responses. Th17 cells, distinguished by their expression of transcription factor RAR-related orphan receptor gamma (RORγ)-t and the secretion of IL-17, are important for protection from fungi and extracellular bacteria. Another two subsets of cells Th9 and Th22, named due to the secretion of IL-9 or IL-22, play similar roles to Th2 and Th17 cells, respectively. The newest lineage of cells, follicular helper T (Tfh) cells are crucial for providing B-cell help by promoting class switching of B-cells and are defined by expression of B-cell lymphoma-6 protein (Bcl-6) and IL-21, along with surface molecules programmed cell death protein (PD)-1, C-X-C

chemokine receptor type (CXCR)-5 and inducible T-cell co-stimulator (ICOS) (Hirahara et al., 2013, Nakayamada et al., 2012).

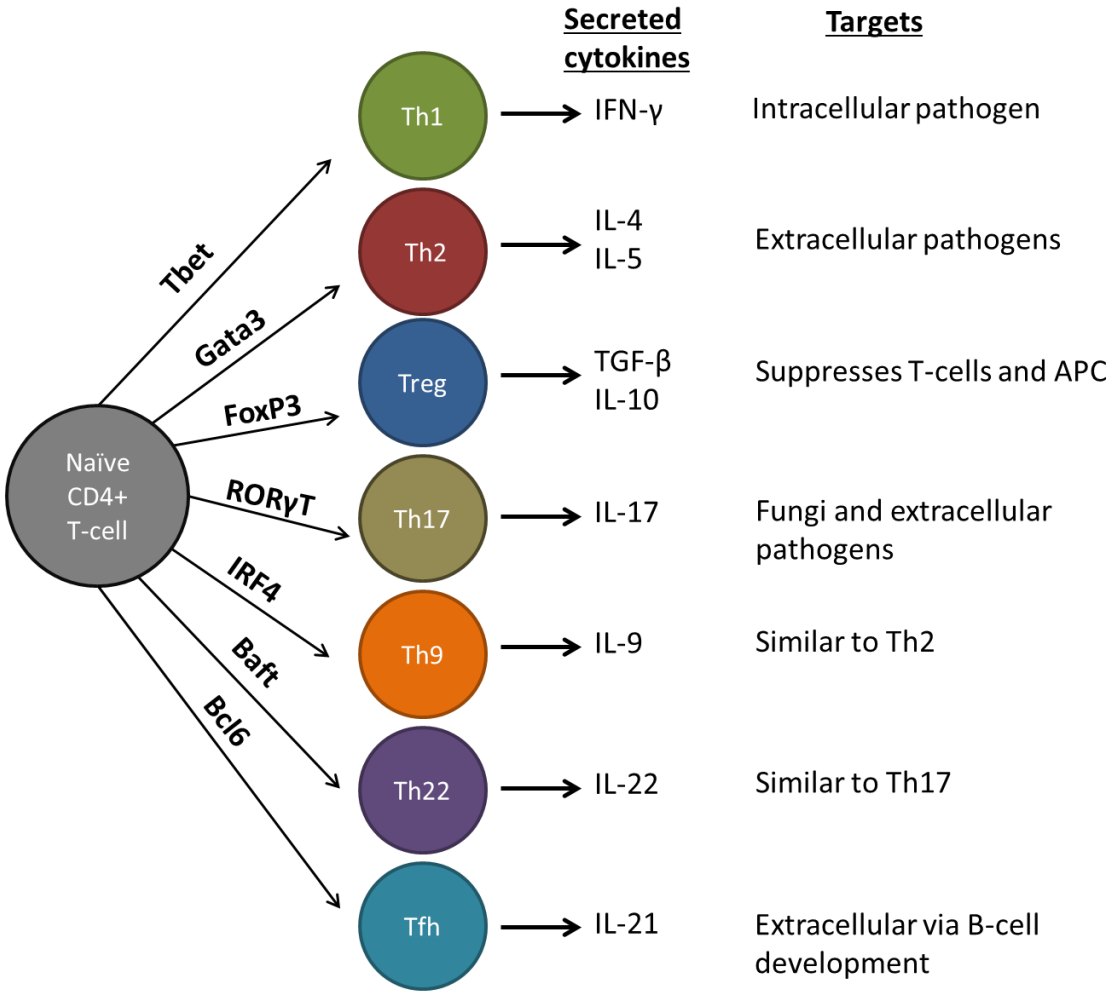

Figure 2. CD4+ T-cell subsets

Naïve CD4+ T-cells differentiate into functionally distinct helper T-cell subsets, defined by expression of particular transcription factors and cytokines, which are imperative for proper host defence and normal immunoregulation.

1.4 The Regulation of T-cell Activation

There are two main types of mechanisms that regulate CD4+ T-cell activity, termed central and peripheral tolerance. Central tolerance mechanisms have, in part been discussed above. As this mechanism relies on avidity interactions between self-peptide MHC class II molecule complexes, low-avidity autoreactive T-cells that are not eliminated, or T-cells bearing reactivity to self-peptide MHC class II not expressed at sufficient quantities on mTECs, escape to the periphery and rely on peripheral tolerance mechanisms to prevent aberrant activation of these cells. Peripheral tolerance mechanisms include: immune deviation, where particular T-cell responses are skewed to a different subset profile; T-cell suppression by Treg or tolerogenic APC; anergy, where T-cells fail to respond to antigenic stimulus; and the existence of immune privileged areas, where antigens from these sites, such as the eye, induce tolerance in the T-cells rather than an inflammatory response.

1.4.1 Control of APC activation

APC require activation before they can assist in T-cell activation, and so serves as a T-cell regulatory mechanism. Prior to migration to a lymph node for antigen presentation, immature DC reside in parenchymal tissues, surveying for infection or injury through constant macropinocytosis of the local environment. DC constantly process available antigens through MHC class II-rich endosomal compartments and are poised to deliver a high density of peptide-MHC class II complexes to the surface should activation occur. The immature DC express a variety of pathogen recognition receptors (PRRs), such as toll-like receptors (TLR), which are activated in response to microbial products, necrosis, mechanical trauma and pro-inflammatory cytokines. As a result of DC activation, DC mature and undergo a dramatic change in their morphology and antigen processing. They up-regulate MHC class II expression and B7 co-stimulatory molecules, CD80 and CD86, as well as C-C chemokine receptor (CCR)-7 and CD40. The DC migrates to T-cell–rich regions of the lymph node where it directs T-cell activation. Full DC maturation is associated with the synthesis of pro-inflammatory cytokines, which can regulate the differentiation of the responder T-cells (Mueller, 2010). Incomplete activation of DC generates tolerogenic DC (tolDC) which induce tolerance in naive T-cells. TolDC induce

tolerance through the presentation of antigen with inadequate co-stimulation and cytokine production for effector T-cell activation, resulting in T-cell anergy, deletion or induction of Treg (Thomson and Robbins, 2008, Jonuleit et al., 2001).

1.4.2 Treg

Treg can arise as a consequence of self-antigen recognition during T-cell maturation in the thymus (nTreg), or following self-antigen recognition in the periphery (iTreg). Both subtypes expand on recognition of antigen and increase their suppressive activity. nTreg are characterised by the high expression of Foxp3, CD25, cytotoxic T-lymphocyte antigen-4 (CTLA-4) and programmed cell death protein-1 (PD-1), which are important for their suppressive function. These cells require TCR triggering and probably IL-2 to exert their suppressive effects on bystander cells (Maggi et al., 2005). iTreg are comprised of transforming growth factor (TGF)-β producing (Th3 cells) and IL-10 producing (Tr1) cells. In pathological conditions, iTreg can revert to effector forms, e.g. Th17, that contribute to immunopathology (Heiber and Geiger, 2012).

1.4.3 Anergy

In T-cells, the term anergy refers to a state of hypo-responsiveness upon antigen encounter. This state requires the cell to remain viable in excess of 24 hours: the time required to initiate an apoptotic death process (Schwartz, 1990). There is no consensus in the literature regarding phenotypic changes and signalling events that occur during the induction of anergy, due to variations in experimental procedure. The type of stimulus seems to be a major variable: for example, T-cells can be stimulated with antigen in the absence of co-stimulation or stimulated persistently to induce anergy. There are also major deviations, explained below, in findings between anergic T-cells studied *in vitro* or *in vivo* (Schwartz, 2003).

Due to this complexity, Schwartz, (2003) has subcategorised anergic phenotypes based on T-cell characteristic traits and proposes a two model anergy system: clonal anergy and adaptive tolerance, although it is stated that there are exceptions which do not fall into either category. Clonal anergy is a growth arrest state occurring when a TCR is stimulated in the absence of co-stimulation or when co-stimulation is present but TCR stimulation is weak.

Adaptive tolerance describes cells which display a state of generalised inhibition of proliferation and effector function, occurring when a T-cell is exposed to a superantigen or repeated exposure to an antigen (Schwartz, 2003). This model of anergy differs from clonal anergy in several ways (Table 1 and Figure 3).

Characteristic traits	Clonal anergy	Adaptive tolerance
T-cell subset	Pre-activated	Naïve
Antigen persistence required	No	Yes
Proliferation upon induction	No	Yes
Inhibition of proliferation	Yes	Yes
Inhibition of IL-2	Yes	Yes
Inhibition of IFN-γ	No	Yes
Inhibition of IL-4	No	Yes
Production of IL-10	No	Some
Major defect in signalling pathway	Ras/MAP kinase	Tyr kinase
Block in IL-2R signalling	No	Yes
Reversible by IL-2	Yes	No

Table 1. Characteristics of the anergy phenotypes

Main characteristic traits of clonal anergy and adaptive tolerance. Table was adapted from Schwartz, (2003).

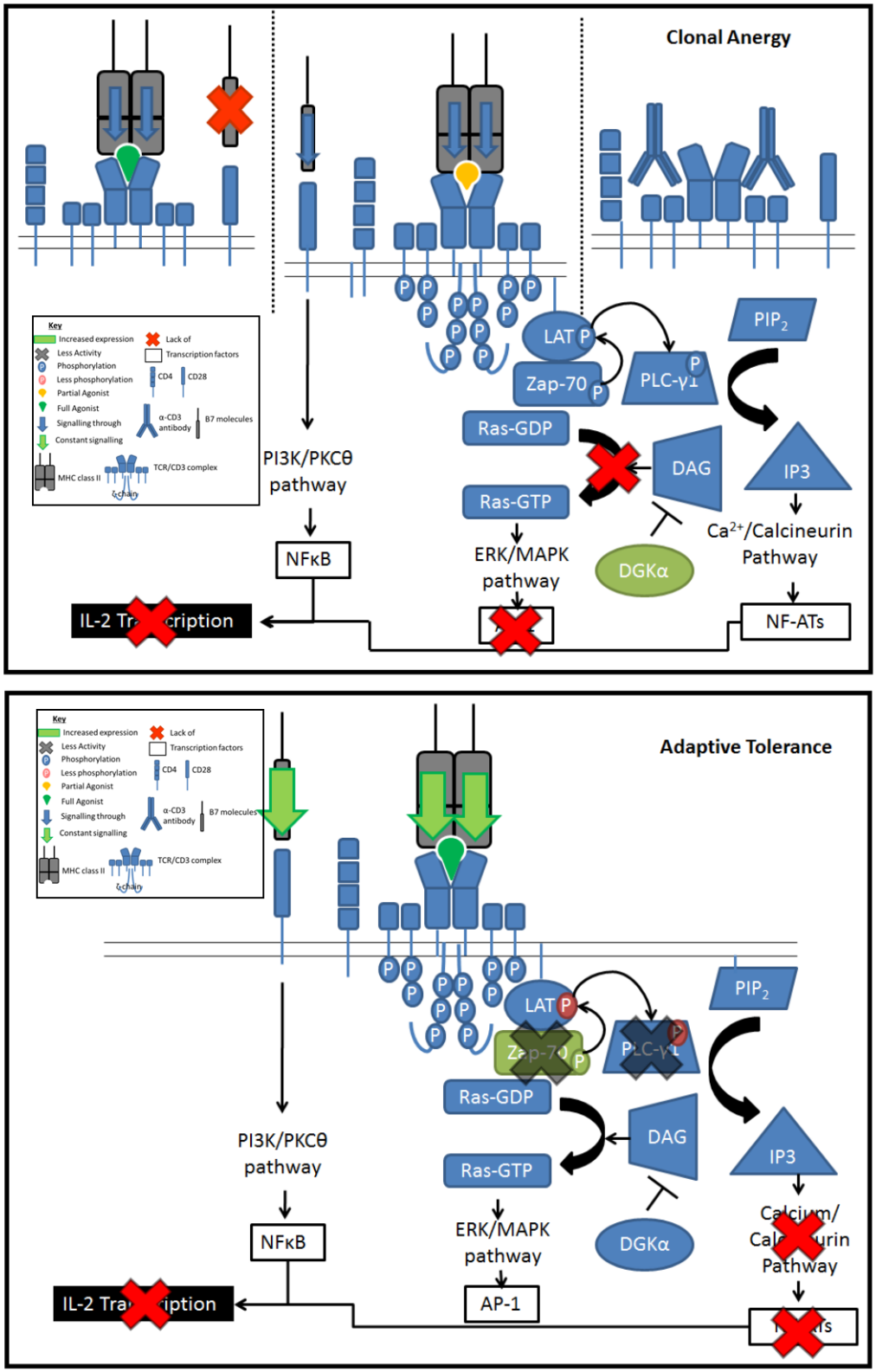

Figure 3. T-cell signalling events during anergic stimulation

Clonal anergy and adaptive tolerance are two distinct anergic states, but both result in abrogated IL-2 transcription. In clonal anergy, sub-optimal TCR triggering through lack of co-stimulation, low antigenic peptide or through CD3 antibody results in defects in the ras/MAPK pathway, preventing the activation of AP-1. In adaptive tolerance, sustained TCR signalling results in proximal TCR signalling defects which affect [Ca]i signalling and subsequent NFAT activation.

Clonal anergy has primarily been regarded to occur in previously activated T-cells and can be reversed by IL-2 (Schwartz, 2003). These cells contain defects in the activation of the MAPK family (Fields et al., 1996, DeSilva et al., 1996), which was localised to ineffective guanosine triphosphate (GTP) loading of ras (Smida et al., 2007, Olenchock et al., 2006) primarily through DAG kinase (DGK)α inhibition (Ebinu et al., 1998, Zhong et al., 2008, Zha et al., 2006). DGKα selectively inhibits AP-1 activation (Olenchock et al., 2006), which is critical for the induction of clonal anergy (Kang et al., 1992). mTOR deficiency under a normally activating stimulus also results in anergy, which has also been linked to the regulation of DGKα (Gorentla et al., 2011, Zheng et al., 2007).

Adaptive tolerance models have proposed defects in the proximal TCR/CD3 signalling pathway. The levels of the src family tyrosine kinase, fyn, are disproportionally increased in adaptive tolerance, compared to lck, yet the importance of this is still to be resolved due to conflicting data from fyn $^{-/-}$ mice (Stein et al., 1992, Choi and Schwartz, 2007). Zap-70 levels are elevated and so tolerant TCR bind more zap-70 than activated TCR; but its function is impaired due to insufficient stabilising phosphorylation events. LAT phosphorylation is also significantly reduced (Choi and Schwartz, 2007). [Ca]i signalling is also impaired, which prevents the activation of NFAT (Chiodetti et al., 2006).

1.4.4 Negative regulators of the immune response

T-cell activation can be controlled by both internal and cell surface proteins, which compete with activating signals. An array of inhibitory molecules have been identified on T-cells, which counteract the induction of the immune response, such as T-cell immunoglobulin-3 (TIM-3) interaction with galectin-9 (gal-9) on APC to induce T-cell death, and lymphocyte activation gene-3 (lag-3), a ligand for MHC class II on DC, which plays an inhibitory role in T-cell activation (Li X et al 2012, Triebel F 2003). Two well established examples of cell surface proteins which control T-cell activation are CTLA-4 and PD-1. CTLA-4 is a structural homologue of CD28 and competes with CD28 signalling in T-cells by binding to the B7 co-stimulatory molecules, CD80 and CD86, on APC. Experiments from CTLA-4$^{-/-}$ mice and the use of CTLA-4-specific monoclonal antibody (mAb) have indicated a role for CTLA-4 in the counter-regulation T-cell activation, as these cells resist anergy induction in response to

antigen administration in the absence of infection or adjuvant (Kearney et al., 1995, Perez et al., 1997, Greenwald et al., 2001). PD-1 is a member of the CD28 and CTLA-4 immunoglobulin superfamily and interacts with PD-L1 and PD-L2 on APC. Evidence from blocking PD-1/PD-L1 interactions with anti-PD-L1 antibody, and from PD-$1^{-/-}$ mice studies, indicate a role for PD-1 in the inhibition of TCR mediated T-cell proliferation and cytokine secretion, through inhibition of proximal TCR phosphorylation events, an independent mechanism to CTLA-4. PD-1 signalling is thought to prevent a decrease in T-cell motility and thus preventing stable T-cell-DC conjugate formation and development of the IS (Freeman et al., 2000, Fife et al., 2009, Gianchecchi et al., 2013).

1.5 Immune Cells in Disease

Circulating autoreactive T-cells are present in all individuals yet as the prevalence of autoimmune disorders affects only a proportion of the population, this suggests that a breakdown in regulation of these autoreactive T-cells is an important mechanism in autoimmune disease initiation. A breakdown in peripheral tolerance mechanisms is thought to play a key role in the pathogenesis of the autoimmune disease, RA.

1.6 RA

RA is a complex, heterogeneous, inflammatory autoimmune disease which has an estimated prevalence of 0.5-1 % in developed regions (Choy, 2012). The disease is systemic, and extra-articular features may be present, but the synovial joints are the primary site of pathology. Although the aetiology of RA is unknown, the susceptibility and severity of RA are likely to encompass both genetic and environmental factors, many of which are still to be elucidated. As characterisation of the disease develops, it is clear that RA can be further subdivided into different disease entities depending on α-citrillunated antibody (CCP) status (Trouw et al., 2013). Within the CCP positive disease setting, the prevalence of shared epitopes found in the human leukocyte antigen (HLA)-DRB1 gene, autoantibodies, the infiltration of immune cells in the joint and the successful application of T- and B-cell ablation strategies all implicate a role for the immune system in the disease (Pratt et al., 2009).

Originally, RA was treated as a disease where joint damage and disability occurred slowly. However, studies have shown that in 90 % of cases, damage

occurs within two years of the disease onset and in some instances is already present at symptom onset (Emery, 1994, McGonagle et al., 1999). The extent of the damage at these time-points reliably correlates with severity of lesions in later stage disease (McQueen et al., 2001). These findings led to the “window of opportunity” hypothesis which is based on the existence of a time frame, of roughly 12 weeks, in which the response to therapy results in long-term sustained benefits of treatment (Quinn and Emery, 2003).

1.7 Synovial Joints

Synovial joints are comprised of several tissues: synovial membrane, articular cartilage and subchondral bone, which are surrounded by the joint capsule (Figure 4). The synovial membrane is comprised of two types of synoviocytes; macrophage- and fibroblast-like. The fibroblast-like cells secrete viscous synovial fluid which both lubricates the joint and allows for the diffusion of nutrients. The articular cartilage is formed by one cell type only, the chondrocyte, which through the secretion of proteins, collagen and proteoglycans, plays a central role in the formation and maintenance of the cartilage. The subchondral bone lies underneath the cartilage and is comprised of collagen, proteoglycans, glycoproteins, glycosaminoglycans and growth factors, calcified in hydroxyapatite. The two primary cell types of the subchondral bone, osteoclasts and osteoblasts, are responsible for the re-modelling of the bone in response to load-bearing requirements and calcium and magnesium homeostasis. In RA, the primary disease target is the synovial membrane (Hui et al., 2012, Datta et al., 2008, Goldring and Marcu, 2009).

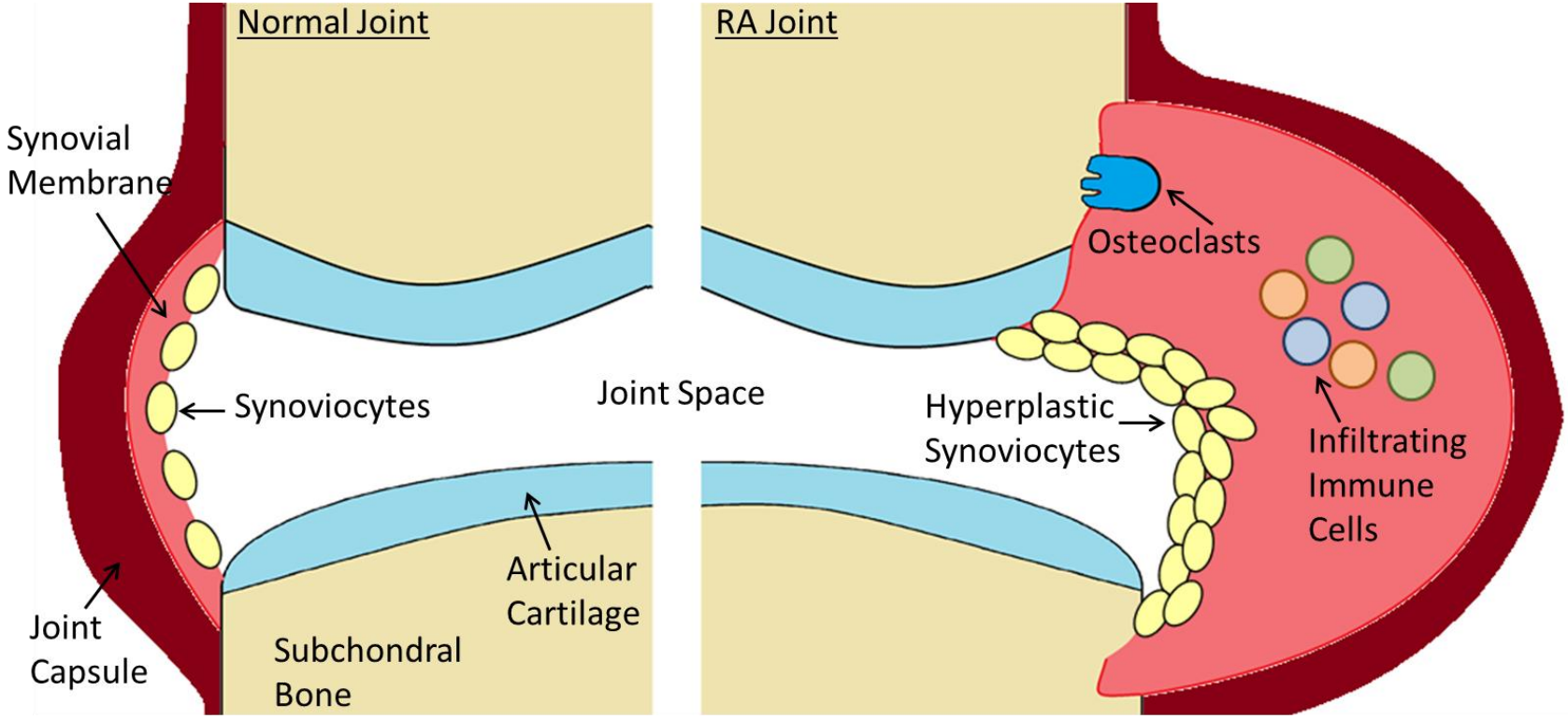

Figure 4. Normal and RA disease joint physiology

In the healthy joint the synoviocytes of the synovial membrane line the joint and secrete synovial fluid to maintain joint homeostasis. In RA, the synovial membrane becomes hyperplastic and infiltrated by chronic inflammatory cells. Expansion of the synovial membrane leads to the degradation of the cartilage and subchondral bone.

1.8 Proposed Models of RA Pathogenesis

The major pathology occurring in RA is destruction of articular cartilage and subchondral bone by the infiltrating synovium, where the disease process begins (Figure 4). Synovitis is initiated by the influx or local activation of mononuclear cells which leads to a hyperplastic synovial lining which expands and forms villi. In late state disease, the dysregulation and expansion of the synovium leads to the degradation of cartilage due to the release of proteolytic enzymes and activation of osteoclasts which destroys the bone (Choy, 2012). There are a number of proposed key players for the pathogenesis of RA, such as B- and T-cells, but disease progression is likely to encompass a complex signalling network between all these factors, described below.

1.8.1 B-cells

The success of rituximab, a B-cell depleting therapy, in the treatment of RA has confirmed the importance of B-cells in disease pathogenesis (Edwards and Cambridge, 2006). As well as their role in the secretion of autoantibodies, B-cells can process and present antigenic peptides to pre-primed CD4+ T-cells, culminating in a classical adaptive immune response (Edwards and Cambridge, 2006). Of the autoantibodies detected in RA, RF and CCP have been identified as markers of disease classification, given their presence before clinical onset of disease (Rantapaa-Dahlqvist, 2009). Deposition of RF immune complexes occurs in the rheumatoid synovium, where these complexes fix complement, leading to a positive-feedback loop whereby B-cell activation is re-enforced and this process can also perpetuate the inflammatory immune response through recognition of antibody constant regions by FCγ-receptors present on a variety of immune cell subsets, such as macrophages and lymphocytes (Edwards and Cambridge, 2006).

1.8.2 T-cells

Both CD4+ and CD8+ T-cells are present in the synovium of RA patients (Matthews et al., 1993, Fox, 1997, Breedveld and Verweij, 1997), with the CD4+ T-cell subset comprising 30-50 % of synovial tissue cells (Zvaifler et al., 1994). In the blood and synovium of RA patients, these cells have an activated phenotype, characterised by the up-regulated expression of HLA-DR, CD69 and CD27 (Cush and Lipsky, 1988, Breedveld and Verweij, 1997, Iannone et al.,

1994). However, *in vitro*, these cells have been shown to proliferate poorly in response to mitogenic stimuli, to have defects in [Ca]i signalling and a similar phenotypic characteristic to anergic T-cells (Carruthers et al., 1996, Ali et al., 2001, Hatachi et al., 2003). Numerous mouse models of RA indicate defects in CD4+ T-cell signalling, with a post-activated memory phenotype and low proliferative capacity (Thomas et al., 2008). These findings along with the therapeutic effects of tolerance inducing mechanisms, such as CLTA-4-Ig, a molecule that mimics the action of CTLA-4 by binding to the B7 molecules CD80 and CD86 on APC (von Kempis et al., 2012), would suggest defects in peripheral tolerance mechanisms in RA, leading to the recognition of autoantigens in the joint and initiation of an autoimmune response.

More recently, a role for Th17 cells has been implicated in not only RA pathogenesis, but in many other autoimmune diseases (Kirkham et al., 2013). Studies have demonstrated elevated levels of IL-17 in the blood and synovium of RA patients, which positively correlate with joint damage (Kirkham et al., 2006). Three therapies that block IL-17 signalling are currently in stage 3 clinical trials (Kirkham et al., 2013). Th17 cells secrete IL-17, which can directly or indirectly exert effects on various cell types to induce chemokine and pro-inflammatory cytokine expression and angiogenesis, which promotes the expansion of the synovium and osteoclastogenesis, which underpins bone resorption, and increased production of cartilage-degrading matrix metalloproteinase (MMPs) (Kirkham et al., 2013).

Given that the pathogenesis of RA is thought to occur as a result of a breakdown in immunological tolerance, the role of Treg in RA has been under intense investigation. It is well established that Treg play a protective role in RA and other autoimmune diseases and dysregulation of this tolerance either through altered Treg levels, reduced suppressive function, or resistance of cells to the suppressive function of Treg may be important in disease pathogenesis (Cooles et al., 2013).

1.8.3 Other players in RA disease pathogenesis

It is well established that pro-inflammatory cytokines are involved in the pathogenesis of RA, in particular IL-6 and tumour necrosis factor (TNF)-α. Through complex signalling pathways, these cytokines trigger gene expression of inflammation-related proteins, including additional cytokines and proteases. A

selection of roles for TNF-α includes increased monocyte activation and subsequent pro-inflammatory cytokine release, and induction of acute-phase protein production, which exacerbate the immune response. IL-6 has important roles in osteoclast activation, neutrophil recruitment, B- and T-cell activation and differentiation and can also induce acute-phase protein production (Choy, 2012).

Over the past two decades, more interest in fibroblast-like synoviocytes (FLS) has developed, expanding on their original role in synovial architecture. RA FLS have long been known to express MHC class II which appears to be up-regulated in the context of inflammation, but it is only more recently that IFN-γ treated RA FLS were shown to be able to extract and present auto-antigen candidates to antigen specific T-cell hybridomas (Leech and Morand, 2013). The cytokine secretion profile of RA FLS is notable for its ability to support the differentiation and activation of T-cells, specifically Th1 and Th17 subsets (Leech and Morand, 2013).

1.9 Therapeutic Tolerance in RA

Given the role for aberrant regulation of the immune system in the pathogenesis of RA, the ideal aim would be to re-instate tolerance as a disease cure. The traditional use of methotrexate for treatment of RA only induces remission in around 30 % of patients. In the 1990s, the development and subsequent approval of biological therapies that targeted pro-inflammatory cytokines or cell surface markers (Table 2) radically changed the course of RA disease. (Upchurch and Kay, 2012). These drugs relieve symptoms effectively but do not provide a cure and moreover, these drugs can increase the risk of serious infections. Preferably, tolerance should be induced in an antigen-specific fashion, possibly only aiming at the pathogenic cells and preserving physiologic defence.

Name	Therapy type	Site of action
Abatacept	CTLA-4 extracellular domain fused to Fc	APC
Adalimumab	mAb	TNF-α
Etanercept	Fusion Protein	TNF-α
Infliximab	Chimeric mAb	TNF-α
Rituximab	Chimeric mAb	CD20+ B-cells
Tocilizumab	Humanised mAb	IL-6R

Table 2. Examples of biological therapies for the treatment of RA
Adapted from Upchurch and Kay (2012).

1.10 Identification of Tolerance Markers in T-cells

The phenotypic link between anergy and RA (Carruthers et al., 1996, Ali et al., 2001) initiated a study to determine gene expression profiles of anergic T-cells and T-cells from established RA patients. In order to help interpret some of the characteristic RA cellular defects, transcriptional similarities between anergic and RA synovial T-cells were explored using the CD4+ T-cell clone, HA1.7, developed by Lamb et al., (1983). This clone is responsive to the influenza virus HA1 peptide 306-329 and will differentially respond when stimulated with different concentrations of HA1 peptide. Stimulating this clone with low doses of peptide (1 μg/ml) induces T-cell proliferation, but increasing the dose (300 μg/ml) stunts T-cell proliferation (Lamb et al., 1983), yet the cells remain viable as they respond to IL-2 (Figure 5). Comparison of the transcriptomes of T-cell anergy and RA synovium identified 11 transcriptional events that were common to both the anergic phenotype and the RA synovium. One example of this is the down-regulation of calmodulin seen in both anergy and the RA synovium, potentially linking the anergic state in HA1.7 with the hyporesponsiveness of RA T-cells. Calmodulin is a calcium-binding protein that binds [Ca]i and regulates other calcium-dependent proteins (Ali et al., 2001).

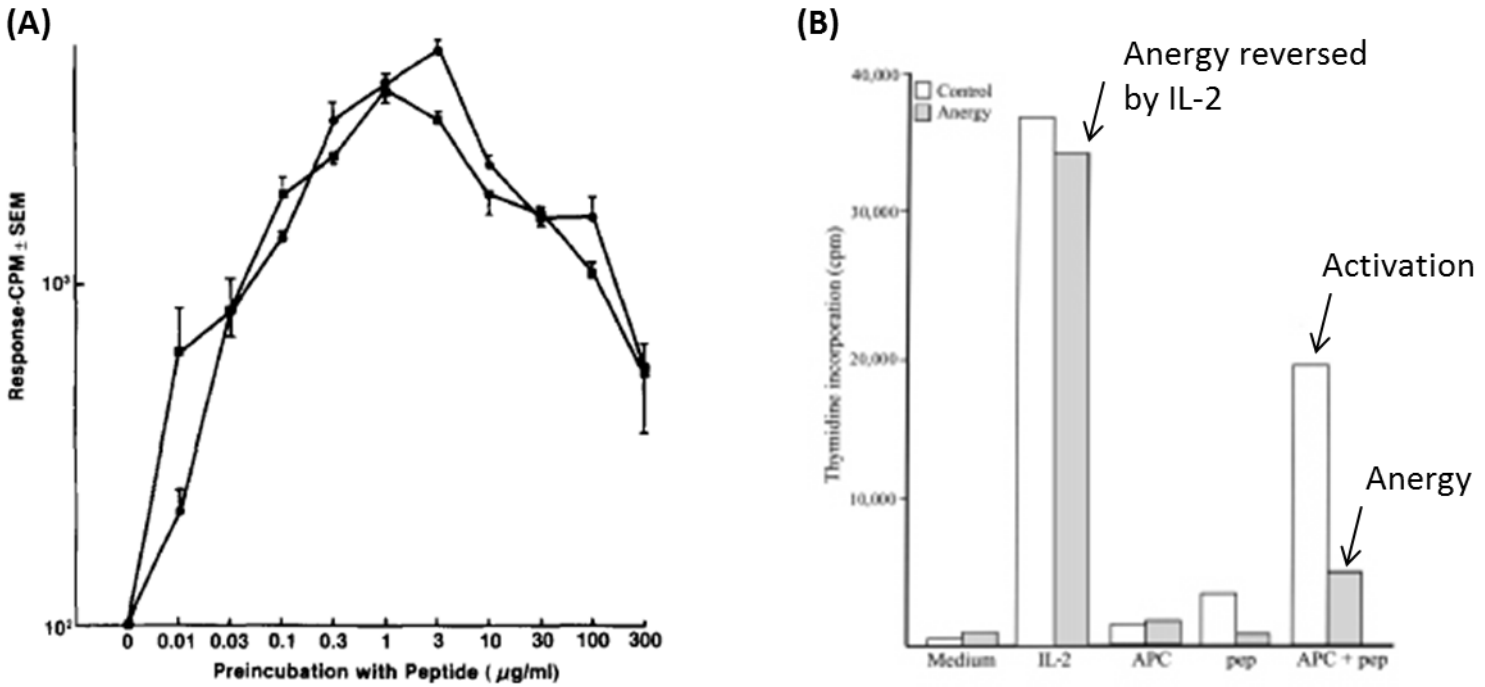

Figure 5. Induction of anergy in the human CD4+ T-cell clone, HA1.7

(A) HA1.7 (●), or HA2.61 (■) were cultured in the presence of differing concentrations of peptides 20 or 11, respectively and proliferation was measured by ^{3}HTdR incorporation after a 72 hour culture. Results are expressed as mean counts per minute (CPM) ± SEM of triplicate cultures. Figure taken from Lamb et al., (1983). (B) HA1.7 was incubated with peptide HA 306-318 for 24 hours (anergy) or with medium alone (control). The anergic state of the cells was subsequently tested by an immunogenic challenge for 48 hours of stimulation, measured as ^{3}HTdR incorporation. Viability was confirmed by responsiveness to exogenous IL-2. Figure adapted from Ali et al., (2001).

To further investigate the different signalling mechanisms in activated and anergic T-cells, comparisons were made between the gene expression profiles of the activated and anergised CD4+ T-cell clone, by differential display (Isaacs, J.D., unpublished data), and identified 37 differentially regulated gene transcripts 2hr or 24hr post-manipulation (Figure 6). Several of the identified genes have subsequently been validated for playing a role in anergy. For example, src-like adaptor protein (SLAP), which was not documented to be expressed by T-cells at the time of the original work, has been shown by others to be important in down-regulating thymocyte and T-cell responses (Myers et al., 2006, Loreto et al., 2002). In our group, interest was drawn to one gene which was differentially expressed between these two states, CLDND1. At a 2hr time-point, the levels of CLDND1 were similar in the anergic state compared to the resting state but fell dramatically in the activated state (Figure 6A). By 24hrs, the levels of CLDND1 were slightly elevated in the anergic state, but still remained low in the activated cells compared to the resting state (Figure 6B).

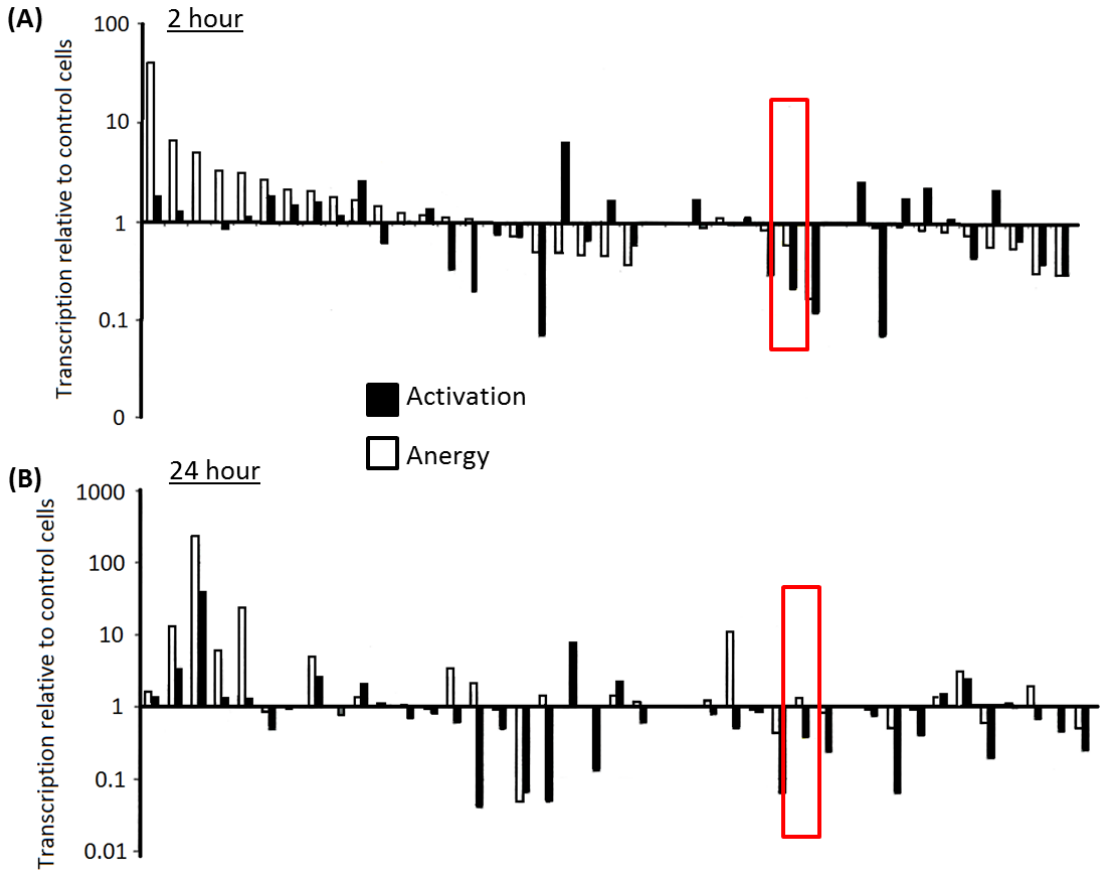

Figure 6. Gene expression profiling in the HA1.7 CD4+ T-cell clone identified CLDND1 to be differentially regulated between activation and anergy

The HA1.7 clone was either activated or anergised with the influenza virus HA1 peptide 306-329 (as described in Ali et al., (2001)) and differential display was performed to identify gene expression profile changes compared to GAPDH. (A) 2hr time-point, post induction. (B) 24hr time-point, post induction. CLDND1 transcript is highlighted in red.

1.11 CLDND1

1.11.1 Discovery of the CLDND1 gene

CLDND1 was originally identified in the human brain, through the screening of an array of clones from the IMAGE Consortium cDNA library 1NIB from infant brain, followed by macro-array analysis of CLDND1 expression in a variety of tissues. These findings were then confirmed using northern blot analysis of 8 human tissues (pancreas, kidney, skeletal muscle, liver, lung, placenta, brain and heart) showing the 2.8 kb CLDND1 transcript levels to be predominantly expressed in brain tissue and faint expression in the heart. Northern blot analysis of different regions of the human CNS identified signals of varying intensities in all the regions tested, with the most intense signals identified in areas corresponding to myelin-rich structures such as the corpus callosm, spinal cord and medulla. Based on these expression profiles, CLDND1 expression in oligodendrocytes was identified by quantitative real-time PCR (qRT-PCR). The coding region of the CLDND1 gene was determined using the Netstart programme and ATGpr, resulting in a transcript of 880 nucleotide long 5’ untranslated region (UTR), followed by a 759 nucleotide open reading frame (ORF) followed by a 3’ untranslated sequence of 1.2 kb (Fayein et al., 2002).

1.11.2 Predicted CLDND1 protein characteristics

C3orf4, which is now known as CLDND1, is the putative protein encoded from the identified coding region above. The CLDND1 protein sequence was processed by the BLAST 1 BEAUTY application, followed by Pfam HMM, TMHMM, ScanProsite and LALIGN (ExPASy) to analyse protein motifs and local alignment. Alternative splicing of the message can generate six transcript variants (variants 1-4, 6-7), from which 3 protein isoforms can be translated (isoforms A, B and D) (Figure 7). Transcript variants 1, 2, 3 and 6 encode the 253 amino acid protein isoform A, while transcript variant 4 encodes protein isoform B: a 276 amino acid protein. Sequence alignments indicate a longer N-terminus on isoform B than isoform A (Figure 7). Transcript variant 7 encodes a shorter 158 amino acid isoform D. The membrane topology was also described for each isoform, with the presence of four transmembrane domains at positions 5–27, 141–163, 175–197 and 212–234 for isoforms A and B, and three transmembrane regions for isoform D. Transmembrane regions correlate with

hydrophobic stretches of amino acids as seen on a hydrophobicity chart. Several putative glycosylation and phosphorylation sites were also predicted (Figure 7). Local alignments were identified in the third transmembrane domain with similar sites in the domain of human and mouse peripheral myelin protein 22-growth arrest specific protein (PMP-22), which identified a consensus sequence with the PMP-22/EMP/MP20/claudin superfamily (Fayein et al., 2002).

```
A ----------------------MDNRFATAFVIACVLSLISTIYMAASIGTDFWYEYRS 37
B MGGDRLENKTSVSVASWSSLNARMDNRFATAFVIACVLSLISTIYMAASIGTDFWYEYRS 60
D ------------------------------------------------------------

A PVQENSSDLNKSIWDEFISDEADEKTYNDALFRYNGTVGLWRRCITIPKNMHWYSPPERT 97
B PVQENSSDLNKSIWDEFISDEADEKTYNDALFRYNGTVGLWRRCITIPKNMHWYSPPERT 120
C ------------------------------------------------------------MG 2

A ESFDVVTKCVSFTLTEQFMEKFVDPGNHNSGIDLLRTYLWRCQFLLPFVSLGLMCFGALI 157
B ESFDVVTKCVSFTLTEQFMEKFVDPGNHNSGIDLLRTYLWRCQFLLPFVSLGLMCFGALI 180
C ESFDVVTKCVSFTLTEQFMEKFVDPGNHNSGIDLLRTYLWRCQFLLPFVSLGLMCFGALI 62
************************************************************

A GLCACICRSLYPTIATGILHLLAGLCTLGSVSCYVAGIELLHQKLELPDNVSGEFGWSFC 217
B GLCACICRSLYPTIATGILHLLAGLCTLGSVSCYVAGIELLHQKLELPDNVSGEFGWSFC 240
D GLCACICRSLYPTIATGILHLLAGLCTLGSVSCYVAGIELLHQKLELPDNVSGEFGWSFC 122
************************************************************

A LACVSAPLQFMASALFIWAAHTNRKEYTLMKAYRVA 253
B LACVSAPLQFMASALFIWAAHTNRKEYTLMKAYRVA 276
D LACVSAPLQFMASALFIWAAHTNRKEYTLMKAYRVA 158
  ***********************************
```

Figure 7. Sequence alignment of CLDND1 protein isoforms

CLDND1 isoforms (A, B and D) were aligned using clustalW2. Transmembrane regions and potential post-translational modifications were taken from www.unitprot.org or www.phosphosite.org. * indicates identical amino acids between the isoforms. Underlined regions indicate transmembrane regions. Red residues indicate potential N-glycosylation sites, orange residues indicate potential ubiquitination sites, purple residues highlight the PMP-22/EMP/MP20/claudin superfamily consensus sequence and blue residues indicate potential phosphorylation sites.

1.11.3 The PMP-22/EMP/MP20/claudin superfamily

The PMP-22/EMP/MP20/claudin superfamily is comprised of a diverse range of proteins with a large variation in function. The major components of this superfamily are the clarin family (IPR026748), the PMP-22/EMP/MP20 family (IPR004032), the claudin family (IPR006187) and the voltage-dependent calcium channel, gamma subunit family (CACNG) (IPR008368). These superfamily members all share a similar tetraspanning transmembrane topology with intracellular N- and C-termini. The similarity of the functional motifs in the superfamily members are illustrated in Figure 8.

1.11.4 The clarin family

The clarin family consist of clarins -1, -2 and -3. Clarin-1 is also known as Usher syndrome type-3 protein as mutations in the gene coding for this protein cause Usher syndrome type 3 (USH3), which is a genetically heterogeneous condition characterised by the association of retinitis pigmentosa and sensorineural deafness (Aller et al., 2004). The functions of clarin-2 and clarin-3 are not clear.

1.11.5 The PMP-22/EMP/MP20 family

PMP-22 and epithelial membrane protein (EMP)-1, -2 and -3 are highly similar, while movement protein (MP)20 is more distantly related. The roles of PMP-22 are still being investigated, but it is known to be involved in promoting and maintaining the myelin sheath: an important insulator of axons. PMP-22 also has a role in controlling cell proliferation, apoptosis and adhesion (Zoidl et al., 1995, Roux et al., 2005, Fabbretti et al., 1995). Circular dichroism and nuclear magnetic resonance (NMR) show that PMP-22 has an alpha-helical secondary structure, with four transmembrane spanning regions, and the protein has strong tendencies to dimerise (Mobley et al., 2007). The PMP-22 deletion results in hereditary neuropathy with liability to pressure palsies (HNPP) (Mouton et al., 1999) and its duplication results in Charcot–Marie–Tooth 1A (CMT1A) disease (Birouk et al., 1997). PMP-22 is also regulated by N-glycosylation in the first extracellular loop and this is required for its cell surface location (Brancolini et al., 2000).

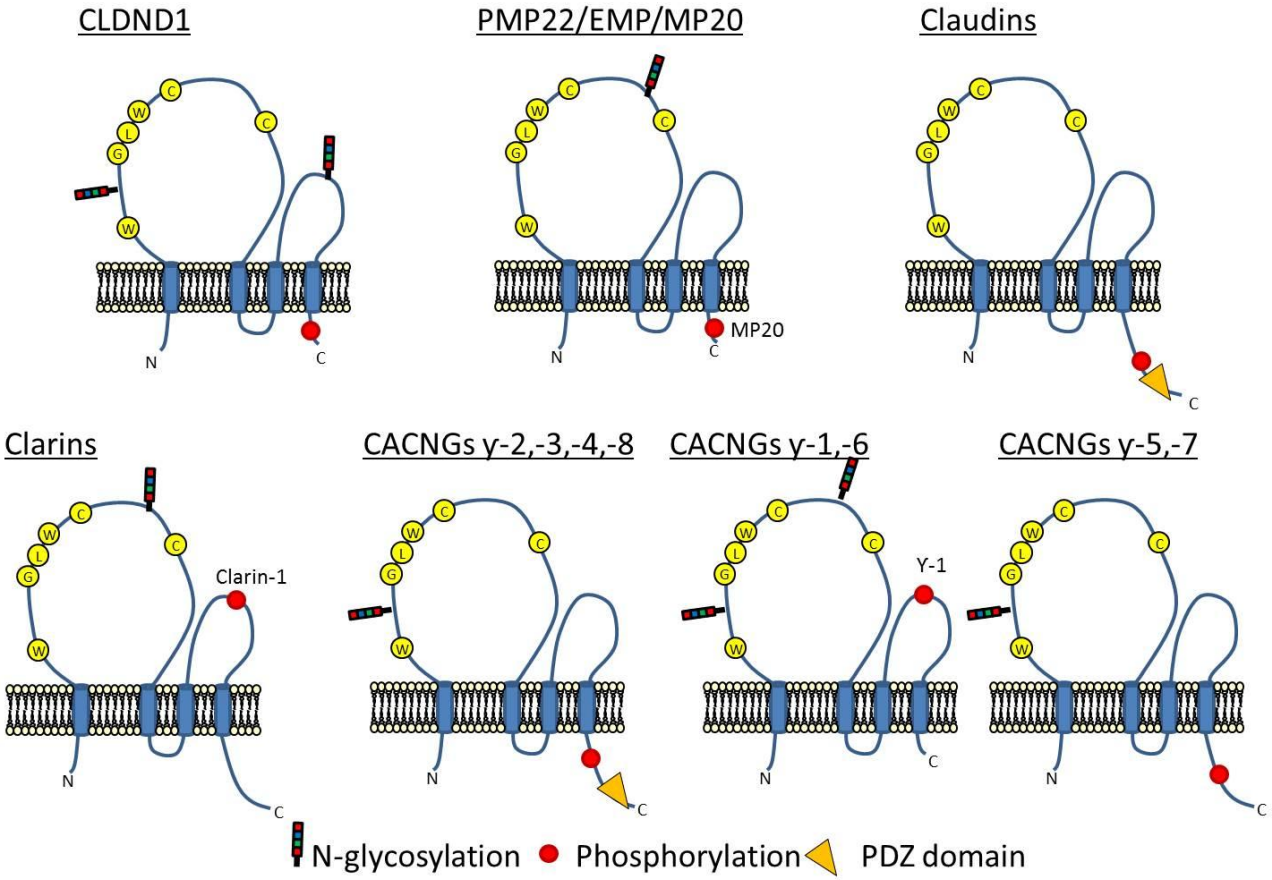

Figure 8. CLDND1 protein motif comparison to PMP-22/EMP/MP20/claudin superfamily members

PMP-22/EMP/MP20/claudin superfamily proteins were grouped according to EBI classification. Transmembrane regions and potential post-translational modifications were taken from uniprot (http://www.uniprot.org/) or cell signalling phosphosite plus (http://www.phosphosite.org). Individual family members with specific motifs are labelled.

The EMP family members bind to a family of ATP-gated ion channels and also play a role in inducing apoptosis in cell culture models (Wilson et al., 2002). The EMPs are expressed in a wide range of tissues, including heart, placenta, lung, skeletal muscle, kidney and small intestine and blood leukocytes (Chen et al., 1997, Taylor and Suter, 1996). A positive role for EMP-1 in proliferating cells has also been suggested (Ben-Porath and Benvenisty, 1996), while EMP-2 also has a suggested role in cell adhesion (Wadehra et al., 2002).

MP20, subsequently renamed to lens intrinsic membrane protein (LMIP), is expressed at extremely high levels in the mammalian eye lens. LMIP has a suggested role in signal transduction as it is phosphorylated by cyclic adenosine monophosphate (cAMP)-dependent kinases (Galvan et al., 1989), and a proposed function as a barrier protein in the eye (Grey et al., 2003), yet its exact role is still to be elucidated.

1.11.6 The claudin family

There are 23 members of the claudin family in humans, ranging from 20 to 34 kDa in size (Lal-Nag and Morin, 2009). Immunofluorescence studies have identified claudins to be located at tight junctions (TJ) (Furuse et al., 1998) and their role in TJ function to be important (Tsukita and Furuse, 2000). TJ are found at the most apical regions of polarised epithelial and endothelial cells and function as a barrier to prevent paracellular transport of solutes and to maintain cellular polarity by preventing lateral diffusion of membrane lipids and proteins (Lal-Nag and Morin, 2009).

Claudin family members show the most heterogeneity in their C-terminal tail, yet all claudins contain a PDZ-domain-binding motif that enables claudins to interact directly with cytoplasmic scaffolding proteins such as the zona occludens (ZO) family (Itoh et al., 1999). The C-terminal tail is also a site of various post-translational modifications that can alter claudin localisation and function (Van Itallie et al., 2005, D'Souza et al., 2005, Aono and Hirai, 2008, Ishizaki et al., 2003, Ikari et al., 2006). The functions of claudins have been determined through the over-expression or down-regulation of claudin genes in a variety of epithelial cell lines and generally they determine the selectivity of paracellular transport of small ions. Specific functions of claudin family members vary depending on the ion and the system in which it is studied (Angelow et al., 2008).

Various human diseases have shown the importance of the claudin family members in TJ function. Mutations of claudin-16 and -19 are associated with familial hypomagnesemia with hypercalciurea and nephroclacinosis (FHHNC), a rare magnesium wasting disorder as a result of loss of Mg^{2+} from malfunctioning kidneys (Simon et al., 1999, Konrad et al., 2006). Claudins are also dysregulated in different cancers which is consistent with TJ disassembly during tumourigenesis (Kramer et al., 2000, Resnick et al., 2005).

1.11.7 The voltage-dependent calcium channel, gamma subunit family

Voltage dependent calcium channels (VDCC) allow the coupling of electrical activity to [Ca]i signalling. The activity of the channel is regulated by four tightly coupled subunits: the pore forming α-1, an intracellular β, a disulphide-linked complex of an α-2 and δ and the CACNG (Catterall et al., 2003). The α, δ and β subunits act as the pore forming unit and aid channel function, while original studies identified the CACNG to regulate the channel (Eberst et al., 1997, Letts et al., 1998). Current understandings suggest a more diverse role for CACNG in the regulation of other channels as well (Chen et al., 2007). The suggested functional and phylogenetic attributes of CACNG have resulted in their division into three groups the γ-2, γ-3, γ-4 and γ-8 subunits are known to act as transmembrane 2-amino-3-(3-hydroxy-5-methyl-isoxazol-4-yl)propanoic acid (AMPA) receptor regulatory proteins (TARP) (Osten and Stern-Bach, 2006), γ-1 and γ-6 are known to regulate VDCC (Freise et al., 2000, Hansen et al., 2004), while γ-5 and γ-7, which have received the least attention, have been shown not to be important in AMPA receptor trafficking and have conflicting evidence for a role in VDCC signalling (Chen et al., 2007).

All CACNG contain N-linked glycosylation sites in the first extracellular loop (Chen et al., 2007); yet other functional motifs are distinct within the subunit clusters. TARP contain a number of regulatory sites in their C-terminal domain, including a PDZ-binding domain, which is important for targeting AMPA receptors to the synapse and acts as a phosphorylation site for PKA, PKC and PKD, which is important for regulating the interactions between TARP and AMPA receptors (Choi et al., 2002) The PDZ-binding domain is lacking in the γ-1 and γ-6 or γ-5 and γ-7 subunits. The C-terminal domain of γ-1 and γ-6 are very short and lack functional motifs.

The original identification of CACNG was the identification of CACNG2 in the stargazin mutant mouse model, which characteristically had spontaneous abnormal head movements and absence seizures with accompanying defects in the cerebellum and inner ear (Letts et al., 1998), yet its role in human disease is yet to be described.

1.11.8 Potential CLDND1 function based on the PMP-22/EMP/MP20/claudin family

Given the diverse functional roles of the PMP-22/EMP/MP20/claudin superfamily members in a range of cell types, it would be difficult to ascribe a specific potential function for CLDND1 in T-cells, from these members' functions. There are, however, similar functional processes that are common between these family members that are also common to T-cells. A large proportion of the superfamily (all the claudins, PMP-22, LMIP and the EMP) have confirmed roles in barrier function or cell adhesion. This may suggest that CLDND1 may also play a role in inter-cellular contacts. Other family members have been identified to be important in controlling cell proliferation and apoptosis (PMP-22 and EMP), and also in the regulation of calcium signalling (CACNG), which both may be linked to the control of T-cell activation, as discussed throughout this chapter, and could potentially link to a function for CLDND1.

1.11.9 CLDND1 gene function

From the literature, there are only a handful of documented cellular expression data for the CLDND1 protein. Gene expression was first described in rat optic nerve cells, in particular on the oligodendrocyte population and so a role for CLDND1 in myelination of the central nervous system was suggested (Fayein et al., 2002). The increasing popularity of RNA microarray analysis of cell types has subsequently lead to the identification of CLDND1 gene expression in mouse hepatoma Hepa-1c1c7 cells (Hao et al., 2012) and within whole blood (Beineke et al., 2012), yet its detection in CD4+ T-cells remained elusive. CLDND1 has been found to be up-regulated in at least 80 % of lung squamous cell carcinomas (Liu et al., 2007), yet its role in these cells still needs to be determined. Advances in mass spectrometric techniques have recently identified CLDND1 protein on both HEK293 cells and human U2OS

osteosarcoma cells, yet no inference was made to its function; apart from the observation that CLDND1 protein can be ubiquitinated, and so is probably targeted for degradation in this manner (Kim et al., 2011, Wagner et al., 2011, Danielsen et al., 2011). There is currently no CLDND1$^{-/-}$ mouse available and so no function for CLDND1 can be determined from these types of studies.

1.11.10 Pilot data indicating a function for CLDND1 in CD4+ T-cells

Preliminary studies in the Isaacs' lab looked at the effect of CLDND1 on CD4+ T-cell function (Isaacs, J.D., unpublished data). In primary human CD4+ T-cells, CLDND1 transcript was targeted for degradation using CLDND1 siRNA (siGENOME Smartpool), or over-expressed using two vectors: pcDNA3.2/GW/V5 (Life technologies, Paisley UK) or the pIRES2- H2K^{k} expression system (Tahvanainen et al., 2006). The use of the H2K^{k} expression vector system allowed for CLDND1 transfected cells to be sorted from the untransfected cells due to the co-expression of a truncated H2K^{k} mouse molecule with CLDND1. Silencing of the CLDND1 transcript was determined by qRT-PCR and was calculated at 70-75 %, while transfection efficiency for over-expression was determined using an e-green fluorescent protein (GFP) expression vector (Amaxa, Lonza, Castleford, UK) and calculated at 50 %. Silencing of the CLDND1 gene resulted in an increase in transfected T-cell proliferation, compared to control cells (Figure 9A). The effect of CLDND1 over-expression on T-cell proliferation was dependent on the vector used. Use of the pcDNA3.2/GW/V5 vector, in which only a proportion of the cells expressed CLDND1, resulted in an increase in transfected T-cell proliferation (Figure 9B), whereas use of the pIRES2- H2K^{k} vector (Figure 9C), where all the cells were both CLDND1 and H2K^{k} positive, showed that CLDND1 reduced T-cell proliferation. From these data, it was hypothesised that the differences in mixed and pure CLDND1-transfected CD4+ T-cell populations may be caused by paracellular homotypic interactions between CLDND1 molecules. Alternatively, the use of the different expression vectors may have resulted in different transfection efficiencies, or affected the viability of the cells. These preliminary results suggest a potential role for CLDND1 in inducing a hypo-proliferative T-cell phenotype, however CLDND1 protein expression was not determined and cell viability was not measured in these limited experiments, and further

investigations are required to investigate these parameters and further elucidate a role for CLDND1 in T-cell tolerance.

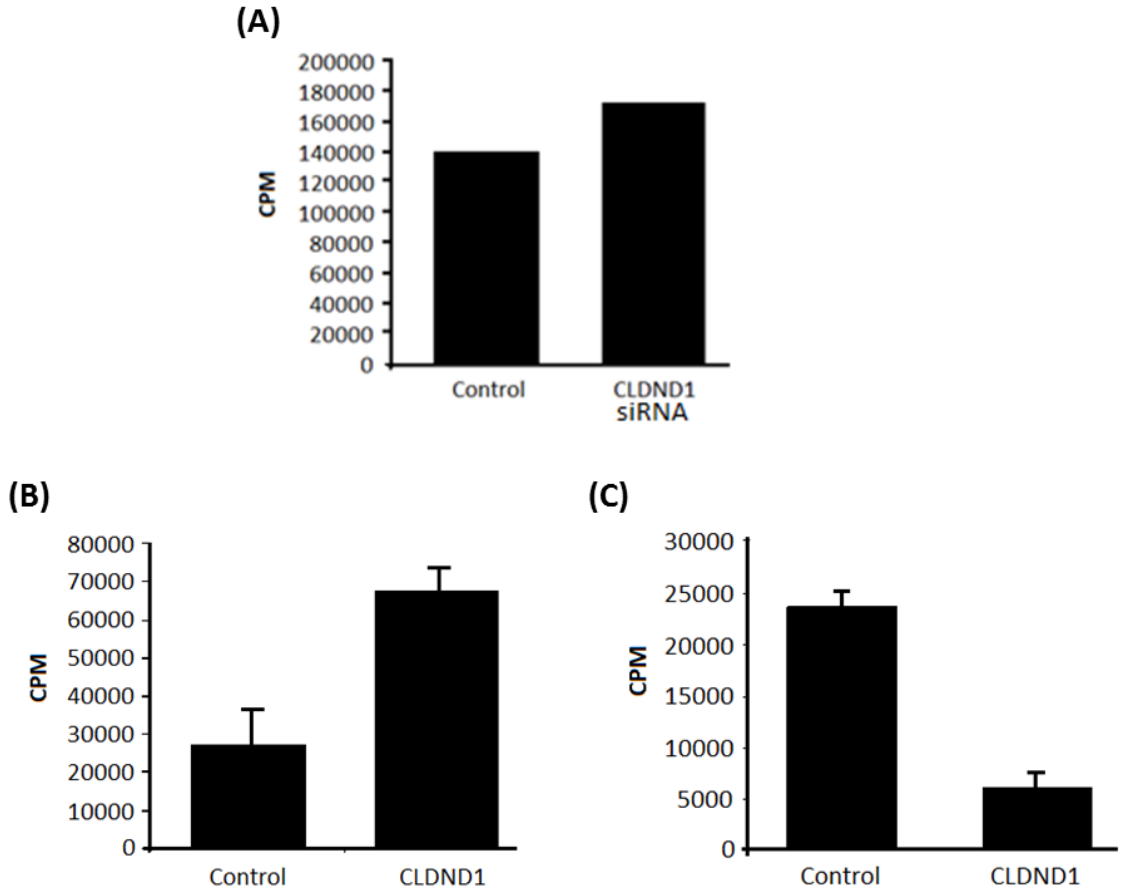

Figure 9. Preliminary work: targeting CLDND1 in primary human CD4+ T-cells reveals a potential role for CLDND1 in the regulation of T-cell proliferation

CLDND1 was silenced (A), or over-expressed (B and C) in primary human CD4+ T-cells. Over-expression was performed with two vectors (B) V5-tagged CLDND1 in pcDNA3.2 or (C) CLDND1 in pIRES-H2K^{k}. 24 hours after transfection, cells were stimulated with 1:1 ratio of α-CD3/CD28 expander beads for 3 days and T-cell proliferation was measured by ^{3}HTdR incorporation. Data illustrate a single experiment.

1.12 Hypothesis and Aims of the Thesis

T-cell activation is under tight regulation to prevent aberrant activation of self-reactive T-cells. A consequence of a breakdown in immunological self-tolerance may lead to autoimmune diseases such as RA. An important therapeutic goal in RA is the reversal of the breakdown in tolerance in order to provide a potential cure. RA T-cell phenotyping revealed similarities to anergic cells and so identifying key players in anergy may yield a potential therapeutic target. CLDND1 expression was differentially regulated during T-cell anergy and activation and preliminary studies suggest a role for this protein in the regulation of T-cell activation. Thus it was hypothesised that CLDND1 may mediate a key mechanism in the regulation of T-cell proliferation and, given its cell surface location, may provide a novel therapeutic target.

The main aims of this thesis were:

- To generate polyclonal antibodies (pAbs) against CLDND1 in order to verify CLDND1 protein expression on CD4+ T-cells
- Document CLDND1 expression during T-cell activation
- Identify CLDND1 expression in early RA patients as both a potential biomarker of early disease and for a role in disease pathogenesis
- Modulate CLDND1 expression by silencing or over-expressing CLDND1 in primary human CD4+ T-cells, to strengthen its hypothesised function in the regulation of T-cell proliferation
- To confirm a role for CLDND1 in anergy

Chapter 2. Methods

2.1 List of Materials

2.1.1 Stocks

Stock solutions were prepared, aliquoted and stored as described below.

4 % formaldehyde: paraformaldehyde (VWR International, Lutterworth, UK) was added to phosphate buffered saline (PBS) for a 4 % (w/v) solution and warmed between 55-60°C until dissolved. The stock was aliquoted and stored at -20°C.

5(6)-carboxyfluorescein diacetate N-succinimidyl ester (CFSE): under aseptic conditions, CFSE (SIGMA Aldrich, Poole, UK) was reconstituted to 10 mM stock solutions with dimethyl sulfoxide (DMSO), aliquoted and stored at -20°C.

Accell siRNA: under aseptic conditions, Accell siRNA (Thermo Scientific, Loughborough, UK) was resuspended to 100 µM stocks with 1x Accell siRNA buffer (Thermo Scientific). Aliquots were stored at -20°C.

ELISA standards: 2 µg/ml stock of recombinant human IL-2, IL-10, IFN-γ and TNF-α (all BD Bioscience, Oxford, UK) were prepared in PBS (Lonza) + 10 mg/mL albumin from bovine serum (BSA) (SIGMA Aldrich) and stored at -80°C. Stocks were diluted 1/1000 in PBS + 1 % BSA for the top ELISA standard.

Fetal bovine serum (FBS): FBS (Lonza) was thawed at 37°C then heat-inactivated at 56°C in a water bath for 1 hour. Under aseptic conditions, the FBS was then aliquoted and re-frozen at -20°C.

Glutamine solution: sterile glutamine solution [200 mM] (SIGMA Aldrich) was thawed at 37°C and was aliquoted and refrozen at -20°C.

LB media: 20.6 g of LB broth EZMix Powder (SIGMA Aldrich) was dissolved in 1 L deionised H_2O and autoclaved.

Methyl-^{3}H thymidine (^{3}HTdR): under aseptic conditions, ^{3}HTdR (Perkin Elmer, Massachusetts, USA) was added to RPMI-1640 (Lonza) to generate a working stock of 0.548 MBq/mL and stored at 4°C.

o-Phenylenediamine dihydrochloride (OPD): each OPD tablet (SIGMA Aldrich) was dissolved in 13 mL citrate phosphate buffer (25 mM citric acid, 50 mM disodium phosphate, 20 mM sodium phosphate dibasic dihydrate) before use, along with 6 µL 30 % hydrogen peroxide solution (SIGMA Aldrich).

Penicillin and streptomycin: sterile penicillin [10,000 units/mL] and streptomycin [10 mg/mL] solution (SIGMA Aldrich) was thawed at 37°C. Under aseptic conditions, the solution was aliquoted and re-frozen at -20°C.

SB-505124: under aseptic conditions, lyophilised SB-505124 hydrochloride hydrate (SIGMA Aldrich) was reconstituted to 28.7 mM with DMSO (SIGMA Aldrich) and stored in aliquots at -20°C, for a maximum of 1 month.

Tissue culture cytokines: the following reagents were prepared under aseptic conditions:

IL-4 lyophilised powder (Miltenyi Biotech, Bergisch Gladbach, Germany) was resuspended to 50 µg/mL in RF-1 (RPMI-1640 medium, 2 mM L-glutamine, 100 U/mL penicillin, 1 µg/mL streptomycin, 1 % FBS). Aliquots were stored at -20°C.

Recombinant human granulocyte macrophage colony-stimulating factor (GM-CSF) (Genzyme, Oxford, UK) was resuspended to 250 µg/mL in RPMI-1640 then further diluted to 5 µg/mL in RF-1, aliquoted and stored at -20°C.

Dexamethasone (SIGMA Aldrich) was reconstituted to 1 mg/mL ($2.55x10^{-3}$ M) in ethanol then further diluted 25.5x in RPMI-1640 to give a $1x10^{-4}$ M stock solution. Aliquots were stored at -20°C.

Calcitrol (vitamin D3) (Tocris Bioscience, Abingdon, UK) was resuspended to $2.4x10^{-3}$ M in ethanol then diluted further in ethanol to $1x10^{-4}$ M and stored in aliquots at -20°C. For use, ethanol was added to each stock to make a $1x10^{-6}$ M solution, then this was diluted 1/100 to give a $1x10^{-8}$ M solution in RF-10 (RPMI-1640 medium, 2 mM L-glutamine, 100 U/mL penicillin, 1 µg/mL streptomycin, 10 % FBS) and used immediately.

LPS from *Escherichia coli* 0111:B4 (SIGMA Aldrich) was reconstituted to 1 mg/mL in RF-1. Aliquots were stored at -20°C. From this, a working stock of 10 µg/mL was prepared in RF-1 and kept for 1 month at 4°C.

Recombinant human TGF-β1 (Peprotech, London, UK) was reconstituted to 1 µg/mL in RF-1 and aliquots were stored at -20°C.

Trypsin: sterile trypsin solution (SIGMA Aldrich) was thawed at 37°C. Under aseptic conditions, the solution was then aliquoted into 5 mL volumes and re-frozen at -20°C until required for tissue culture media.

2.1.2 Antibodies

Primary antibody	Manufacturer	Clone	Catalogue	Dilution
Alexa Fluor® 647 α-human Foxp3	BioLegend	206D	320114	1/50
Annexin V- allophycocyanin	BD Bioscience	-	550474	3 µL/test
α-human CD3- allophycocyanin	eBioscience	UCHT1	17-0038-43	1/200
α -human CD3- fluorescein isothiocyanate	BD Bioscience	HIT3a	555339	1/10
α-human CD3- peridinin chlorophyll protein	BD Bioscience	SK7	345766	1/20
α-human CD4- fluorescein isothiocyanate	eBioscience	RPA-T4	11-0049-42	1/200
α-human CD4- phycoerythrin cyanin7	eBioscience	SK3	25-0047-42	1/50
α-human CD4- peridinin chlorophyll protein	BD Bioscience	SK3	345770	1/20
α-human CD8- allophycocyanin	BD Bioscience	RPA-T8	555369	1/20
α-human CD8- peridinin chlorophyll protein	BD Bioscience	SK1	345774	1/20
α-human CD14- fluorescein isothiocyanate	BD Bioscience	M5E2	555397	1/20
α-human CD19- allophycocyanin	BD Bioscience	HIB19	555415	1/20
α-human CD25- fluorescein isothiocyanate	BD Bioscience	M-A251	555431	1/20
α-human CD25-phycoerythrin	BD Bioscience	M-A251	555432	1/20
α-human CD28- fluorescein isothiocyanate	BD Bioscience	CD28.2	555728	1/20
α-human CD45RA- fluorescein isothiocyanate	BD Bioscience	HI100	555488	1/20
α-human CD56- fluorescein isothiocyanate	BD Bioscience	NCAM16.2	345811	1/10
α-human CD80- fluorescein isothiocyanate	BD Bioscience	L307.4	557226	1/50

Primary antibody	Manufacturer	Clone	Catalogue	Dilution
α-human CD83- allophycocyanin	BD Bioscience	HB15e	551073	1/20
α-human CD86- allophycocyanin	BD Bioscience	2331 (FUN-1)	555660	1/50
α-human CD282 (TLR2)- allophycocyanin	eBioscience	TL2.1	17-9922	1/10
α-human HLA-DR- peridinin chlorophyll protein	R&D Systems	L203	FAB4869C	1/20
α-human LAP (TGF-beta 1) phycoerythrin	R&D Systems	27232	FAB2463P	1/10
MACSelect control fluorescein isothiocyanate	Miltenyi Biotech	Polyclonal	130-090-326	1/10
Mouse α- H2K^{k} -phycoerythrin	Miltenyi Biotech	H100-27.R55	130-094-867	1/10
Via-Probe™	BD Bioscience	-	555815	5 µL/test

Table 3. Directly-conjugated antibodies

A list of the directly-conjugated antibodies, along with the manufacturer and clone of antibody, used for flow cytometry. The quantity of antibody used for each reaction is expressed as a dilution of the antibody stock, or a set volume per reaction.

Primary antibody	Manufacturer	Clone	Dilution		
			Flow cytometry	Western blot	Immunofluorescence
α-CLDND1 (in-house)	UCB Celltech	Polyclonal	1 µg/test	1 µg/mL	-
α-CLDND1 pre- and anti-sera	UCB Celltech	Polyclonal	1/100, 1/2000	1/100	1/100
Goat α-human-CLDND1	Santa Cruz	Polyclonal	5 µg/mL	1 µg/mL	-
Mouse monoclonal α-FLAG® M2	SIGMA Aldrich	M2	-	-	1/100
Mouse monoclonal α-α-tubulin	SIGMA Aldrich	B-5-1-2	-	1/1000	-
Rabbit α-human-CLDND1	ProSci	Polyclonal	5 µg/mL	1 µg/mL	-
Rabbit α-human-CLDND1	Abcam	Polyclonal	5 µg/mL	1 µg/mL	-
Rabbit α-human-CLDND1-SIGMA 1	SIGMA Aldrich	Polyclonal	1 µg/mL	1 µg/mL	-
Rabbit α-human-CLDND1-SIGMA 2	SIGMA Aldrich	Polyclonal	1 µg/mL	1 µg/mL	-
Rabbit α-DYKDDDDK tag	Cell Signaling Technology	Polyclonal	-	1/1000	-
Rabbit α-GAPDH XP®	Cell Signaling Technology	D16H11	-	1/10000	-

Table 4. Primary antibodies

A list of the primary antibodies, along with the manufacturer and clone of antibody where applicable, used for flow cytometry, Western blot and immunofluorescence techniques. The quantity of antibody used for each reaction is expressed as a dilution of the antibody stock, or a set concentration or amount per reaction.

Secondary antibody	Manufacturer	Dilution		
		Flow cytometry	Western blot	Immunofluorescence
Alexa Fluor® 488 goat α-rabbit IgG (H+L)	Molecular Probes	-	-	1/750
Alexa Fluor® 594 goat α-mouse IgG (H+L)	Molecular Probes	-	-	1/750
Alexa Fluor® 594 goat α-rabbit IgG antibody, ReadyProbes™ reagent	Molecular Probes	-	-	1/750
α-mouse IgG (H+L) HRP-linked	Cell Signaling Technology	-	1/3000	-
α-rabbit IgG (H+L) HRP-linked	Cell Signaling Technology	-	1/3000	-
Fluorescein isothiocyanate-affinipure F(ab')$_2$ fragment goat α-rabbit IgG, Fc fragment specific	Jackson ImmunoResearch	1/100	-	-
Goat serum	SIGMA Aldrich	2 %	-	2 %
Human IgG (138.5 mg/ml)	Gift from Sophie Hambleton	0.2 µg/test	-	-
R-phycoerythrin-affinipure F(ab')$_2$ fragment goat α-rabbit IgG (H+L)	Jackson ImmunoResearch	1/200	-	-

Table 5. Secondary antibodies

A list of secondary antibodies, along with the manufacturer, used to detect the primary antibodies used in flow cytometry, Western blot or immunofluorescence techniques. The quantity of antibody used for each reaction is expressed as a dilution of the antibody stock, a percentage of the final reaction volume, or a set amount per reaction.

2.1.3 Buffers

	Buffer alias	Components
Tissue culture	RF-10	RPMI-1640 medium, 2 mM L-glutamine, 100 U/mL penicillin, 1 µg/mL streptomycin, 10 % FBS
	RF-5	RPMI-1640 medium, 2 mM L-glutamine, 100 U/mL penicillin, 1 µg/mL streptomycin, 5 % FBS
	RF-1	RPMI-1640 medium, 2 mM L-glutamine, 100 U/mL penicillin, 1 µg/mL streptomycin, 1 % FBS
	RF-0	RPMI-1640 medium, 2 mM L-glutamine, 100 U/mL penicillin, 1 µg/mL streptomycin
	Amaxa culture medium	RPMI-1640 medium, 4 mM L-glutamine, 10 % FBS
	SW1353 culture medium	DMEM, high glucose, 2 mM L-glutamine, 100 U/mL penicillin, 1 µg/mL streptomycin, 10 % FBS
	Rab-9 culture medium	RPMI-1640 medium + 10 % FBS + 1 mM L-glutamine +100 µg/mL normacin (InvivoGen)
	MACS Buffer	PBS pH 7.2, 0.5 % BSA, 2 mM EDTA
DNA	1xTAE	40 mM tris-acetate pH 8, 1 mM EDTA
	TAE-agarose loading buffer	0.125 M tris pH 6.8, 2% (w/v) SDS, 10 % (v/v) glycerol, 0.001 % bromophenol blue
Protein identification	RIPA lysis buffer	50 mM tris HCl pH 8, 150 mM NaCl, 1 % (v/v) triton-X 100, 0.5 % (v/v) sodium deoxycholate, 0.1 % SDS (w/v), protease inhibitor cocktail (Roche)
	Triton-X permeabilisation buffer	PBS pH 7.2, 0.5 % (w/v) BSA, 1 % (v/v) fish skin gelatin, 0.5 % (v/v) triton-X 100
	Coomassie brilliant blue R250 staining buffer	45 % methanol, 10 % glacial acetic acid, 45 % water, 3 g/L coomassie brilliant blue R250
	Coomassie destaining buffer	45 % methanol, 10 % glacial acetic acid, 45 % water

	Buffer alias	Components
	5x laemmli loading buffer	0.1 M tris HCl, pH 6.8, 0.35 M SDS, 20 % (v/v) glycerol, 0.01 % bromophenol blue and 5 % (v/v) β-mercaptoethanol
	Transfer buffer	20 mM tris HCL, 0.65 M glycine, 20 % (v/v) methanol
	TBS-T	10 mM tris pH 7.5, 150 mM NaCl, 0.1 % tween 20 (v/v)
	Red blood cell lysis buffer	0.1 M NH_4Cl, 1 mM $KHCO_3$, 0.1 mM EDTA
	10X Annexin V binding buffer	0.1 M HEPES, pH 7.4, 1.4 M NaCl, 25 mM $CaCl_2$
	FACS buffer	PBS pH 7.2, 3 % (v/v) FBS, 100 µM (v/v) EDTA, 0.01% (v/v) sodium azide
ELISA	Citrate phosphate buffer	25 mM citric acid, 50 mM disodium phosphate, 20 mM sodium phosphate dibasic dihydrate
	Coating buffer	15 mM disodium phosphate, 20 mM monosodium phosphate sodium phosphate monobasic
	ELISA wash buffer	PBS pH 7.2+ 0.1 % (v/v) tween 20
	Blocking buffer	PBS pH 7.2 + 1 % (w/v) BSA
	Diluent	PBS pH 7.2 + 1 % BSA + 0.1 % (v/v) tween 20

Table 6. Buffers

Alias and composition of the buffers used for tissue culture, molecular biology (DNA), protein identification and ELISA techniques.

2.2 Vector Generation

The CLDND1-autofluorescent protein (AFP) vector was pre-made by Kerry Tyson (UCB Celltech). All vector information can be found in Table 7.

2.2.1 PCR amplification of DNA inserts

The human CLDND1 (UCB) fragment, stuffer fragment and immunoglobulin κ light chain fragment were pre-amplified and digested with HindIII and EcoRI restriction enzymes by Kerry Tyson (UCB Celltech). CLDND1 cDNA was purchased from abgene (MHS1010-58003). The CLDND1 (UCB) fragment and CLDND1 abgene sequences differ in their nucleotide composition.CLDND1 (UCB) was codon-optimised for mammalian expression (performed by Kerry Tyson, UCB Celltech) yet both translated proteins have the same protein sequence. All vectors generated from UCB Celltech (PIMMS2011, pQBI25-fN1, pVSV40E-ELF, pVSV40E-FerL, pVSV40E-hCMV and pKH10) utilised the CLDND1 (UCB) insert, whereas the remaining vectors contained the abgene CLDND1 sequence. Amplification of the CLDND1 abgene cDNA sequence was required to generate CLDND1-FLAG and CLDND1-H2K. CLDND1 (UCB) sequence amplification was required to generate human CLDND1 (UCB)-truncated, human CLDND1 (UCB)-GPI1 and human CLDND1 (UCB)-GPI2 sequences.

For CLDND1 abgene cDNA sequence amplification, the following 20 µL reaction mix was created, according to manufacturer instruction: 2 ng of CLDND1 cDNA, 0.1 U Phusion hot start II high-fidelity DNA polymerase (Thermo Scientific), 500 nM forward and reverse primers. The sample mix was subjected to the following cycle conditions in a PCR thermocycler: 98°C for 30 seconds; then 25 cycles of 98°C (10 seconds), 69-80°C (30 seconds) and 72°C (90 seconds), followed by a final extension time at 72°C for 5 minutes.

For human CLDND1 (UCB)-truncated, human CLDND1 (UCB)-GPI1 and human CLDND1 (UCB)-GPI2 sequence generation, 50 ng of human CLDND1 (UCB) sequence was used as a template and amplification was performed using 1 U Platinum® Taq DNA polymerase high fidelity (Thermo Scientific) with 400 nM forward and reverse primers in a 50 µL reaction mix according to manufacturer instruction. The samples were subjected to the following cycle conditions in a PCR thermocycler: 94°C for 60 seconds; then 40 cycles of 94°C

(30 seconds), 68-75°C (30 seconds) and 68°C (60 seconds), followed by a final extension time at 68°C for 5 minutes.

A 5 µL aliquot of each PCR reaction was run on a 1 % (w/v) tris-acetate-ethlenediamine tetraacetic acid (TAE) (tris-acetate 40 mM pH 8, 1 mM EDTA)-agarose gel, in loading buffer (0.125 M tris pH 6.8, 2 % (w/v) sodium dodecyl sulphate (SDS), 10 % (v/v) glycerol, 0.001 % bromophenol blue). Bands were visualised with 0.02 % ethidium bromide (SIGMA Aldrich) on a G:BOX Chemi system (Syngene, Cambridge, UK) to confirm construct sizes. The PCR products were then purified from the remaining sample using the QIAquick PCR purification kit (Qiagen, Crawley, UK), according to manufacturer instruction and eluted in 50 µL DNase and RNase free H_2O (SIGMA Aldrich)

2.2.2 Restriction digests

PCR products and vectors (5 µL) were digested with 10 U of the each restriction enzymes (see Table 7) (all Thermo Scientific) in a total volume of 20 µL. Vector digests were run on a 1 % TAE-agarose gel as described above to verify correct digestion. The digested vector was incubated with 1 U FastAP thermosensitive alkaline phosphatase (Thermo Scientific) at 37°C for 10 minutes to remove 5' phosphate groups in order to prevent vector ends from re-joining. The vectors were re-purified using commercially available kits (Qiagen) as described in Section 2.2.1.

2.2.3 Ligations and transformations

Ligations were performed using 1 U T4 DNA ligase (Thermo Scientific) with a 3:1 molar ratio of DNA to vector for at least 1 hour at room temperature (RT), according to manufacturer instruction. Following ligation, 3 µL of the reaction was transformed into 100 µL of JM109 cells (Promega, Madison, USA) or 30 µL of XL1-blue competent cells (Agilent, Wokingham, UK). Cells were incubated on ice for 10 minutes, or 20 minutes respectively. The cells were heat shocked for 45-50 seconds at 42°C before transferring to ice for 2 minutes. 900 µL LB medium or 125 µL of SOC medium (Life technologies) was added, respectively and cells were incubated at 37°C for 90 minutes. 100-150 µL of the cell mixture was plated onto a 30 µg/mL kanamycin (SIGMA Aldrich) or 50 µg/mL ampicillin (SIGMA Aldrich) 1.5 % LB-agar plates. The next day, several colonies were

selected and incubated, in 5 mL LB supplemented with 30 µg/mL kanamycin or 50 µg/mL ampicillin, at 37°C and 200 rpm overnight in an orbital shaker.

2.2.4 In-house minipreps

Following overnight culture, the bacteria were pelleted, resuspended in 100 µL P1 resuspension buffer, lysed with 200 µL P2 lysis buffer and neutralised with 150 µL P3 neutralisation buffer (all Qiagen). The DNA-containing supernatant was then precipitated in 1 mL 100 % (v/v) ethanol, vortexed and centrifuged at 13,000 x g for 10 minutes. The pellet was air dried and resuspended in 50 µL DNase and RNase free H_2O. A 5 µL aliquot was digested using the appropriate restriction enzymes, as described above and run on a 1 % 1xTAE-agarose gel to verify the plasmids had the correct inserts.

2.2.5 DNA sequencing

Vector sequences were confirmed by DNA sequencing performed either by Genome Enterprise Limited (commercial service, Norwich, UK) using Life Technologies 3730XL sequencers or by UCB Celltech. At UCB Celltech, DNA sequencing reactions were performed using the Big Dye® Terminator v3.1 cycle sequencing kit (Applied Biosystems, catalogue no. 4336921), by Kerry Tyson, UCB Celltech. The reactions were run on a 3130xL Genetic Analyzer automated sequencer (Applied Biosystems), and sequencing data were analysed using the Vector NTI Advance (Version 11) ContigExpress program (Life Technologies).

2.2.6 Qiagen maxi and giga preps

Following identification of correct vector inserts, DNA was transformed as described in Section 2.2.3. After an 8 hour culture in 5 mL LB medium, the culture was transferred to 250 mL LB medium supplemented with 30 µg/mL kanamycin or 50 µg/mL ampicillin and cultured at 200 rpm in an orbital shaker at 37°C overnight. Following overnight culture, the bacteria were pelleted and DNA was extracted using the endoFree plasmid maxi kit or the QIAfilter plasmid giga kit (both Qiagen), as per manufacturer's instruction. DNA concentration was determined using the NanoDrop ND-1000 spectrophotometer.

Vector alias	Vector	Inserted sequence	Primers to amplify inserted sequence	Digest sites	Promoter	Resistance gene	Protein encoded	Use
CLDND1 -trunc	PIMMS 2011	CLDND1 (UCB)-truncated	Fwd: 5' ACGAAGCTTGCCACCA	HindIII	hCMV-MIE	Kanamycin	CLDND1 (UCB)-truncated	Rab-9, primary CD4+ T-cell
			Rev: 5' CCCGAATTCTCATTCCT TCCGATTTGTATGGGCAGC	EcoRI				
CLDND1 -GPI1	PIMMS 2011	CLDND1 (UCB)-GPI1	Fwd: 5' ACGAAGCTTGCCA CCATGGACAACCGTTTTGCC	HindIII	hCMV-MIE	Kanamycin	CLDND1 (UCB)-GPI1	Rab-9, primary CD4+ T-cell
			Rev: 5' CCCGAATTCCTATATCA GAGCCACCCTGGCCAGCACTC CAATCGTGATGCCGACGGTGG CCACAGCTGAGAGGACCGGT GCACTTCCAGATTCTCCGGAA ACATTGTCAGGGAG	EcoRI				
CLDND1 -GPI2	PIMMS 2011	CLDND1 (UCB)-GPI2	Fwd: 5' ACGAAGCTTGCCACC ATGGACAACCGTTTTGCC	HindIII	hCMV-MIE	Kanamycin	CLDND1 (UCB)-GPI2	Rab-9, primary CD4+ T-cell
			Rev: 5' CCCGAATTCCTATATCA GAGCCACCCTGGCCAGCACTC CAATCGTGATGCCGACGGTGG CCACAGCTGAGAGGACCGGT GCACTTCCAGATTGGCATCTC CAAAGATATGTGCG	EcoRI				

Vector alias	Vector	Inserted sequence	Primers to amplify inserted sequence	Digest sites	Promoter	Resistance gene	Protein encoded	Use
CLDND1-FLAG	modified pcDNA4/myc-His B	CLDND1-FLAG	Fwd: 5' TGCAAGATCTCACCATGGATAACCGTTTTG	BglII	CMV	Ampicillin	CLDND1	FreeStyle293-F, SW1353
			Rev: 5' TACGCTGCAGATGCCACACGATATGCCT	PstI				
CLDND1-AFP	pQBI 25-fN1	CLDND1 (UCB)-AFP	UCB Celltech made	HindIII	CMV	Ampicillin	CLDND1 (UCB)-AFP	SW1353, Jurkat
				NheI				
CLDND1-PIMMS	PIMMS 2011	CLDND1 (UCB)	UCB Celltech made	HindIII	hCMV-MIE	Kanamycin	CLDND1 (UCB)	Rab-9, primary CD4+ T-cell
				EcoRI				
CLDND1-Elf	pV SV40E-ELF	CLDND1 (UCB)	UCB Celltech made	HindIII	SV40E-ELF	Kanamycin	CLDND1 (UCB)	Rab-9, primary CD4+ T-cell
				EcoRI				
CLDND1-FerL	pV SV40E-FerL	CLDND1 (UCB)	UCB Celltech made	HindIII	SV40E-FerL	Kanamycin	CLDND1 (UCB)	Rab-9, primary CD4+ T-cell
				EcoRI				
CLDND1-HCMV	pV SV40E-hCMV	CLDND1 (UCB)	UCB Celltech made	HindIII	SV40E-hCMV	Kanamycin	CLDND1 (UCB)	Rab-9, primary CD4+ T-cell
				EcoRI				

Vector alias	Vector	Inserted sequence	Primers to amplify inserted sequence	Digest sites	Promoter	Resistance gene	Protein encoded	Use
PIMMS-non-coding	PIMMS 2011	Stuffer fragment	UCB Celltech made	HindIII / EcoRI	hCMV-MIE	Kanamycin	Stuffer fragment	Primary CD4+ T-cell
PIMMS-coding	PIMMS 2011	Immunoglobulin κ light chain	UCB Celltech made	HindIII / EcoRI	hCMV-MIE	Kanamycin	Immunoglobulin κ light chain	Primary CD4+ T-cell
CLDND1-Screen	pKH10	Human CLDND1 (UCB)	UCB Celltech made	HindIII / EcoRI	hCMV-MIE	Kanamycin	CLDND1 (UCB)	FreeStyle293-F
CLDND1-H2K	pIRES2-H2K^{k} (1)	Human CLDND1 (H2K)	Fwd: 5' CGCAGCTAGCATGGA TAACCGTTTTGC / Rev: 5' TGCAGGATCCTCATGC CACACGATAT	NheI / BamHI	CMV	Kanamycin	CLDND1	Primary CD4+ T-cell

Table 7. DNA vectors

Throughout the thesis, vectors are referred to by the 'Vector alias'. The vector backbone and inserted sequences are detailed for each vector, along with the primer sequences required for inserted sequence amplification, where required. Restriction digest sites are listed along with the type of promoter present within the vector backbone and antibiotic resistance gene. The CLDND1 protein sequence translated from each vector is also described, along with the technique each vector was used for. (1) vector information (Tahvanainen et al., 2006).

2.3 Antibody Generation

2.3.1 Peptide generation

The peptide generation work was performed by Terry Baker, UCB Celltech. Human (NP_001035289.1) and mouse (NP_741968.1) CLDND1 protein sequences were aligned to the PMP-22/EMP/MP20/claudin superfamily members and regions of exclusivity in the extracellular loops of the mouse and human CLDND1 homologues were identified. Four peptides were generated from these exclusive regions, utilising the most immunogenic amino acids in the available sequences (Table 8). Peptides were made cyclic and attached to one of three hapten carriers: keyhole limpet hemocyanin (KLH), ovalbumin (OVA) or human serum albumin (HSA), through a maleimide structure.

Peptide number	Loop position	Peptide sequence	Immunisation number
CLE11	1st	cyclo[cys*KSIWDEFISDEADEKTY]	2675, 2676
CLE12	1st	cyclo[cys*ITIPKNMHWYSPPER]	2677, 2678
CLE13	1st	cyclo[cys*VSFTLTEQFMEK]	2679, 2680
CLE21	2nd	cyclo[cys*[ELLHQKLELPDNVSG]	2681, 2682

Table 8. Immunisation peptides

Name of peptide, along with extracellular loop position, sequence and immunisation number are shown. Cyclo[cys] indicates where the peptides were made cyclic and linked to the haptens, through the maleimide structure of the cysteine residue.

2.3.2 Immunisation strategy

The immunisation group at UCB Celltech performed the immunisations. Five immunisations were performed at 3 week intervals alternating the peptide-conjugate as follows; KLH, OVA, HSA, KLH, then OVA, using 100 µg antigen per immunisation in HsdIF:NZW rabbits along with Imject Freund's complete (FCA) or Freund's imcomplete (FIA) adjuvant. Immunisations were performed subcutaneously. 10 mL bleeds were taken prior to the first immunisation and at

subsequent immunisations. Prior to immunisation, a preserum bleed was performed, for use as a negative control. At the end of the immunisation protocol, blood was drawn for antibody assessment and spleen and bone marrow cells were collected and stored at -80°C. Serum was prepared from the blood. An aliquot of serum was taken for antibody validation and the remaining serum was stored at -80°C.

2.3.3 Antibody purification

Antisera was centrifuged at 4000 x g for 10 minutes and filtered through a Whatman 0.22 µm bottle-top filter (GE Healthcare, Chalfont St Giles, UK). The serum was passed over a NHS-activated column (GE healthcare) loaded with streptavidin (SA) containing the biotinylated peptide: CTLESIMNTLESEEDFRYKY (Terry Baker, UCB Celltech) to remove any non-specific antisera binding. 400 µL of 10 mM CLE11, the immunisation peptide, was added to 2676 antiserum and incubated overnight at 4°C.

2.3.4 Affinity purification column generation

130 mg SA (Terry Baker, UCB Celltech) was dissolved in 0.2 M $NaCHO_3$ and purified using a disposable PD-10 column (GE healthcare), to remove low molecular weight contaminants. The NHS-activated HP 5 mL column (GE healthcare) was activated with 1 mM HCl according to manufacturer instruction, loaded with SA (NHS load) and re-circulated for 30 minutes. Unbound SA was eluted (NHS eluate) with 0.2 M $NaHCO_3$. The SA coupling efficiency was measured as follows, according to manufacturer instruction:

$$Coupling\ Yield\ (\%) = \frac{A - B}{A} * 100$$

where: $A = Absorbance@280nm\ of\ NHS\ load * NHS\ load\ volume$

$$B = \frac{Absorbance@280nm\ of\ NHS\ eluate * NHS\ load * NHS\ eluate\ volume}{starting\ volume\ of\ streptavidin}$$

and was calculated at 95.4 %. The SA-NHS column was de-activated according to manufacturer instruction and a mock elution performed, using 0.1 M glycine/HCl pH 2.7, 20 % glycerol, followed by 0.58 % acetic acid then PBS.

2.3.5 Affinity purification

The 2676 antiserum containing biotinylated CLE11 was loaded onto the SA-NHS-CLE11 column, and washed in PBS. The bound antibodies were eluted in 5 mL fractions using 0.1 M glycine/HCl pH 2.7, 20 % glycerol into a bijoux containing 0.5 mL 1 M tris pH 8, 0.5 M NaCl, to neutralise the acidity of the eluate. Absorbance at 280 nm was measured for each fraction. The purification process was repeated for 2675 antiserum. 2675 and 2676 antisera were chosen for purification due to their most convincing α-CLDND1 binding data.

2.3.6 Antibody concentration and buffer exchange

Fractions from the affinity purification containing functional antibody were pooled and concentrated using an Ultra-15 centrifugal filter unit with ultracel-30 membrane (Merck Millipore, MA, USA) and buffer exchanged into PBS. Absorbance was measured at 280 nm and protein concentration was determined. Concentrated antibody was aliquoted into 1 mg/mL fractions and stored at -20°C.

2.4 Cell Line Culture

2.4.1 SW1353 cells

The SW1353 cell line was initiated from a primary grade II chondrosarcoma in the right humerus of a 72 year old Caucasian female. Full details of the cell line can be found at the ATCC company website (www.atcc.org). Cells were purchased from ATCC (catalogue HTB-94). The cell line was cultured in SW1353 culture medium (DMEM, high glucose, 2 mM L-glutamine, 100 U/mL penicillin, 1 µg/mL streptomycin, 10 % FBS). Cells were plated into vented T75 cm^2 flasks, grown at 37°C in 5 % (v/v) CO_2/humidified air until approximately 80 % confluent. Cells were detached with trypsin and split into the appropriate culture vessel for experimentation or into further T75 cm^2 flasks for continuation of the line every 2-3 days. Experiments were performed on cells between passage 3 and 25.

2.4.2 FreeStyle™ 293-F cells

Cells were grown and maintained by Ashley Hudson, UCB Celltech. The FreeStyle™ 293-F cell line (Life Technologies) is derived from the 293 cell line and is adapted for suspension culture. The cells were maintained in Gibco® FreeStyle™ 293 expression medium (Life Technologies) and passaged at 1-2x10^5 cells/mL every 3-4 days at 37°C in 5 % (v/v) CO_2/humidified air. Cells were maintained in suspension by culturing cells with shaking and used until passage 30.

2.4.3 E6-1 Jurkat cells

The Jurkat cell line was established in the late 1970s from the peripheral blood of a 14 year old boy with T-cell leukemia. The E6-1 Jurkat cells are a clone of the Jurkat-FHCRC cell line, a derivative of the Jurkat cell line. Full details of the cell line can be found at the ATCC company website (www.atcc.org). Cells were purchased from ATCC (catalogue TIB-152). The cell line was cultured in vented T75 cm^2 flasks, grown at 37°C in 5 % (v/v) CO_2/humidified air in RF-10. Cells were passaged into the appropriate culture vessel for experimentation or into further T75 cm^2 flasks for continuation of the line every 2-3 days.

2.4.4 Rab-9 cells

Cell maintenance was performed by Sophie Shaw, UCB Celltech. The Rab-9 cell line is a rabbit fibroblast cell line from an adult female *Oryctolagus cuniculus*. Full details of the cell line can be found at the ATCC company website (www.atcc.org). Cells were purchased from ATCC (catalogue CRL-1414). Cells were cultured in Rab-9 culture medium (RPMI-1640 medium + 10 % FBS + 1 mM glutamine +100 µg/mL normacin (InvivoGen)) and passaged when confluency was reached. Cells were harvested with Accutase® (PAA Laboratories Ltd, Yevil, UK) and passaged to continue the stock.

2.5 Cell Line Transfections

2.5.1 SW1353 cell transfections

For chamberslide transfections for immunofluorescence, SW1353 were harvested, as described in Section 2.4.1 and resuspended to $5x10^4$/mL in DMEM. $1.5x10^4$ cells were added per well of a chamberslide and cultured overnight at 37°C in 5 % (v/v) CO_2/humidified air prior to transfection with Fugene® HD (Promega) or ExGen 500 *in vitro* (Thermo Scientific) transfection reagents, in order to determine the transfection reagent with the highest transfection efficiency.

FuGENE® HD transfection reagent: vector DNA was added to 11 µL of DMEM, to which FuGENE® HD transfection reagent was added, at differing ratios (Figure 10A). The mixture was vortexed and incubated at RT for 20 minutes then added to the cells. Cells were incubated for 24 hours at 37°C in 5 % (v/v) CO_2/humidified air. The ExGen 500 *in vitro* transfection reagent resulted in higher transfection than the FuGENE® HD transfection reagent, so no optimal conditions were chosen for this transfection reagent.

ExGen 500 *in vitro* transfection reagent: the volume of vector DNA was increased to 33 µL in 150 mM NaCl, to which varying concentrations of ExGen 500 *in vitro* transfection reagent was added (Figure 10B). The mixture was incubated at RT for 10 minutes before removing the SW1353 culture medium and adding 33 µL of the DNA/ExGen 500 *in vitro* transfection reagent mixture per chamberslide well. 300 µL of SW1353 culture medium was added to the cells and the chamberslide was incubated at 37°C in 5 % (v/v) CO_2/humidified air for 24 hours. From the optimisations, 0.5 µg vector DNA with a 1:3.8 ratio of ExGen 500 *in vitro* transfection reagent was chosen as this conditions resulted in the highest transfection efficiency, observed visually by AFP fluorescence.

To generate cell lysates for Western blotting, the ExGen 500 *in vitro* transfection reagent transfection method was used with the following modifications: SW1353 cells were resuspended to $1.15x10^5$/mL in SW1353 culture medium and added to a 6-well plate at a final density of $3.5x10^5$ cells/well. 2 µg vector DNA and 13 µL of ExGen 500 *in vitro* transfection reagent was used in 300 µL of 150 mM NaCl. 300 µL of the mixture was added to the cells and 3 mL SW1353 culture medium was added.

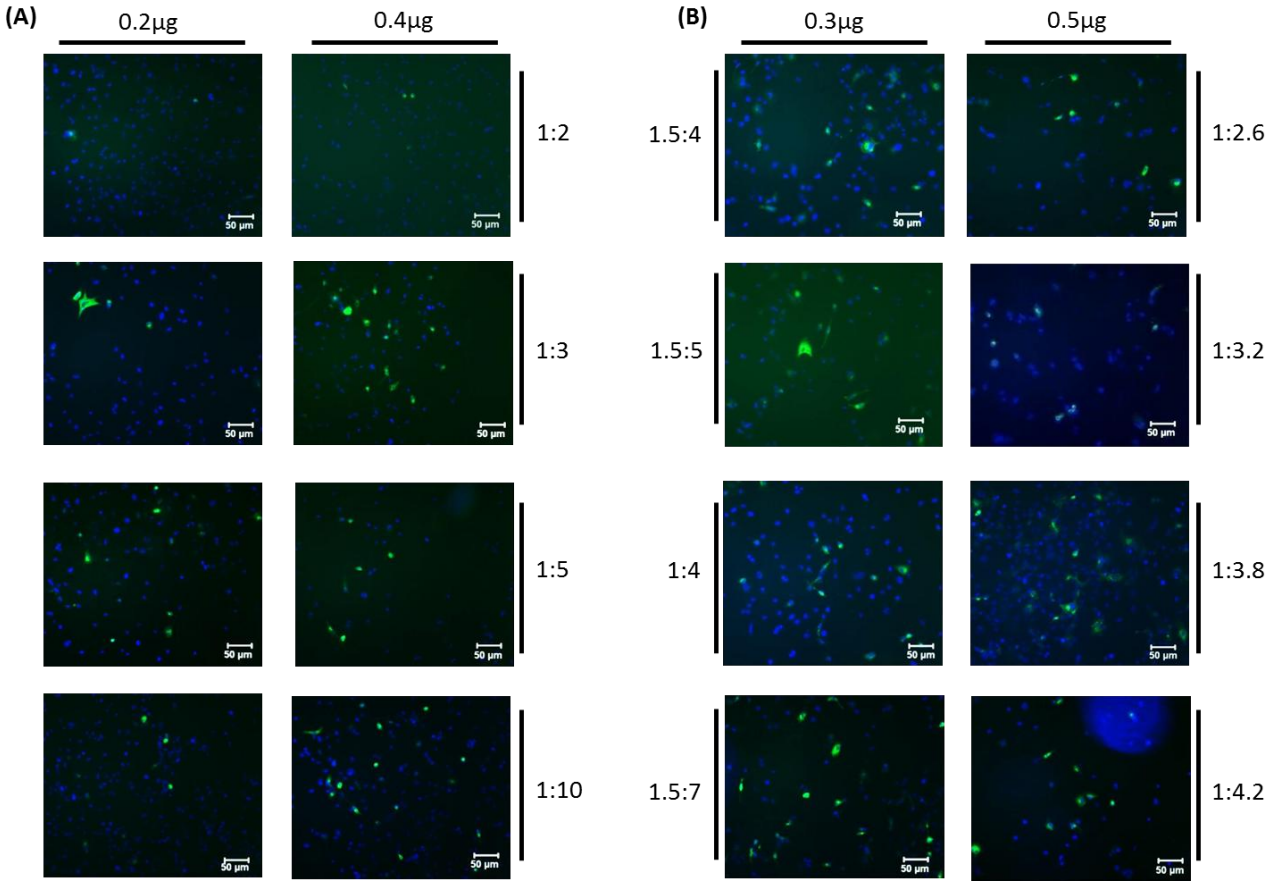

Figure 10. SW1353 transfection optimisations: CLDND1-AFP

SW1353 cells were transfected with the CLDND1-AFP vector using transfection reagents: (A) FuGENE® HD transfection reagent or (B) ExGen 500 *in vitro* transfection reagent. The µg values represent the amount of DNA used and the ratios represent DNA quantity to transfection reagent ratios. Transfection efficiencies were visualised by the amount of AFP fluorescence detected. Nuclear staining was performed with DAPI and is illustrated by the blue fluorescence.

2.5.2 FreeStyle™ 293-F cell transfections

FreeStyle™ 293-F cells were harvested and washed in PBS. Cells were resuspended to a density of $1x10^6$/mL in NM6 medium (SIGMA Aldrich) and 5 mL was added per well of a 6-well plate. 5 µg of vector DNA was diluted into 170 µL of Opti-PRO medium (Life Technologies) in polycarbonate tubes. 10 µL of 293fectin (Life Technologies) was diluted into 170 µL of Opti-PRO medium in polycarbonate tubes and incubated for up to 5 minutes. The DNA and 293fectin mixtures were combined and incubated for 20 minutes at RT before adding to the FreeStyle™ 293-F cells. Cells were incubated with shaking at 37°C in 5 % (v/v) CO_2/humidified air for 24 hours.

2.5.3 E6-1 Jurkat cell transfections

E6-1 Jurkat cells were nucleofected using the Neon® transfection system (Life Technologies). Initially, optimisations were performed (Table 9), varying the nucleofection parameters. Based on cell viability and transfection efficiency, the following parameters were chosen for subsequent experiments: 1600 V pulse voltage, 10 pulse width, 3 pulse number (Table 9A). The transfection protocol was optimised further by varying the number of cells transfected and the amount of CLDND1-AFP vector used (Table 9B).

(A)

Voltage	Width	Number	Efficiency (%)	Viability (%)
1400	20	1	2.95	84
1600	20	1	13.9	72
1100	30	1	0.77	91.97
1300	30	1	5.69	86
1000	40	1	0.88	93
1200	40	1	7	85
1200	20	2	3	87
1400	20	2	19.5	76
950	30	2	0.81	93
1150	30	2	7.58	81
1400	10	3	6.39	86
1600	10	3	23.5	81

(B)

Cell Number	Vector DNA (µg)	Efficiency (%)	Viability (%)
1x10^5	0.5	35	71
1x10^5	1	48.6	69.5
1x10^5	1.5	42.2	56.7
1x10^5	3	27.6	34.39
2x10^5	0.5	27.4	67.2
2x10^5	1	44.3	68.5
2x10^5	1.5	49.2	66.7
2x10^5	3	31.7	39.15

Table 9. Jurkat transfection optimisations

Jurkat cells were transfected with the CLDND1-AFP vector and cultured for 18 hours before determining transfection efficiency and cell viability by flow cytometry. Transfection efficiency was determined by AFP fluorescence and viable cell numbers were obtained from cells staining negative for Via-Probe™. (A) Nucleofection pulse parameters were varied, using 0.5 µg DNA and 1x10^5 cells. (B) Using the nucleofection parameters: 1600 V, pulse width 10 and pulse number 3, cell number and amount of DNA was varied.

For all subsequent transfections, 2x10^5 cells and 1 µg of CLDND1-AFP vector was used using the transfection method below:

Two days prior to electroporation, Jurkats were harvested and passaged at 1:20 dilution in RF-10. On the day of transfection, 500 µL of RF-10 was pre-equilibrated in a 24-well plate at 37°C in 5 % (v/v) CO_2/humidified air. Cells were harvested, centrifuged at 400 x g and washed in PBS. Cells were resuspended in resuspension buffer R at a final density of 1x10^7/mL. The Neon® transfection system was set-up to manufacturer instruction. Briefly, 3 mL electrolytic buffer E was added to the Neon™ pipette station and the nucleofection conditions were entered. 1 µg of CLDND1-AFP vector was transferred to a sterile 1.5 mL microcentrifuge tube and the cells were added and gently mixed. The cell/DNA mix was taken into the nucleofection pipette and the nucleofection was carried out. Post nucleofection, the pipette was emptied into the 24-well plate and the plate was gently rocked to assure even

distribution of the cells. The plate was incubated at 37°C in 5 % (v/v) CO_2/humidified air, for 24 hours.

$H2K^k$ transfected Jurkats were purified against the $H2K^k$ tag using MACSelect K^k microbeads (Miltenyi Biotech), according to manufacturer instruction. Prior to selection, dead cells were removed using the dead cell removal kit (Miltenyi Biotech), to prevent dead cells from binding the K^k microbeads. Dead cell removal was performed according to manufacturer instruction. Briefly, $1x10^7$ cells were resuspended in 100 µL of dead cell removal microbeads, mixed and incubated for 15 minutes at RT. An MS column was placed in the MACS separator and prepared by rinsing with binding buffer (Miltenyi Biotech). The sample was added to the column and effluent was collected as live cells. For dead cell fraction analysis, the column was removed from the MACs separator and dead cells were eluted in binding buffer.

The effluent was prepared for MACSelect K^k microbead selection, according to manufacturer instruction. Cells were resuspended in 320 µL of buffer PBE (PBS pH 7.2 supplemented with 0.5 % BSA, 5 mM EDTA) per $1x10^7$ cells, to which 80 µL of MACSelect K^k microbeads were added and incubated at 4°C for 15 minutes. The volume was adjusted to 2 mL in buffer PBE. An MS column was prepared by placing in a MACS separator and rinsed with 500 µL of buffer PBE. The cell suspension was applied to the column and unlabelled cells were collected in the effluent. The column was washed 3 x 500 µL in buffer PBE before the column was removed from the MACS separator and positively selected cells were eluted in 1 mL if buffer PBE. Cells were analysed for viability with Via-Probe™ (BD Bioscience) and $H2K^k$ positivity using mouse anti- $H2K^k$-phycoerythrin and MACSelect control FITC antibody (both Miltenyi Biotech), as the MACSelect K^k microbeads bind to the same epitope as the mouse anti-$H2K^k$-phycoerythrin and so could have masked binding.

2.5.4 Rab-9 cell transfections

Cells were harvested according to Section 2.4.4, upon confluency. The cells were washed with PBS by centrifugation at 400 x g. Cells were resuspended at $5x10^7$/mL in Earles solution (SIGMA Aldrich). 250 µg DNA at 1 mg/mL was added to 600 µL of cells and the cells were electroporated with a using the conditions 8.4 A, 20 ms in an in-house electroporator (UCB Celltech). Cells

were transferred to warm Rab-9 culture medium and cultured for 24 hours at 37°C in 5 % (v/v) CO_2/humidified air.

2.6 Primary Cell Culture

2.6.1 Ethics

All research was performed under favourable ethical opinion for the Newcastle autoimmune inflammatory rheumatic diseases research biobank (NAIRD) and healthy controls and RA patients gave informed consent. The study has been reviewed by the South West 3 Research Ethics committee and by the Newcastle upon Tyne Hospitals NHS Foundation Trust Research and Development Department.

2.6.2 Blood collection and culture

Peripheral blood was collected into spray-coated K_2EDTA or sodium heparin vacutainers (BD Bioscience). Peripheral blood was cultured in 24 well plates, with 1 mL blood per well. Where dilutions were required, RPMI-1640 was used.

2.6.3 Buffy cone collection

Buffy cones were bought from the national blood bank. Cells were removed from the cone using Hanks balanced salt solution (HBSS) supplemented with 2 mM EDTA to a final volume of 50 mL.

2.6.4 Peripheral blood mononuclear cell isolation

Peripheral blood or processed buffy cone was diluted 1:1 with HBSS supplemented with 2 mM EDTA and layered onto Lymphoprep™ according to manufacturer's instruction. Blood was centrifuged at 895 x g for 30 minutes at RT with no brake. Peripheral blood mononuclear cells (PBMC) were collected from the sample/medium interface. Two wash steps were performed with HBSS supplemented with 1 % FBS: 600 x g for 7 minutes at 4°C then 250 x g for 7 minutes at 4°C to remove platelets. Cells were counted using a Burker haemocytometer.

2.6.5 CD4 T-cell isolation: positive selection

The EasySep™ human whole blood CD4 positive selection kit (StemCell Technologies, Grenoble, France) and human CD4 microbeads (Miltenyi Biotech) specifically target the CD4 protein. CD4 is a 55 kDa cell surface protein highly expressed on T-cells, with lower expression on monocytes and dendritic cells. On T helper cells, CD4 acts as an accessory molecule for the recognition of MHC class II/peptide complexes by the TCR. Both systems utilise α-CD4 antibody and magnetic bead complexes which allow for labelled cells to be isolated through magnetic separation. The EasySep™ human whole blood CD4 positive selection kit uses a tube held within a magnet to maintain the positively selected cells whereas the human CD4 microbeads utilise a column held within a magnet to positively select for cells.

EasySep™ human whole blood CD4 positive selection: peripheral blood was incubated with a 1/40 dilution of RosetteSep™ human monocyte depletion cocktail (StemCell Technologies) for 15 minutes at RT. This product couples CD36 expressing monocytes to red blood cells resulting in large aggregate formations. Blood was then inverted with 1/5 dilution of Hetasep™ solution (StemCell Technologies), a density centrifugation medium, prior to centrifugation at 50 x g for 5 minutes at RT. The blood was incubated at RT for 10 minutes, to allow for the red blood cell/monocyte aggregates to settle. CD36 expressing monocytes would therefore be eliminated prior to CD4 positive selection to reduce monocyte contamination in the purified fraction. The upper fraction was collected and washed in HBSS supplemented with 1 % FBS. Cells were resuspended with HBSS supplemented with 1 % FBS to 1/5 of the total volume of whole blood. CD4 expressing T-cells were isolated automatically with the RoboSep (StemCell Technologies) using the EasySep™ human whole blood CD4 positive selection kit. Purified cells were resuspended to $1x10^6$ cells/mL in X-vivo-15 medium (Xv15) (Lonza) unless otherwise specified.

Human CD4 microbead positive selection: CD4 positive selection was carried out using human CD4 microbeads (Miltenyi Biotec) according to manufacturer instructions. Briefly, PBMC (see Section 2.6.4 for isolation method) were resuspended in 80 µL of MACS buffer (PBS pH 7.2, 0.5 % BSA, 2 mM EDTA) and 20 µL of human CD4 microbeads per $1x10^7$ cells and refrigerated for 15 minutes. Cells were washed in MACS buffer then resuspended in 2 mL MACS

buffer. The MS column (Miltenyi Biotech) was prepared by placing it in the magnetic field of a MACS separator (Miltenyi Biotech) and by rinsing with 500 µL of MACS buffer. The cell suspension was applied onto the column and unlabelled cells were eluted. The column was washed prior to removing the column from the MACS separator and eluting the CD4 labelled cells in 1 mL of MACS buffer. Positively selected cells were washed and resuspended in the appropriate culture medium.

2.6.6 CD4 T-cell isolation: enrichment

RosetteSep™ human CD4+ T-cell enrichment involves the depletion of other cell types than CD4 expressing cells through antibody targeted depletion of the surface antigens CD8, CD16, CD19, CD36, CD56, CD66b and TCRγδ. The antibodies crosslink these surface antigens to red blood cells through glycophorin A, resulting in immunorosette aggregates. These rosette cells have a greater density and so pellet faster than unrosetted cells when centrifuged over a buoyant density medium.

Non-CD4 expressing cells were depleted from whole blood or buffy cone using the RosetteSep™ human CD4+ T-cell enrichment cocktail (StemCell Technologies) using 50 µL or 75 µL per mL of blood or cone, respectively. Cells were incubated for 20 minutes at RT before diluting in PBS supplemented with 2 % FBS at a 1:1 ratio. 20 mL of diluted cells were layered onto 15 mL of Lymphoprep™ (Axis-Shield, Dundee, Scotland), a density centrifugation medium, according to manufacturer's instruction and centrifuged at 895 x g for 30 minutes at RT with no brake. Cells were collected from the sample/medium interface and washed twice in PBS supplemented with 2 % FBS prior to use.

2.6.7 Monocyte isolation

PBMC were isolated from processed buffy cone according to Section 2.6.4. Monocytes were isolated using human CD14 microbeads (Miltenyi Biotech), according to revised manufacturer's instruction. Briefly, cells were resuspended in 80 µL MACS buffer and 10 µL CD14 microbeads per $10x10^6$ cells. Cells were incubated at 4°C for 15 minutes. Cells were washed and resuspended in 2 mL ice cold MACS buffer. The LS column (Miltenyi Biotech) was placed in the MACs separator and pre-rinsed with 3 mL ice-cold MACs buffer before the PBMC were added. LS column was washed 3 times with ice-cold MACs buffer.

The effluent fraction contained unlabelled cells. The LS column was removed from the magnet and the positively selected cells were flushed from the column with 5 mL of ice-cold MACS buffer. Cells were washed and resuspended in cold culture medium.

2.6.8 nTreg isolation

CD4+ T-cells were isolated according to Section 2.6.6. CD4+CD25^{high} T-cells were isolated using human CD25 microbeads II (Miltenyi Biotech) according to revised manufacturer instruction. Briefly CD4+ T-cells were resuspended in 98 µL MACS Buffer per 1x10^{7} cells in with 2 µL of CD25 microbeads II, in order to obtain only the highest CD25 expressing cells, and refrigerated for 15 minutes. Volumes were scaled up as required. Cells were washed and resuspended in 500 µL MACS buffer. The LS column was prepared by placing it in the magnetic field of a MACS separator and rinsing with 3 mL of MACS buffer. The cell suspension was applied onto the column and unlabelled cells were eluted and stored as effector T-cells (Teff). The column was washed prior to removing the column from the MACS separator and eluting the CD4+CD25^{high} expressing cells in 5 mL of MACS buffer. Purity was determined by flow cytometry using CD3-FITC, CD4-PerCP, CD25-PE (all BD Bioscience) and Foxp3-AF647 (BioLegend, San Diego, USA).

2.6.9 Platelet rich and platelet poor plasma preparation

K_2EDTA sprayed vacutainers containing peripheral blood were centrifuged at 2000 x g or 200 x g for 10 minutes at RT. The upper layer was collected as platelet poor (PPP) or platelet rich plasma (PRP), respectively. Where dilutions were required, RPMI-1640 was used.

2.6.10 Serum preparations

Peripheral blood was drawn into serum vacutainers (BD Bioscience) and incubated for 30 minutes to allow the blood to clot. Vacutainers were centrifuged at 1500 x g for 15 minutes and upper layer was collected as serum. Where dilutions were required, RPMI-1640 was used.

2.6.11 Monocyte differentiation

Monocytes were differentiated into DC using a 7 day differentiation protocol (Anderson et al., 2008). Monocytes were isolated and cultured according to

Section 2.6.7. Cells were seeded at $0.5x10^6$ /mL in RF-10. IL-4 and GM-CSF were added at a final concentration of 50 ng/mL and cultured at 37°C in 5 % (v/v) CO_2/humidified air. At day 3, the culture medium was refreshed by removing 450 µL medium and replacing with a 500 µL mastermix containing RF-10 supplemented with 50 ng/mL final concentrations of IL-4 and GM-CSF for mature DC (matDC) and IL-4, GM-CSF and 10^{-6} M dexamethasone for tolDC. At day 6, LPS at a 0.1 µg/mL final concentration was added to each well for matDC and a 0.1 µg/mL final concentration of LPS, 10^{-6} M dexamethasone and 10^{-10} M calcitriol were added for tolDC. At day 7, cells were incubated on ice for 1 hour prior to harvesting by pipetting and scraping the well with a pipette tip. Cell were washed extensively in HBSS + 1 % FBS prior to use. A recovery rate of 20-40 % was expected.

2.6.12 Cell cryopreservation and thawing of cryopreserved cells

Freezing: surplus cells were resuspended in 1 mL in FBS containing 10 % DMSO at $2x10^7$ cells for T-cells or $1x10^6$ for DC and transferred to cryovials. Cells were frozen at -80°C in polystyrene boxes then transferred to liquid nitrogen for longer term storage.

Thawing: cells were removed from liquid nitrogen and gases were allowed to equilibrate by incubating the vial on ice for 5 minutes. Vials were thawed at 37°C and immediately transferred to warm cell culture medium. Cells were washed twice in cell culture medium before counting in a 0.2 % trypan blue solution (final concentration) (SIGMA Aldrich) to assess cell viability.

2.7 Primary Cell Transfections

2.7.1 Accell siRNA original protocol

CD4+ T-cells were isolated according to Section 2.6.5 “EasySep™ human whole blood CD4 positive selection” and rested overnight at $1x10^6$/mL in Xv15 at 37°C in 5 % (v/v) CO_2/humidified air. Cells were harvested in PBS and plated at $1x10^5$ per well of a 96 well plate, to which a 1 µM final concentration of Accell siRNA (Table 10) was added. Cells were incubated for 72 hours at 37°C in 5 % (v/v) CO_2/humidified air.

siRNA alias	Reference	Sequence
NT1	D-001910-01	UGGUUUACAUGUCGACUAA
NT2	D-001910-02	UGGUUUACAUGUUUUCUGA
NT3	D-001910-03	UGGUUUACAUGUUUUCCUA
NT4	D-001910-04	UGGUUUACAUGUUGUGUGA
C1	A-020682-13	UUGUUAUGUUGCUGGAAUU
C2	A-020682-14	CCGGUGAAUUUGGAUGGUC
C3	A-020682-15	CUGGUGUGUAUCAACAUUA
C4	A-020682-16	CCAGGGTTATTAAAAGTGT
CD4SMARTpool	E-005234-00	UCCUUUUCCUUCAAGCCUA
		CCUUUGACCUGAAGAACAA
		GGAGGAGGUGCAAUUGCUA
		CCCCUGAGCUGAAAUAAAA

Table 10. Accell siRNA

Accell siRNA are referred to by the “siRNA Alias” throughout the thesis.

2.7.2 Accell siRNA literature recommended protocol (72hrsiBead)

CD4+ T-cells were isolated according to Section 2.6.5 “EasySep™ human whole blood CD4 positive selection”. nTreg were isolated according to Section 2.6.8. Isolated cells were rested overnight at $1x10^6$/mL in Xv15 at 37°C in 5 % (v/v) CO_2/humidified air. Cells were harvested in PBS and plated in a 96-well flat bottom plate at $1x10^5$ cells/well. α-CD3/CD28 expander beads (Life Technologies) were added to the cells at a 1:10 ratio, to make a final volume of 100 µL. Accell siRNA was also added to give a final concentration of 1 µM per well. Cells were incubated for 72 hours at 37°C in 5 % (v/v) CO_2/humidified air. As minimal differences were seen in cell viability between the NT siRNA samples, for proliferation assays, a selection of NT siRNA was chosen.

Cells were then either taken for ^{3}HTdR incorporation (see Section 2.8.5), or harvested for RNA extraction, protein analysis or for further culture. For further culture, cells were harvested in PBS and α-CD3/CD28 expander beads were removed using a magnet. Cells were cultured at $1x10^6$/mL in Xv15 to rest for 72

hours. Cells were harvested and $1x10^5$ cells were added per well of a 96-well plate in Xv15. A 1:10 ratio of α-CD3/CD28 expander beads were added to the cells to create a final volume of 100 µL per well. Cells were cultured for 72 hours at 37°C in 5 % (v/v) CO_2/humidified air.

2.7.3 T-cell nucleofection: Amaxa

CD4+ T-cells were isolated according to Section 2.6.6 from buffy cone. Cells were resuspended to $47.6x10^6$/mL in RPMI-1640 medium. Master mixes were prepared containing 5 µg vector DNA and $5x10^6$ CD4+ T-cells per condition. Cells were nucleofected using program U-14 on the Amaxa Nucleofector™ II Device (Lonza). Cells were immediately transferred to pre-equilibrated Amaxa culture medium (RPMI-1640 medium, 4 mM L-glutamine, 10 % FBS). Cells were cultured for 18 hours at 37°C in 5 % (v/v) CO_2/humidified air.

Cells were harvested and washed in PBS + 2 % FBS. Cells were resuspended in HBSS supplemented with 1 % FBS and layered over an equal volume of Lymphoprep™. Cells were centrifuged at 895 x g for 30 minutes RT in order to remove dead cells. Cells were washed twice with PBS + 2 % FBS. Cells were resuspended to $2x10^6$/mL in RF-10 for T-cell activation studies.

2.8 Cellular Assays

2.8.1 T-cell stimulation

For isolated CD4+ T-cell proliferation assays, a 1:10 ratio of stimulus to T-cells was used. Stimuli were matDC, tolDC or α-CD3/CD28 expander beads. CD4+ T-cell numbers varied depending on the type of assay:

For CLDND1 over-expression studies, $2x10^5$ transfected CD4+ T-cells were cultured in a flat bottom 96-well plate in RF-10 at 37°C in 5 % (v/v) CO_2/humidified air for 3 or 6 days. For re-stimulations, $5x10^4$ transfected CD4+ T-cells were cultured in a flat bottom 96-well plate in RF-10 at 37°C in 5 % (v/v) CO_2/humidified air for 3 days.

For CLDND1 kinetics experiments, $1x10^6$ enriched CD4+ T-cells were cultured in a 24-well flat bottom plate in Xv15 or with RF-10 for the DC co-culture experiments, in a final volume of 1 mL. Where PBMC were used, $1x10^6$ PBMC were cultured in 1 mL RF-10 in a 24-well plate with a final concentration of 1 µg/mL LEAF purified anti-human CD3 (BioLegend) and 1 µg/mL of LEAF

purified anti-human CD28 (BioLegend). Cells were cultured at 37°C in 5 % (v/v) CO_2/humidified air for the time-points specified.

2.8.2 Anergy induction

CD4+ T-cells were isolated according to Section 2.6.6. The *in vitro* anergy protocol attempted was based upon similar experiments performed (Safford et al., 2005). A 24-well tissue culture plate was coated with 1 µg/mL LEAF purified anti-human CD3 in PBS and incubated for 1 hour at 37°C. Solution was removed from each well, to which $1x10^6$ CD4+ T-cells were added with 1 µg/mL LEAF purified anti-human CD28 in RF-10 medium. Cells were incubated overnight at 37°C in 5 % (v/v) CO_2/humidified air. Cells were harvested and washed in HBSS + 1 % FBS and rested for 7 days at $1x10^6$/mL in RF-10. Cells were harvested and $2x10^5$ cells were added to a 96-well plate pre-coated, as before, with 1 µg/mL LEAF purified anti-human CD3. 1 µg/mL LEAF purified anti-human CD28 was added in RF-10 medium and cells were cultured for 3 days at 37°C in 5 % (v/v) CO_2/humidified air.

2.8.3 nTreg suppression assay

Suppression assays were set up using the following ratios of cells: 1 allogeneic matDC: 40 Teff: 20 nTreg cells in a final volume of 200 µL RF-10 in a 96-well round bottom plate. The following wells were prepared for each experiment:

1. $5x10^4$ Teff + $1.25x10^3$ matDC
2. $5x10^4$ Treg + $1.25x10^3$ matDC
3. $5x10^4$ Teff + $2.5x10^4$ Teff + $1.25x10^3$ matDC
4. $5x10^4$ Teff + $2.5x10^4$ Treg + $1.25x10^3$ matDC

Cultures were incubated for 5 days at 37°C in 5 % (v/v) CO_2/humidified air.

2.8.4 CFSE staining

A 1 µM 2x working solution of CFSE was prepared in PBS + 0.1 % FBS immediately before use. Transfected CD4+ T-cells were washed twice in RPMI-1640. The third wash step was performed in PBS + 0.1 % FBS at 800 x g for 10 minutes. All supernatant was aspirated and cells were resuspended to $20x10^6$/mL in PBS + 0.1 % FBS, or to 1 mL if fewer cells were used. $1x10^7$ cells were incubated for 5 minutes at 37°C in 0.5 M CFSE. 5 mL cold RF-10 was added to the mixture to terminate the staining and cells were incubated on ice

for 5 minutes. Cells were washed twice at 800 x g in cold RF-10 and resuspended in RF-10 for use.

2.8.5 ^{3}HTdR incorporation

20 µL of the 0.548 MBq/mL methyl-^{3}H thymidine working stock was added to each well of a 96 well plate and plates were incubated for 8 hours at 37°C in 5 % (v/v) CO_2/humidified air. Plates were harvested onto A, GF/C filtermats (Perkin Elmer) and air-dried overnight. Filters were placed in MicroBeta® Trilux sample bags (Perkin Elmer) and 5 mL of scintillation fluid (Perkin Elmer) was added. Filters were read on the Microbeta TriLux 1450 LSC luminescence counter (Perkin Elmer).

2.9 RNA and Protein Quantification: Flow Cytometry

2.9.1 Peripheral blood: immune cell subset staining

200 µL of whole blood was used per stain. Cell surface marker antibodies were added directly to whole blood (at the concentrations listed in Table 3) and incubated at RT for 30 minutes in the dark. 800 µL of pre-warmed red blood cell lysis buffer (0.1 M NH_4Cl, 1 mM $KHCO_3$, 0.1 mM EDTA) was added and samples were incubated at 37°C for 5 minutes. Cells were centrifuged at 400 x g for 5 minutes and washed twice in FACS buffer (PBS pH 7.2, 3 % (v/v) FBS, 100 µM EDTA, 0.01 % (v/v) sodium azide). Cells were then stained for CLDND1 according to Section 2.9.3. Cell populations were identified by lineage marker during flow cytometric analysis according to Section 2.9.9.

2.9.2 Cell populations: immune cell subset staining

For cell surface marker staining on PBMC, PBMC were resuspended in FACS buffer and non-specific antibody binding was blocked by pre-incubating the cells with 2 % human IgG (kind gift from Sophie Hambleton, Newcastle University). Directly conjugated cell surface markers were added to the cell populations at the dilutions described in (Table 3) for 30 minute at 4°C. Cells were washed twice prior to acquisition, or further stained for CLDND1. Cell surface marker abundance was measured as geometric mean fluorescence intensity (GMFI) or comparatively by over-laying histograms of the fluorescence.

2.9.3 CLDND1 cell surface staining

For CLDND1 staining, cell surface marker staining was performed if required (lineage markers were not used on isolated cell populations). Apart from where indicated in the antisera binding chapter, cells were fixed in 4 % formaldehyde for 30 minutes at RT. Cells were washed twice in FACS buffer. Cells were blocked in 2 % goat IgG (SIGMA Aldrich) and 1 µg α-CLDND1, or pre- or anti-sera was added for 30 minutes at RT (at 1/100 or 1/2000 dilutions), in the dark. Cells were washed twice in the appropriate buffer before incubation with 1:200 dilution of R-phycoerythrin-affinipure $F(ab')_2$ fragment goat anti-rabbit IgG (H+L) (Jackson ImmunoResearch, PA, USA) for 30 minutes at RT in the dark. Cells were washed twice, resuspended in FACS buffer and stored at 4°C, if required, before acquisition.

2.9.4 CLDND1 intracellular staining

Cells were stained according to Section 2.9.3, with the following addition: post cell fixation, cells were permeabilised. Two different permeabilisation buffers were used depending on the type of staining. For staining of cells for commercial antibody and pre- and antisera analysis, cells were permeabilised in permeabilization buffer (10X), diluted to 1X (eBioscience, San Diego, UK). The permeabilisation buffer (10X) was diluted in deionised H_2O, according to manufacturer instruction. All other flow cytometry staining that required permeabilisation used triton-X permeabilisation buffer (PBS pH 7.2, 0.5 % (w/v) BSA, 1 % (v/v) fish skin gelatin, 0.5 % (v/v) triton-X 100). The sample was incubated in either buffer for 30 minutes at RT. All subsequent staining steps were also performed in each permeabilisation buffer.

2.9.5 Viability staining

Where viability staining was required, post lineage marker staining, cells were resuspended in 100 µL of Annexin V binding buffer (diluted from a 10X stock (0.1 M HEPES, pH 7.4; 1.4 M NaCl; 25 mM $CaCl_2$) in deionised H_2O). Annexin V antibody (BD Bioscience) and Via-Probe™ (BD Bioscience) were added 15 minutes prior to acquisition, according to manufacturer instruction.

2.9.6 CLDND1 antibody blocking

CLE11, CLE12, CLE13 and CLE21 peptides were incubated at a final concentration of 1 µg/mL with a 1/200 dilution of α-CLDND1 pre- or anti-sera in PBS, overnight at 4°C. The mixture was added at a 1/20 dilution to the cells, at the equivalent step as the CLDND1 or sera staining in Section 2.9.3.

2.9.7 Determining nTreg purity.

Purified CD4+ T-cell and corresponding purified nTreg cell populations were stained for CD3, CD4 and CD25 according to Section 2.9.2. Cells were then fixed and permeabilised with Foxp3 fixation/permeabilization concentrate and diluent (eBioscience), according to manufacturer instruction. Alexa Fluor® 647 anti-human Foxp3 antibody (BioLegend) was added and samples were incubated for 30 minutes at 4°C, in the dark. Cells were washed twice and resuspended in FACS buffer before acquisition. Sample purity was determined according to the strategy outlined in Figure 11.

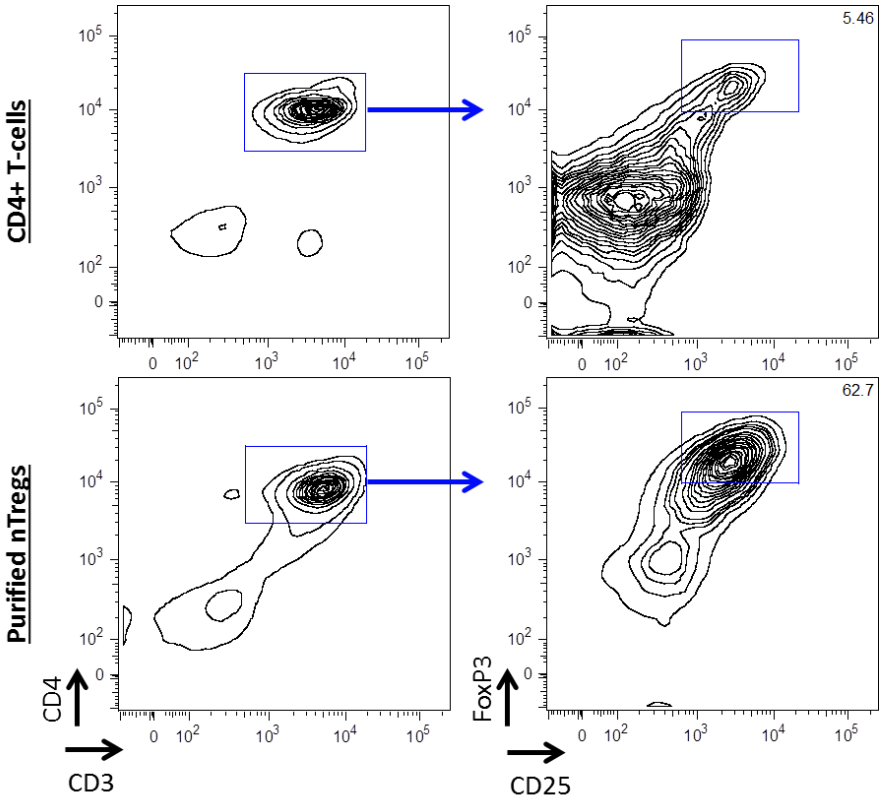

Figure 11. Gating strategy to determine nTreg purity

CD4+ T-cells or purified nTreg were stained for CD3, CD4, CD25 and Foxp3. CD3/CD4 double positive cells were gated on and from this, CD25high Foxp3 positive cells were determined, as identified by the boxed cells. The average number of cells identified in the box was 59 %.

2.9.8 Acquisition

Samples were acquired in a FACSCanto II (BD Biosciences) with 2 lasers (488nm, 635nm) using FACSDiva software (BD Bioscience). Data was analysed with FlowJo software (Tree Star, OR, USA).

2.9.9 Gating strategy

For analysis of T-cells, a lymphocyte gate was drawn from the whole population. Cells were then selected for CD3 expression and from this gate, CD4+ or CD8+ T-cells were selected (Figure 12A). For analysis of monocytes and B-cells, a PBMC gate was drawn from the whole population and cells were then either selected for CD14 or CD19 expression, respectively (Figure 12B). The large population of cells present in the centre of the plots probably represent granulocytes.

CLDND1 staining was determined by two methods: the percentage of CLDND1 positive cells (Figure 12C) or by GMFI. Both methods required the negative control of cells stained with phycoerythrin-affinipure $F(ab')_2$ fragment goat anti-rabbit IgG (H+L) detection antibody only (detection only). For determining the percentage of CLDND1 positive cells, a CLDND1 positive gate was set above the staining profile in the “detection only” population of cells and transferred to the CLDND1 stained cells to determine CLDND1 positivity. The GMFI was also calculated for both the detection only sample and the CLDND1 stained sample and the detection only value was subtracted from the CLDND1 stained GMFI value to obtain a GMFI value for CLDND1 staining intensity.

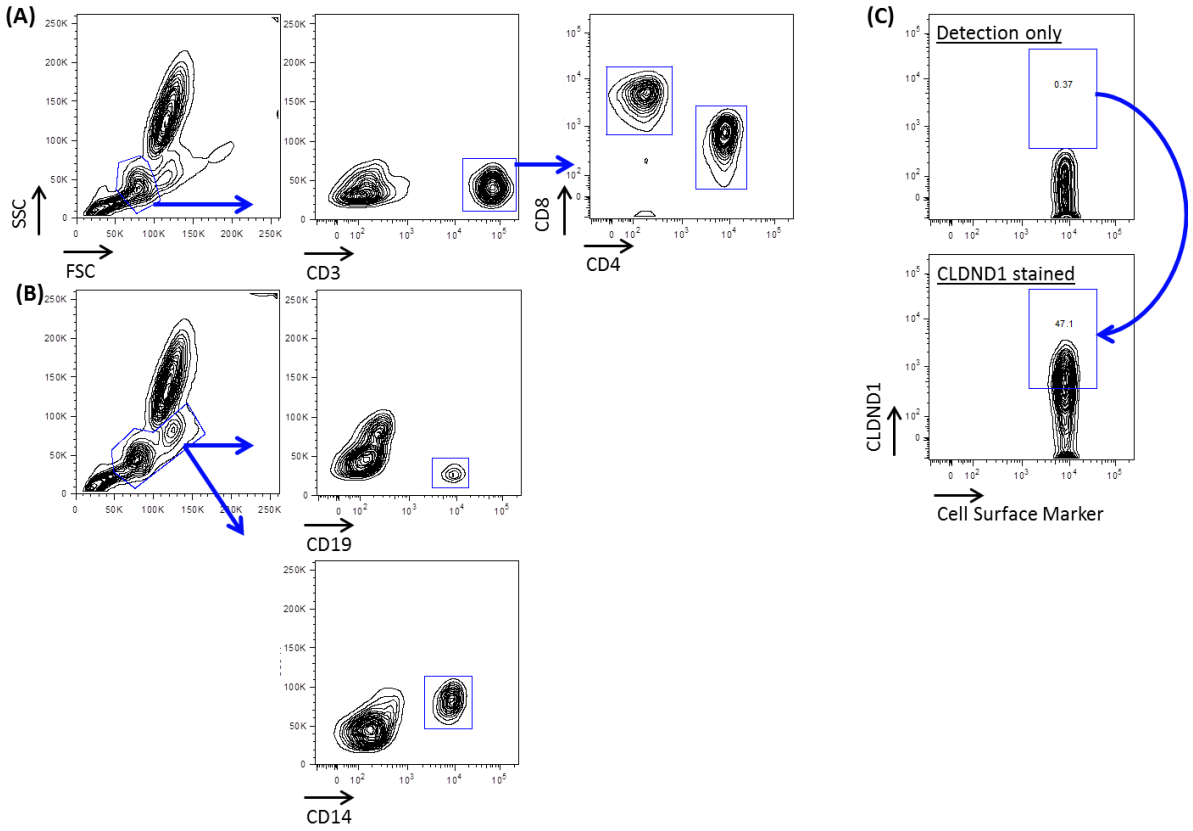

Figure 12. Gating strategy to determine cell subsets and CLDND1 positivity

Staining from whole blood is shown, and a similar gating strategy was applied to PBMC populations. Whole blood was stained for CD3, CD4, CD8, CD14 and CD19. (A) Identification of T-cells. The lymphocyte population was gated and T-cells were selected based on CD3 positivity. CD4+ and CD8+ T-cell were separated. (B) Identification of B-cells and monocytes. The PBMC population was gated around and B-cells or monocytes were selected based on CD19 or CD14 staining (C) CLDND1 staining was determined using FMO analysis. Cells were stained with secondary detection antibody only and a gate was drawn above the population of cells. When the gate was transferred to CLDND1 antibody stained cells, the cells within this gate related to CLDND1 positive cells.

2.10 RNA and Protein Quantification: Western Blotting

2.10.1 Lysate generation

For adherent cells: after desired cell incubation, cell culture medium was removed and cells were rinsed with cold PBS. The PBS was then removed and replaced with 100 µL ice-cold RIPA lysis buffer (50 mM tris HCl pH 8, 150 mM NaCl, 1 % (v/v) triton-X 100, 0.5 % (v/v) sodium deoxycholate, 0.1 % SDS (w/v), protease inhibitor cocktail (Roche, Burgess Hill, UK)). To detach the cells they were scraped and then transferred into an eppendorf on ice.

For suspension cells: after desired cell incubation, cells were washed in PBS and then pelleted. 50-100 µL ice-cold RIPA lysis buffer was added to the cells, depending on the number of cells.

Samples were incubated on ice for 30 minutes with periodic vortexing. Samples were centrifuged at 10, 000 x g for 3 minutes and the supernatant was transferred into a new eppendorf and frozen at -20°C.

2.10.2 Bradford protein assay

A 0.4 mg/mL BSA protein stock was prepared in PBS and was diluted to produce a range of standard from 0 - 0.4 mg/mL in 0.04 mg/mL increments and added to a flat bottom 96-well plate. Cell lysates and equal quantities of cell lysis buffer were added to act as blanks. BradfordUltra (Expedeon, Harston, UK) assay reagent was then added to the wells containing the standards and the samples, according to manufacturer instruction. The samples were gently mixed and left to stand for 5 minutes before the absorbance was read at 595 nm using a Tecan Sunrise microplate absorbance reader.

2.10.3 SDS-PAGE

Cell lysates were thawed on ice and dilutions were made to correct for protein concentration. 5x laemmli loading buffer (0.1 M tris HCl, pH 6.8, 0.35 M SDS, 20 % (v/v) glycerol, 0.01 % bromophenol blue and 5 % (v/v) β-mercaptoethanol) was added at 1/5 of the lysate volume. The resulting mixtures were heated to 100°C for 5 minutes, cooled and then electrophoresed on a 12.5 % SDS-polyacrylamide gel. For SDS-PAGE analysis, gels were stained with SilverQuest™ silver staining kit (Life Technologies), according to manufacturer

instruction or transferred into coomassie brilliant blue R250 staining buffer (45 % methanol, 10 % glacial acetic acid, 45 % water, 3 g/L coomassie brilliant blue R250). Gels were destained in coomassie destaining buffer (45 % methanol, 10 % glacial acetic acid, 45 % deionised H_2O). Samples for western blot were then transferred to polyvinylidene fluoride (PVDF) membrane by electroblotting in a Scie-Plas V20-SDB 20X20 cm semi-dry blotter for 1.5 hours at 1 mA/cm^2 in transfer buffer (20 mM tris HCl, 0.65 M glycine, 20 % (v/v) methanol).

Membranes were covered in blocking buffer (TBS-T (10 mM tris pH 7.5, 150 mM NaCl, 0.1 % tween 20 (v/v)), 5 % non-fat dry milk powder (w/v)) for 1 hour at RT. Membranes were washed 3 times for 5 minutes in TBS-T. Washed membranes were incubated overnight at 4°C with primary antibody or sera, diluted in TBS-T, 5 % BSA with gentle agitation. Following incubation, membranes were washed 3 times for 5 minutes with TBS-T and then incubated with anti-mouse IgG (H+L) HRP-linked or anti-rabbit IgG (H+L) HRP-linked antibody (both Cell Signaling Technology, MA, USA) in TBS-T, 5 % milk for 1 hour at RT with gentle agitation, then washed a further 3 times in TBS-T. Blots were visualised using ECL detection reagents (Merck Millipore) and the G:BOX Chemi system.

2.11 RNA and Protein Quantification: Immunofluorescence

Medium was removed from the chamberslide and the wells were washed twice with PBS. Cells were fixed in 4 % formaldehyde for 15 minutes at RT. Cells were washed once in PBS before permeabilisation using triton-X permeabilisation buffer for 15 minutes at RT. Samples were blocked with 2 % goat serum for 15 minutes before primary antibody or α-CLDND1 sera and mouse monoclonal anti-FLAG® M2 (SIGMA Aldrich) was added a 1/100 final dilution. Samples were incubated for 1 hour at RT before washing twice in triton-X permeabilisation buffer. Alexa Fluor® 488 goat anti-rabbit IgG (H+L), Alexa Fluor® 594 goat anti-mouse IgG (H+L) and Alexa Fluor® 594 goat anti-rabbit IgG (all Life Technologies) secondary antibodies were added and cells were incubated for 30 minutes at RT, in the dark. Samples were washed twice, the final wash in PBS. The chambers were removed from the slide. Cells were mounted with VECTASHIELD mounting media with 4',6-diamidino-2-phenylindole (DAPI) (Vector Laboratories, Orton Southgate, UK) and

fluorescence was detected with a LEICA DMLB fluorescent microscope and associated SPOT RT camera and software.

For confocal microscopy, analysis was performed using a Zeiss Axio Imager II and associated AxioVision software. Between 8 and 12 z-stacks were taken for each analysis, and one of these images were presented.

2.12 RNA and Protein Quantification: RNA Analysis

2.12.1 RNA extraction

$1x10^5$ CD4+ T-cells were pelleted and RNA extracted using the RNeasy plus micro kit (Qiagen), according to manufacturer instruction, eluting in 14 µL DNase and RNase free H_2O. For transfected CD4+ T-cells, an additional on column DNAse I treatment was performed using RNase-Free DNase set (Qiagen) as follows: after cell lysate was loaded onto the Qiagen spin purification column, 30 Kunitz units of DNase I was added to the column for 15 minutes at RT. DNase was eluted from the column with RW1 buffer as part of the RNeasy plus micro kit protocol and the remaining RNA purification steps were performed according to manufacturer protocol.

2.12.2 Reverse transcription

For reverse transcription, 8 µL of eluted sample was transferred to a 96-well PCR plate. Following this, 0.375 mM dNTPs (Bioline, London, UK) and 0.2 µg of random hexamers $p(dH)_6$ (GE healthcare) (final concentrations) were added to each well and the plate incubated at 70°C for 5 minutes. Samples were then placed on ice followed by the addition of a reaction mix consisting of 10 mM DTT (final concentration), 200 U MMLV-RT and the appropriate volume of 5X first strand buffer (all Life Technologies) to each well and the plate was incubated at 37°C for 50 minutes followed by 70°C for 15 minutes. The stable cDNA was then diluted 1.5 times in DNase and RNase free H_2O and stored at -20°C for further use.

2.12.3 qRT-PCR

Fluorescence-based, qRT-PCR was used to measure mRNA expression in cells. When analysed with a stably expressed ‘housekeeping’ gene, such as pol2a, a subunit of RNA polymerase II, the relative expression of a gene was determined.

Forward and reverse primers were designed with the universal ProbeLibrary (Roche) (Table 11) or CLDND1 was detected with the CLDND1 TaqMan® gene expression assay (Hs00219886_m1, Life Technologies). To prevent amplification of any residual genomic DNA present, the primers were placed to span an intron/exon boundary.

Gene	Primers	Probe library
Pol2a	Fwd 5' TTGTGCAGGACACACTCACA	1
	Rev 5' CAGGAGGTTCATCACTTCACC	
CD4	Fwd 5' GGCAGTGTCTGCTGAGTGAC	18
	Rev 5' GACCATGTGGGCAGAACC	
CLDND1 (UCB)	Fwd 5' AATTCATGGCCTCTGCACTT	26
	Rev 5' GGGTGTATTCCTTCCGATTTG	
CD25	Fwd 5' ACGGGAAGACAAGGTGGAC	54
	Rev 5' TGCCTGAGGCTTCTCTTCA	

Table 11. qRT-PCR primers for Taqman based assay

Primers were designed using the universal ProbeLibrary assay design centre (Roche Diagnostics) to complement existing Roche probes for analysis of the genes listed by qRT-PCR.

For qRT-PCR, 15 µL of a master mix containing 100 nM universal ProbeLibrary probe (Roche), 200 nM of each primer (SIGMA Aldrich) and 7.5 µL TaqMan® gene expression master mix (Life Technologies) was added to 5 µL of cDNA, or for the CLDND1 TaqMan® gene expression assay, 5 µL cDNA was mixed with 20x CLDND1 TaqMan® gene expression assay to a final volume of 15 µL. mRNA expression was determined using a TaqMan 7900HT fast-real time PCR system (Life Technologies) with the thermal cycler set to 50°C x 2 minutes, 95°C x 10 minutes, then (95°C x 15 seconds, 60°C x 1 minute) X 40. CLDND1 cDNA levels were normalised to the level of pol2a using the calculation $2^{e-\Delta CT}$, where ΔCT represents CT(target gene) – CT(pol2a). Results were analysed using SDS 2.4 software (Life Technologies).

2.13 RNA and Protein Quantification: Immunoprecipitation

2.13.1 CLDND1 antibody immunoprecipitation

Several different methods to couple antibody to resin for immunoprecipitation (IP) are available. The Pierce direct IP kit (Thermo Scientific) was chosen as the antibody can be directly coupled to the resin through the interaction of lysine epsilon-amines on the antibody with aldehyde groups on the resin, stabilised by cyanoborohydride.

IP were carried out according to manufacturer protocol. Briefly, 10 µg of α-CLDND1 antibody was coupled to 20 µL of the AminoLink plus coupling resin in the presence of 75 mM sodium cyanoborohydride solution for 2 hours at RT. The column was washed and IP was performed.

Cells were pelleted, lysed in 500 µL ice-cold IP lysis/wash buffer per 50 mg of wet cell pellet and incubated on ice for 5 minutes. Cell debris was removed by centrifugation at 13000 x g for 10 minutes and supernatant concentration was determined by Pierce BCA protein assay (Thermo Scientific), according to manufacturer instruction. The lysate was pre-cleared using 80 µL of control agarose resin per 1 mg of lysate. 1000 µg of pre-cleared lysate was added to the α-CLDND1 antibody coupled resin and incubated overnight at 4°C with rotation. The column was washed and the eluted fractions were kept as flowthrough (FT) fractions. CLDND1-antibody specific proteins were eluted from the IP matrix using 100 µL of elution buffer. Fractions were collected in 8 µL of 1 M tris pH 9.5, to neutralise the acidity of the eluate.

For the addition of SDS, 0.1 % SDS (w/v) was added to the IP lysis/wash buffer prior to cell lysis. For scale-up experiments, 50 µg of α-CLDND1 antibody as coupled to 200 µL of AminoLink plus coupling resin with other solution volumes and concentrations scaled-up accordingly.

2.13.2 FLAG IP

FLAG IP was performed using the FLAG IP kit (SIGMA Aldrich) according to manufacturer instruction. Briefly, transfected cells were pelleted and resuspended in 10^6-10^7 cells/mL and incubated for 15 minutes on a shaker. To remove cellular debris, cell lysates were centrifuged at 12000 x g for 10 minutes. 500 µL of supernatant was added to 40 µL of anti-FLAG M2 affinity gel

resin and incubated for 2 hours at 4°C. Unbound proteins were washed from the column and kept as column FT. FLAG-proteins were eluted from the column by competitive binding with FLAG peptide. A 150 ng/µL FLAG peptide solution was prepared, 100 µL of this solution was added to the resin and the samples were incubated for 30 minutes at 4°C. Samples were eluted using 100 µL elution buffer at RT. For scale-up experiments, all volumes used were doubled.

2.14 RNA and Protein Quantification: ELISA

ELISAs for IL-5 and IL-17 were bought as kits (Peprotech and eBioscience, respectively) and were performed according to manufacturer instruction. Individual IFN-γ, IL-2, IL-10 and TNF-α capture and biotinylated secondary antibodies (all BD Bioscience) were purchased and ELISAs were performed as described below.

96-well high-affinity plates were coated with 4 µg/mL IL-2, 2 µg/mL IL-10 or TNF-α or 1 µg/mL IFN-γ capture antibodies in coating buffer (15 mM disodium phosphate, 20 mM monosodium phosphate sodium phosphate monobasic) and incubated overnight at 4°C. Wells were washed in ELISA wash buffer (PBS pH 7.2 + 0.1 % (v/v) tween 20) before wells were blocked in PBS pH 7.2 + 1 % (w/v) BSA. Samples were diluted accordingly in PBS pH 7.2 + 1 % BSA + 0.1 % (v/v) tween 20 before adding to the plate. 2000 pg/mL standards were diluted 2-fold in PBS + 1 % BSA + 0.1 % (v/v) tween 20 to create a standard curve. Plates were incubated overnight at 4°C. Plates were washed in ELISA wash buffer before biotinylated detection antibody was added at 1 µg/mL for IL-2, IL-10, IFN-γ or 0.5 µg/mL for TNF-α. Samples were incubated for 1 hour at RT. Plates were washed again in ELISA wash buffer before a 1/1000 dilution of ExtrAvidin®−peroxidase (SIGMA Aldrich) was added for 30 minutes at RT. Plates were washed in ELISA wash buffer before OPD susbstrate was added. Plates were developed for 30-40 minutes before the reaction was stopped with 3 M sulphuric acid. Absorbances were read at 490 nm using a Tecan Sunrise microplate absorbance reader.

2.15 Bioinformatics

2.15.1 BLAST Search

Sequence alignments were performed against the CLDND1 protein sequence (NP_001035289.1) with the basic local alignment search tool (BLAST) (NCBI) using the algorithm blastp against the human genome. The search parameters were ranked according to max score, query coverage and E-value. Max score ranks the highest alignment score between the query and the database sequence, with higher scores corresponding to a better alignment. This score covers alignment of similar or identical residues and any gaps introduced to align the sequences. Values are normalised so different alignments can be compared. The query coverage identifies the length of the aligned sequence matching the hit within the database. The E-value describes the number of hits expected to be seen by chance when searching the database of a particular size. The lower the E-value, the more significant the alignment.

2.15.2 PMP-22/EMP/MP20/claudin superfamily sequence alignment and phylogenetic analysis

Phylogenetic analysis was carried out on the same sequences as Maher et al., (2011) (Appendix Table 1). Sequences were aligned using clustalW2-MUSCLE (EBI), followed by phylogenetic analysis using the Seaview software, on observed distance, with gap sites ignored. Bootstrap proportions were used to assess the robustness of the tree with 10000 bootstrap replications. Clarin-1 was used as an out group.

2.16 Fold Change Calculations

Several data are expressed as a fold change compared to a control value for qRT-PCR and flow cytometric analysis. Control values were set to a value of 1, through the division of the value by itself. Subject values were also divided by the control value to give a value expressed as fold change. A fold change of 1 represents no change from the control, values above 1 represent an increase in read-out in the subject sample compared to the control and a value below 1 represents a decrease in read-out value in the subject sample compared to the control value.

2.17 Statistical Analysis

Various statistical analyses were performed on the data to determine whether the data collected represented changes between two populations, as apposed to natural variance within each population. Where applicable, data was tested for fit to the Gaussian distribution using D'Agostino and Pearson omnibus normality test, as recommended by GraphPad PRISM and parametric or non-parametric tests were used accordingly. Statistical testing was applied to experiments where three or more replicates were performed.

For parametric data, Student's t-test analysis was performed on normalised data or paired Student's t-test was performed on raw data values. Where more than three groups of raw data were analysed repeated-measures ANOVA was performed on dependent groups or a 1way ANOVA was performed on independent samples, with Bonferroni's correction to account for generation of a statistically significant result by chance from testing multiple parameters.

For non-parametric data, Wilcoxon matched paired t-test was used for comparison between two dependent samples or a man-Whitney U test was performed for independent data. Where samples were not large enough to test for normality, both statistical testing was performed. If p values less than 0.05 were only determined with parametric tests, these values were shown, but where both parametric and non-parametric tests gave p values lower than 0.05, the non-parametric test was shown.

Data illustrate the mean value of the data plus the standard error of the mean (SEM). Significance values are illustrated by *, ** or ***, which correspond to $p<0.05$, $p<0.01$ and $p<0.001$, respectively.

Chapter 3. Generation of CLDND1 Antibodies

3.1 Aims

One aim of this chapter was to validate the commercially available antibodies against CLDND1 by firstly determining whether these antibodies definitely recognised CLDND1 and secondly whether they could be used to manipulate CLDND1 function. In addition, I sought to generate in-house antibodies against extracellular regions of CLDND1 which would be thoroughly validated. These latter antibodies would then be screened for functional effects to further elucidate a role for CLDND1 in the immune response.

3.2 Introduction

3.2.1 Antibody characteristics

Antibodies are glycoproteins produced by B-cells, as the main effector of the humoral immune response. Belonging to the immunoglobulin superfamily, they typically conform to a basic “Y”-shaped structure, comprising two large heavy chains and two small light chains. The five heavy chains determine the class of antibody: γ for IgG, α for IgA, μ for IgM, δ for IgD and ε for IgE antibodies. The class of the antibody dictates the effector function of the antibody. The κ or λ light chains are found on any class of antibody, but are restricted to one isoform per antibody molecule.

Both heavy and light chains have a variable and a constant region. The variable region determines antigen specificity through its complimentary determining regions (CDRs) and framework regions. The framework regions define the placement of the three CDRs for each chain, so when the heavy and light chains are joined, the six CDRs form a surface that serves as the antigen-binding site, of which there are two per antibody molecule.

Each antibody is specific for a single epitope and antibody gene rearrangements enable the generation of different antibodies that are estimated to recognise 10^9 distinct epitopes. Further diversity can also be introduced by somatic hypermutation of the variable regions, which introduces additional point mutations in the coding sequences (Janeway et al., 2001).

3.2.2 Antibody production for research

Immunising animals with an antigen can result in the development of pAbs in the serum of the animal, or mAbs can be developed from the B-cells in the spleen. Antibodies can also be made through *in vitro* selection protocols, such as phage display (Uhlen and Ponten, 2005).

3.2.3 pAbs

pAbs are produced by a population of non-identical B-cells, so are comprised of a mixture of antibodies with varying affinities and recognising different epitopes. The antiserum collected from the blood from animal immunisations, typically contains 1 % of antigen specific antibodies. Epitope specific affinity purification can separate the antibody from the antiserum, to reduce interference by the non-specific antibodies (Uhlen and Ponten, 2005).

pAbs are suited to many technical applications due to their ability to recognise several epitopes within a target protein. The polyclonality of antiserum is an advantage in techniques such as immunohistochemistry, where some epitopes can be destroyed by chemical fixation (Fritschy, 2008), however include the disadvantage of non-specific binding, as mentioned above.

3.2.4 mAbs

mAbs are also generated from animal immunisations with antigen, utilising the spleen cells. The B-cells from the spleen are fused with a myeloma cell line to create immortal hybridomas that secrete antibodies, whose specificity is determined by the B-cell fusion partner. Each hybridoma can produce large amounts of antibody and this population of hybridomas can be screened to allow selection of one or more that secrete antibody of requisite specificity (Kohler and Milstein, 1975). mAbs confer an advantage over polyclonal antisera as a preparation containing one specificity of antibody can consistently be re-made, whereas different batches of antiserum can have different properties.

3.2.5 Types of antigens for immunisation

Immunisation protocols use different types of antigen, depending on the desired properties of the antibody. There are three main types of antigen: synthetic peptides that mimic protein sequences, full length protein, or recombinant protein fragments.

The use of synthetic peptides is technically simple and relatively straight forward, as pure peptides can be readily prepared. As the peptides are usually less than 40 amino acids in length they are not likely to resemble folded protein structures. If peptide epitopes are hidden within the folded protein structure, however, the antibodies generated could be non-functional, recognising only denatured antigen (Uhlen and Ponten, 2005).

Immunisation with full length protein is a way of generating antibodies that recognise folded protein. Full length proteins can be expressed in eukaryotic systems provided the cells are equipped for correct protein manufacture. Alternatively, protein can be purified from the appropriate tissue, but the yield is usually low. Purification methods are most suited to soluble proteins, as obtaining pure transmembrane protein samples is technically challenging. The use of folded protein for immunisation has been questioned as proteins can be denatured during the immunisation protocol (Uhlen and Ponten, 2005).

Protein fragments are portions of the full length protein and maintain the potential to retain structural features seen in the full length protein. The use of protein fragments is often more straightforward than generating full length protein, partly due to using affinity tags for protein purification. For example, a small histidine tag on either terminus of the protein fragment allows for quick purification using resin immobilised nickel. The use of protein fragments risk incorrectly folded protein structures, however this can be partially overcome by strategic selection of protein fragments with increased structural integrity and architecture (Uhlen and Ponten, 2005).

3.2.6 Antibody design for CLDND1 structure

CLDND1 is a hypothesised tetra-spanning transmembrane protein, consisting of intracellular N- and C-termini and two extracellular loops. The large first loop contains the conserved PMP-22/EMP/MP20/claudin superfamily motif and three cysteine residues, which are important for function by forming disulphide bridges in other superfamily members (Wen et al., 2004). The first loop also contains potential phosphorylation and glycosylation sites (Figure 7). The presence of these potential features within the CLDND1 molecule needs to be considered when designing immunisation strategies to ensure CLDND1 specific antibody generation.

3.3 Results

3.3.1 Commercial antibody validation

Five commercially available α-CLDND1 antibodies were available at the time of validation, so they were tested on CLDND1-transfected cells, to determine their CLDND1 binding characteristics, before the in-house antibodies were produced. CLDND1 folded protein binding was measured by flow cytometry and denatured protein binding was analysed by Western blot (Figure 13). The commercial antibodies had different CLDND1 staining patterns. Compared to each isotype control, positive cell surface staining was detected on all cell populations probed with the SIGMA 2 or the Santa Cruz antibody or in the CLDND1-transfected cells for SIGMA 1 antibody (Figure 13A). The CLDND1-transfected cell staining profile of SIGMA 2 and the Santa Cruz antibody was less compared to the mock-transfected cells stained with each commercial antibody, suggesting these antibodies were not specific to CLDND1, transfected CLDND1 behaved differently to native CLDND1, or transfected-CLDND1 levels were low.

At the time the experiments were performed, the hypothesised location of CLDND1 was at the plasma membrane, but as this was not validated, commercial antibody binding to total CLDND1 was also assessed. For total CLDND1 expression, the transfected cells were fixed and permeabilised prior to staining (Figure 13B). Compared to each isotype control, CLDND1 staining mirrored the cell surface staining for the CLDND1-transfected cells probed with commercial antibody. A small shoulder was seen on the histogram of the CLDND1-transfected cells probed with the SIGMA antibodies, above any staining of the control cells. The Abcam, Santa Cruz and the Prosci antibodies had similar staining profiles between the CLDND1-transfected and the mock transfected samples. These data suggest that the two SIGMA antibodies were potentially recognising a small amount of CLDND1. These cells were prepared by UCB Celltech, but transfection efficiency was not determined and so the level of transfection remains unknown.

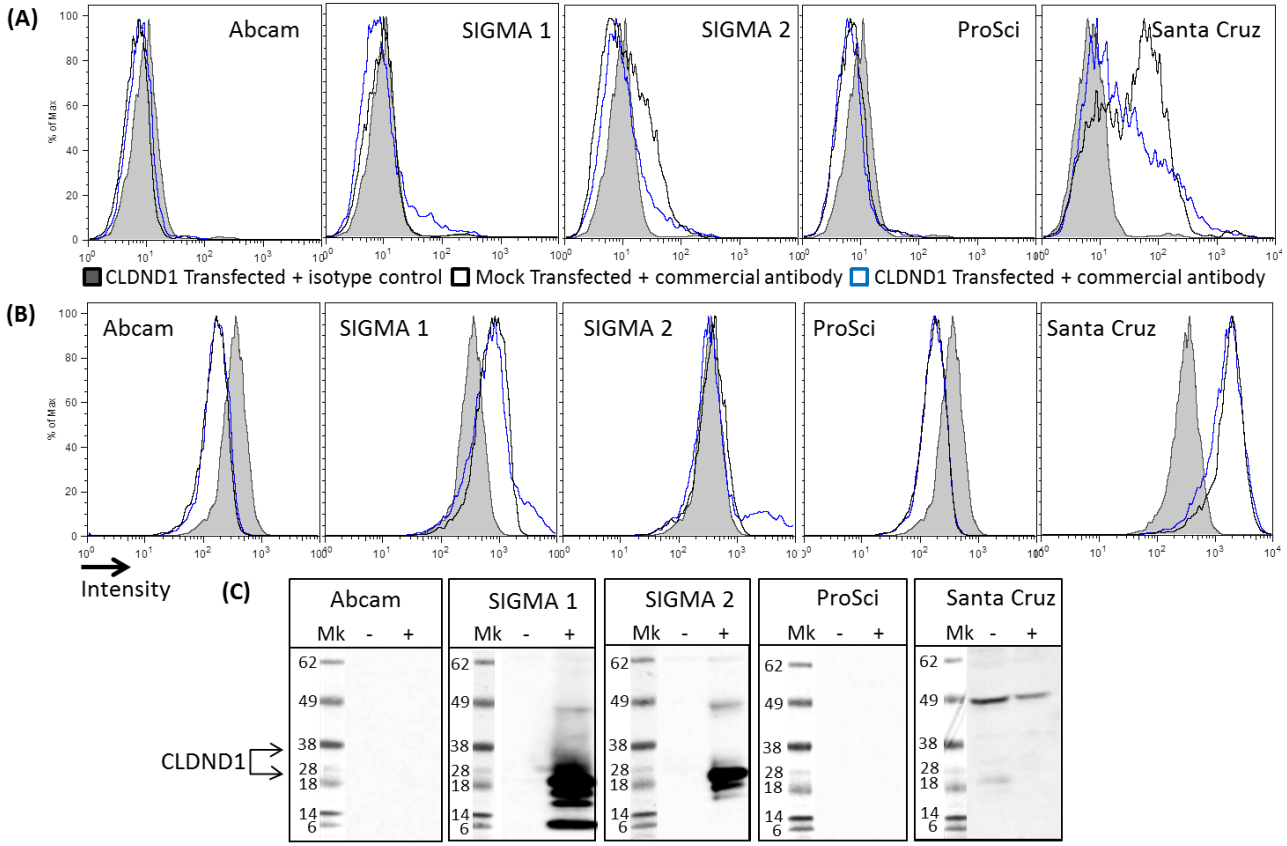

Figure 13. Validation of commercial antibodies

Mock-transfected (-) and CLDND1-transfected (+) FreeStyle™ 293-F cells were stained with each commercial antibody or isotype control before flow cytometry or Western blot analysis. Detection of native CLDND1 expression (A) on the cell surface or (B) total cellular CLDND1 expression by flow cytometry. (C) Western blot of total CLDND1 in cell lysates. Mk represents protein ladder marker. Data illustrate one experiment.

At the time these experiments were performed, there were conflicting datasets regarding CLDND1 RNA expression in HEK293 cells (www.genecards.org, www.biogps.org) and so we were uncertain whether the commercial antibodies were detecting native protein on mock-transfected cells. CLDND1 protein expression has subsequently been confirmed on HEK293 cells by mass spectrometry (Kim et al., 2011, Danielsen et al., 2011, Wagner et al., 2011), suggesting the staining identified by the SIGMA and Santa Cruz antibodies on mock-transfected cells may have been native CLDND1. If the staining with the Santa Cruz antibody was true CLDND1 staining, it may suggest that induced expression of CLDND1 may disrupt the detection of endogenous expression.

Due to the conflicting RNA expression data, Western blotting validation of the commercial antibodies was also performed on CLDND1-transfected cell lysates. The molecular weight of CLDND1 is predicted at 28 kDa, yet a phenomenon is known to occur with helical transmembrane proteins where aberrant migration by up to 20 % of the predicted molecular weight of the protein is observed by SDS-PAGE relative to standard protein markers (Rath and Deber, 2013). Given this fact, bands between 34 kDa and 22 kDa were ascribed to CLDND1.

No bands were visualised on the Western blots probed with either the Abcam or ProSci antibodies (Figure 13C). Bands were identified with the Santa Cruz antibody, yet these were nearly double the predicted molecular weight of CLDND1 and were present at similar intensities in both the mock- and CLDND1-transfected cell lysates. There was also an additional band present in the mock-transfected sample, around the predicted molecular weight of CLDND1, which wasn't present in the CLDND1-transfected sample. Given the discrepancy in RNA expression profiling, it was difficult to determine whether the band present in the mock-transfected sample was true staining. Staining results were, however, expected to be more intense in the CLDND1-transfected sample, and so the bands identified with the Santa Cruz antibody were dismissed as non-specific interactions.

Bands were also visualised in the CLDND1-transfected lysates using either SIGMA antibody. The SIGMA 1 antibody detected 5 main bands, two of which had the predicted molecular weight of CLDND1 and three of which migrated lower than predicted. There was also a faint band present around 50 kDa, similar to the one identified by the Santa Cruz antibody. Two main bands were

identified in the CLDND1-transfected lysate with the SIGMA 2 antibody, one of which was the correct molecular weight for CLDND1 and one of which migrated lower than predicted. Similar to the SIGMA 1 and the Santa Cruz antibody, a band around 50 kDa was also detected with the SIGMA 2 antibody.

The data presented showed that two (SIGMA1 and SIGMA2) of the five commercial antibodies may detect CLDND1 by Western blot; however the binding of the antibodies to native CLDND1 was low. The quantity of CLDND1 detected in the CLDND1-transfected cell lysates by Western blot was not reflected in the flow cytometry data, as a minimal difference in cell surface staining between mock-transfected and CLDND1-transfected cell populations was seen. It can be argued that there was a small amount of total CLDND1 expression detected, yet as the antibodies were to be preferentially used for functional studies, the conditions (fixation and permeabilisation) required to obtain positive staining were not suitable. Additionally, as both antibodies highlighted several bands by Western blot, it is not known whether all these bands corresponded to CLDND1. The definitive way to assess specific binding would have been to block the epitope binding site of the antibody with specific substrate or peptide, but it was not feasible to perform this experiment, due to the lack of reagent availability. With the hope of generating an antibody which could be used for functional studies as well as for protein detection, in-house antibodies were generated and full antibody validation was performed to confirm specificity to CLDND1.

3.3.2 In-house antibody generation

Synthetic peptides were chosen for antibody immunisations as this method is the most straightforward way for generating antibodies and avoids the generation of overlapping specificities to other PMP-22/EMP/MP20/claudin superfamily members. Although antibodies generated in this manner may be non-functional, a tool to detect CLDND1 protein would be the first step in definitively identifying CLDND1 protein expression. Attempting to generate cells expressing CLDND1 protein to use for immunisation would be challenging without an antibody to detect whether cell surface protein expression was being achieved.

Four peptides were generated against CLDND1-specific extracellular regions of CLDND1, taking into account any potential functional motifs (Figure 7), and used in the immunisation protocol described (See Sections 2.3.1 and 2.3.2). Serum obtained from the rabbits, pre (preserum) and post (antiserum) immunisation, were tested for the presence of α-CLDND1 peptide antibodies. Each serum was tested for binding with its cognate or non-cognate peptide: 2675-78 sera with CLE11 and CLE12 peptides (2675 and 76 cognate peptide is CLE11, 2677 and 78 cognate peptide is CLE12) and 2679-82 sera with CLE13 and CLE21 peptides (2679 and 2680 cognate peptide is CLE13, 2681 and 82 cognate peptide is CLE21) (Figure 14). All antisera bound to their cognate immunisation peptide in a dose dependent manner. There was minimal cross-reactivity of 2675 and 2676 antisera with CLE12 (Figure 14B), 2678 antiserum with CLE11 (Figure 14A), 2679 antiserum with CLE21 (Figure 14D) and 2681 and 2682 antisera with CLE13 (Figure 14C). Non-cognate peptide binding was seen with 2677 antiserum and CLE11 and 2680 antiserum with CLE21, suggesting some non-specific activity of those antisera.

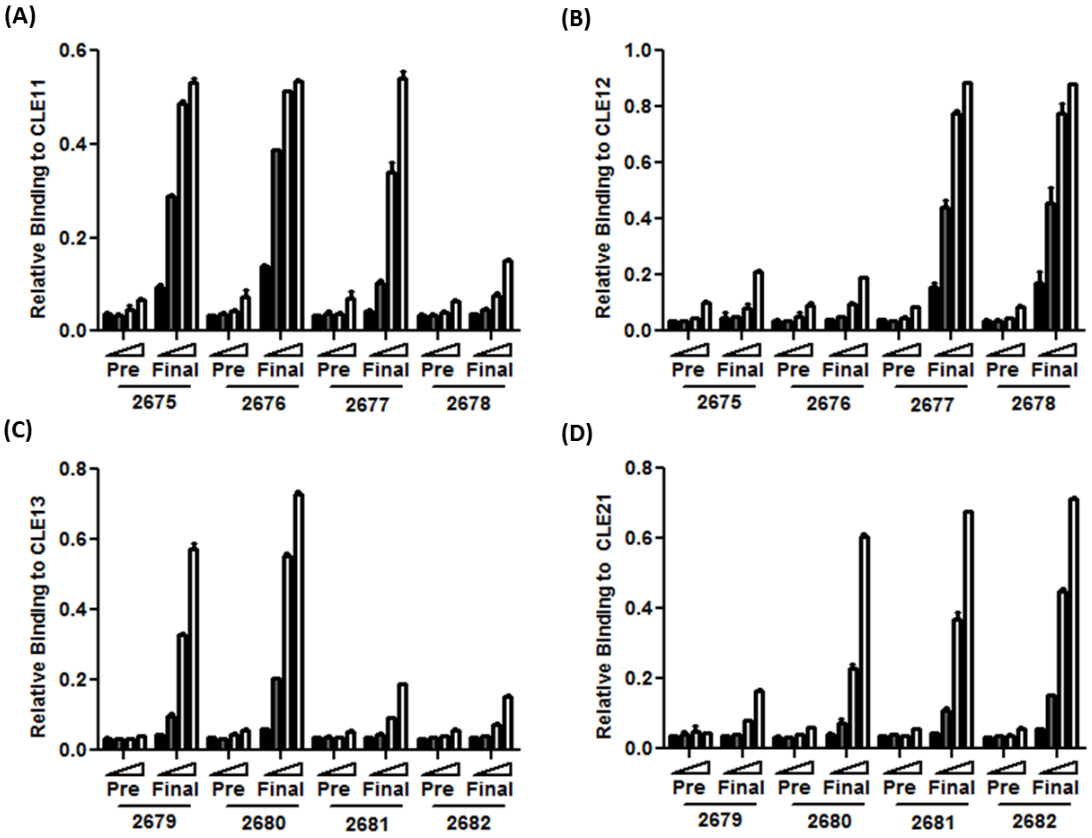

Figure 14. CLDND1 peptide binding by immunisation serum

Binding of (A) 2675-2678 antisera to peptide CLE11, where CLE11 is cognate peptide for 2675 and 2676, (B) 2675-2678 antisera to peptide CLE12, where CLE12 is cognate peptide for 2677 and 2678, (C) 2679-2682 antisera to peptide CLE13, where CLE13 is cognate peptide for 2679 and 2680, (D) 2679-2682 antisera to peptide CLE21, where CLE21 is cognate peptide for 2681 and 2682. Arrows indicate increasing concentrations of serum used in the ELISA. Mean values were plotted with error bars illustrating SEM. Data illustrate one experiment performed in duplicate.

After clarification that all antisera recognised cognate peptide, the ability of each antiserum to recognise native protein was assessed in CLDND1-AFP-transfected cells. As the transfected CLDND1 is fused with the fluorescent AFP molecule, the fluorescence of AFP should mirror the antibody staining. The CLDND1-AFP-transfected cells were stained with each of the antisera and positive staining was assessed using fluorescence microscopy by merging the fluorescence of the antisera stain with the AFP fluorescence (Figure 15). Dual fluorescence was detected with all antisera except 2680 and 2682. However, only weak staining was detected with 2679 and 2681 antisera.

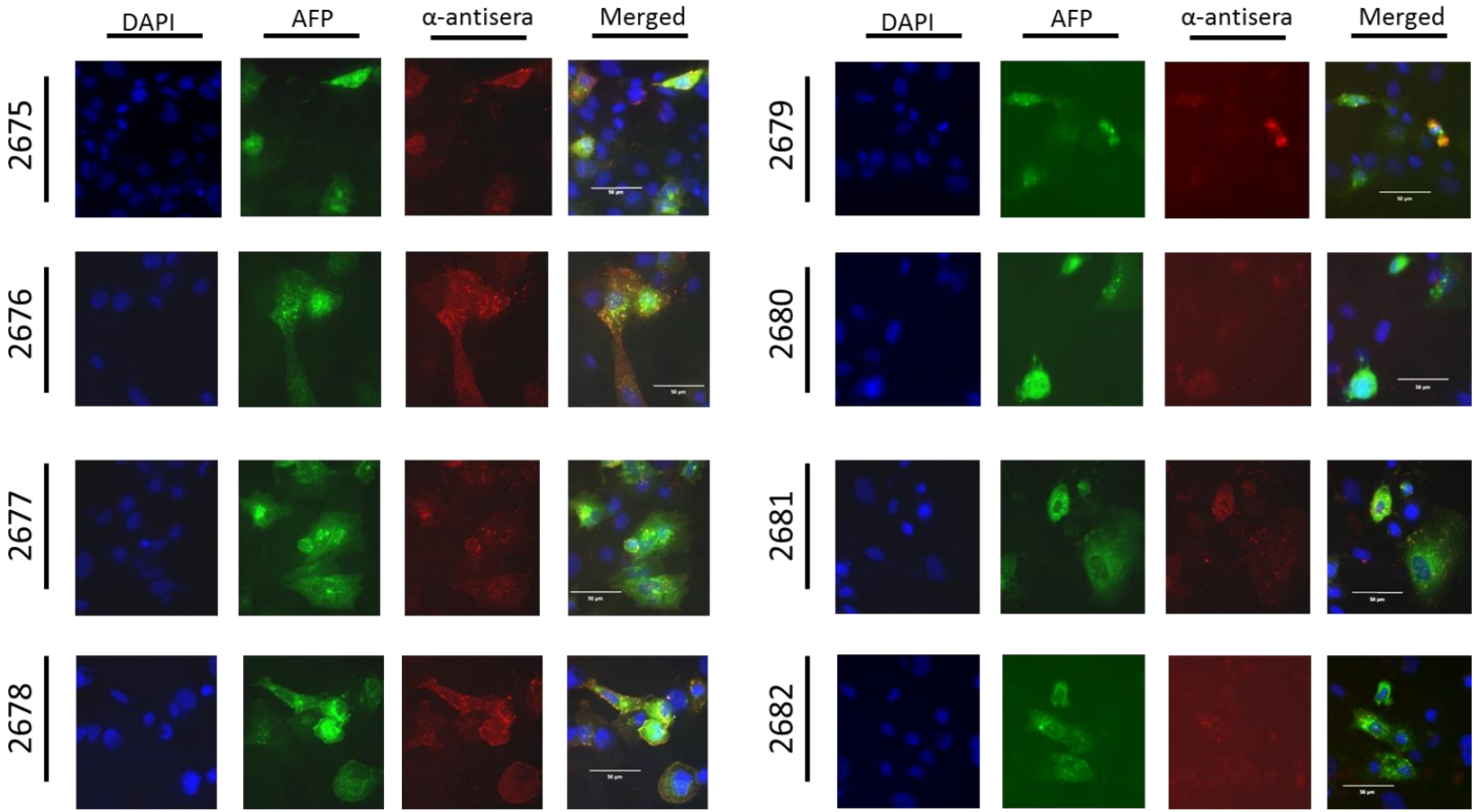

Figure 15. Antisera binding to CLDND1 protein: CLDND1-AFP transfection

SW1353 cells transfected with the CLDND1-AFP vector were fixed and permeabilised prior to staining with DAPI (blue) and antiserum followed by α-rabbit IgG-Alex Fluor® 594 (red). Cells were visualised via fluorescence microscopy and images were merged to assess for co-localisation with AFP fluorescence (green). Data illustrate one experiment.

To confirm the staining wasn't due to antisera binding to epitopes within the AFP molecule, a second construct was used for transfection, CLDND1-FLAG. The availability of robust α-FLAG antibodies allowed for the dual validation of antiserum CLDND1 binding by fluorescence microscopy and by Western blot (Figure 16). 2675, 2676, 2678 and 2681 antisera were tested owing to the most prominent staining with the CLDND1-AFP transfected cells. Additionally, the corresponding presera were also used to stain the western blots to look at non-specific banding patterns.

Immunofluorescence analysis revealed that the four antisera stained the CLDND1-FLAG-transfected cells in the same manner as the α-FLAG antibody, suggesting each antiserum recognised the CLDND1-FLAG protein (Figure 16A). Western blot analysis showed a similar binding pattern of 2675, 2676 and 2678 antisera to the α-FLAG antibody in the CLDND1-FLAG transfected cell lysates (Figure 16B). Interestingly, two bands were identified on the western blot with the α-FLAG antibody. Similar size bands were also identified in the CLDND1-FLAG transfected sample with the 2681 antiserum, yet these bands were present in different proportions to the α-FLAG control.

A similar size band was also present on the 2678 and 2681 preserum blots, suggesting that the bands identified by 2678 and 2681 antiserum may not be CLDND1 specific, or the bands may be masked by non-specific staining at that size. There were no similar banding patterns on the presera blots of 2675 and 2676 as the bands identified on the antiserum blots, strengthening the evidence that these two antisera recognised CLDND1.

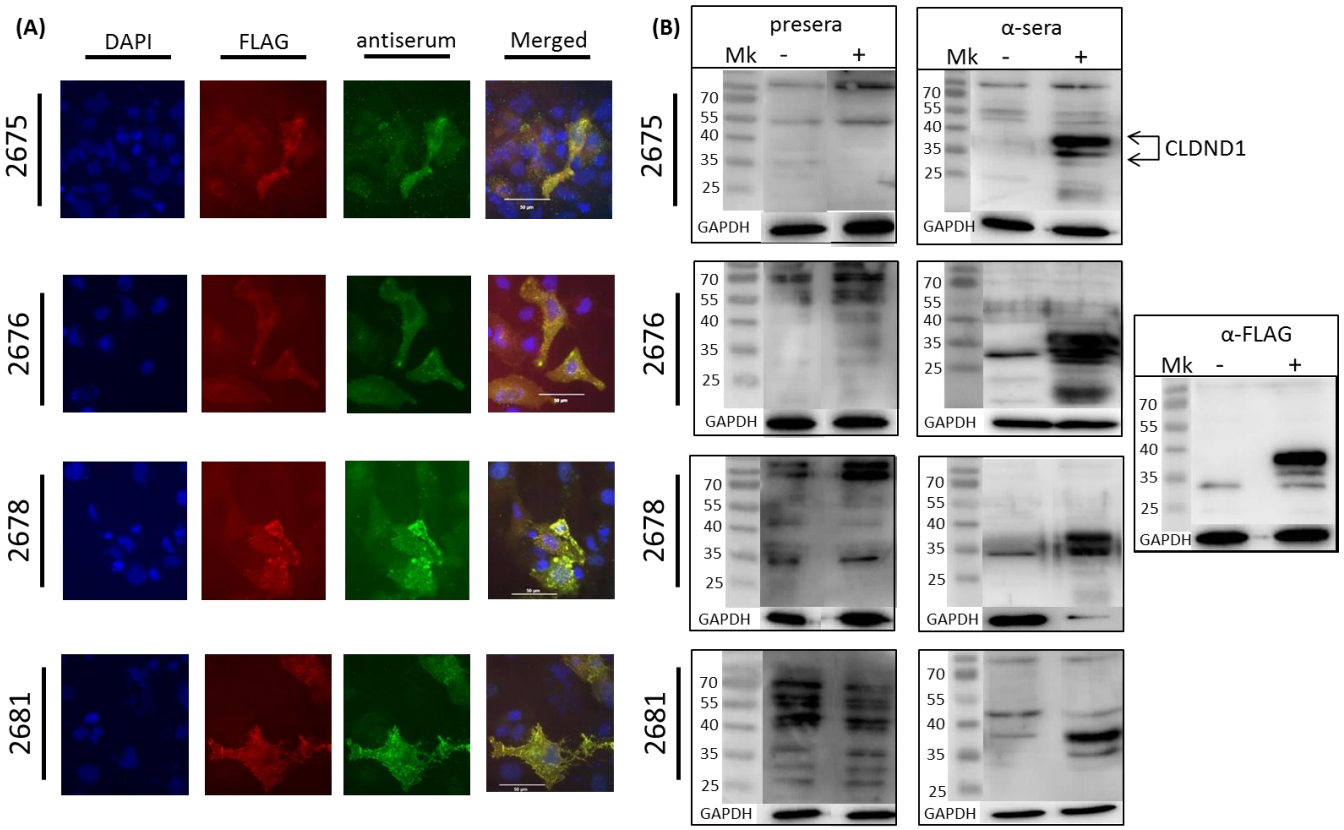

Figure 16. Antisera binding to CLDND1 protein: CLDND1-FLAG

(A) SW1353 cells transfected with CLDND1-FLAG vector were fixed and permeabilised prior to staining with antiserum followed by α-rabbit IgG Alexa Fluor® 488 (green), α-FLAG antibody (red) and DAPI (blue). Cells were visualised by fluorescence microscopy. Images were merged to assess for co-localisation of CLDND1 and FLAG fluorescence (B) Mock transfected (-) or CLDND1-FLAG transfected (+) cell lysate blots were probed with preserum, antiserum or α-FLAG antibody. Protein loading was confirmed with GAPDH. Mk represents protein ladder marker. Data illustrate one experiment.

A definitive way to determine whether an antibody is binding specifically to the target of interest is to block antibody binding with the epitope specific peptide used for the immunisation. The Jurkat T-cell line was transfected with CLDND1-AFP and stained with 2675 or 2676 antisera. Each antiserum was also pre-incubated with CLE11 peptide or the non-epitope specific peptide, CLE12. As 2681 antiserum binding appeared not to recognise CLDND1-FLAG protein, its staining pattern was used as a negative control.

Figure 17 showed that both 2675 and 2676 antisera bound to CLDND1, as double positive staining was seen in the top right hand quadrant of the plot. This staining was not present in the presera samples. After pre-incubation of each antiserum with CLE11, the double positive staining was lost, but staining was still present when each antiserum was pre-incubated with the non-epitope specific peptide, CLE12, showing the specific blocking activity of the peptide. No CLDND1 staining was seen with the negative control antiserum 2681 (Figure 17B), regardless of whether the antibody was pre-incubated with epitope specific peptide, or not.

The double positive staining seen with 2676 antiserum was more pronounced than with 2675 antiserum. There was also an additional population identified with 2676 antiserum in the non-AFP-positive cells (Figure 17A*). An independent finding that CLDND1 is expressed on Jurkat cells (Wollscheid et al., 2009), suggests that the staining seen with the 2676 antiserum is due to native CLDND1 expression on Jurkats. Naturally, as both antisera were used at the same dilution, the differences in staining intensity could have arisen from differences in the proportions of CLDND1 specific antibodies in each antiserum.

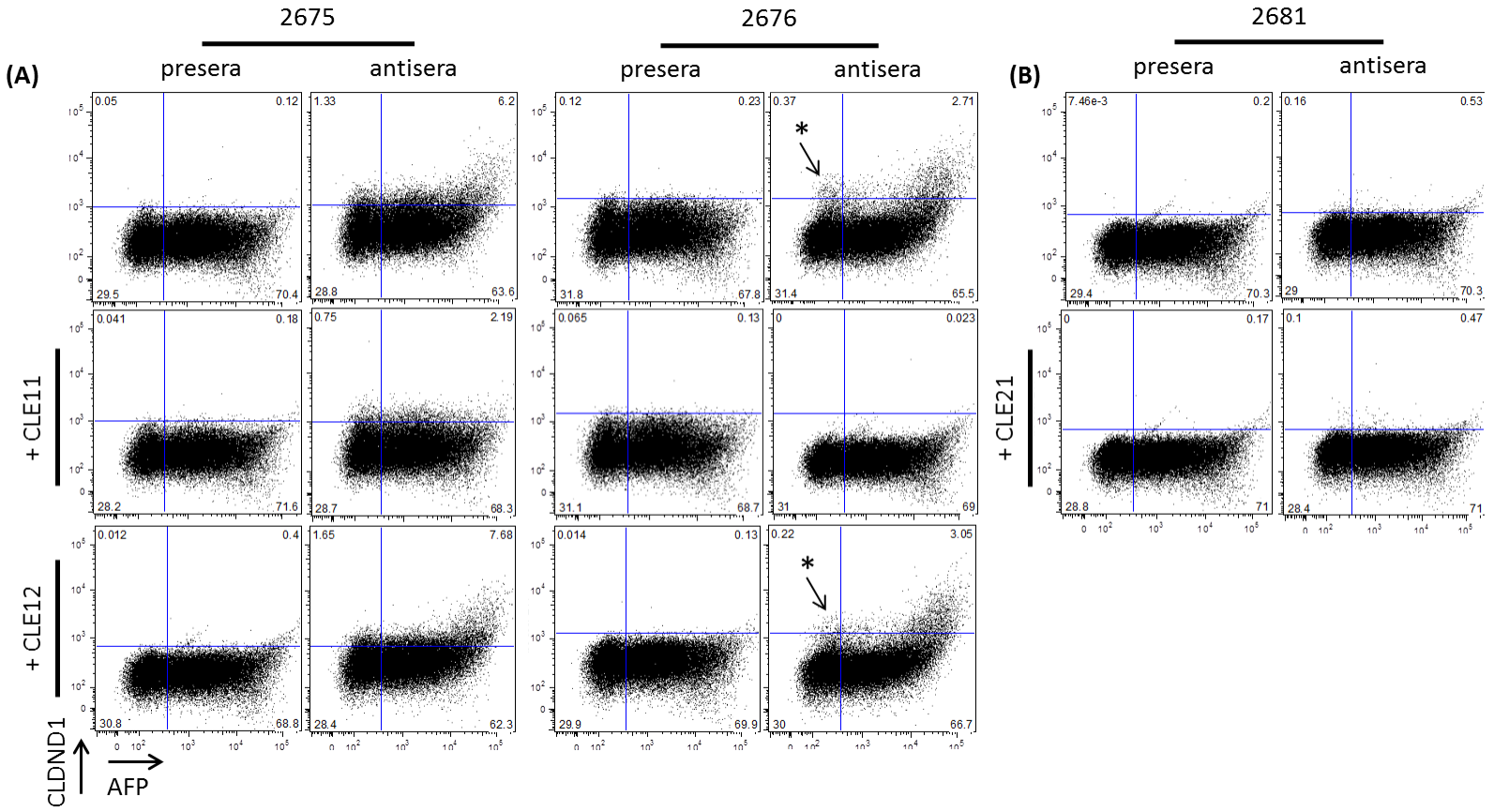

Figure 17. Antisera binding to CLDND1 protein: peptide blocking

CLDND1-AFP transfected Jurkat cells were fixed and permeabilised prior to staining with 2675 or 2676 pre or antiserum (A) pre-incubated with cognate CLE11 peptide or non-cognate CLE21 peptide. (B) 2681 pre and antiserum was used as a negative control and was also pre-incubated with peptide CLE12. AFP and CLDND1 dual staining was assessed by flow cytometry. * possible native CLDND1 expression on Jurkats.

The experiments described above investigated CLDND1 on fixed and permeabilised cells to increase the positive staining intensity therefore endogenous native CLDND1 surface expression was not determined. I therefore sought to determine whether the antisera recognised endogenous native CLDND1 on the surface of Jurkat cells. CLDND1 staining was seen with fixed Jurkat cells, so this population was used as a positive control to determine whether the antisera also bound to native CLDND1 (Figure 18). Fixed Jurkats stained with 2675 and 2676 antisera showed increased CLDND1 staining above each of the preserum, as expected (Figure 18A). No native staining was seen with any of the other sera (data not shown). Comparing the staining profiles of the non-fixed cells identified that although both antisera showed positive staining above the detection antibodies, the intensity of CLDND1 staining in the antisera populations were comparable to each of the presera stains, suggesting that the antisera did not recognise expression of endogenous native CLDND1.

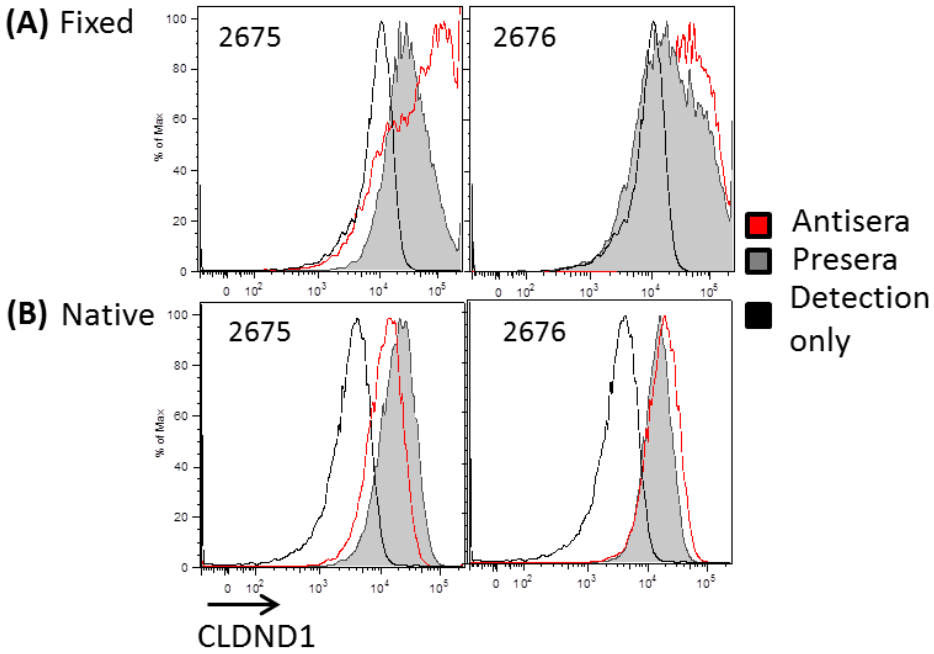

Figure 18. Antisera binding to CLDND1 protein: native versus fixed CLDND1

CLDND1 expression was examined with 2675 and 2676 pre- or antiserum in Jurkat cells that were (A) fixed (B) or not, prior to CLDND1 staining. CLDND1 staining was detected using α-rabbit IgG (H+L) PE conjugated antibody (detection). Staining was assessed by flow cytometry. Data illustrate one experiment.

From the data presented, 2675 and 2676 antisera consistently bound CLDND1 by Western blot and on fixed cells, but not on non-fixed cells so both antisera were used to purify CLDND1 antibodies using a two-step affinity purification method, followed by buffer exchange and concentration.

3.3.3 Purified antibody re-validation

The CLDND1-specific antibodies present in 2675 antiserum were all captured during the affinity purification, as no CLE11 binding activity was detected in the non-column binding FT (Figure 19A). The column-eluted fractions (F1-6) retained α-CLDND1 antibody activity, as these antibodies bound CLE11 peptide in a dose dependent manner in an ELISA based assay (Figure 19B). The amount of CLDND1-specific antibody in the 2676 antiserum was greater than the 2675 antiserum, as CLDND1 peptide binding activity was still seen in the FT fraction (Figure 19A). Although binding activity was detected in the FT fraction, the highest affinity antibodies would have bound and been eluted from the affinity column. Again the eluted 2676 antiserum fractions also retained CLE11 binding activity (Figure 19B).

The purified antibody fractions were pooled, buffer-exchanged and concentrated before analysing antibody integrity by SDS-PAGE. Samples of each of the purified antibodies were loaded under reducing and non-reducing conditions. In the reduced fractions, ratios of the heavy (H) and light (L) chains of antibody are shown (Figure 19C). These proteins migrated to approximately 55 kDa and 25 kDa, respectively (Lewis et al., 2008). The band intensity around 25 kDa was higher in the 2675 purified fraction. As equal concentrations of each antibody were loaded, this suggests that the integrity of the antibodies in 2675 was greater, as individual proteins less than 30 kDa would have been lost during the concentration process, due to the size of the filter. In both fractions, there was a contaminating band around 70 kDa. This molecular weight corresponded to SA monomers that could have disassociated from the affinity purification column.

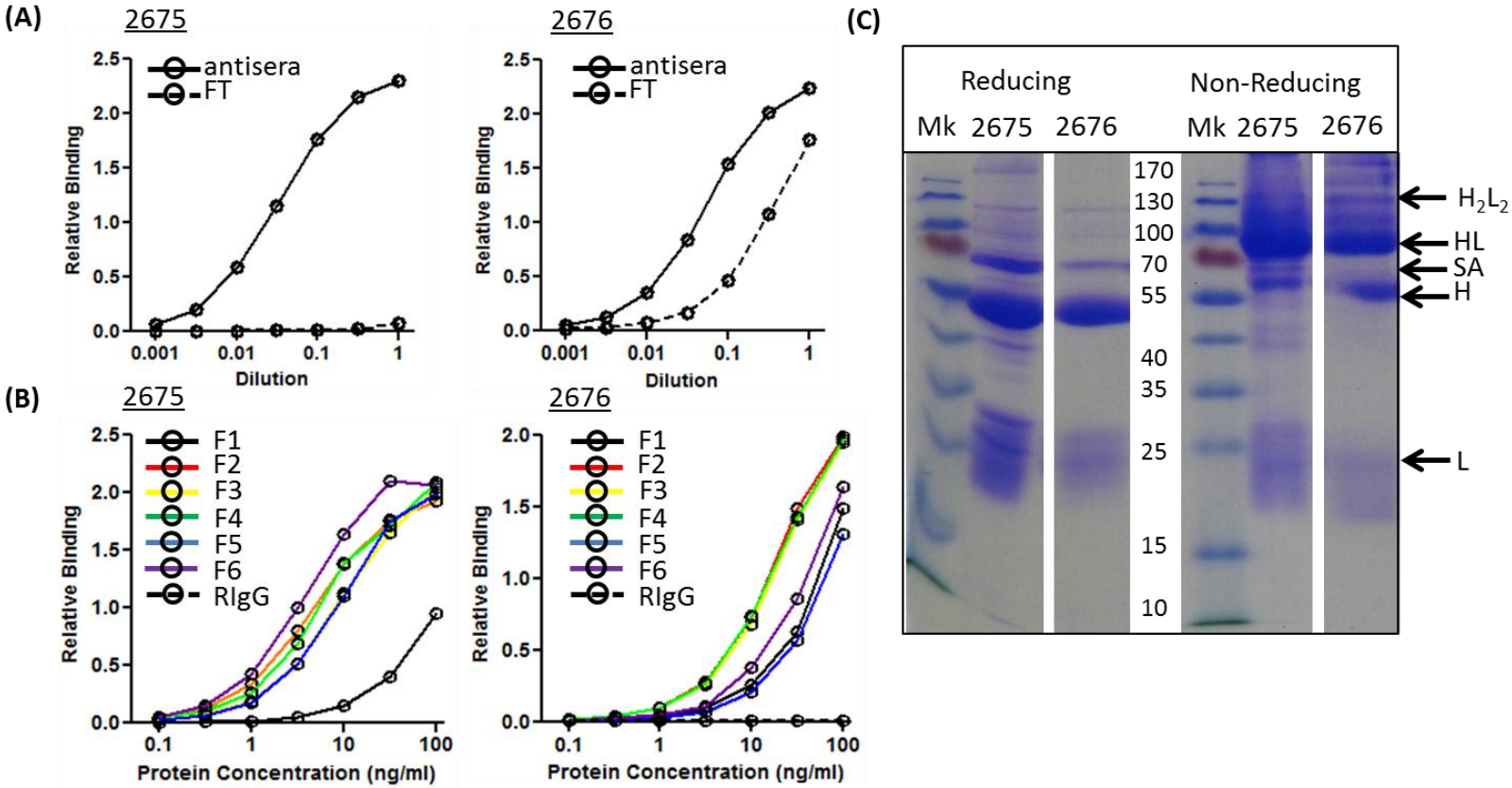

Figure 19. Antisera purification

2675 and 2676 antisera were purified by CLE11 affinity chromatography. (A) Binding of antisera and non-column bound FT to CLE11. (B) Binding of purified fractions (F1-6) to CLE11. (C) SDS-PAGE analysis of purified fractions, under reducing or non-reducing sample conditions. H_2L_2 represents intact antibody, HL represents half an antibody comprising one heavy chain and one light chain, H represents heavy chain monomer and L represents light chain monomer.

Comparison of the non-reduced samples showed that there was relatively little intact antibody (H_2L_2) in either of the purified samples. The low amount of full length antibody present in both the samples may be a consequence of the harsh elution conditions from the affinity purification. The large band that was present between 70-100 kDa may have represented half an antibody structure, comprising one heavy and one light chain (HL) (Beenhouwer et al., 2007). Further analysis of these samples by size exclusion chromatography followed by mass spectrometry would have clarified these bands.

3.3.4 Antibody titrations for experimental techniques

Both the purified antibody samples were re-validated for CLDND1 binding by flow cytometry and Western blot, as per the screening experiments (Figure 20). The intensity of CLDND1 staining was reduced in the presence of cognate peptide (Figure 20A), showing that the purified antibodies were specific to CLDND1, however not all the antibody binding was blocked, suggesting that the amount of CLDND1 antibodies present were greater than in the initial antisera. Western blot analysis identified that the purified antisera had more intense and a sharper staining pattern that the antisera, without emphasising the non-specific bands detected outside the molecular weight range of CLDND1 (Figure 20B). Throughout the antibody validation experiments, 2676 antisera and purified antibody had greater staining intensities and bound to both endogenous and over-expressed CLDND1, so purified 2676, herein referred to as α-CLDND1 antibody, was taken forward for use in all characterisation experiments.

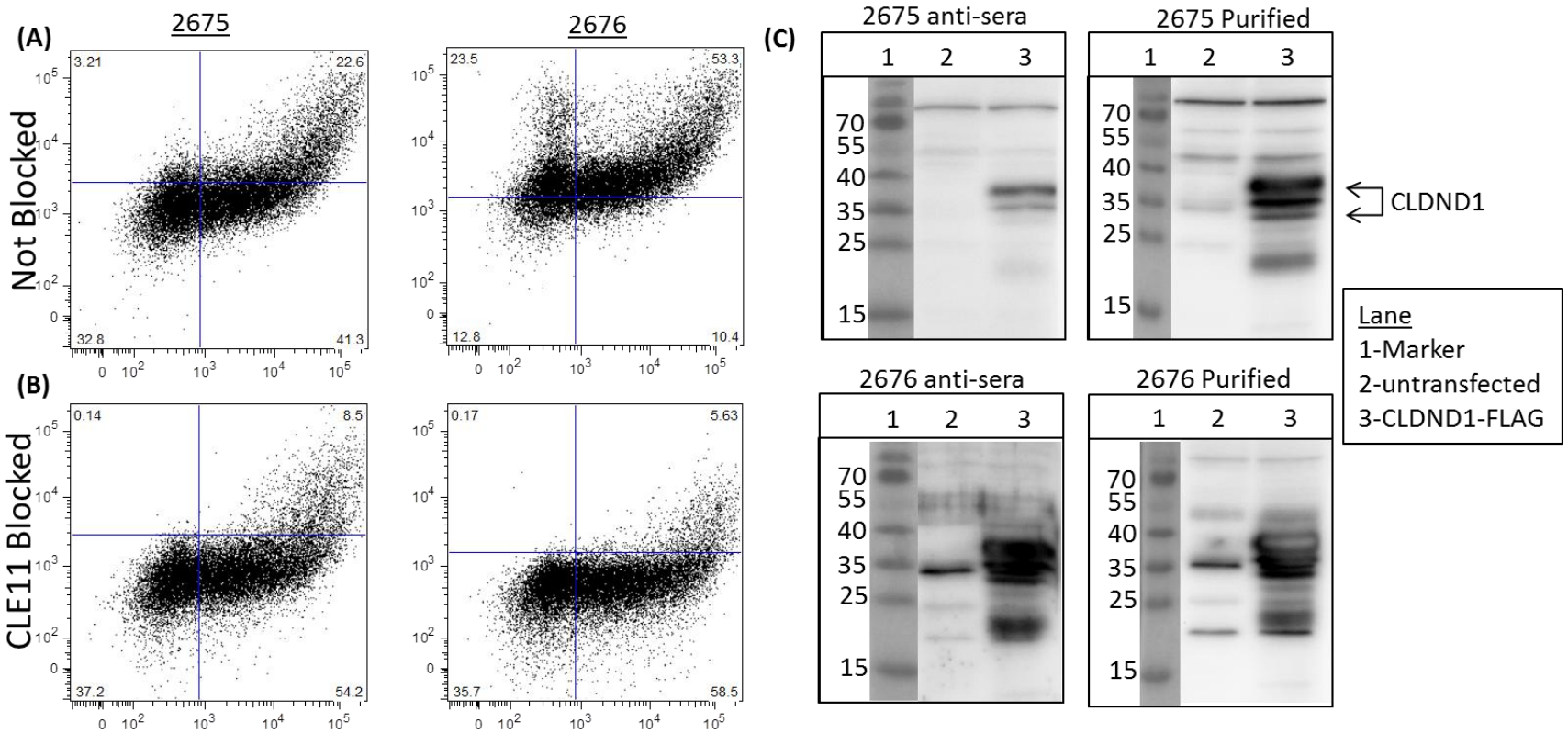

Figure 20. Antibody re-validation

CLDND1-AFP transfected cells were fixed and permeabilised prior to staining with purified antibody (A), or antibody pre-incubated with cognate peptide CLE11 (B). The gate was set on the CLE11 blocked-stained cells for each purified antisera and was copied to the not blocked populations. (C) Western blot of CLDND1-FLAG transfected SW1353 cell lysates probed with antiserum or purified antibody.

Before CLDND1 expression characterisation experiments were performed, optimisations of CLDND1 and detection antibody concentrations were performed for Western blotting to determine the best signal ratio over background. The α-CLDND1 antibody was also pre-incubated with CLE11 prior to Western blot probing to confirm the specificity of the bands identified (Figure 21 and Figure 22). Western blot titrations were performed on lysates from both CLDND1-FLAG-transfected SW1353 cells (Figure 21) and in CD4+ T-cells (Figure 22) as different staining patterns were seen between the two different lysates and confirmation of CLDND1 specificity was therefore required for both cell types. In the presence of a 5 times molar excess of peptide to antibody, all bands seen with the α-CLDND1 antibody were diminished, indicating that all bands identified by the α-CLDND1 antibody were specific to the CLDND1 peptide. Based on the staining profiles seen, a concentration of 1:1000 α-CLDND1 antibody and 1:3000 secondary antibody were chosen for subsequent experiments as these conditions resulted in high CLDND1 staining in both the CLDND1-FLAG-transfected SW1353 cell and CD4+ T-cell lysates, while minimising the excess use of reagents. CLDND1 and detection antibody titrations were also performed for flow cytometry staining (Figure 23). Based on the staining profiles observed, 1 µg of α-CLDND1 antibody and 1:200 dilution of secondary antibody were chosen for subsequent experiments. These conditions enabled the detection of CLDND1 from the secondary antibody only stained control, without using concentrations of both α-CLDND1 and secondary antibody surplus to requirements.

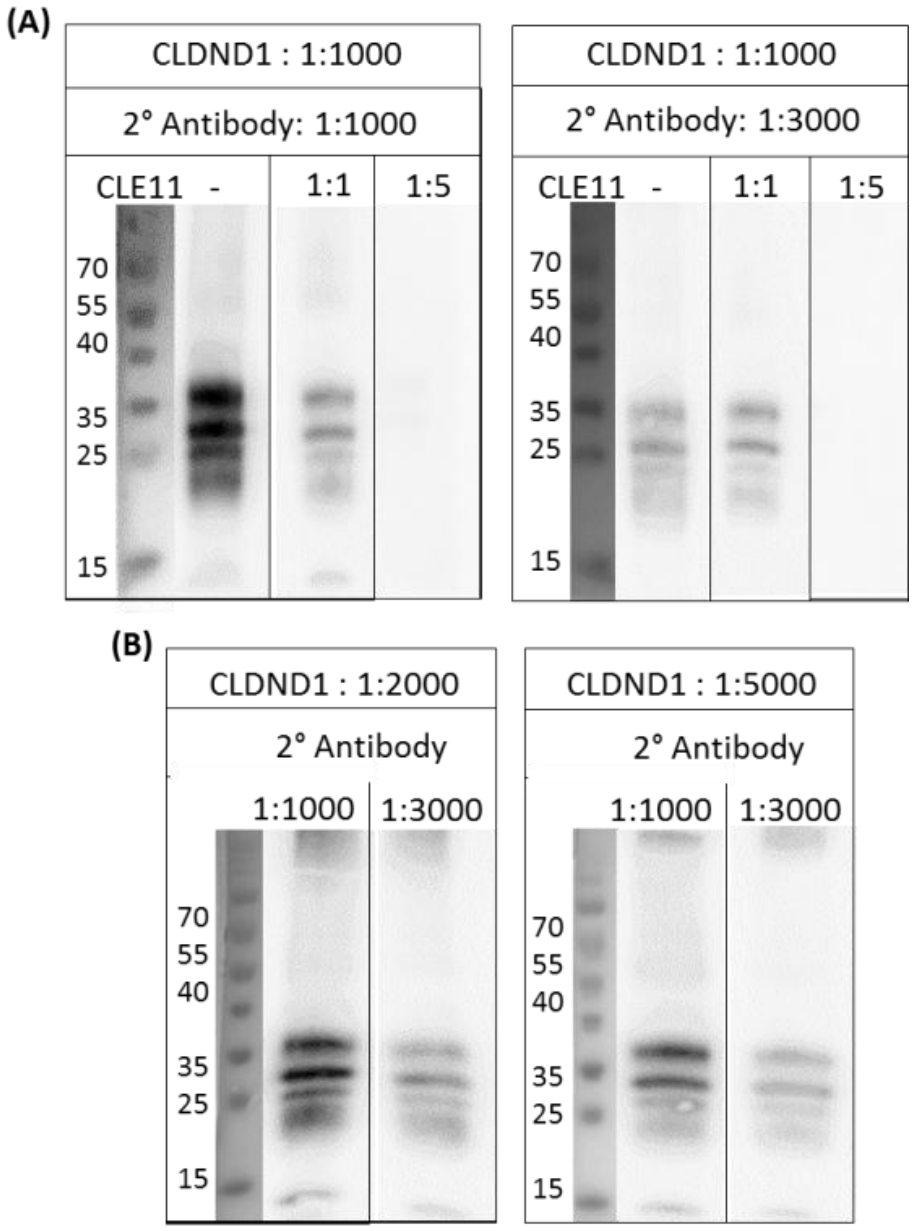

Figure 21. Antibody Western blot titrations: transfected cell lysates

CLDND1-FLAG transfected SW1353 cell lysate Western blots were probed with a 1:1000 dilution of 1 mg/mL α-CLDND1 antibody pre-incubated with none, 1:1 or 1:5 molar ratio of cognate peptide CLE11, followed by differing dilutions of secondary antibody, respectively (A). 1:2000 or 1:5000 dilutions of 1 mg/mL α-CLDND1 antibody were used to probe the Western blots, followed by 1:1000 or 1:3000 dilutions of secondary antibody (B). Data illustrate one experiment.

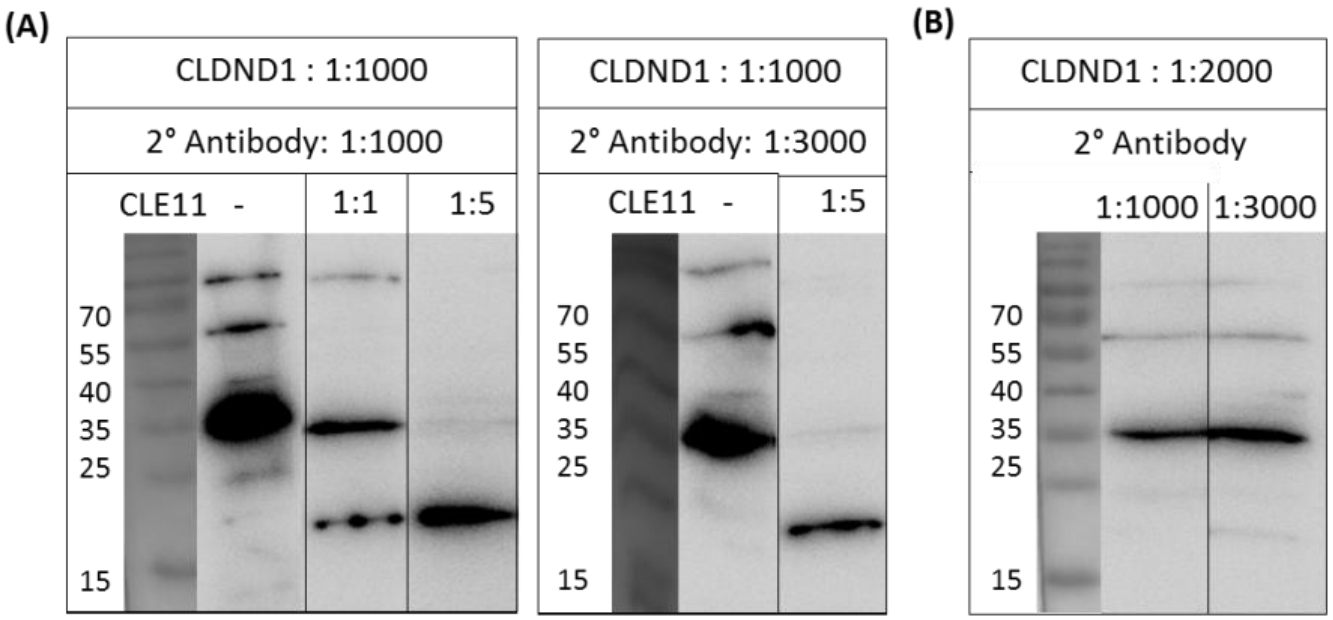

Figure 22. Antibody Western blot titration: CD4+ T-cell lysates

48 hour α-CD3/CD28 expander bead activated CD4+ T-cell lysate Western blots were probed with 1:1000 dilution of 1 mg/mL α-CLDND1 antibody pre-incubated with none, 1:1 or 1:5 molar ratio of cognate peptide CLE11, followed by either a 1:1000 or 1:3000 dilution of secondary antibody, respectively (A). A 1:2000 dilution of 1 mg/ml CLDND1 was used to probe the Western blot followed by either a 1:1000 or 1:3000 dilution of secondary antibody. Data illustrate one experiment.

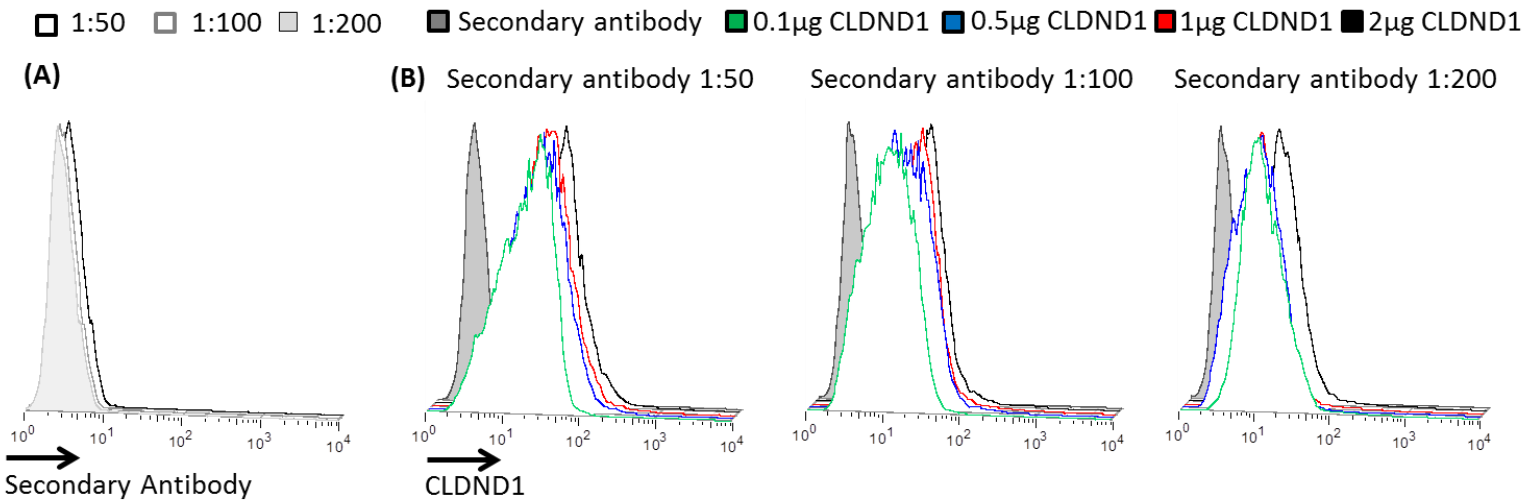

Figure 23. Antibody flow cytometry titrations

FreeStyle™ 293-F cells were stained with varying concentrations of α-CLDND1 antibody (0.1, 0.5, 1 or 2 µg) and secondary antibody (1:50, 1:100 or 1:200 dilution). (A) Concentrations of secondary antibody only. (B) Varying concentrations of CLDND1 and secondary antibody. Data illustrate one experiment.

3.3.5 Immunoprecipitation

IP is one way to potentially determine a function of CLDND1 (as discussed in Section 4.4.2), through the identification of binding partners. IP utilises target specific antibodies to purify out the target from a given preparation, for example a cell lysate. As a CLDND1 specific antibody has been generated, I could potentially use this antibody for IP. Classically, IP utilises the binding characteristics of Protein A or Protein G to IgG molecules, to capture antibody-bait complexes. Since the α-CLDND1 antibody was purified by affinity chromatography, the proportions and activity of the antibody may not be restricted to the IgG subclass, and although the immunisation process will have been designed to maximise IgG production, there may be a possibility that selecting for antibodies using this method may impact negatively on findings. Alternatively, an antibody can be covalenty immobilised to aldehyde-activated agarose resin. Lysine molecules available on amino acid side chains of the antibody react with the aldehyde on the agarose resin, which can be stabilised in the presence of cyanoborohydride. This technique can be applied to any purified antibody sample regardless of species or class of antibody, and so was tested for the α-CLDND1 antibody.

The potential of the α-CLDND1 antibody to bind to endogenous CLDND1 in activated CD4+ T-cell lysates was determined. The reactions were performed in SDS-free conditions, according to manufacturer recommendations. SDS can dissociate disulphide bonds present between antibody chains, so compromising the structural integrity of the antibody. No bands were detected in the fractions eluted from the IP column (Figure 24A, lanes 4 and 5), suggesting that CLDND1 was not bound or eluted, at least not at high enough concentrations to be detected. If bands cannot be detected by Western blot, there wasn't sufficient protein for sequencing analysis. Worryingly, the amount of CLDND1 detected in the cell lysate (Figure 24A, Lane 2) was low compared to other experiments at similar time-points (Section 5.3.1, Figure 39A), which were performed using SDS-containing RIPA lysis buffer. As the IP was performed in SDS-free conditions, there was a concern that CLDND1 may not be sufficiently dissociated from the cell membrane, explaining the low levels detected by western blot.

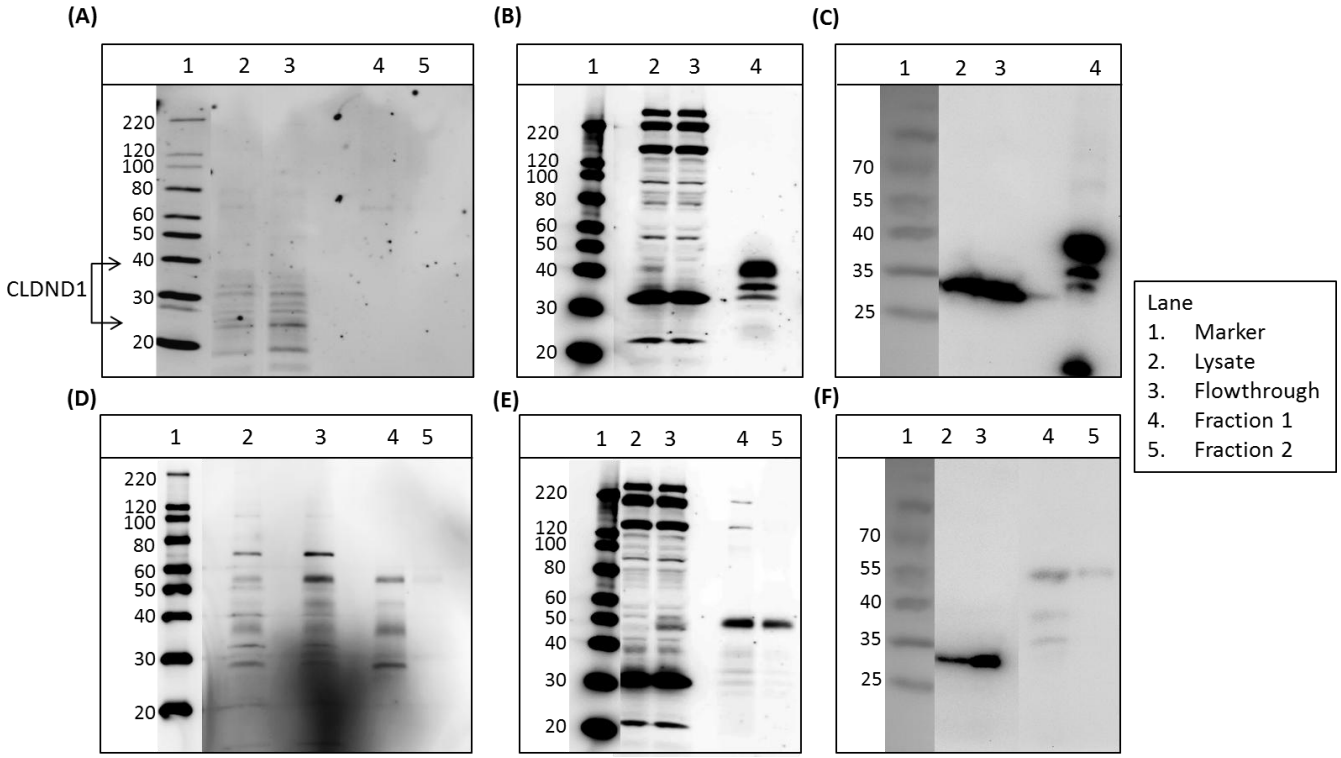

Figure 24. Antibody IP: Western blot analysis

IP were performed on 48 hour α-CD3/CD28 expander bead activated CD4+ T-cell lysates or CLDND1-FLAG transfected Freestyle™ 293-F cell lysates using α-CLDND1 antibody or α-FLAG antibody. (A) Blot probed with α-CLDND1 antibody for CLDND1 antibody IP on CD4+ T-cells under SDS free conditions. (B) Blot probed with α-CLDND1 antibody or (C) probed with α-FLAG antibody for FLAG IP on Freestyle™ 293-F CLDND1-FLAG transfected cells under SDS free conditions. (D) Blot probed with α-CLDND1 antibody for CLDND1 antibody IP on CD4+ T–cell lysates in 0.1% SDS. (E) Blot probed with α-CLDND1 antibody or (F) probed with α-FLAG antibody for scaled-up CLDND1 IP on Freestyle™ 293-F CLDND1-FLAG transfected cells in 0.1% SDS.

In order to determine whether SDS was required for CLDND1 extraction from the cell membrane, an alternative approach was adopted. Throughout this chapter, CLDND1-FLAG-transfected cell lysates have been used to identify the antiserum binding characteristics. FLAG based IP methods were readily available, so as a positive control, FLAG IP was performed on CLDND1-FLAG transfected cell lysates, under SDS-free conditions (Figure 24B). The quantity of CLDND1-FLAG identified in the whole cell lysate was quite low (Figure 24B, Lane 2), yet this population was substantially enriched after the IP (Figure 24B, Lane 4). Similar bands identified by the α-CLDND1 antibody were also detected on Western blots probed with α-FLAG antibody (Figure 24B and C). These findings suggested that SDS was not required for extraction of CLDND1 from cell membranes, and was a reflection of the binding properties of the α-CLDND1 antibody during the IP.

Three cysteines residues are present in the first extracellular loop of CLDND1, which, in other PMP-22/EMP/MP20/claudin superfamily members, form disulphide bridges (Wen et al., 2004). It was hypothesised that disulphide bridges were interfering with α-CLDND1 antibody recognition as the α-CLDND1 antibody epitope lies within CLDND1s first extracellular loop. To try to enhance antibody recognition, 0.1 % SDS was added to the cell lysis buffer and CLDND1 antibody IP was performed on the same activated CD4+ T-cell lysate. Four bands were detected in Western blot of the eluted fraction probed with α-CLDND1 antibody (Figure 24D, lane 4). The two bands that were present at 55 kDa and 25 kDa might have corresponded to α-CLDND1 antibody heavy and light chain monomers, while the band identified near 35 kDa could correspond to CLDND1. Unfortunately, not enough material was recovered to perform protein sequencing.

The requirement for SDS in α-CLDND1 antibody mediated IP meant that the potential to identify CLDND1 binding partners was eliminated, as the SDS would have disrupted any potential interactions. It was still worthwhile performing the CLDND1 antibody IP to confirm the proteins identified by the α-CLDND1 antibody were CLDND1. The CLDND1 antibody IP protocol was scaled up and repeated with CLDND1-FLAG transfected lysate in the presence of SDS (Figure 24E and F). Again, a band was detected at 55 kDa, in both the CLDND1 and FLAG antibody probed western blots. There were also 3 bands

detected on the Western blots in the eluted fraction probed by α-CLDND1 antibody (Figure 24E, lane 4) and two bands in the eluted fraction detected by the α-FLAG antibody (Figure 24F, lane 4) which potentially corresponded to endogenous CLDND1 and transfected CLDND1-FLAG. However, when these samples were analysed by SDS-PAGE and detected using Silver Staining, there were a number of proteins in both the samples (Figure 25). It was not clear which bands corresponded to CLDND1 and so protein sequencing was not performed.

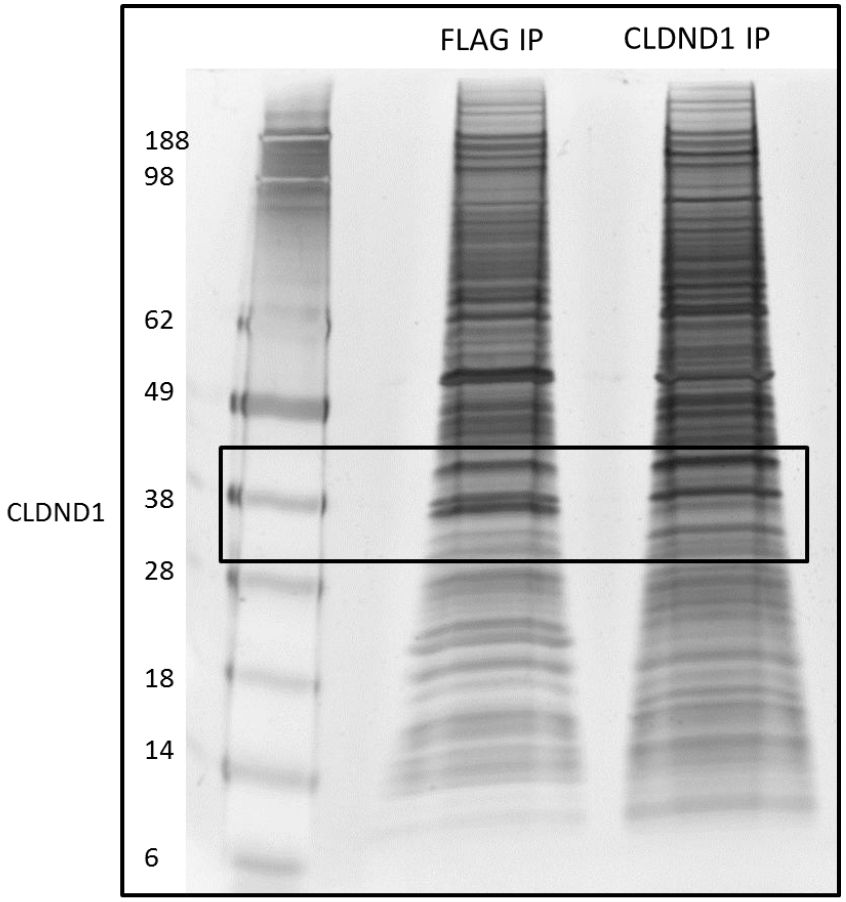

Figure 25. Antibody IP: SDS-PAGE analysis

Eluted CLDND1-FLAG protein IP fractions from the scaled-up CLDND1 and FLAG IP were analysed by SDS-PAGE with silver staining.

3.3.6 Post translational modifications of CLDND1

Throughout this chapter, several bands have been identified around the predicted molecular weight of CLDND1. Some members of the PMP-22/EMP/MP20/claudin superfamily, but not the claudins, have the potential to be N-glycosylated in the first extracellular loop (Maher et al., 2011), and such sites are present in the first extracellular loop of CLDND1 (Figure 7). Therefore the glycosylation status of CLDND1 was examined using PNGase F; an amidase that cleaves between the innermost N-Acetylglucosamine (GlcNAc) and asparagine residues of high mannose, hybrid, and complex oligosaccharides from N-linked glycoproteins (Maley et al., 1989). CLDND1-FLAG transfected SW1353 cell lysates were incubated with PNGase F or with PBS prior to analysing protein banding patterns by Western blot (Figure 26). The three bands usually identified between 30-40 kDa were reduced to one band in lysates pre-incubated with PNGase F. This finding was consistent with CLDND1 being differentially glycosylated, but could only be confirmed through mutational analysis of the potential glycosylation sites.

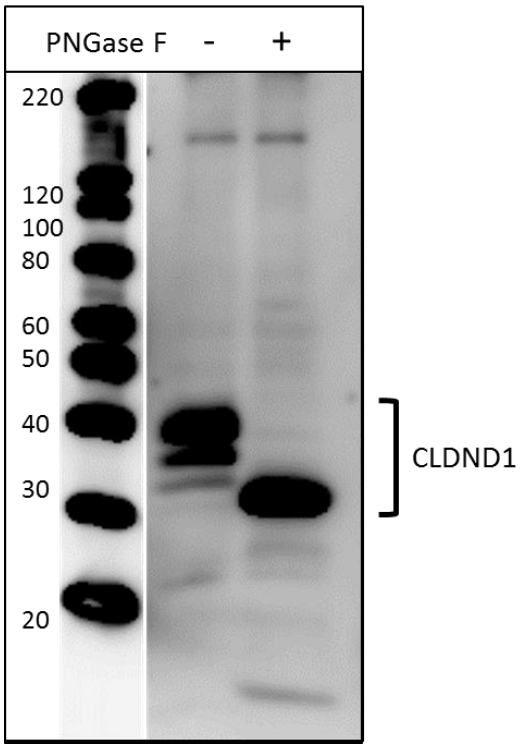

Figure 26. Analysis of glycosylation status of CLDND1

CLDND1-FLAG transfected SW1353 cell lysates were incubated with PNGase F for 1 hour prior to Western blot analysis, probed with α-CLDND1 antibody.

3.3.7 Efforts to generate an antibody to native CLDND1

Based on the data presented in this chapter, it was clear that the α-CLDND1 antibody generated in response to peptide immunisation was not adequate for binding to native CLDND1, limiting the potential use of this antibody in functional studies. The advantages and disadvantages of using full length protein as an immunisation antigen have already been discussed but given that using synthetic peptides for immunisation did not produce antibodies with the correct characteristics, it was worth looking again at the potential to immunise with full length CLDND1 protein. Protocols using full length protein typically use artificially synthesised full length protein with adjuvant as the antigen. However, given the complications associated with isolating transmembrane proteins due to high hydrophobicity and lack of protein structure in the absence of the membranes, cellular immunisation using CLDND1-transfected fibroblasts seemed a better approach. Transfection of the cell surface immunogen into the fibroblasts would increase the likelihood of fully folded protein being expressed on the cell surface, and so produce a native protein conformation against which antibodies could be raised, as part of the humoral immune response.

Four different CLDND1-expressing vectors were generated containing different promoters, with the idea to balance high CLDND1 expression with cell viability. The different vectors were transfected into the rabbit fibroblast cell line, Rab-9, and CLDND1 expression was examined (Figure 27). While there was a slight increase in cell surface expressed CLDND1 in all the transfected populations compared to the mock-transfected population, the increased level of protein expression would not have been substantial enough to generate a sufficient antibody response against CLDND1. On examination of total CLDND1 expression (Figure 27B), there was an increase in CLDND1 expression with all the vectors, in a portion of the population. This staining profile indicated that CLDND1 was not trafficking appropriately to the cell surface.

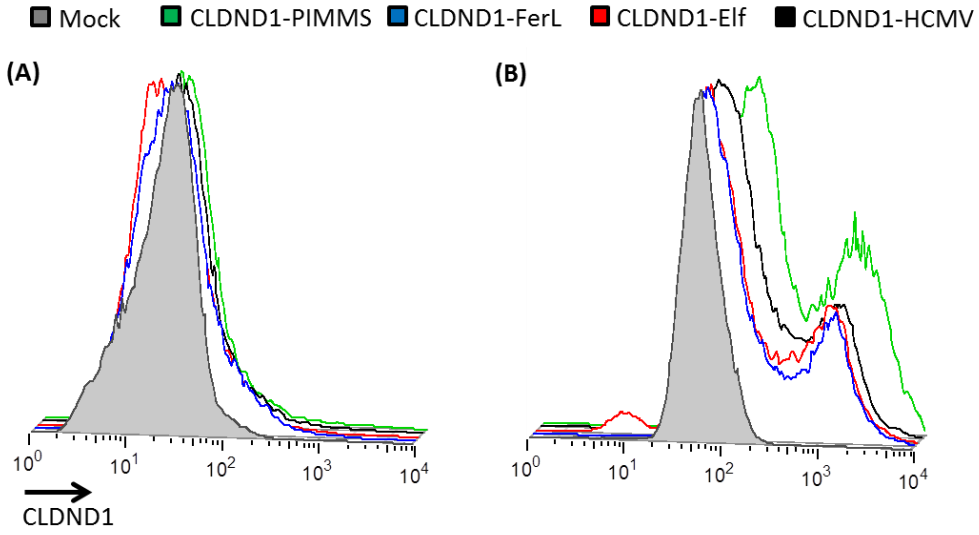

Figure 27. Native CLDND1 immunisations: Rab-9 transfections

The rabbit fibroblast cell line, Rab-9 was transfected with one of the four CLDND1 containing constructs; CLDND1-PIMMS, CLDND1-FerL, CLDND1-Elf or CLDND1-HCMV. 24 hour post transfection cells were fixed and cell surface expression was measured (A), or cells were fixed and permeabilised and total CLDND1 expression was measured (B), by flow cytometry.

CLDND1 cell surface expression was not seen in the Rab-9 fibroblast cell line, so the transfected cells would not make a good immunisation tool. To try to overcome the problem of minimal cell surface CLDND1 expression, protein engineering strategies were approached. Transmembrane proteins can be internalised by clathrin- or caveolin- mediated endocytotic pathways (Lodish et al., 2000b). CLDND1 contains a clathrin-mediated endocytosis signal in its C-terminal tail, suggesting it may be internalised in this manner. Previous studies have shown that protein truncation to remove the clathrin-mediated endocytosis signal allowed for high cell surface protein expression compared to the wildtype protein (Finney, H., UCB Celltech, unpublished data).

Three truncated forms of CLDND1 were cloned into the PIMMS vector backbone (Figure 28A). The CLDND1-trunc construct had an introduced stop codon prior to the YTLM clathrin-mediated endocytosis motif and the CLDND1-GPI1 and CLDND1-GPI2 constructs truncated after the second and first extracellular loops, respectively, and were fused directly to the glycosylphosphatidylinositol (GPI) sequence indicated.

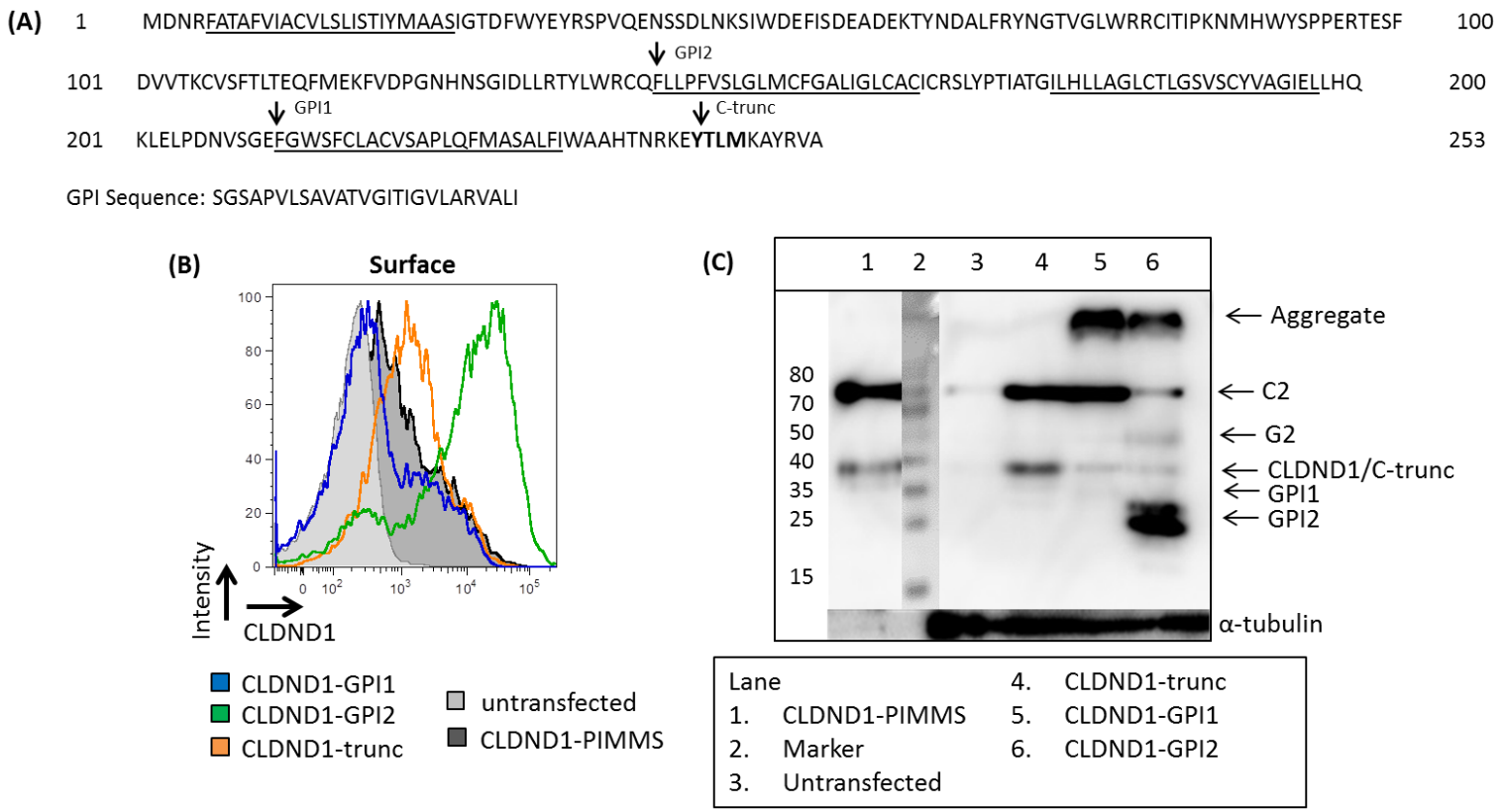

Figure 28. Native CLDND1 immunisations: CLDND1 engineering

Three truncated versions of CLDND1 were made: CLDND1-trunc (C-trunc), CLDND1-GPI1 (GPI1) and CLDND1-GPI2 (GPI2). (A) Mutated CLDND1 construct sequences. Underlined amino acids indicate transmembrane regions. The YTLM sequence is the clathrin-mediated endocytosis signalling motif. Arrows indicate CLDND1 sequence termination for each CLDND1 construct.For C-trunc, a TGA stop sequence was inserted and for GPI1 and 2 the GPI sequence replaced the remaining amino acids. (B) CLDND1 cell surface expression in transfected CD4+ T-cells. (C) Total CLDND1 expression in transfected CD4+ T-cells lysates. Western blot were probed with α-CLDND1 antibody. C2 represents CLDND1/C-trunc/GPI1 dimer, G2 represents GPI2 dimer. α-tubulin was used to control for protein loading.

Construct transfection into primary human T-cells effectively altered CLDND1 cell surface expression (Figure 28B). Removal of the clathrin-endocytosis signal increased the CLDND1 cell surface expression when comparing CLDND1-trunc to full length CLDND1, but removal of both the clathrin-endocytosis signal and the second extracellular loop (CLDND1-GPI1) reverted the surface expression profile back to similar levels of full length CLDND1. Incorporation of a GPI anchor after the first extracellular loop resulted in a large cell surface expression of CLDND1.

Total CLDND1 expression was also examined to determine whether the differences in cell surface expression were due to differences in total protein expression (Figure 28C). Comparable band intensities were seen between full length CLDND1 and CLDND-trunc but no loading control was detected in the full length CLDND1 sample. The reason for this is unknown. Total protein levels were normalised prior to loading on the gel and so may suggest CLDND1 expression was greater with the full length CLDND1 expression vector based on these differences between the loading controls. Overall, the increased cell surface expression of CLDND1 in the CLDND1-trunc cells was not due to increased quantities of total CLDND1 protein in this sample.

The predicted molecular weights for CLDND1-GPI1 and CLDND1-GPI2 are 24 kDa and 16 kDa, respectively. There was marginal CLDND1 expression in CLDND1-GPI1 transfected cells but high expression in CLDND1-GPI2 transfected cells. Two large bands were detected at the top of each lane for both GPI constructs, indicating protein aggregation. In the CLDND1-GPI2 transfected cell lysates, two bands were present, suggesting protein glycosylation. Interestingly, in all the samples there was a band present at approximately double the molecular weight of CLDND1 (Figure 28C, C2) and also a band approximately double the molecular weight of CLDND1-GPI2 (Figure 28C, G2), potentially suggesting dimer formation between CLDND1 proteins. High cell surface CLDND1 expression has been achieved with the CLDND1-GPI2 vector in primary human CD4+ T-cells but in order to test the suitability of this vector for immunisations, transfections still need to be performed in the Rab-9 fibroblast cell line, which is an area for future investigation.

3.4 Discussion

This chapter has followed the binding characteristics of both commercial and in-house generated CLDND1 antibodies. Due to the unsuitability of the commercial antibodies, a decision was made to generate in-house antibodies, so full validation experiments could be performed. These experiments confirmed the generation of a CLDND1 specific antibody for use with Western blotting. The antibody was also suitable for the detection of CLDND1 cell surface expression by flow cytometry, provided the cells were fixed in formaldehyde prior to staining. The antibody has also revealed that CLDND1 exists in a glycosylated state, yet mutational analysis would be needed to confirm the glycosylation sites. The results obtained have given some insight into the potential structures and functional qualities of CLDND1. Both points will be discussed below.

3.4.1 Formaldehyde fixation and CLDND1 structure

A confounding finding in this chapter is the ability of the α-CLDND1 antibody to recognise CLDND1 in its fixed conformation but not in its native conformation. As the antibody was raised against a linear epitope, this would suggest that the extracellular loop in its native state is arranged in such a way that the epitope is not available for antibody binding; but on the addition of formaldehyde, this region becomes available for antibody binding.

Formaldehyde is known to cause four different modifications on proteins: hydroxyl methyl (methylol) adducts, Schiff base adducts, 4-imidazolidinone adducts and methyl bridges. Formaldehyde can react with primary amines (lysine) and thiol groups (cysteine) to form metholyl groups. The methylol groups can then cross-link with the nucleophiles tyrosine, arginine, asparagine, glutamine, histidine, and tryptophan. 4-imidazolidinone adducts form at the N-terminal site of proteins (Metz et al., 2004, Fowler et al., 2011), and so are unlikely to be involved in the α-CLDND1 antibody mechanism. The consequences of these reactions are well documented in immunohistochemistry leading to epitope masking and loss of antibody signal (Fritschy, 2008); yet conversely, the α-CLDND1 antibody binds in the presence of formaldehyde fixation, which is a less well documented phenomenon and indicates a mechanism that opens up the CLDND1 extracellular loop structure to allow for α-CLDND1 antibody binding.

Aqueous formaldehyde primarily exists in the form of methylene glycol, which alters protein tertiary structure by two mechanisms: promoting protein unfolding by weakening the hydrophobic stability of the protein core; or inducing β-sheet secondary conformation through interactions with the protein backbone, thus causing a collapse of the tertiary structure (Fowler et al., 2011). Either mechanism may explain CLDND1 epitope exposure during fixation. This information may also indicate a predominantly α-helical secondary structure in the first extracellular loop of CLDND1, yet to prove this, structural techniques such as x-ray crystallography would need to be performed.

An alternative suggestion which enables α-CLDND1 antibody binding after formaldehyde fixation includes steric-hindrance or epitope sequestration by CLDND1-protein binding partners. Formaldehyde fixation may act on the CLDND1-binding partner(s), disrupting their conformation and allowing access for the α-CLDND1 antibody, although there is little evidence in the literature to support this model.

3.4.2 CLDND1 glycosylation states

Western blot analysis of CLDND1-transfected cell lysates confirmed CLDND1 exists in different glycosylation states, which is consistent with several of the PMP-22/EMP/MP20/claudin superfamily members. The family member sharing the most homology to CLDND1, TMEM114, demonstrates glycosylation which is critical for cell surface location (Maher et al., 2011). The importance for glycosylation to help maintain TMEM114 protein stability and folding (Lodish et al., 2000a), was not addressed and, therefore may account for the phenotype observed. Mutational analysis of the sequence of CLDND1 would confirm whether glycosylation is important for its cellular distribution, but the effects of glycosylation on CLDND1 stability would need to be controlled for.

A band of approximately double the molecular weight of CLDND1 was observed during Western blot analysis of CLDND1-transfected CD4+ T-cells, which was CLDND1 specific. These bands were also detected with the SIGMA and Santa Cruz antibodies during the commercial antibody validation. Independent studies in the PMP-22/EMP/MP20/claudin superfamily members, integral plasma membrane protein (IP) 39 and PMP-22, detected protein dimer formation by Western blot (Suzuki et al., 2013, Mobley et al., 2007), suggesting that CLDND1 may also exist in dimers.

3.4.3 Rate-limiting factors for antibody generations

One of the main limiting factors at the start of the project was the lack of evidence supporting CLDND1 protein expression in different cell types, which could have been used for the screening of both the commercial and in-house antibodies. At the time the experiments were undertaken, the choice to use CLDND1-transfected cells was most suited to assess for antibody binding. Alternatively, rat optic nerve cells or cultured oligodendrocytes (Fayein et al., 2002) from where CLDND1 was originally discovered could have been used; yet protein expression was also not confirmed in these cells. The lack of experimental data assessing CLDND1 protein expression meant that robust validation techniques were required to identify true CLDND1 staining. The variety of techniques and experiments performed in this chapter has validated 2676 antiserum as a CLDND1 binder.

CLDND1-transfected cells were the most suited tool for screening α-CLDND1 antibody specificity, but in the absence of a direct way to detect over-expressed CLDND1 protein, a CLDND1-AFP fusion protein was instead used to indirectly detect CLDND1, through AFP expression. The large AFP molecule shares a similar molecular weight to CLDND1 and raised potential issues with proper CLDND1 protein folding and trafficking to the cell surface membrane. Consequently, the CLDND-AFP transfected cells were fixed and permeabilised to help achieve the greatest intensity of staining over the high non-specific background binding of the preserum. Unfortunately, screening by this technique identified antibodies which only recognised fixed-conformation CLDND1.

During the in-house α-CLDND1 antibody validation experiments, all antiserum binding was compared to the corresponding preserum, acting as a control. Upon purification of the CLDND1-specific antibodies, there was no equivalent isotype control as rabbit serum would contain a lot more non-specific binding properties than the purified antibody samples. Ideally, purification of antibodies from scrambled peptide sequence immunisations would have provided a similar preparation to the purified antibody to use as an isotype control. As a result, the percentage of CLDND1 positive cells was only determined by using fluorescence minus one (FMO) analysis.

In retrospect, some of the commercial antibodies displayed similar binding properties as the in-house antibody, in particular the SIGMA antibodies, and

could potentially have been used as a positive control to screen for CLDND1 binders. These antibodies however, were not used for this purpose as the quantities required for staining were large and not cost effective.

For future immunisation strategies, it is a prerequisite to consider CLDND1 cell surface expression in Rab-9 rabbit fibroblast cells. The lack of cell surface CLDND1 expression seen may reflect the cell culture techniques: Rab-9 cells are an adherent cell line and require Accutase® treatment to remove them from tissue culture flasks. Accustase® treatment may have cleaved CLDND1 from the cell surface. Additionally, CLDND1 staining reflects one time-point, which may not represent normal CLDND1 expression profiles. The use of live cell imaging would resolve this issue, but would first require generation of a native-CLDND1 binding antibody. Understanding this pathway could also infer mechanisms regarding CLDND1 regulatory mechanisms by cellular location.

In conclusion, the generation of in-house antibodies has provided insight into potential CLDND1 extracellular loop structures and although these antibodies could not be used functionally, they have highlighted other strategies for production of functional antibodies, along with interesting features of the CLDND1 protein, which can be validated with further studies.

Chapter 4. Optimisation of CD4+ T-cell siRNA Transfection

4.1 Aims

The aim of this chapter was to identify a role for CLDND1 in the regulation of T-cell activation by assessing the phenotype of CD4+ T-cells lacking endogenous CLDND1, targeted by short interfering RNA (siRNA). Firstly, a procotol for siRNA transfection needed to be optimised. At the time, due to a lack of a CLDND1-specific antibody, CLDND1 silencing was measured by qRT-PCR and protein silencing was assessed using siRNA and a monoclonal antibody against CD4. In CLDND1 silenced cells, T-cell proliferation was measured in response to α-CD3/CD28 expander bead stimulus along with their pro-inflammatory cytokine profile.

4.2 Introduction

CLDND1 function remains elusive owing to a lack of published evidence in any cell type. A regulatory function in CD4+ T-cells has been hypothesised from preliminary studies on the CD4+ T-cell clone, HA1.7, which showed lower levels of CLDND1 transcript in activated compared to anergic cells (Figure 6). Other suggestions for CLDND1 function have been predicted based on homology to the PMP-22/EMP/MP20/claudin superfamily. The claudins are important structural components of TJ, as well as mediating inter-cellular communication through signalling via the ZO protein family. Different claudins have been shown to interact homotypically and heterotypically with other claudin family members and these interactions impart specific function (Angelow et al., 2008).

4.2.1 RNA interference

RNA interference (RNAi) is evolutionary conserved in eukaryotes and has an essential role in the clearance of viral RNA. The effect of double stranded RNA (dsRNA) on the translational efficiency of messenger RNA (mRNA) was first described in *Caenorhabditis elegans* (Montgomery et al., 1998) and subsequent experiments unravelled the mechanism involved (Kurreck, 2009). In brief, dsRNA is processed by Dicer into siRNA around 21 nucleotides in length with 3' unpaired ends. Once unwound, the siRNA duplex guides the RNA induced silencing complex (RISC) to complementary target mRNA. Site specific cleavage of the mRNA occurs 10 nucleotides from the 5' end of the siRNA

strand by the catalytic component Argonaut 2 (Valencia-Sanchez et al., 2006). Post cleavage, the RNA is degraded by cellular exonucleases such as XRN1 or the exosome (Orban and Izaurralde, 2005).

Early use of this technique in mammalian cells proved problematic as dsRNA sequences over 30 nucleotides in length mediated biological responses against the dsRNA, known as the interferon response, where general RNA degradation and shutdown of cellular processes occurs. The subsequent discovery that 21-nucleotide siRNA could be transfected into cells while evading host responses, minimised off-target effects (Elbashir et al., 2001).

4.2.2 Current CD4+ T-cell siRNA transfection techniques

The prevalent transient transfection method of primary human CD4+ T-cells is electroporation: a transfection technique where the cell membrane phospholipid bilayer is disrupted by electrical pulses. Temporary pores are formed, through which small molecules such as DNA can pass into the cell. While nucleofection, a trade name for electroporation, is versatile and can be used with many cell subsets, it results in high cell toxicity and allows non-specific transport of material both in and out of the cell, which can lead to ion imbalance (Weaver, 1995).

4.2.3 Accell siRNA

Dharmacon offer a variety of different siRNA and transfection moieties. Their Accell siRNA range is specifically designed for use with difficult to transfect cell types, such as primary human T-cells. Dharmacon claim Accell siRNA can achieve “delivery into difficult-to-transfect cells without additional reagents, virus, or instruments”. The modifications to the siRNA to facilitate transfection are novel and proprietary, but claim to facilitate siRNA stability and uptake while maintaining specificity and knockdown efficiency.

Several recommendations are provided when using this product. Firstly, Accell siRNA works at a 1 µM working concentration, higher than conventional siRNA. Secondly, siRNA delivery may be inhibited by the presence of BSA in serum, so transfection with serum-free media formulations or less than 2.5 % serum in standard media are recommended. Dharmacon claim optimal mRNA silencing is typically achieved by 72 hours, or up to 96 hours for protein knockdown.

4.3 Results

4.3.1 CD4+ T-cell isolation methods

A highly pure isolated CD4+ T-cell population was required for the siRNA transfection experiments to prevent contaminating cells skewing any data interpretation. There are several methods for isolating CD4+ T-cells from whole blood, which fall under two categories: positive selection, where the cells of interest are selected using a specific cell surface marker; or cell enrichment, where undesired cells are depleted from the population, leaving an untouched cell population of interest. Three different CD4+ T-cell isolation protocols were therefore tested, monitoring CD4+ T-cell purity, CD14 contamination and cell viability (Table 12). CD14 contamination was monitored as monocytes express low levels of CD4, and so can be co-purified with CD4+ T-cells during positive selection. The highest percentage of CD3+/CD4+ cells (98.3%) were isolated using StemCell positive selection, followed by Miltenyi CD4 positive selection (94%). The lowest purity was obtained using StemCell CD4 enrichment (85.4%); however this protocol also had the lowest monocyte contamination (1.15%). The Miltenyi CD4 positive selection had the highest monocyte contamination (2.31%). Viability of the purified cell population was comparable between the different isolation methods. The StemCell CD4 positive selection method was chosen due to the high purity of the isolated CD4+ T-cell population.

Isolation method	CD3/4+ (%)	CD4/14+ (%)	Viable (%)
StemCell CD4 positive selection	98.3	1.24	96.3
Miltenyi CD4 positive selection	94	2.31	96.3
StemCell CD4 enrichment	85.4	1.15	97.6

Table 12. CD4+ T-cell isolation methods

CD4+ T-cells were isolated from PBMC using Miltenyi CD4 positive selection, or from whole blood for StemCell positive selection and enrichment. Isolated populations were stained for CD3, CD4 and CD14 expression and viability determined with Annexin V and Via-Probe™.

4.3.2 Cell culture media optimisation

After cell isolation but prior to transfection, Dharmacon recommend resting the cells by incubating them overnight. Two different cell culture media were tested for the rest incubation and the 72 hour transfection period: RPMI supplemented with 5 % FBS, 100 U/ml penicillin, 100 µg/ml streptomycin and 2 mM L-glutamine, followed by RPMI supplemented as above but without FBS for the siRNA transfection period (RF-5/RF-0), against Xv15, a serum free T-cell medium. The RF-5/RF-0 media were used for comparison based on previous work (Crossland, K., 2010 Masters Dissertation).

Transfection efficiencies for the RF-5/RF-0 and Xv15 media were examined using siGLO positive control siRNA (Figure 29). Dharmacon siGLO siRNA is a non-targeting (NT) positive control siRNA, labelled with Dy-547, a red fluorophore similar to PE. Transfection efficiencies using siGLO siRNA were equivalent with RF-5/RF-0 and Xv15 (Figure 29A). To determine the siRNA efficiency to silence protein, CD4 was used as a positive control and targeted using Accell CD4 SMARTpool siRNA (Figure 29B-E). Previous studies have shown that CD4 can be successfully targeted with siRNA in mouse CD4+ T-cells (Mantei et al., 2008) and both CD4 mRNA and protein are easy to measure, due to high expression on CD4+ T-cells.

CD4 mRNA levels were significantly reduced in both RF-5/RF-0 and Xv15 media when normalised to the untransfected control (Figure 29B-C) (68 % in RF-5/RF-0 media compared to 50 % in Xv15). The reduction in CD4 mRNA also translated to a reduction in CD4 protein. Using GMFI to quantify CD4 protein, a 61 % or 55 % decrease in CD4 was seen for RF-5/RF-0 or Xv15, respectively. Although there was a greater reduction in CD4 protein in RF-5/RF-0, the reduction in CD4 protein was more consistent between experiments in Xv15. Untransfected cells had a more uniform expression of CD4 in Xv15 compared to RF-5/RF-0, identified by the single peaked histogram (Figure 29D).

T-cell recovery after culture in RF-5/RF-0 or Xv15 was better with Xv15, after the rest incubation (Figure 29E). Post 72 hour siRNA transfection, there were significantly more cells recovered in Xv15 than RF-5/RF-0. The presence of siRNA in either culture did not affect CD4+ T-cell recovery. Xv15 was chosen for all subsequent transfection experiments.

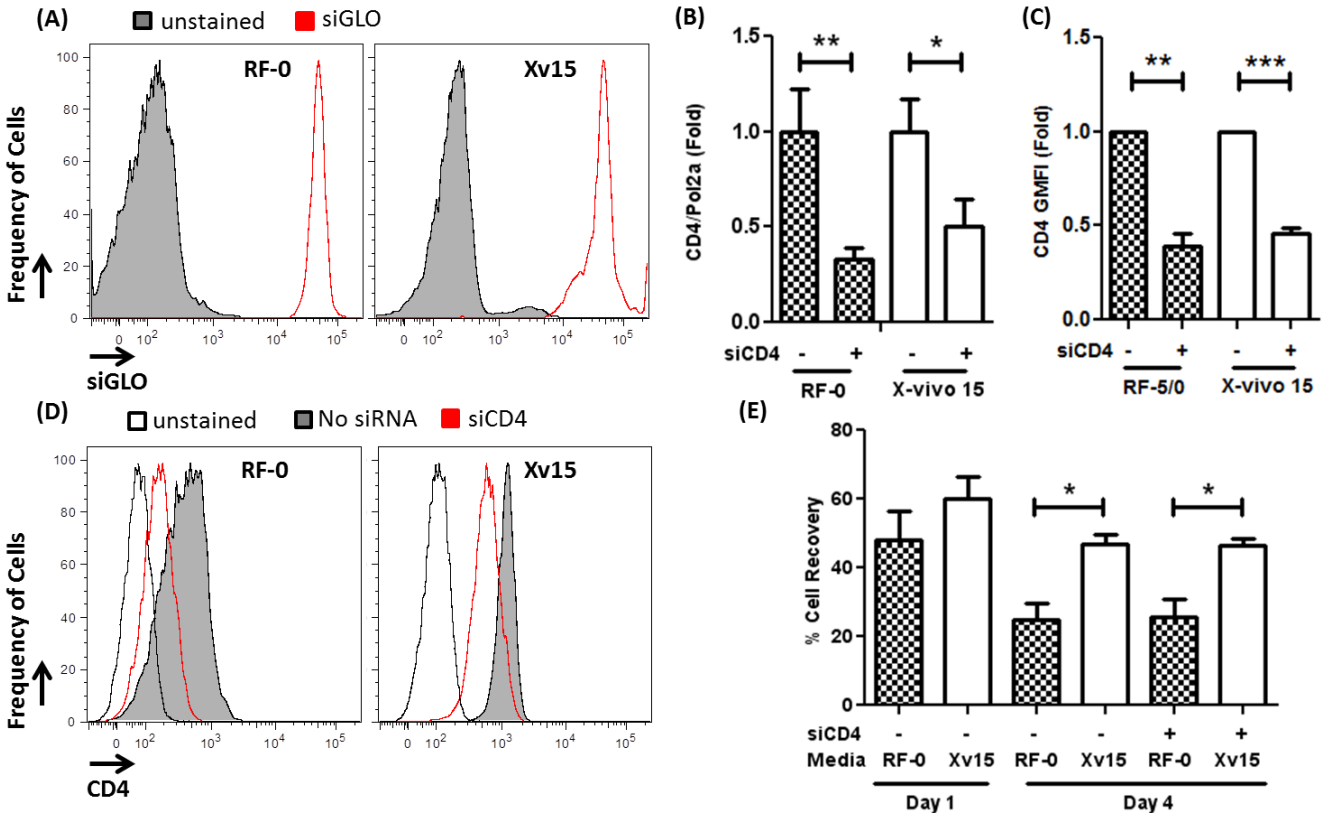

Figure 29. Accell siRNA transfection: cell culture media optimisation

Positively isolated CD4+ T-cells were incubated in RF-5/RF-0 or Xv15 media in the presence of 1 µM Accell siRNA for 72 hours. (A) Histogram illustrating data from one siGLO siRNA transfection experiment. Cells were incubated with CD4 SMARTpool siRNA. (B) CD4 mRNA levels were detected by qRT-PCR and normalised to pol2a. (C) CD4 protein levels were determined by GMFI. (D) Representative histogram of CD4 fluorescence on CD4 siRNA transfected cells or untransfected cells. (E) Cell recovery was assessed during the transfection protocol. Data illustrate at least 3 independent experiments. Mean values were plotted with error bars illustrating SEM. Student's t-test analysis was performed. *p<0.05, **p<0.01, ***p<0.001.

4.3.3 siRNA transfection protocol optimisation: manufacturer recommendations

Although introduction of siRNA into immune cells is thought to bypass the interferon response, there have been reports that siRNA can actually trigger immune activation (Sioud, 2010). NT siRNA was therefore required to account for any off-target effects on T-cell function. Dharmacon offer four NT Accell siRNA. These siRNA were tested with CD4 SMARTpool siRNA (Figure 30). A significant reduction in CD4 mRNA was still achieved when normalising CD4 mRNA levels in the NT 2, 3 and 4 siRNA samples. Contrary to the initial findings (Figure 29B), silencing was not reproduced using the no siRNA control (Figure 30A), suggesting variability between experimental replicates. The reduction in CD4 mRNA seen in the CD4 siRNA sample compared to NT 2, 3 and 4 siRNA did not translate to an equivalent reduction in CD4 protein (Figure 30B), although protein levels were lower than control siRNA. The only significant reduction was found when normalising CD4 protein levels to the no siRNA control, indicating CD4 protein levels were lower in the NT siRNA samples compared to the no siRNA sample.

All four NT siRNA and no siRNA were used as controls to validate the four CLDND1 Accell siRNA (C1-4). C1 and 2 siRNA bind within the CLDND1 ORF and CLDND1 siRNA 3 and 4 bind in the 3' UTR (Appendix Figure 1). Post siRNA transfection, no consistent reduction in CLDND1 mRNA in the C1-4 siRNA samples were seen when CLDND1 mRNA levels were normalised to any of the NT siRNA CLDND1 mRNA values (Figure 30C). There were large differences in relative CLDND1 mRNA expression in the C1-4 siRNA samples depending on the CLDND1 mRNA values used for normalisation from each control siRNA.

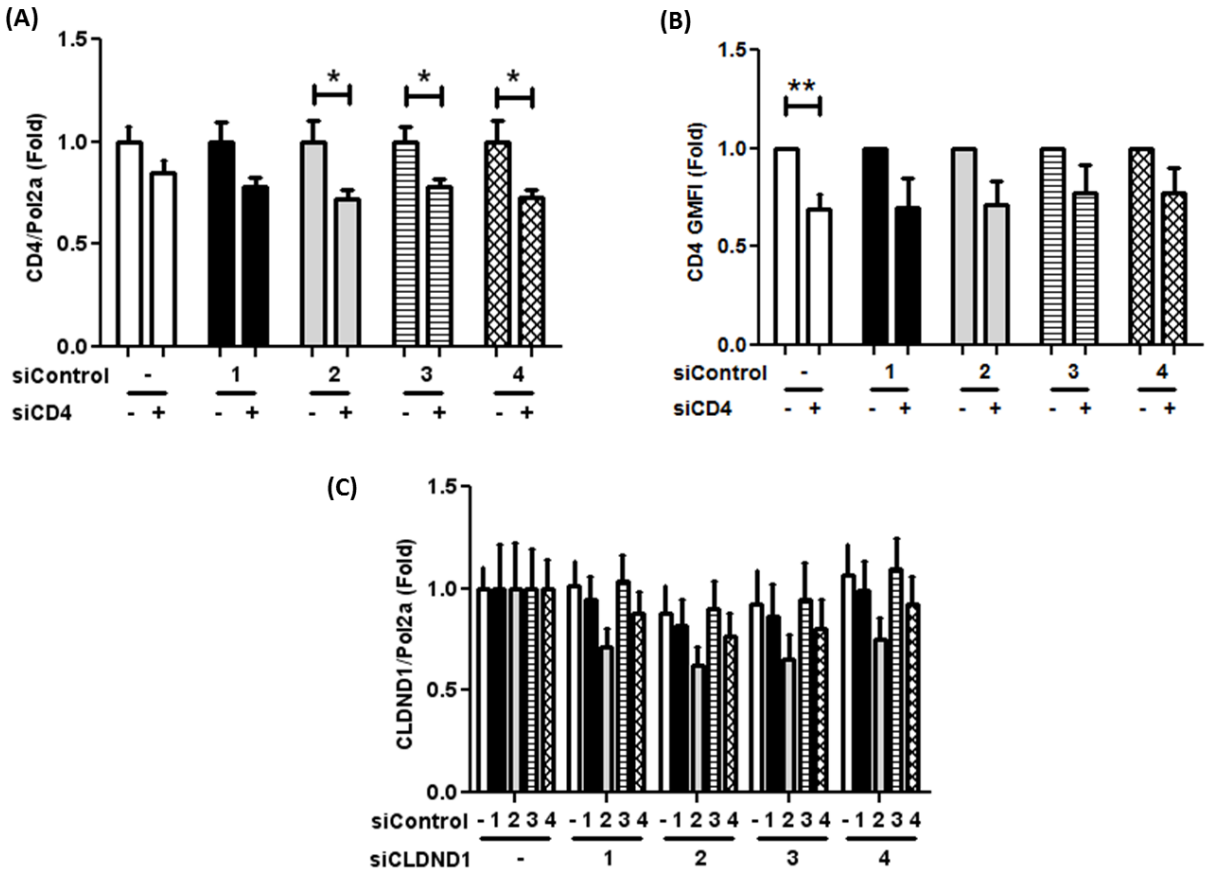

Figure 30. Accell siRNA transfection: manufacturer protocol

Positively selected CD4+ T-cells were transfected with 1 µM Accell siRNA for 72 hours. All values are given as fold change in RNA compared to each control siRNA, after normalisation to pol2a mRNA. (A) CD4 SMARTpool siRNA: fold change in CD4 mRNA (B) CD4 SMARTpool siRNA: fold change in CD4 protein MFI. (C) Accell C1-4 siRNA: fold change in CLDND1 RNA. Data illustrate at least four independent experiments. Mean values are plotted and error bars illustrate SEM. *p<0.05, **p<0.01, Student's t-test.

Due to the variation in relative CLDND1 gene expression, CD4+ T-cell viability was assessed post transfection, to determine whether gene expression profiles were being altered due to cell death (Table 13). There was no significant difference in T-cell viability post transfection with any of the Accell siRNA, suggesting the differences in CLDND1 mRNA levels were due to other factors.

siRNA	Viability (%)
No siRNA	82 ± 10
NT1	79 ± 6
NT2	83 ± 7
NT3	75 ± 8
NT4	81 ± 6
C1	81 ± 8
C2	80 ± 8
C3	80 ± 6
C4	78 ± 6
CD4	85 ± 5

Table 13. Accell siRNA transfection cell viabilities: manufacturer recommended protocol

CD4+ T-cells were transfected with 1 µM Accell siRNA for 72 hours. Post culture, cell viability was assessed using Annexin V and Via-Probe™. Values illustrate at least three independent experiments ± SD.

4.3.4 siRNA transfection protocol optimisation: literature recommendations

Two independent groups using Accell siRNA in human T-cells (Apetoh et al., 2010, http://www.systemsimmunology.org/, no date), used the siRNA in the presence of TCR stimulation, so this approach was attempted with CD4 and CLDND1 siRNA. Initially, optimisations were performed using CD4 SMARTpool siRNA: CD4+ T-cells were stimulated with a 10:1 α-CD3/CD28 expander bead ratio for 72 hours in the presence of 1 µM CD4 SMARTpool or NT siRNA (Figure 31). This protocol will be referred to as the 72hrsiBead protocol. A significant reduction in CD4 mRNA and protein was seen in the CD4 siRNA sample compared to NT siRNA samples (Figure 31A-B): 54 ± 4 % for CD4 mRNA and 36 ± 5 % for CD4 protein.

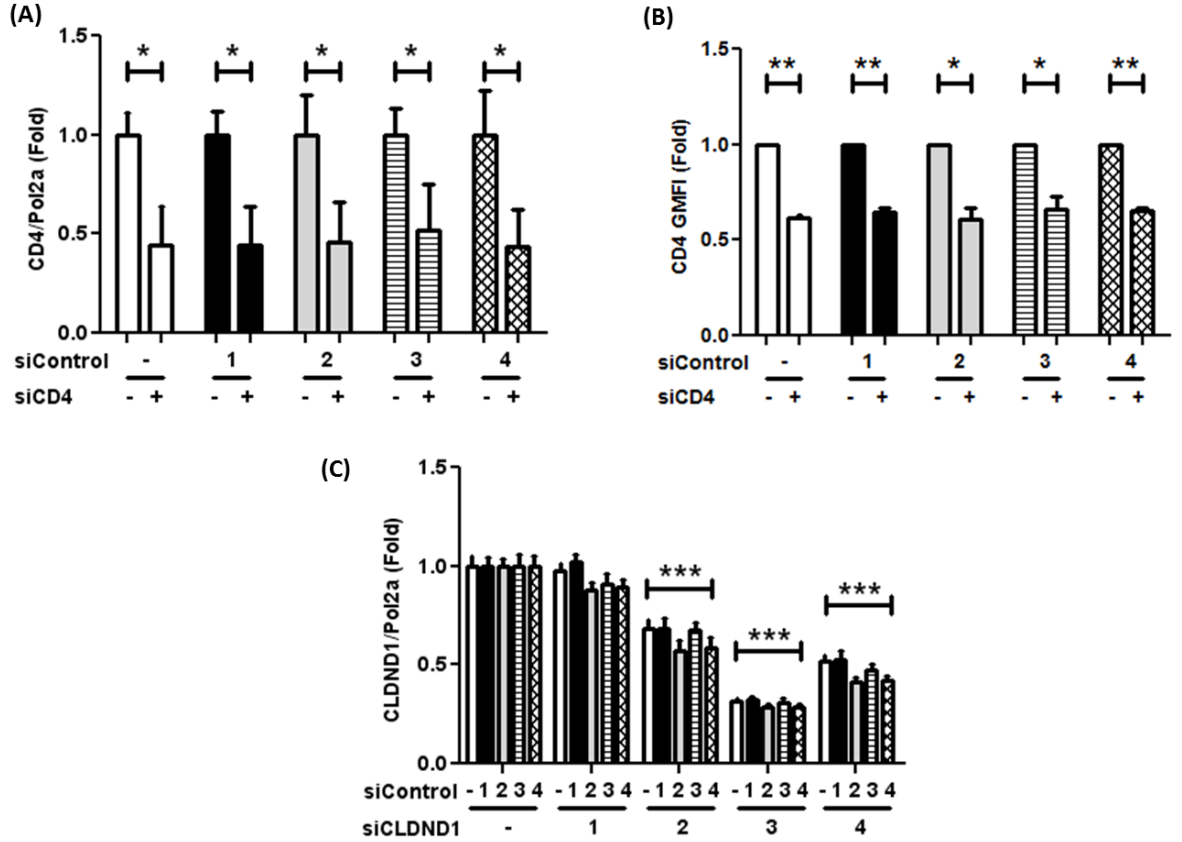

Figure 31. Accell siRNA transfection: modified protocol (72hrsiBead)

Positively selected CD4+ T-cells were transfected with 1 µM Accell siRNA for 72 hours with 10:1 ratio of α-CD3/CD28 expander beads. Each bar illustrates the values of target mRNA levels in the given target siRNA sample, compared to the value in the given control siRNA or no siRNA sample (-), plotted as fold change. CLDND1 RNA values were first normalised to pol2a. (A) CD4 SMARTpool siRNA: fold change in CD4 mRNA. (B) CD4 SMARTpool siRNA: fold change in CD4 GMFI. (C) Accell C1-4 siRNA: fold change in CLDND1 RNA. Data illustrate at least 4 independent experiments. Mean values are plotted and error bars illustrate SEM. Student's t-test analysis was performed. *p<0.05, **p<0.01, *** p<0.001.

CLDND1 gene silencing was assessed using C1-4 siRNA. A significant decrease in CLDND1 mRNA was achieved for C2-4 siRNA samples (35.9 %, 69.7 % and 53.0 % respectively), when normalised to any NT siRNA CLDND1 mRNA values, yet no reduction was seen in the C1 siRNA sample (6.3 %). The reduction in CLDND1 mRNA was consistent regardless of the NT siRNA used for normalisation (Figure 31C) and cell viability varied from 47 to 52% with the different CLDND1 siRNA (Table 14).

siRNA	Viability (%)
No siRNA	46 ± 8
NT1	55 ± 12
NT2	51 ± 8
NT3	50 ± 21
NT4	52 ± 16
C1	50 ± 11
C2	47 ± 13
C3	50 ± 5
C4	52 ± 13
CD4	42 ± 9

Table 14. Accell siRNA transfection cell viabilities: literature recommended protocol

CD4+ T-cells were transfected with 1 µM Accell siRNA for 72 hours with 10:1 ratio of α-CD3/CD28 expander beads. Cell viability was assessed using Annexin V and Via-Probe™. Data illustrate two independent experiments ± SD.

4.3.5 siRNA transfection: effect on T-cell function

Post the 72hrsiBead protocol, T-cell proliferation was assessed. Based on higher CLDND1 expression in anergic cells compared to activated counter-parts (Section 1.10, Figure 6) a reduction in CLDND1 transcript should correlate with increased T-cell proliferation. Instead, a significant reduction in T-cell proliferation was seen in cells incubated with C4 siRNA compared to no siRNA and NT2 siRNA samples (51 % reduction, on average) (Figure 32).

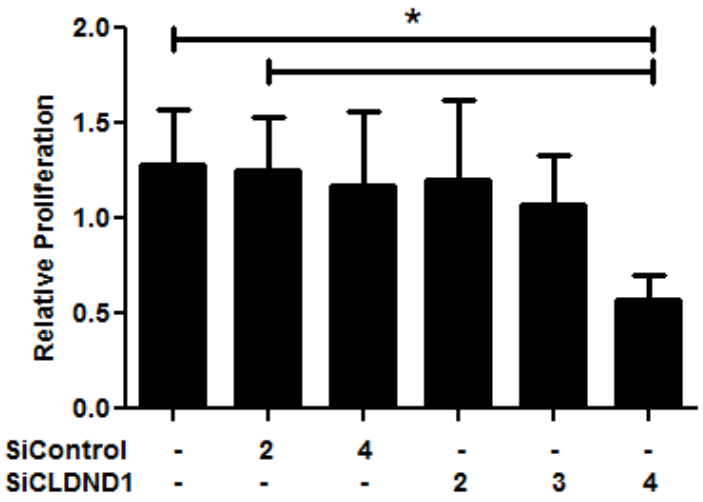

Figure 32. CLDND1 gene silencing and T-cell function: 72hrsiBead

Positively selected CD4+ T-cells were transfected with 1 µM Accell C2-4 siRNA for 72 hours with 10:1 ratio of α-CD3/CD28 expander beads. Proliferation was determined by ^{3}HTdR incorporation. Data illustrate at least 5 independent experiments where each experimental replicate was normalised to one data value in the no siRNA control, for every independent experiment. Mean values are plotted and error bars illustrate SEM. Student's t-test analysis was performed. *$p<0.05$.

A reduction in proliferation was only seen for the C4 siRNA sample, and not in C2 and C3, where there was also a reduction in CLDND1 mRNA. One possible explanation is different levels of CLDND1 protein within the siRNA transfected cells, as a result of different CLDND1 transcript degradation rates of each siRNA. The lack of CLDND1 specific antibodies available at that time, and an unknown CLDND1 protein half-life meant protein levels could not be measured, so the protocol was further optimised to account for a lag time between reduced CLDND1 RNA levels resulting in reduced CLDND1 protein levels.

After the 72hrsiBead protocol, the α-CD3/CD28 expander bead stimulus was removed; the cell medium was refreshed and the cells were rested for a further 3 days (72hrsiBeadRest). CLDND1 mRNA levels were examined after the 3 day rest (Figure 33A), prior to re-stimulation. At this time-point, CLDND1 mRNA levels in the CLDND1 siRNA samples were starting to return to the CLDND1 mRNA levels seen in the NT siRNA samples, but were still significantly reduced in C3 and C4 siRNA samples when normalised to the CLDND1 mRNA levels in the no siRNA and NT2 siRNA samples.

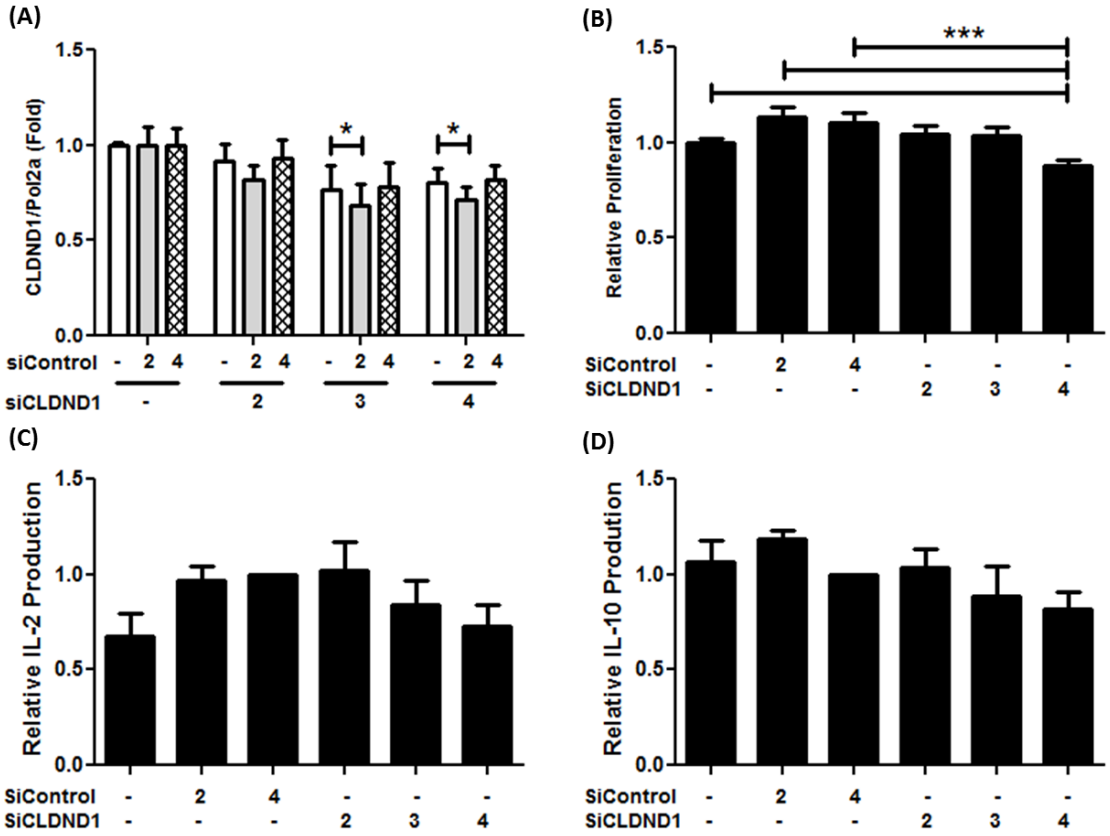

Figure 33. CLDND1 gene silencing and T-cell function: 72hrsibeadRest

Positively selected CD4+ T-cells were transfected with 1 µM Accell C2-4 or NT 2 or 4 siRNA for 72 hours with 10:1 ratio of α-CD3/CD28 expander beads. Cells were rested for 72 hours prior to re-stimulation with 10:1 ratio of α-CD3/CD28 expander beads. (A) CLDND1 RNA levels relative to control siRNA. Each bar illustrates the CLDND1 mRNA level in the CLDND1 siRNA sample, compared to the value in the control siRNA or no siRNA sample (-), plotted as fold change. CLDND1 RNA values were first normalised to pol2a. (B) Proliferation was determined by ^{3}HTdR incorporation. (C) IL-2 production or (D) IL-10 production measured by ELISA. For (B-D), data illustrate three independent experiments where values were normalised to one data point in the no siRNA control or NT4 siRNA for (C) and (D), for each independent experiment. Mean values are plotted and error bars illustrate SEM. Student's t-test analysis was performed. * $p<0.05$, *** $p<0.001$.

Using the 72hrsiBeadRest protocol, the effect of CLDND1 silencing on T-cell proliferation was examined. A significant reduction in T-cell proliferation in cells pre-incubated with C4 siRNA was seen (Figure 33B). It is unclear whether there was a reduction in IL-2 and IL-10 production, due to the variability in the control siRNA values (Figure 33C and D) and no difference in IFNγ, IL-5 or IL-17 production (data not shown). The reduction in proliferation was more subtle with this protocol than the 72hrsiBead protocol (Figure 32).

4.3.6 siRNA transfection: effect on nTreg function

The 72hrsiBead protocol was tested in an isolated nTreg population and the ability of the nTreg to suppress Teff proliferation in a mixed lymphocyte reaction (MLR) was assessed. Post siRNA transfection, nTreg CLDND1 mRNA levels were significantly reduced in the C3 siRNA sample but the decrease in CLDND1 mRNA levels in the C4 siRNA sample was not significant (Figure 34A). There was a trend for an increase in Teff proliferation when cultured with the nTreg that was pre-incubated with C4 siRNA (Figure 34B), yet this was very variable between experimental replicates. There was also variability in IFN-γ production between the siRNA samples (Figure 34C) and so it was difficult to draw a conclusion on a function for CLDND1 in nTreg.

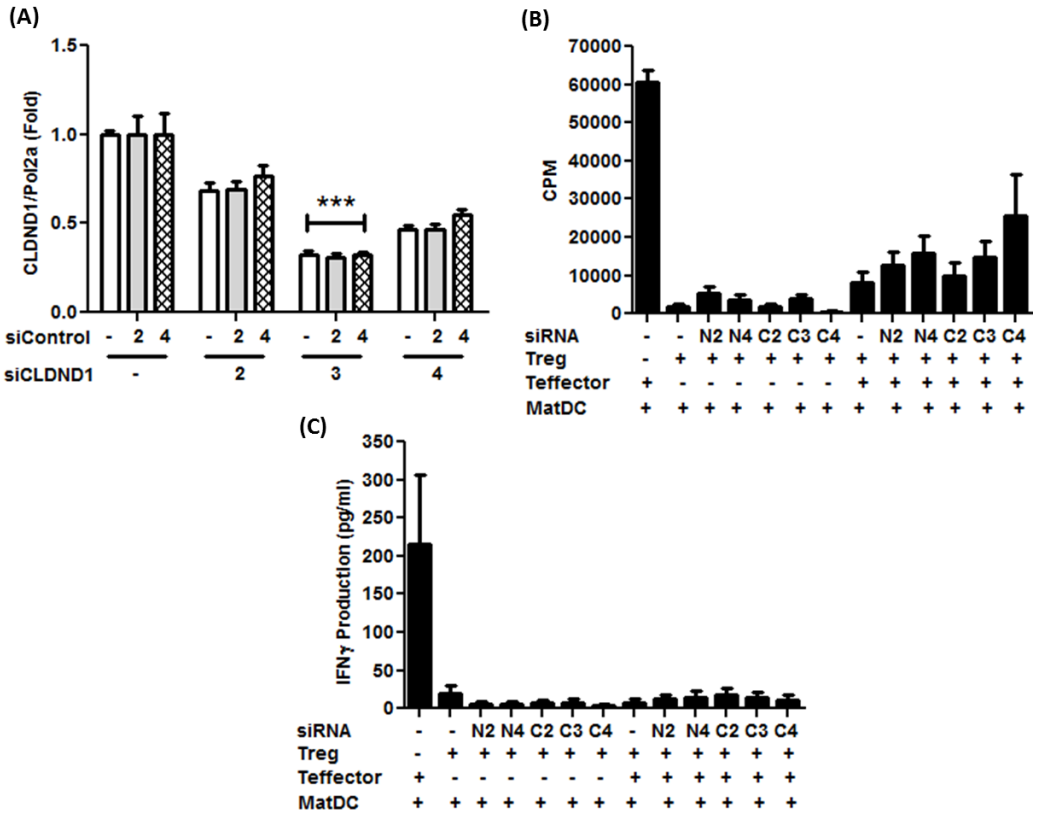

Figure 34. CLDND1 gene silencing: nTreg suppression assay

nTreg cells were transfected using the 72hrsiBead protocol, prior to performing a suppression assay. (A) Fold change in CLDND1 RNA relative to control siRNA. Each bar illustrates CLDND1 mRNA levels in the CLDND1 siRNA sample, compared to the value in the control siRNA or no siRNA sample (-), plotted as fold change. CLDND1 RNA values were first normalised to pol2a. (B) Proliferation of Teff were determined by ^{3}HTdR incorporation. (C) IFNγ production was measured by ELISA. Data illustrate four independent experiments. Mean values are plotted and error bars illustrate SEM. Student's t-test analysis was performed. *** $p<0.001$.

4.3.7 siRNA transfection: CLDND1 protein

On completion of the in-house antibody validation (see Section 3.3.3), cell surface and total CLDND1 protein levels were determined in cells transfected with Accell siRNA, for both 72hrsiBead and 72hrsiBeadRest protocols. Correlating differences in CLDND1 protein levels to reduced T-cell proliferation in the C4 siRNA sample may allude to CLDND1 function.

Characterising CLDND1 protein expression in CLDND1 siRNA transfected cells showed that regardless of the optimised protocol used, there was no consistent reduction in cell surface or total CLDND1 protein in the CLDND1 siRNA samples, when normalising CLDND1 protein levels to control siRNA (Figure 35). A reduction in CLDND1 cell surface protein was observed in the CLDND1 siRNA samples compared to a no siRNA control in the 72hrsiBeadRest protocol (Figure 35C), and indicates that the transfection protocol is altering CLDND1 protein expression itself. Contrary to expected findings, there was a trend for a minimal increase in CLDND1 protein at the cell surface with C4 siRNA, and a total increase in CLDND1 protein with C3 and C4 siRNA (Figure 35A and B).

The non-concordance of CLDND1 mRNA values to CLDND1 protein levels in all of the siRNA transfected cells has significantly affected the interpretation of my experimental series. Even though the reduction in CLDND1 mRNA was not reflected in a reduction in CLDND1 protein, there were still functional differences observed between the C4 siRNA sample and the control siRNA, albeit subtle. Instead of a reduction in CLDND1 protein in the C4 siRNA sample, there was a slight increase in CLDND1 protein, suggesting the increased CLDND1 protein expression in the C4 siRNA sample may account for the decrease in proliferation seen in this transfected sample, although the increase in CLDND1 protein is minimal. Overall, the results are still consistent with the hypothesis that CLDND1 acts as a negative regulator of T-cell proliferation, rather than a positive regulator of T-cell proliferation as suggested by the CLDND1 siRNA and mRNA data.

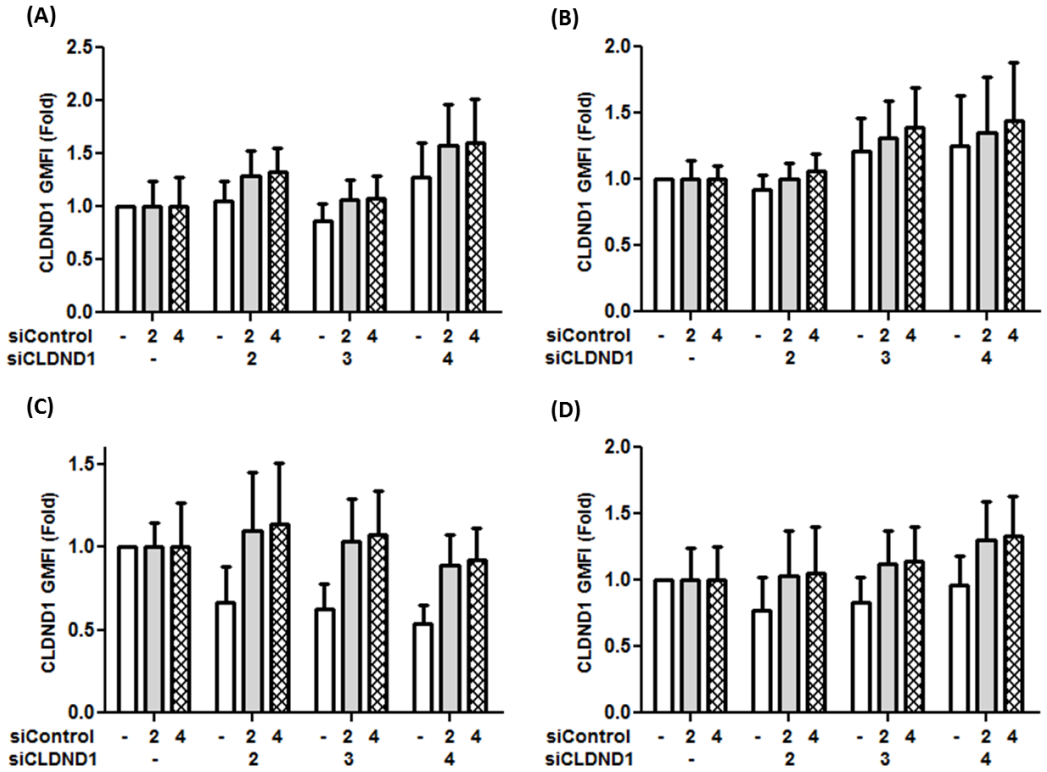

Figure 35. Accell siRNA transfection: CLDND1 protein

CD4+ T-cells were transfected with 1 µM Accell C2-4 or NT 2 or 4 siRNA using the 72hrsiBead protocol. Each bar illustrates CLDND1 protein levels, determined by CLDND1 GMFI, in the CLDND1 siRNA sample compared to the value in the control siRNA or no siRNA sample (-), plotted as fold change. Data illustrate three independent experiments. (A) Surface CLDND1 GMFI. (B) Total CLDND1 GMFI. Cells were transfected using the 72hrsiBeadRest protocol. (C) Surface CLDND1 GMFI. (D) Total CLDND1 GMFI. Data illustrates five independent experiments. Mean values are plotted and error bars illustrate SEM. Student's t-test analysis was performed.

4.4 Discussion

This chapter has studied an alternative method of introducing siRNA into primary human CD4+ T-cells, omitting the need for nucleofection. However, although this method could silence the CLDND1 gene, no consistent effect was seen on CLDND1 protein and so a function for CLDND1 in the regulation of CD4+ T-cell proliferation could not be determined. Even though the Accell method was apparently not suitable for CLDND1, different Accell siRNA have since been successfully used in primary human T-cells (Gomez-Valades et al., 2012), validating the Accell CD4 siRNA silencing performed in this chapter. Documented success with Accell siRNA would suggest an issue using the RNAi technique for CLDND1, rather than a problem with the Accell siRNA. There are numerous technical and theoretical considerations to explore to help explain the issues of silencing CLDND1 in primary human CD4+ T-cells, which will be addressed accordingly.

4.4.1 Technical considerations

It has been widely argued that isolating T-cells using CD4 positive selection may lead to altered function of the T-cell and skew data interpretation, due to the targeting of a co-receptor. Nonetheless, microarray data analysing positively and negatively selected T-cells suggests that gene expression profiling in each CD4+ T-cell population is comparable regardless of the T-cell isolation technique (Lyons et al., 2007). Additionally, the effects of T-cell function during CLDND1 silencing were compared to controls, which have also been subjected to the same isolation method. Any difference mediated through silencing CLDND1 should therefore remain identifiable.

Evidence suggests that the siRNA silencing technique is applicable to primary human CD4+ T-cells, so discrepancies between the CLDND1 mRNA and protein data may be a due their detection techniques. Measuring siRNA mediated mRNA silencing using qRT-PCR has the potential to generate false positives and false negatives. An independent study identified how positive results can be missed due to inadequate primer design (Holmes et al., 2010). Designing primer sets downstream of the siRNA binding site may give false negatives due to primer binding to the 3’ mRNA degradation product even though the cleavage of RNA is sufficient to reduce RNA translation. In the case

of the CLDND1 silencing experiments, the design of CLDND1 primers could potentially have resulted in a false negative observation for C1 siRNA, as CLDND1 primer sites sit downstream of where this siRNA binds.

Similarly, false positives can be generated when using qRT-PCR primers that flank the siRNA-mediated cleavage site. For *in vivo* siRNA mediated gene silencing in animal studies, higher concentrations of siRNA are required. Excess siRNA can be purified with cellular RNA and can interfere with RNA amplification during reverse transcription, lowering the perceived amount of target RNA during qRT-PCR (Herbert et al., 2011). As the Accell method requires higher concentrations of siRNA than other transfection methods, false positives could be a concern. In order to prevent detection of false negative and positives, it is proposed that qRT-PCR primers should be designed to bind upstream of the siRNA binding site (Herbert et al., 2011). In fact, analysis of the qRT-PCR primers used to detect CLDND1 transcripts reveals that the primers bind upstream of all the siRNA (Appendix Figure 1), and so excludes the possibility of detecting false positives and negatives in these experiments.

Thus the likelihood of differences in CLDND1 protein and mRNA detection being due to the mRNA technique used is unlikely. Focus next falls on the method of detecting CLDND1 protein using the in-house antibody. The antibody specificity was confirmed by performing peptide blocking experiments (see Section 3.3.2) so it was improbable that the α-CLDND1 antibody generated bound to other proteins that mask any changes in the levels of CLDND1 protein.

4.4.2 Theoretical considerations

From the points discussed, technical errors to account for differences in detecting CLDND1 RNA and protein seem unlikely. Instead these discrepancies may represent a method of CLDND1 translational regulation.

One possibility looks at the translation of CLDND1 transcript as its own regulatory mechanism for protein expression, independent of the level of mRNA in the cell. This type of regulation has been shown for another protein BiP, an ER-stress protein, where increased cellular RNA levels were not reflected by increased protein, which remained constant under steady state conditions. When ER stress was induced, transcript translation was disproportionally

increased from the same amount of transcript, compared to the steady state condition (Gulow et al., 2002).

Similarly, the quantity of CLDND1 mRNA may not prove essential in the role of CLDND1 protein expression, if the position of CLDND1 within the cell is part of a mechanism to regulate protein function. For example, CTLA-4 is a potent negative regulator of CD4+ T-cell proliferation and its cell surface location is tightly regulated. CTLA-4 is not present on the surface of resting T-cells and is only up-regulated upon T-cell activation, where it can exert its effect. The CTLA-4 protein is primarily localised to intracellular vesicles and cycles between there and the cell surface (McCoy and Le Gros, 1999).Whilst these two mechanisms could potentially explain my findings, there may also be additional reasons to explain the discrepancies between CLDND1 mRNA and protein observed during the siRNA silencing experiments.

During the siRNA experiments, four different CLDND1 siRNA were used to target the CLDND1 transcript. I have shown that these four siRNA differed in their efficiency to down-regulate the CLDND1 transcript. Based on the sites the siRNA binds to within the CLDND1 mRNA, the efficiency of these siRNA could allude to potential regulation of the CLDND1 transcript post-transcriptionally, namely by microRNAs. MicroRNAs are endogenous double-stranded RNA sequences that have been shown to regulate protein expression through repressing translation of RNA transcripts. C3 and C4 siRNA showed the most efficient targeting of the CLDND1 transcript and these siRNA bind to the 3'UTR of the CLDND1 transcript. One group have reported that 3' UTR targeting is the most effective way of targeting transcripts in primary T-cells, while ORF-binding siRNA was ineffective and this targeting was identified in several types of cells. Although their studies are limited and they admit that further screening may identify ORF siRNA repressors, they suggest that the 3' UTR of genes that can be silenced by siRNA may also be targets for regulation by microRNAs (McManus et al., 2002). Also interestingly, genes that avoid microRNA regulation have transcripts that have varying 3' UTR lengths (Cheng et al., 2009). The CLDND1 siRNA that are most effective target the 3'UTR of the transcripts. In addition, all CLDND1 transcripts have the same length 3'UTR (Appendix Figure 1). These two factors may suggest that CLDND1 may be regulated by microRNAs.

The presence of the siRNA, a double stranded RNA molecule, may itself alter CLDND1 protein expression, as TLR signalling in the CD4+ T-cells may have been induced. It has been shown in PBMC that siRNA mediated silencing can induce immune activation through endogenous TLR triggering, as well as TLR-independent mechanisms (Sioud, 2010). Most TLR are expressed on and in T-cells and activation of TLR can induce co-stimulatory molecule expression (CD69) on T-cells (Simone et al., 2009). We have shown than CLDND1 is up-regulated upon TCR-induced T-cell activation (Section 5.3.2, Figure 38) with a modest increase in CLDND1 RNA (Section 5.3.2, Figure 39). Therefore if Accell siRNA activated TLR in lymphocytes and induced CLDND1 translation, this could overcome the effects of siRNA silencing. Similarly the activation of CD4+ T-cells by α-CD3/CD28 expander beads during the siRNA transfection period could also over-ride any down-regulatory effects of the CLDND1 siRNA. These mechanisms may provide a useful insight into how CLDND1 protein function is regulated, however an extensive amount of research would need to be performed to verify any such mechanisms.

This chapter has revealed that silencing the CLDND1 gene is not a suitable way of determining CLDND1 function. An alternative method to investigate the CLDND1 protein would be to over-express the protein. This would be the next step in trying to identify CLDND1 function. Failing this, it may be worthwhile visiting other methods of determining protein interactions to determine a function for CLDND1. As protein-protein interactions are critical for cellular function, there are several techniques that identify the interactions of a given protein in its environment. Two examples of these techniques are yeast-two hybrid screening systems, and co-IP.

Yeast-two hybrid screening allows for large scale screening of potential protein binding partners. The basic principle of this technique utilises the binding and interaction characteristics of transcription factors. A bait protein is fused to the DNA binding domain of a transcription factor and the prey protein is fused to the transcriptional activation domain of that transcription factor. Expression and interaction of the two proteins results in the transcription of a transcription factor specific reporter gene (Ratushny and Golemis, 2008). This technique is performed in a host cell, such as yeast, that is predominately easier to manipulate than the cell subsets of interest and, as such, false positive

interactions may be highlighted, as cell-specific regulation of proteins is not accounted for. It has been recorded that non-specific interactions can account for up to half of the results collected (von Mering et al., 2002). Initial studies using the yeast-two hybrid screening approach were limited to soluble protein interactions and so may not be suited to identifying binding partners for CLDND1. However, a variant of this technique, termed the split-ubiquitin membrane-based yeast two-hybrid system, allows for integral membrane protein interactions to be studied (Thaminy et al., 2004). To determine CLDND1 binding partners a high-throughput screen would be required, as potential types of interacting partners are unknown and therefore cannot be pre-selected for. Given the reported number of false positive results generated using this, it would be challenging to verify actual binders. The yeast two-hybrid system could be utilised after functional studies confirmed a role for CLDND1 in the regulation of CD4+ T-cell activation, to validate potential CLDND1 interactions.

A different method for determining protein-protein interactions is to perform co-IP experiments using cell lysates containing CLDND1. Lamentably, IP performed with either the α-CLDND1 antibody or using α-FLAG, to isolate binding partners to FLAG tagged CLDND1 over-expressed protein (see Section 3.3.5), were unsuccessful to identify potential CLDND1 binding partners.

Another method reliant on robust functional antibodies is to perform antibody blocking experiments to determine whether blocking potential interaction sites on CLDND1 may disturb its function, or alternatively act in an agonistic fashion and increase any function that CLDND1 may possess. With this approach, potential CLDND1 interaction sites would need to be identified along with a function for CLDND1 in order to have a read-out on the functional effects of the antibody. More immediately, functional antibodies would also have to be generated. In order to determine the function of CLDND1 in the absence of these reagents, over-expression studies would give the best insight into the role of CLDND1 in primary human CD4+ T-cells.

Chapter 5. CLDND1 Expression Profiling

5.1 Aims

The aim of this chapter was to identify a role for CLDND1 in primary human CD4+ T-cells through its expression profiling under a range of different stimuli. In order to understand roles of CLDND1 within the immune response as a whole, CLDND1 protein expression was also sought on a variety of different immune cell subsets. CLDND1 expression patterns were documented during CD4+ and CD8+ T-cell TCR-mediated activation and also in the presence of the immunoregulatory cytokine, TGF-β, as CLDND1 expression patterns could infer roles for CLDND1 in the regulation of the immune response. CLDND1 protein expression was identified with the in-house generated α-CLDND1 antibody using flow cytometry and, where individual subsets were isolated, CLDND1 protein expression was confirmed by Western blotting and CLDND1 mRNA by qRT-PCR. Finally the expression of CLDND1 was determined in early arthritis (EA) patients, with focus on the early RA subgroup to determine a potential role for CLDND1 in arthritic disease progression.

5.2 Introduction

Characterisation of different immune cell subsets and functions has been aided through the division of these subsets by distinct cell surface protein expression profiles. These sub-divisions have allowed for separation between pro-inflammatory immune responders and those involved in regulating immune responses. One type of regulatory immune response that has generated interest from an immunotherapeutic perspective is the hypo-responsive state of anergy. Although several proteins have been identified in the process of anergy, many of these proteins are present within the cytoplasm, and so are not ideal targets for biological therapy. Identification of a cell surface protein that can specifically modulate an aspect of the immune response would make a more tractable therapeutic target.

5.2.1 Documented expression of CLDND1 to date

CLDND1 is a tetraspanning transmembrane protein of unknown function. CLDND1 gene and protein expression has been documented on only a handful of cell types. Gene expression was first described in rat optic nerve cells, with

focus drawing on the oligodendrocyte population and so a role for CLDND1 in myelination of the central nervous system was suggested (Fayein et al., 2002). The increasing popularity of RNA microarray analysis of cell types has subsequently lead to the identification of CLDND1 gene expression in mouse hepatoma Hepa-1c1c7 cells (Hao et al., 2012) and within whole blood (Beineke et al., 2012), yet it's detection in CD4+ T-cells remained elusive. Advances in mass spectrometric techniques has recently detected CLDND1 protein on both HEK293T cells and in human U2OS osteosarcoma cells, yet no inference was made to its function apart from the fact that CLDND1 protein can be ubiquitinated, and so is probably targeted for degradation in this manner (Kim et al., 2011, Wagner et al., 2011, Danielsen et al., 2011). The potential presence of CLDND1 on the cell surface of CD4+ T-cells, as well as its differential expression between activated and anergic CD4+ T-cell clones has sparked our interest in the function of CLDND1 in the CD4+ T-cell immune response. Elucidating a role for CLDND1 in the CD4+ T-cell immune response may open avenues of research into a novel therapeutic target.

5.2.2 Expression of the PMP-22/EMP/MP20/claudin superfamily members in T-cell subsets

CLDND1 shares homology to the PMP-22/EMP/MP20/claudin superfamily which contains a diverse population of proteins of differing cellular functions and distributions. One sub-group of this family, the claudins, are important structural and functional components of epithelial TJ. Based on shared homology, the documented expression of PMP-22/EMP/MP20/claudin superfamily members on T-cells was investigated. Expression of some claudins has been documented in different stages of T-cell development and function.

Claudin-4 is expressed in CD4/CD8 double positive thymocytes and is diffusely distributed on the cell surface of these cells, independently of CD3 but in association with CD4 and lck (Kawai et al., 2011). Upon TCR engagement, claudin-4 recruits to the IS and co-ligates with CD3, resulting in a marked increase in T-cell activation. Claudin-4 is subsequently down-regulated in the thymocytes post TCR activation, leading to a theory that claudin-4 is important in thymocyte positive selection, independently of its known function in TJ. Claudin -10, -11, -12 and -20 transcript is also present in these thymocytes, their function remains unknown (Kawai et al., 2011).

Both claudin-1 and -5 are expressed on CD20+ B-cells, CD14+ monocytes and CD4+ and CD8+ T-cells and co-localise with the integral TJ proteins ZO-1 and ZO-2 (Mandel et al., 2012). In the presence of α-CD3 stimulus, claudin-1 protein levels increase on CD4+ T-cells by four times the resting levels. Claudin-5 levels are not affected by T-cell stimulation (Mandel et al., 2012).

5.2.3 TGF-β signalling in T-cells

In the work that follows, CLDND1 cell surface expression was partially regulated by TGF-β and so it is important to understand the roles of TGF-β in the immune response. TGF-β signalling induces a diverse range of outcomes depending on the cell type studied and the environment in which TGF-β signalling takes place. There are three isoforms of TGF-β, of which TGF-β1 is expressed predominantly in haematopoietic cells. Even within T-cells, TGF-β signalling plays different roles depending on the stage of T-cell development and function. In brief, TGF-β is produced in an inactive form, which requires proteolytic cleavage before it can bind to the TGF-β receptor (TGFBR). The TGFBR is made up of two different polypeptides, TGRBR type I and II. TGF-β binds directly to TGFBRII, which results in TGFBRII mediated phosphorylation of the regulatory domain of TGFBRI. TGFBRI phosphorylation results in its activation and subsequent phosphorylation of SMAD (mothers against decapentaplegic homologue) proteins. These proteins, through an array of interactions, transduce signals to the nucleus. The regulation of TGF-β signalling can be modulated by many mechanisms, from the TGF-β ligand being sequestered in its latent form by latency associated protein (LAP), to post signalling regulation by SMAD specific E3 ubiquitin protein ligases (SMURFS), making TGF-β signalling difficult to predict. The activation of the TGF-β signalling pathway can prevent both naïve CD4, helper, and CD8 cytolytic T-cell responses, in part due to the inhibition of IL-2 production (Rubtsov and Rudensky, 2007, Gorelik and Flavell, 2002).

5.3 Results

5.3.1 CLDND1 expression in immune cell subsets

Gene expression analysis of the CD4+ T-cell clone, HA1.7, (Figure 6) identified CLDND1 transcript expression; the first record of CLDND1 expression in CD4+ T-cells. CLDND1 protein cell surface expression was confirmed in a selection of immune cells, as a result of generating the in-house CLDND1-specific antibody. PBMC were isolated from whole blood by density centrifugation and the cell populations were fixed prior to CLDND1 staining. The percentage of CLDND1 positive cells was determined using FMO analysis, and the amount of CLDND1 expressed on the cell surface was determined using CLDND1 GMFI (see Section 2.9.3 Figure 36).

The profile of CLDND1 expression was similar between the different immune cell subsets, irrespective of the flow cytometry analysis used. Identification of CLDND1 protein on the CD4+ T-cell population, along with the CD8+ T-cell population, supported the RNA expression profiling data from the preliminary differential display experiment. Interestingly, CLDND1 was identified on only a subset of each of the cell types, as determined from the percentage of CLDND1 positive cells. This finding was similar to the expression profiles identified for claudin-1 and -5 on immune cell subsets (Mandel et al., 2012). The CLDND1 positive CD4+ T-cell subset did not correlate with antigen experience as CLDND1 levels were similar between the naïve and memory subsets.

Natural killer (NK) T-cells had lower CLDND1 cell surface expression and percentage of CLDND1 positive cells than both the T-cell and the NK cell population, suggesting that CLDND1 may not play a substantial role in this subset, under resting conditions. The highest level of CLDND1 cell surface expression was detected on CD14+ monocytes, yet both the percentage of cells expressing CLDND1 and the quantity of CLDND1 was very variable between individuals.

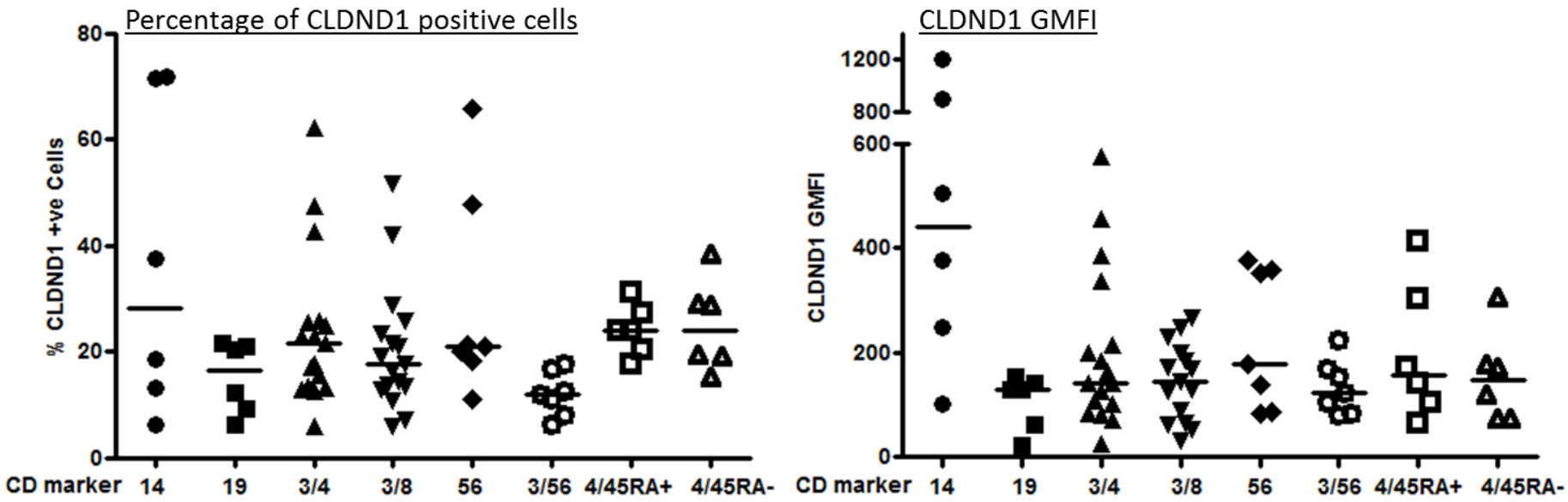

Figure 36. CLDND1 expression on immune cell subsets

PBMC were isolated from whole blood by density centrifugation prior to surface staining for cell subsets. The CD markers relate to the following cell types; CD14: monocytes, CD19: B-cells, CD3/4: CD4+ T-cells, CD3/8: CD8+ T-cells, CD56: NK cells, CD3/56: NK T-cells. For naïve and memory CD4+ T-cells, CD45RA staining was used to segregate naïve (CD45RA+) and memory (CD45RA-) cells. Cells were fixed in 4 % formaldehyde prior to staining for CLDND1. Percentage of CLDND1 positive cells, using FMO analysis, and amount of CLDND1, using CLDND1 GMFI, was measured. Median values are indicated by the corresponding line for each subset. Data illustrate at least six independent experiments.

5.3.2 CLDND1 expression during T-cell activation

The CLDND1 transcript is differentially expressed between activated, resting and anergic states of the CD4+ T-cell clone, HA1.7, and so to strengthen these data, CLDND1 protein expression was sought. Revival of the CD4+ T-cell clone was unsuccessful, as the clone did not respond to stimulatory activation (Amy Anderson, unpublished data), so no comparison between RNA and protein could be made. Instead, primary CD4+ T-cells were used as a model, however as a result, an anergic state could not be generated for comparison. There are several published methods claiming to induce non-clonal anergy (Hoves et al., 2006, Davies et al., 2011, Heissmeyer et al., 2004), yet it is well documented different types of anergy are induced depending on the stimulus used, resulting in different phenotypic characteristics of the cells (Schwartz, 2003, Lechler et al., 2001). Due to the complexities of these interactions and differences in effects, these methods were not used as an alternative model for T-cell anergy. Additionally, a CD3-based anergy model was attempted, but proved unsuccessful in inducing an anergic state (Figure 37).

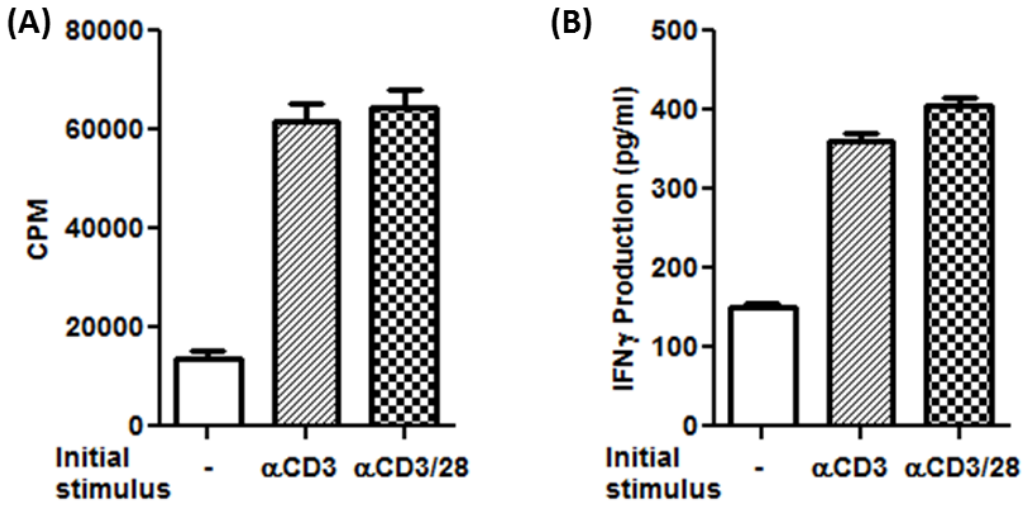

Figure 37. CD3-based *in vitro* CD4+ T-cell anergy model

CD4+ T-cells were incubated with no stimulus (-), 1 µg/mL plate-bound α-CD3 or with 1 µg/mL plate-bound α-CD3 and soluble α-CD28 overnight, before resting for 7 days. Cells were re-stimulated with 1 µg/mL plate-bound α-CD3 and soluble α-CD28 for 72 hours. (A) Proliferation was measured by ^{3}HTdR incorporation. (B) IFNγ levels were measured in the supernatants of cultures by ELISA. Mean values were plotted with error bars illustrating SEM. Data illustrate one experiment performed in triplicate.

CD4+ T-cells were activated with α-CD3 and α-CD28, as part of a PBMC or isolated cell population, and CLDND1 cell surface protein levels, total CLDND1 protein levels and CLDND1 RNA levels were measured. Non-activated (resting) T-cells were used as the control to assess for changes in CLDND1 protein and RNA expression in the activated cells.

An increase in CLDND1 cell surface protein was seen in the activated population compared with the resting counterpart (Figure 38), peaking during day 2 of stimulation (6.0 ± 1.33 SEM fold change). The change in the amount of CLDND1 cell surface expression during the stimulation was more pronounced than the change in the percentage of cells expressing CLDND1. A substantial decrease in the amount of CLDND1 cell surface expression and number of CLDND1 expressing cells was seen during the first 24 hours of resting cell culture. The amount of CLDND1 remained low throughout the culture of the resting cells and although the number of CLDND1 positive cells started to recuperate, there were still less CLDND1 positive cells than in freshly isolated cells.

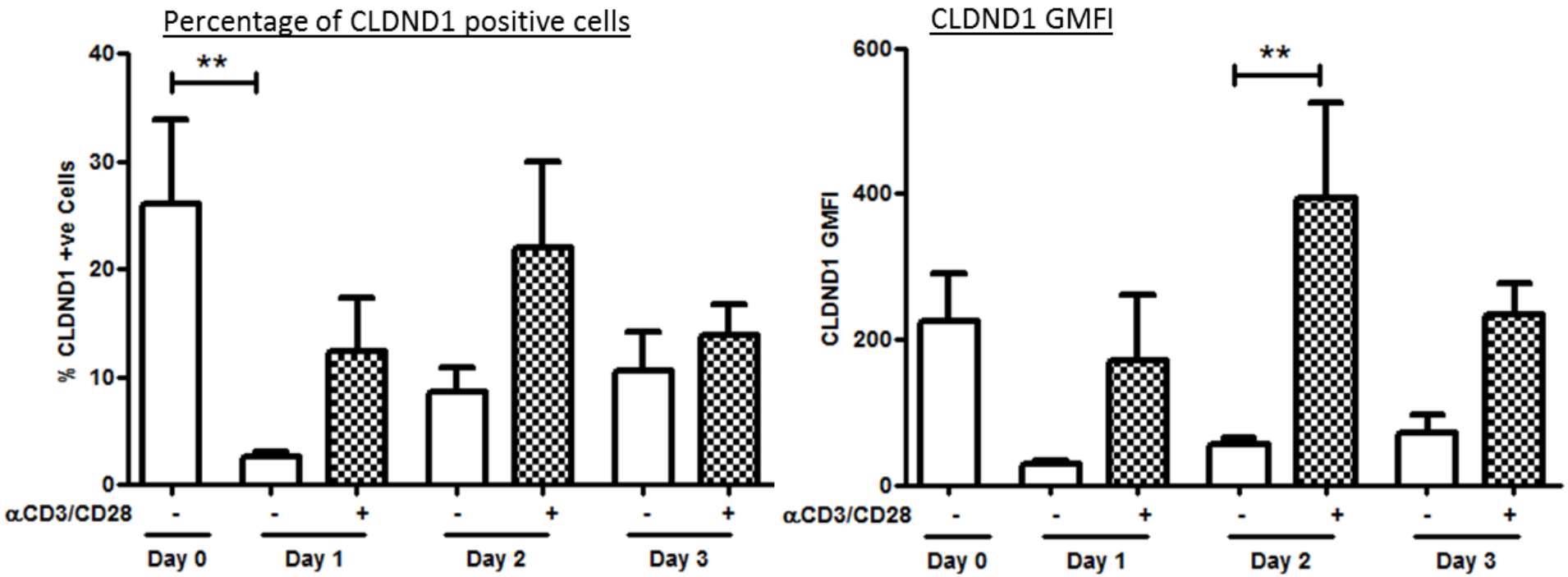

Figure 38. CD4+ T-cell CLDND1 protein expression during PBMC activation

PBMC were rested or activated for 3 days with 1 µg/ml soluble α-CD3 and α-CD28 then stained for CD3 and CD4 expression prior to cell fixation in 4 % formaldehyde for CLDND1 staining. Cell surface CLDND1 protein expression was measured by percentage of CLDND1 positive cells, using FMO analysis, and by CLDND1 GMFI. Data illustrate six independent experiments. Mean values were plotted with error bars illustrating SEM. **p<0.01, repeated measures ANOVA with Bonferroni correction comparing unstimulated to stimulated cells at each time-point, and day 0 values to day 1 and day 3 unstimulated values.

CLDND1 total protein was also up-regulated at day 2 and 3 during stimulation (Figure 39A). Modest amounts of CLDND1 protein were detected in the resting cells at day 0, day 2 and day 3, and CLDND1 protein was undetectable at day 1, mirroring the cell surface expression flow cytometry data. These data suggested CLDND1 protein was being internalised and degraded or that CLDND1 was being cleaved, yet as there were no antibodies available against different epitopes, this theory could not be tested.

To determine whether the increased CLDND1 protein expression was a result of increased gene transcription, CLDND1 RNA levels were compared between the resting and activated T-cell populations (Figure 39B). At 2 hours post-stimulation, there was a marginal decrease in the amount of CLDND1 transcript in the activated cells compared to the resting counterparts and, although not significant, this showed a similar trend to the same time-point in the initial differential display study (Section 1.10, Figure 6). Post 2 hours, CLDND1 RNA levels increased significantly in activated cells, although the RNA levels never exceeded more than 1.9 ± 0.3 SEM fold more than the resting T-cell RNA values.

The increase in CLDND1 cell surface expression on the T-cells was not linked to CD25 expression (Figure 40), as both CLDND1 positive and negative populations has comparable CD25 expression during T-cell activation. There was however a link between CD25 expression and CLDND1 cell surface expression in resting cells (Figure 40, day 0), as the CLDND1 positive cells were predominately also CD25 positive.

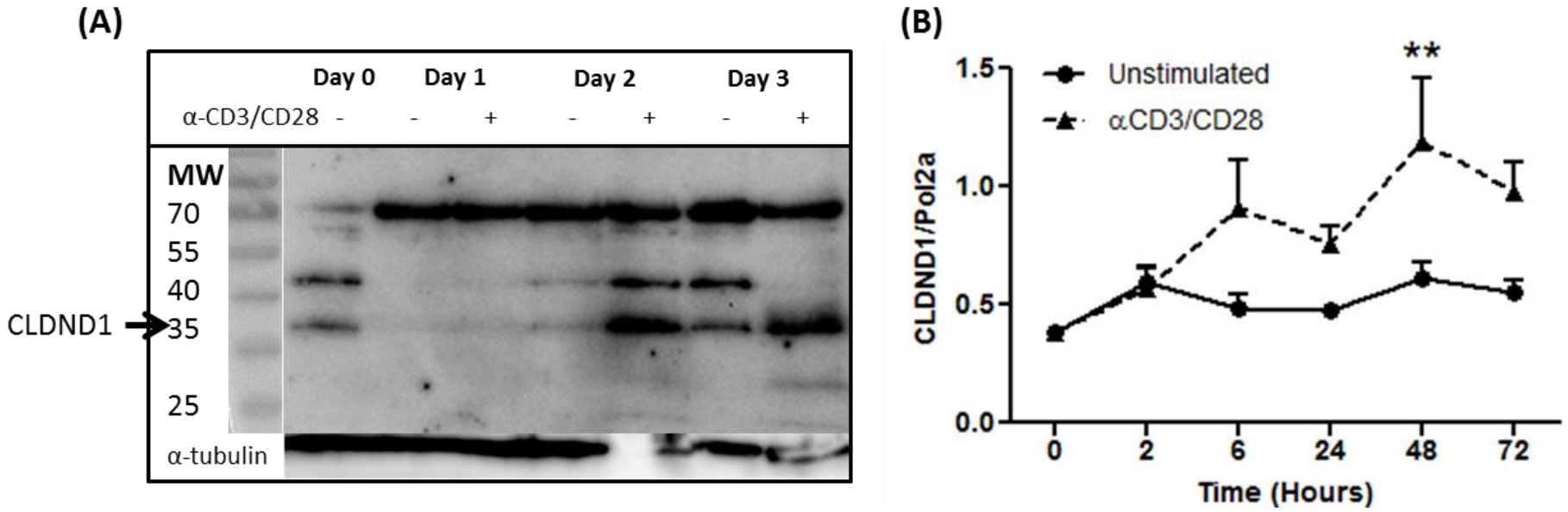

Figure 39. CLDND1 expression during CD4+ T-cell activation

CD4+ T-cells were rested or activated with 10:1 ratio of α-CD3/CD28 expander beads for 3 days. Cell lysates were prepared and (A) CLDND1 protein expression was examined by Western blot, using α-tubulin to account for total protein or (C) RNA was extracted and CLDND1 mRNA levels were determined by qRT-PCR, normalising to the housekeeping gene pol2a. Data illustrate three or six independent experiments, respectively Mean values were plotted with error bars illustrating SEM. **p<0.01, repeated measures ANOVA with Bonferroni correction comparing unstimulated to stimulated cells at each time-point, and day 0 values to day 1 and day 3 unstimulated values.

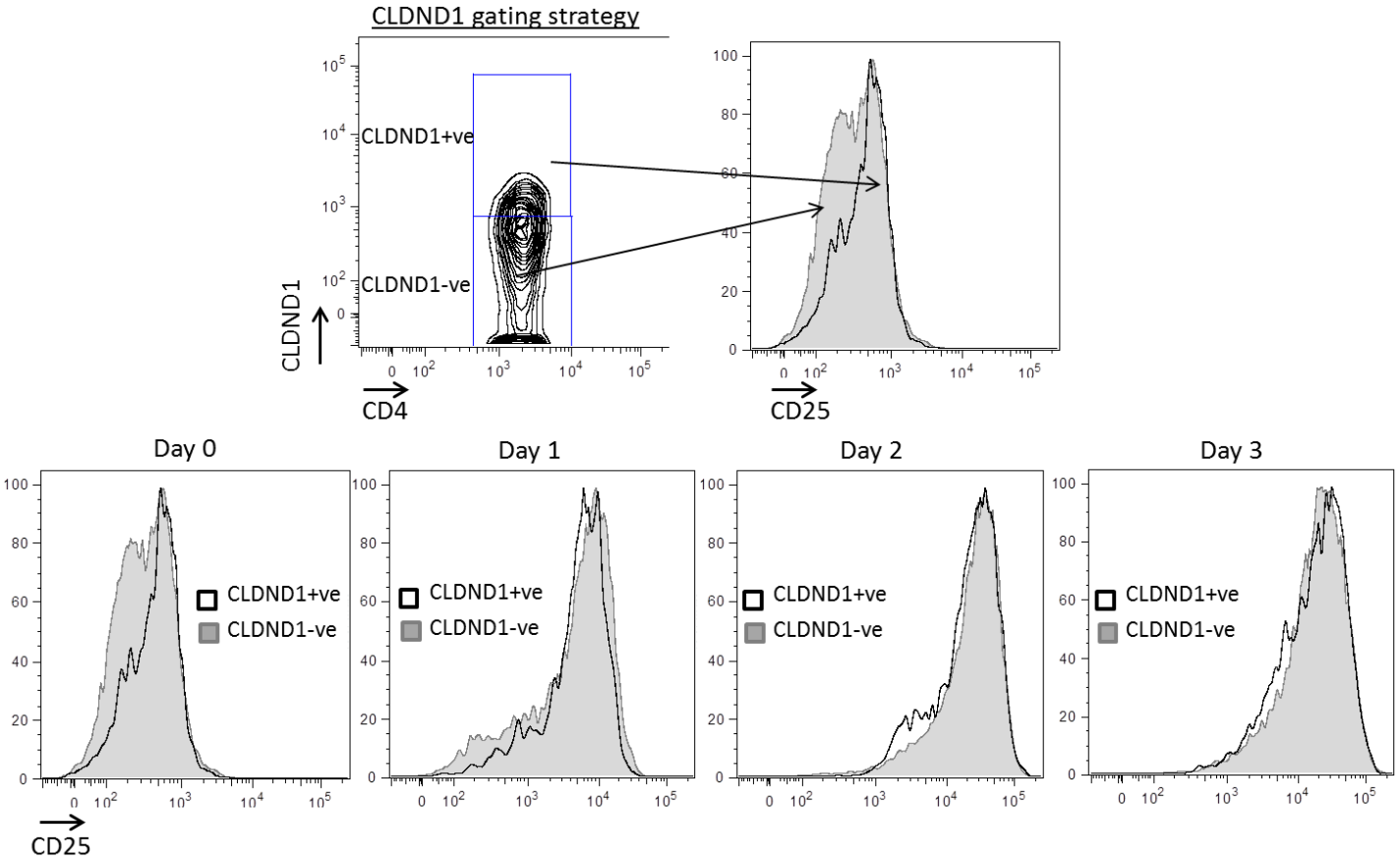

Figure 40. CLDND1 and CD25 expression during CD4+ T-cell activation

PBMC were activated with 1 µg/mL soluble α-CD3 and α-CD28 for 3 days. At each time-point, PBMC were stained for CD3, CD4 and CD25 expression prior to cell fixation in 4 % formaldehyde for CLDND1 staining. The CLDND1 gate was determined from the CD3/CD4 positive gate, based on FMO analysis. The CLDND1 gated populations were analysed for CD25 expression. Data represent two independent experiments.

To further visualise CLDND1 expression in resting and activated T-cells, confocal microscopy analysis was performed, using CD3 staining to identify the cell surface plasma membrane, and DAPI staining to identify non-cytoplasmic regions (Figure 41). CLDND1 protein was present on the surface of resting CD4+ T-cells, post isolation, in agreement with the flow cytometry data. Interestingly, in some of the cells visualised, CLDND1 expression looked to be polarised (Figure 41, day 0 arrow). Intracellular CLDND1 localises to the cytoplasm. Post CD4+ T-cell activation, total CLDND1 levels increase and show punctate staining, indicative of localised pockets of CLDND1, yet further analysis would be required to determine whether these foci localise to intracellular vesicles. CLDND1 cell surface expression post activation looked polarised (Figure 41, day 3 arrow). CLDND1 expression did not co-localise with CD3, suggesting CLDND1 has distinct functions from claudin-4 during T-cell activation, as this protein was shown to co-ligate with CD3 in the IS (Kawai et al., 2011).

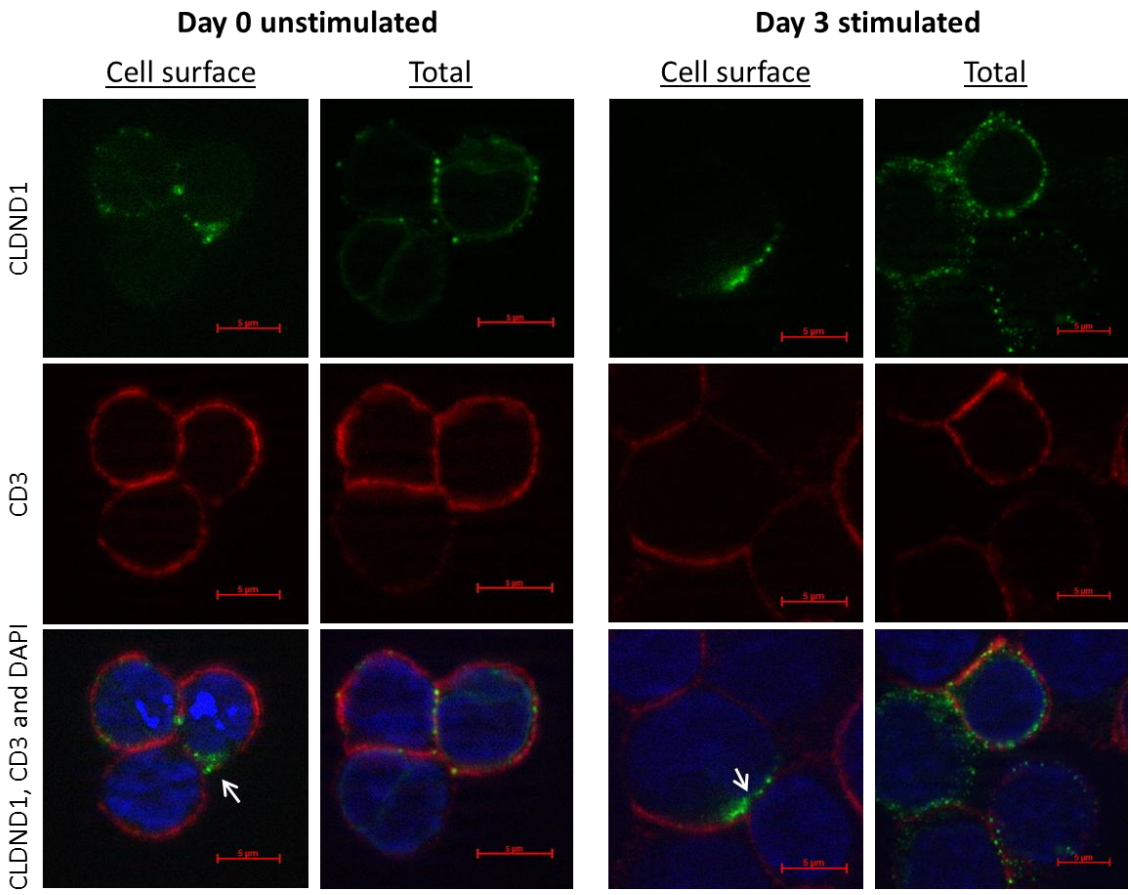

Figure 41. CLDND1 expression during CD4+ T-cell activation: visualisation

CD4+ T-cells were stained immediately, or stimulated for 3 days with α-CD3/CD28 expander beads before fixation in 4 % formaldehyde and stained for CD3 expression. Cells were then stained for CLDND1 expression (unpermeabilised), or permeabilised prior to CLDND1 staining. Nuclear staining was performed with DAPI. Confocal microscopy analysis was performed and one cross-sectional image is displayed. Arrow indicates proposed polarisation of CLDND1. Data represent two independent experiments.

The expression profiling of CLDND1 protein during T-cell activation was also investigated in the CD8+ T-cell population to determine whether increased CLDND1 protein expression occurred as part of generic T-cell activation events (Figure 42). Similar CLDND1 cell surface expression kinetics were seen in the activated CD8+ T-cell subset as for the CD4+ T-cell subset, however the change in CLDND1 cell surface expression was smaller (4.02 ± 0.96 SEM fold change). These findings suggested CLDND1 expression was modulated by generic T-cell activation events. The same pattern in CLDND1 cell surface expression as the CD4+ T-cells was seen in resting CD8+ T-cells during the first 24 hours in culture, suggesting a generic regulation of CLDND1 in response to *in vitro* culture.

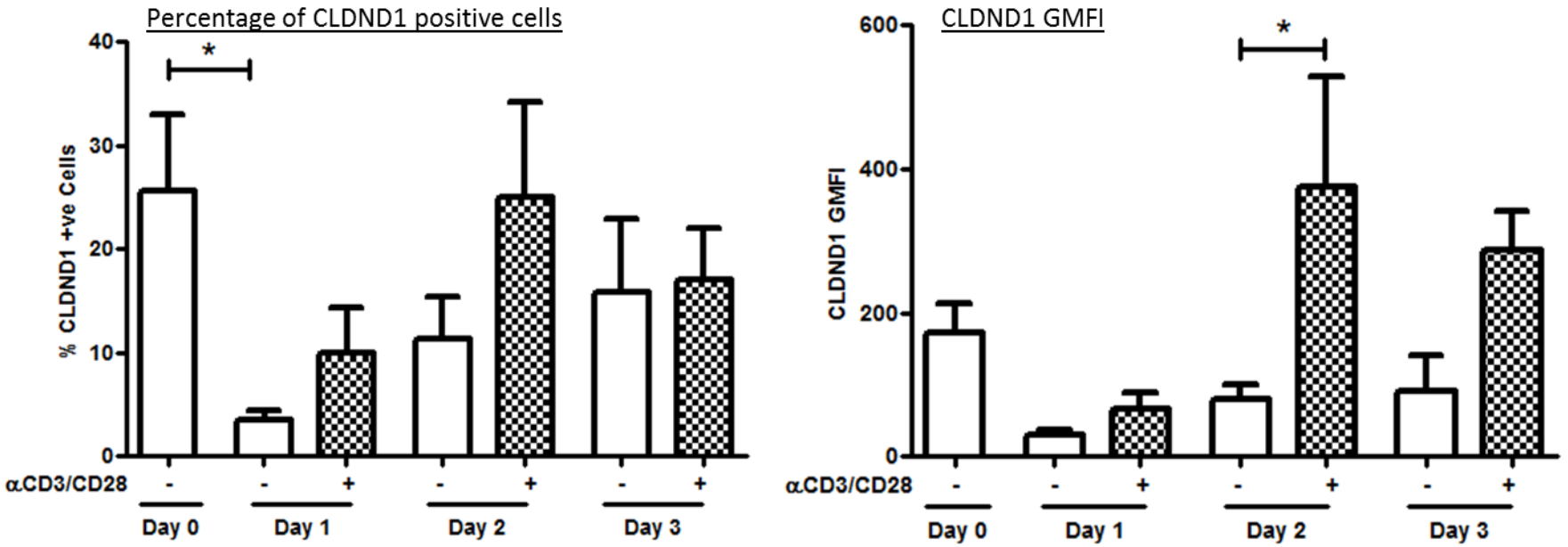

Figure 42. CLDND1 expression during CD8+ T-cell activation

PBMC were rested or activated with 1 μg/ml soluble α-CD3 and α-CD28 for 3 days. PBMC were stained for CD3 and CD8 expression prior to cell fixation in 4 % formaldehyde for CLDND1 staining. CLDND1 expression was determined from the CD3/CD8 positive gate. Cell surface CLDND1 protein expression was measured by percentage of CLDND1 positive cells, using FMO analysis, and amount of CLDND1, using CLDND1 GMFI. Data illustrate five independent experiments. Mean values were plotted with error bars illustrating SEM *$p<0.05$, repeated measures ANOVA with Bonferroni correction comparing unstimulated cells to stimulated cells at each time-point, and day 0 values to day 1 and day 3 unstimulated values.

5.3.3 Effect of experimental parameters on CLDND1 expression

As a distinct loss of CLDND1 protein expression was identified during T-cell culture, a couple of parameters were tested in order to see whether this was a direct effect of cellular manipulation and culture. Firstly, the cell density of the cultures was assessed as CLDND1 shares homology to proteins with roles in cell-cell interactions and so cell-to-cell proximity may have influenced CLDND1 protein levels (Figure 43). No significant association was identified between cell culture density and CLDND1 cell surface expression, indicating cell culture density was not important for maintenance of CLDND1 cell surface expression, at least over the range of cell densities tested.

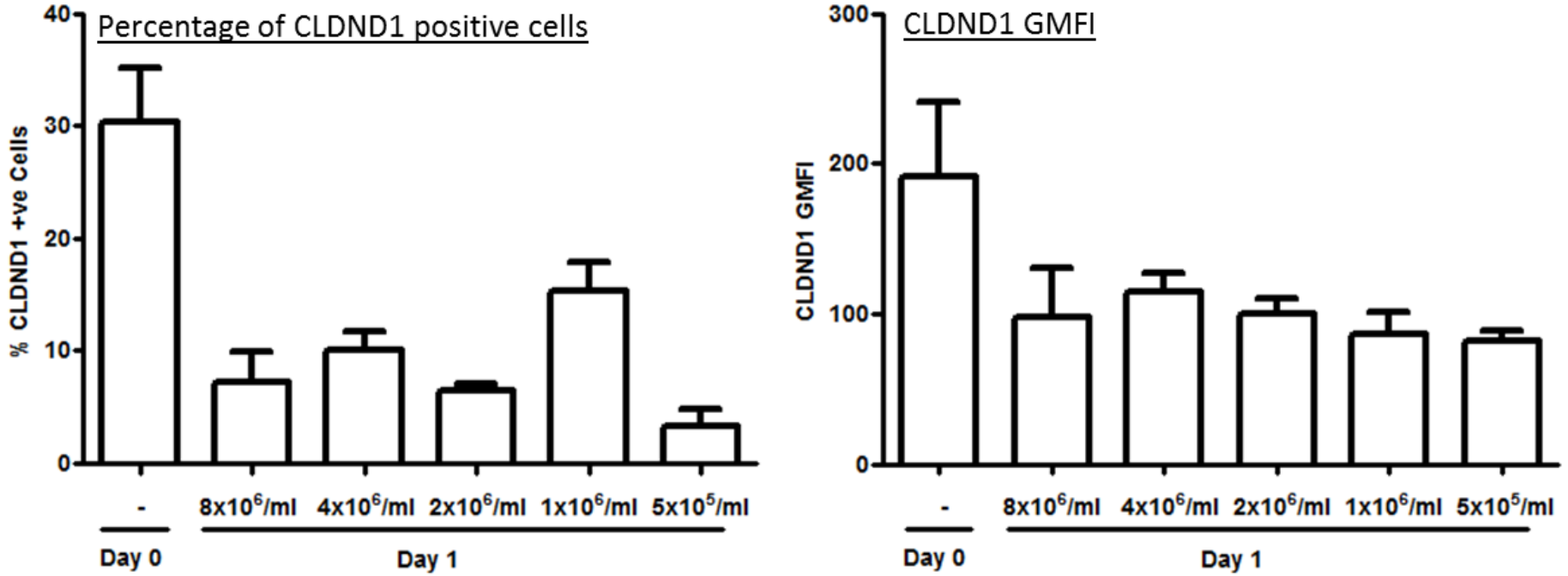

Figure 43. The effect of cell density on CLDND1 expression

PBMC were cultured at different cell densities for 24 hours. PBMC were stained for CD3 and CD4 expression prior to cell fixation in 4 % formaldehyde for CLDND1 staining. CLDND1 expression was determined from the CD3/CD4 positive gate. Cell surface CLDND1 protein expression was measured by percentage of CLDND1 positive cells, using FMO analysis, and CLDND1 GMFI. Data illustrate three independent experiments. Mean values were plotted with error bars illustrating SEM.

Secondly, all the preceding experiments used cells isolated from whole blood drawn into the anticoagulant EDTA, which acts as a chelating agent. Chelation of metal cations may have affected the expression of CLDND1, as specific claudins are known to be expressed where specific metal cation uptake occurs (Angelow et al., 2007). The anticoagulants EDTA and heparin sulphate, an antithrombin III activator which does not chelate metal ions, were compared. PBMC were isolated from the two blood preparations and were cultured for 24 hours (Figure 44). A significant decrease in both the percentage of CLDND1 positive cells and the amount of CLDND1 protein was detected after 24 hour culture in the cell preparations from EDTA-containing blood, as seen previously. A similar trend in CLDND1 cell surface expression was also seen in cell preparations from heparin sulphate-containing blood. These findings suggested that the anticoagulant was not the confounding factor in the reduction of CLDND1 cell surface expression during cell culture and that metal chelation is not important for CLDND1 cell surface expression. All subsequent experiments were performed using blood anticoagulated using EDTA.

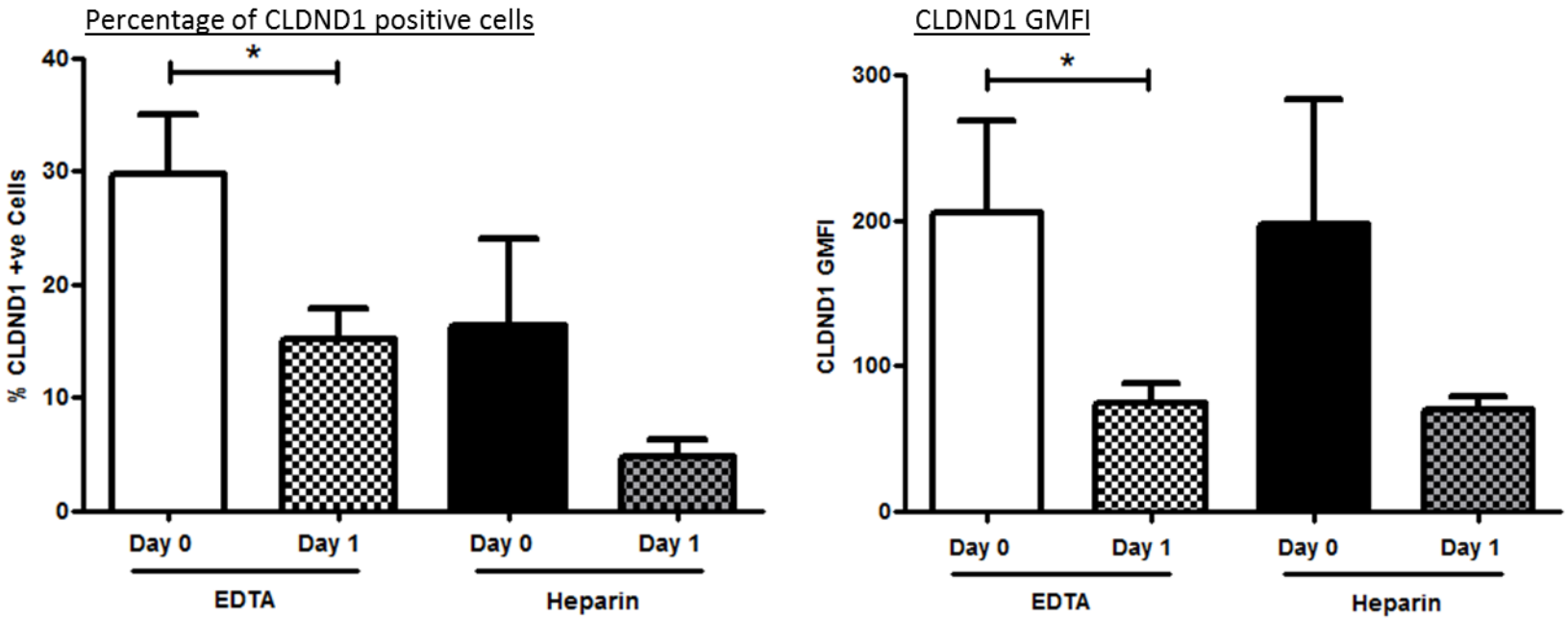

Figure 44. The effect of anticoagulant of CLDND1 expression

Whole blood was collected in EDTA based or Heparin based anticoagulant vacutainers. Blood was stained immediately or cultured for 24 hours. Cells were stained for CD3 and CD4 expression prior to cell fixation in 4 % formaldehyde for CLDND1 staining. CLDND1 expression was determined from the CD3/CD4 positive gate. Cell surface CLDND1 protein expression was measured by percentage of CLDND1 positive cells, using FMO analysis, and CLDND1 GMFI. Data illustrate five independent experiments. Mean values were plotted with error bars illustrating SEM.*$p<0.05$, Wilcoxon matched pairs test.

A further possible factor underpinning loss of CLDND1 cell surface expression was the cell isolation methods used. Cell surface expression of various chemokines is irreversibly lost during the isolation of cell types from whole blood (Nieto et al., 2012). In light of this, CLDND1 cell surface expression was compared between CD4+ T-cells from whole blood and PBMC cultures (Figure 45A). Comparison of day 0 and day 1 cultured CD4+ T-cells in whole blood showed no difference in the amount of cell surface CLDND1 or the percentage of CLDND1 expressing cells, whereas as previously shown the PBMC CD4+ T-cells had reduced CLDND1 cell surface expression after culture (Figure 44). Additionally, comparison of CD4+ T-cells at day 0 in whole blood to the freshly isolated PBMC revealed that CLDND1 expression was significantly lower in the CD4+ T-cells of the isolated PBMC population even prior to cell culture (Figure 45B).

These findings suggested that either factors within whole blood maintained CLDND1 cell surface expression; or specific elements of PBMC isolation resulted in its loss. Understanding factors that regulate CLDND1 expression would facilitate *in vitro* study of this molecule. Components of blood were addressed individually to determine their importance in maintaining CLDND1 cell surface expression. Blood is made up of a mixture of 45 % cellular and 55 % soluble material. The soluble fraction is termed plasma and comprises a mixture of water, sugar, fat, protein, and salts. The cellular portion comprises red blood cells, which occupy approximately 40-45 % of the blood's volume, leukocytes and platelets.

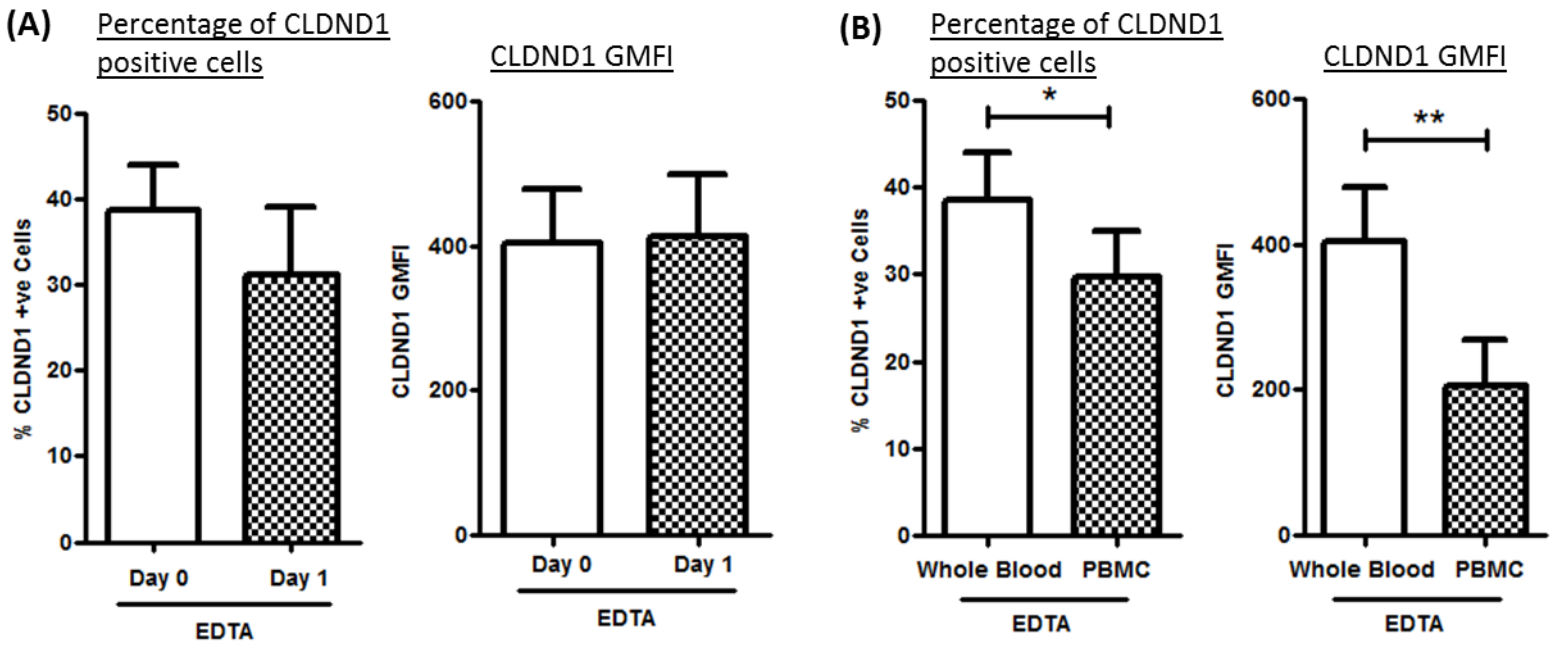

Figure 45. The effect of cell isolation on CLDND1 expression

Whole blood was collected in EDTA based vacutainers. Blood or isolated PBMC were stained immediately, or cultured for 24 hours. Cells were stained for CD3 and CD4 expression prior to cell fixation in 4 % formaldehyde for CLDND1 staining. CLDND1 expression was determined from the CD3/CD4 positive gate. Cell surface CLDND1 protein expression was measured by percentage of CLDND1 positive cells, using FMO analysis, and CLDND1 GMFI. (A) Whole blood CLDND1 cell surface levels. (B) Day 0 (immediate) stain of whole blood and isolated PBMC. Data illustrate ten independent experiments. Mean values were plotted with error bars illustrating SEM.*$p<0.05$, **$p<0.01$, Wilcoxon matched pairs test.

Initially, whole blood was separated into its cellular and soluble fractions by centrifugation, to address the importance of soluble factors. Varying centrifugation speed enabled the separation of two different plasma preparations: low speed centrifugation for the separation of plasma which was rich in platelets (PRP) whereas higher speeds eliminated the platelet portion from the plasma (PPP). Visually, the clarity of the plasma post centrifugation confirmed the presence or absence of platelets. Both these preparations were compared with serum, the soluble fraction of blood obtained after blood clotting has taken place. These preparations differ in their levels of soluble factors (Ayache et al., 2006), which could influence CLDND1 cell surface expression. PBMC were cultured in varying concentrations of these plasma and serum preparations for 24 hours. PBMC were also maintained in cell culture media as a positive control and whole blood was cultured as a negative control. CLDND1 cell surface expression was analysed pre- and post-culture (Figure 46). As the previous experiments have shown, isolation and culture of PBMC in culture medium resulted in a substantial decrease in CLDND1 cell surface expression whereas CLDND1 cell surface expression was maintained in all dilutions of cultured whole blood. Loss of CLDND1 cell surface expression was also seen in PBMC cultured in PPP or serum. There was however, maintenance of CLDND1 cell surface expression in the PBMC cultured in the PRP, comparable to the CLDND1 levels identified in the whole blood samples. The differences between the two plasma preparations suggested that platelets or platelet related factors may play a role in the maintenance of CLDND1 cell surface expression in culture. Platelet-related effects could have been mediated through cell-platelet contact, or through soluble mediators released by the platelet, such as PDGF and TGF-β.

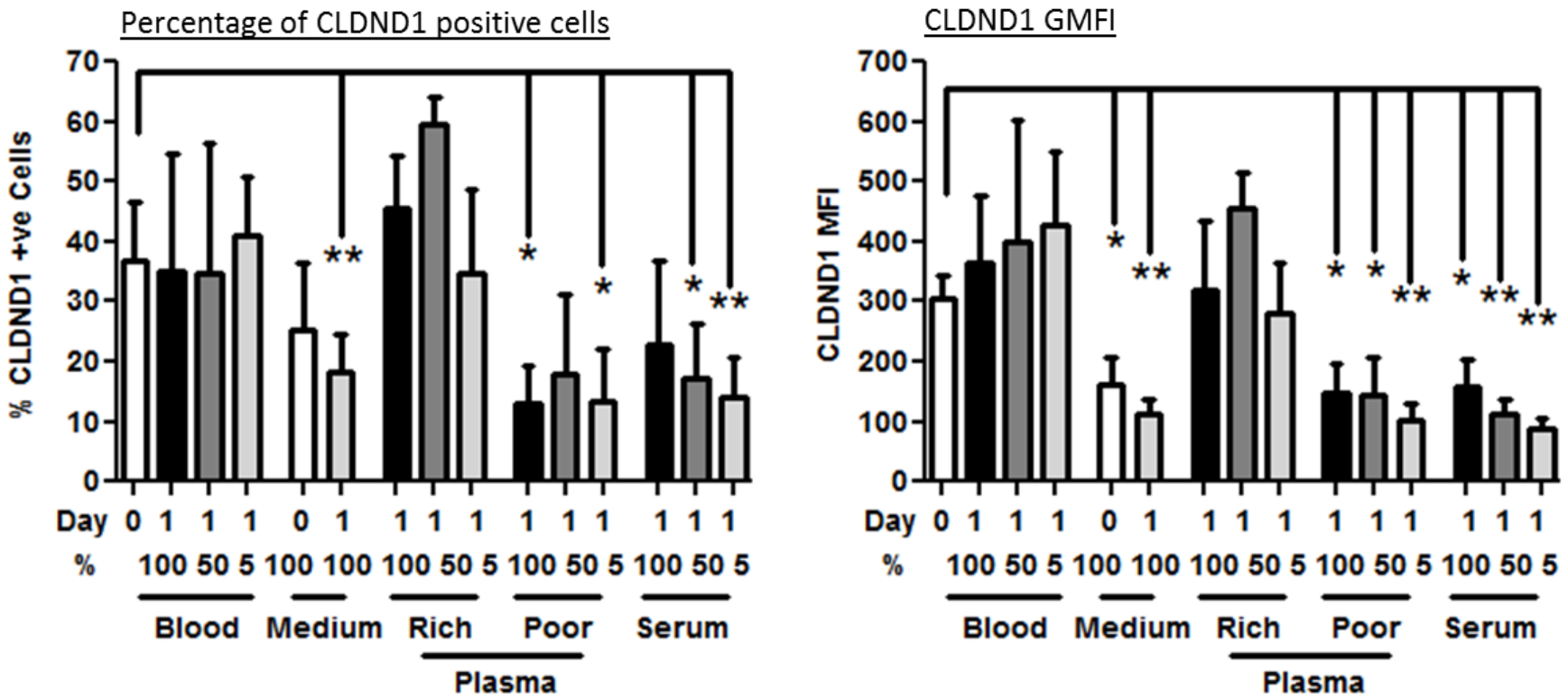

Figure 46. The effect of plasma on CLDND1 expression

Whole blood or isolated PBMC were stained immediately or cultured for 24 hours. Whole blood was cultured at 100 %, 50 % or 5 % concentrations and PBMC were cultured in 100 %, 50 % or 5 % concentrations of PRP (rich), PPP (poor) or serum. Cells were stained for CD3 and CD4 expression prior to cell fixation in 4 % formaldehyde for CLDND1 staining. CLDND1 expression was determined from the CD3/CD4 positive gate. Cell surface CLDND1 protein expression was measured by percentage of CLDND1 positive cells, using FMO analysis, and CLDND1 GMFI. Data illustrate at least four independent experiments. Mean values were plotted with error bars illustrating SEM. *p<0.05, **p<0.01, paired Student's t-test.

5.3.4 TGF-β and CLDND1 expression

Within the CLDND1 promoter, potential binding sites for an array of different transcription factors exist, one of which is the binding element CAGACA, for the SMAD transcription factors (Jonk et al., 1998), major transcription factors downstream of TGF-β ligands. I therefore sought an effect of TGF-β on CLDND1 expression.

PBMC were cultured and activated with α-CD3 and α-CD28 in the presence of TGF-β for 3 days (Figure 47). A significant increase in the percentage of CLDND1 positive cells was seen by day 3 in the resting CD4+ T-cells cultured with TGF-β compared to the no-TGF-β control. A more distinct change in the amount of cell surface CLDND1 was seen in the presence of α-CD3 and α-CD28: in contrast to the finding that CLDND1 levels were increased in the presence of T-cell activation, the presence of TFG-β with α-CD3 and α-CD28 stimulus reduced the amount of cell surface CLDND1 compared to no-TGF-β at the same time-point. Significance was determined through the use of a paired t-test, and did not include a correction for multiple sample comparison. As twelve different parameters were compared in these experiments a Bonferroni multiple correction analysis was performed, to account for a type I error, where the null hypothesis is rejected when it is true. The p value threshold of <0.05 was adjusted to account for this. As 12 different variables were tested, the p value was adjusted to $p<0.004$ ($=0.05/12$), and so would yield these findings insignificant. There is much debate as to whether the Bonferroni correction is constructive in determining true statistical significance (Perneger, 1998).

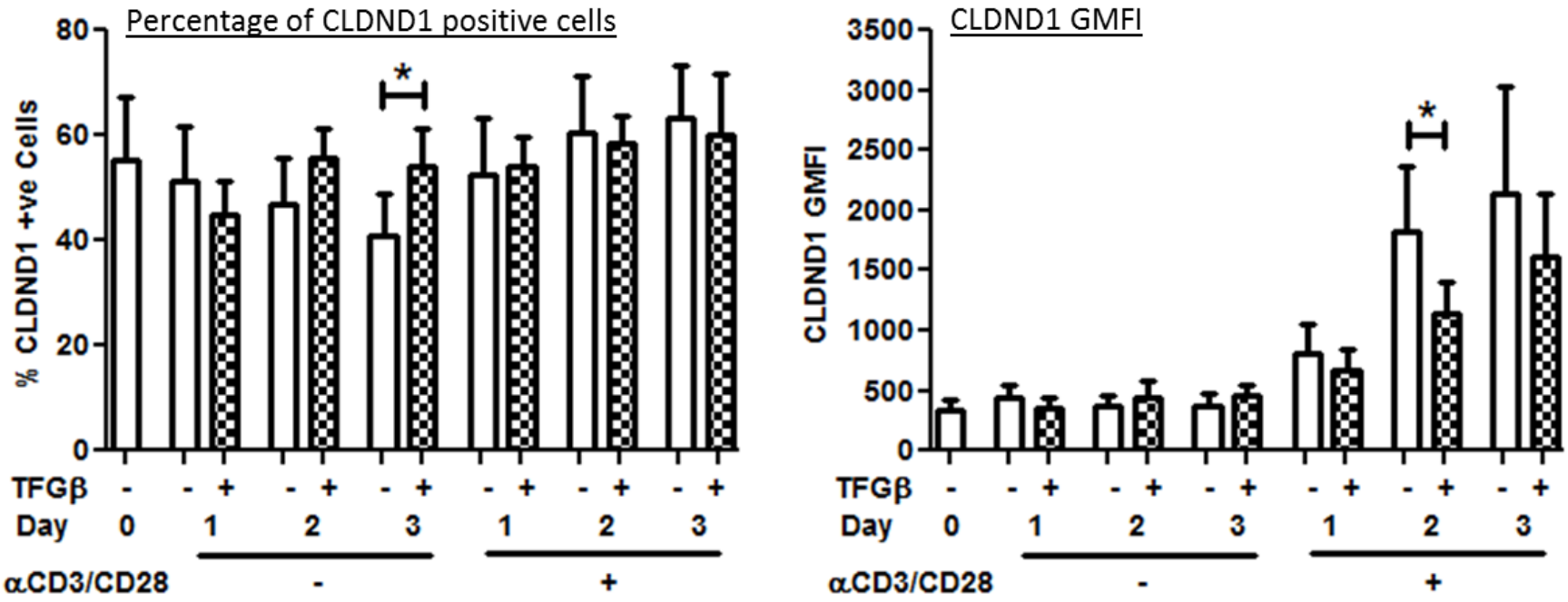

Figure 47. The effect of TGF-β on CLDND1 expression: T-cell activation

Isolated PBMC were stained immediately or cultured for 24, 48 or 72 hours in the presence of 10 ng/ml TGF-β and 1 µg/ml soluble α-CD3 and α-CD28. Cells were stained for CD3 and CD4 expression prior to cell fixation in 4 % formaldehyde for CLDND1 staining. CLDND1 expression was determined from the CD3/CD4 positive gate. Cell surface CLDND1 protein expression was measured by percentage of CLDND1 positive cells, using FMO analysis, and CLDND1 GMFI. Data illustrate at least five independent experiments. Mean values were plotted with error bars illustrating SEM. *$p<0.05$, paired Student's t-test.

To validate further the effects seen with TGF-β, the TGF-β signalling pathway was targeted with the small molecule inhibitor SB-505124. This molecule selectively inhibits the TGFBRI, ALK-4, -5 and -7, preventing TGF-β dependent down-stream activation of SMAD2 and 3 signalling (DaCosta Byfield et al., 2004). As the hypothesis for TGF-β involvement was predicted from the PRP and PPP preparation experiment, this experiment was performed again, in the presence of SB-505124 (Figure 48). As expected, CLDND1 cell surface expression was maintained in whole blood cultures and decreased in PBMC cultured in media. Contrary to the initial findings, the amount of cell surface CLDND1 was not maintained in platelet rich plasma, and the presence of SB-505124 showed no difference in CLDND1 cell surface expression in these cells. As CLDND1 cell surface levels were maintained in whole blood, the effect of SB-505124 could be tested. A small decrease in the amount of CLDND1 cell surface expression was detected in the 100 % blood cultures in the presence of SB-505124; suggesting TGF-β signalling may be playing some role in maintaining CLDND1 expression, however the limited decrease suggests that TGF-β signalling may not be a major contributing factor to CLDND1 expression. Again, as multiple analyses were performed, application of a Bonferroni correction would re-adjust the p-value required for significance to <0.008 (=0.05/6). As the PRP experiment did not maintain CLDND1 cell surface expression, these data were omitted from the statistical analysis. Again, application of the Bonferroni correction yielded an insignificant difference between the day 1 100 % blood samples in the absence or presence of SB-505124. The underlying aim of these experiments was to determine optimal culture conditions for maintaining CLDND1 cell surface expression. This proved challenging with some inconsistencies potentially suggesting donor dependent factors.

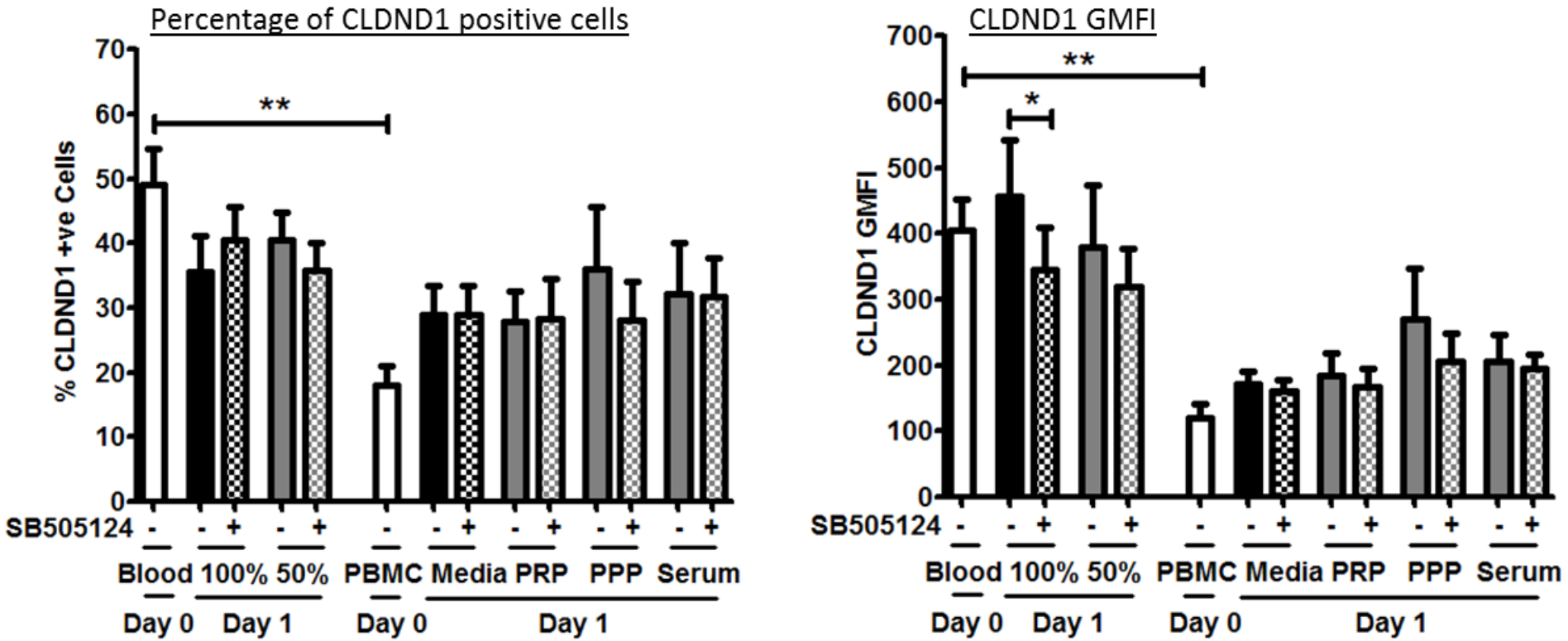

Figure 48.The effect of TGF-β on CLDND1 expression: SB-505124

Whole blood or isolated PBMC were stained immediately or cultured for 24 hours with 1 μM SB-505124. Whole blood was cultured at 100 % or 50 % concentration, diluting in RPMI and PBMC were cultured in 50% concentrations of PRP,PPP or serum. Cells were stained for CD3 and CD4 expression prior to cell fixation in 4 % formaldehyde for CLDND1 staining. CLDND1 expression was determined from the CD3/CD4 positive gate. Cell surface CLDND1 protein expression was measured by percentage of CLDND1 positive cells, using FMO analysis, and CLDND1 GMFI. Data illustrate at least five independent experiments. Mean values were plotted with error bars illustrating SEM. *p<0.05, **p<0.01, paired Student's t-test.

5.3.5 CLDND1 expression on CD4+ T-cell and DC co-cultures.

The CLDND1 protein expression data obtained during T-cell activation used α-CD3 and α-CD28 as a stimulus. Based on homology to the PMP-22/EMP/MP20/claudin superfamily members and their roles in cell-cell interactions, I hypothesised a role for CLDND1 in the interaction between T-cells and APC. DC are the archetypal APC, can be differentiated from blood monocytes and are widely used to activate T-cells *in vitro*. Depending on the differentiation process used, DC can be matured with LPS (matDC) or become tolerogenic (tolDC) with dexamethasone and calcitriol.

These two DC subsets were generated to determine CLDND1 expression profiles on co-cultured CD4+ T-cells. Firstly, DC characterisation was performed to confirm mature and tolerogenic phenotypes (Figure 49). TolDC had lower CD80 and CD83 co-stimulatory molecule expression than matDC and marginally lower expression of CD86. TolDC had higher HLA-DR expression, suggesting they maintain the capability to present to T-cells, and higher TLR-2 expression. Increased TLR-2 expression has been associated with a lower pro-inflammatory immune profile (Chamorro et al., 2009, Harry et al., 2010). The tolDC had higher LAP expression, a marker for TGF-β, but no comparable difference in CLDND1 expression.

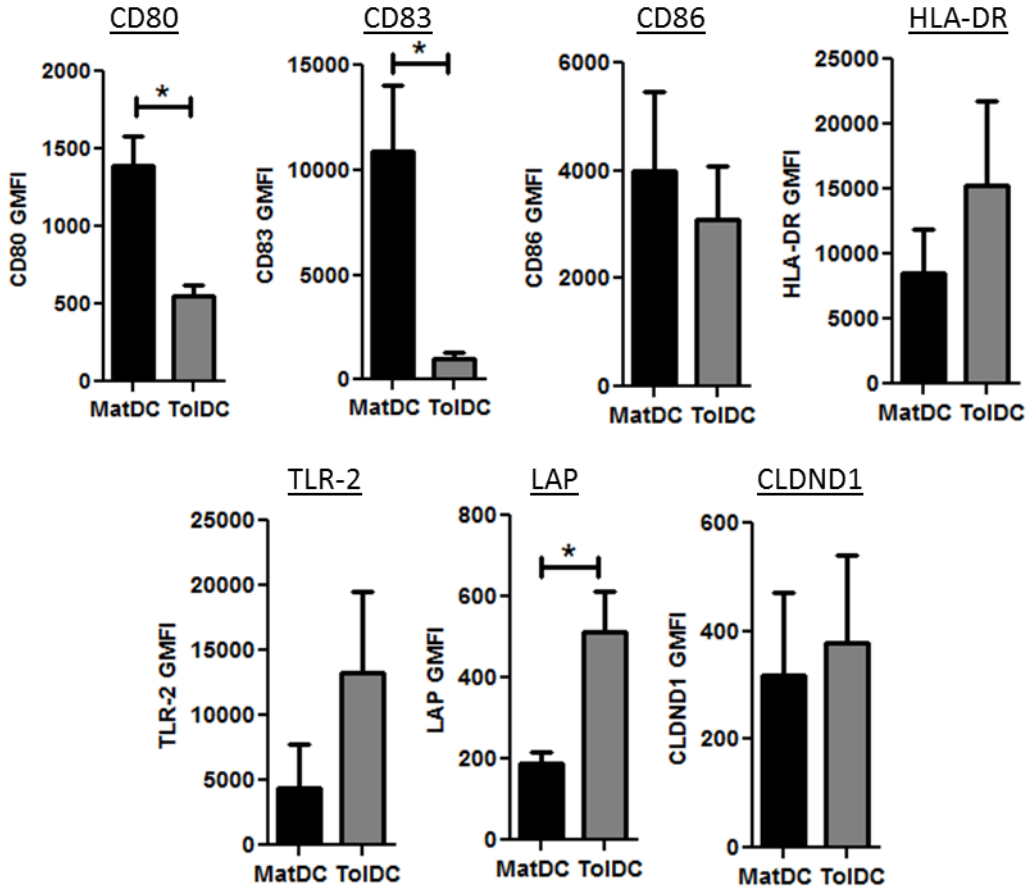

Figure 49. Characterisation of mat- and tolDC

Mat- and tolDC were differentiated from CD14+ monocytes. (A) Post differentiation the DC were stained for the different cell surface markers shown. Data illustrate at least four independent experiments. Mean values were plotted with error bars illustrating SEM. *p<0.05, paired Student's t-test.

CD4+ T-cells co-cultured with matDC or tolDC had different proliferation kinetics and cytokine expression profiles (Figure 50). The matDC stimulated T-cells had higher proliferation counts at day 3 than the T-cells stimulated with the tolDC (Figure 50A). Both proliferation values were lower than the value obtained with α-CD3/CD28 expander bead stimulus. The cytokine expression profile also mirrored the proliferation data, with less IFN-γ, TNF-α and IL-10 production by the T-cells stimulated with tolDC (Figure 50B). The day 6 data revealed that proliferation counts were comparable between the DC stimulated T-cells (Figure 50C). The cytokine expression profiling showed that T-cells stimulated with tolDC secreted less IFN-γ (Figure 50D).

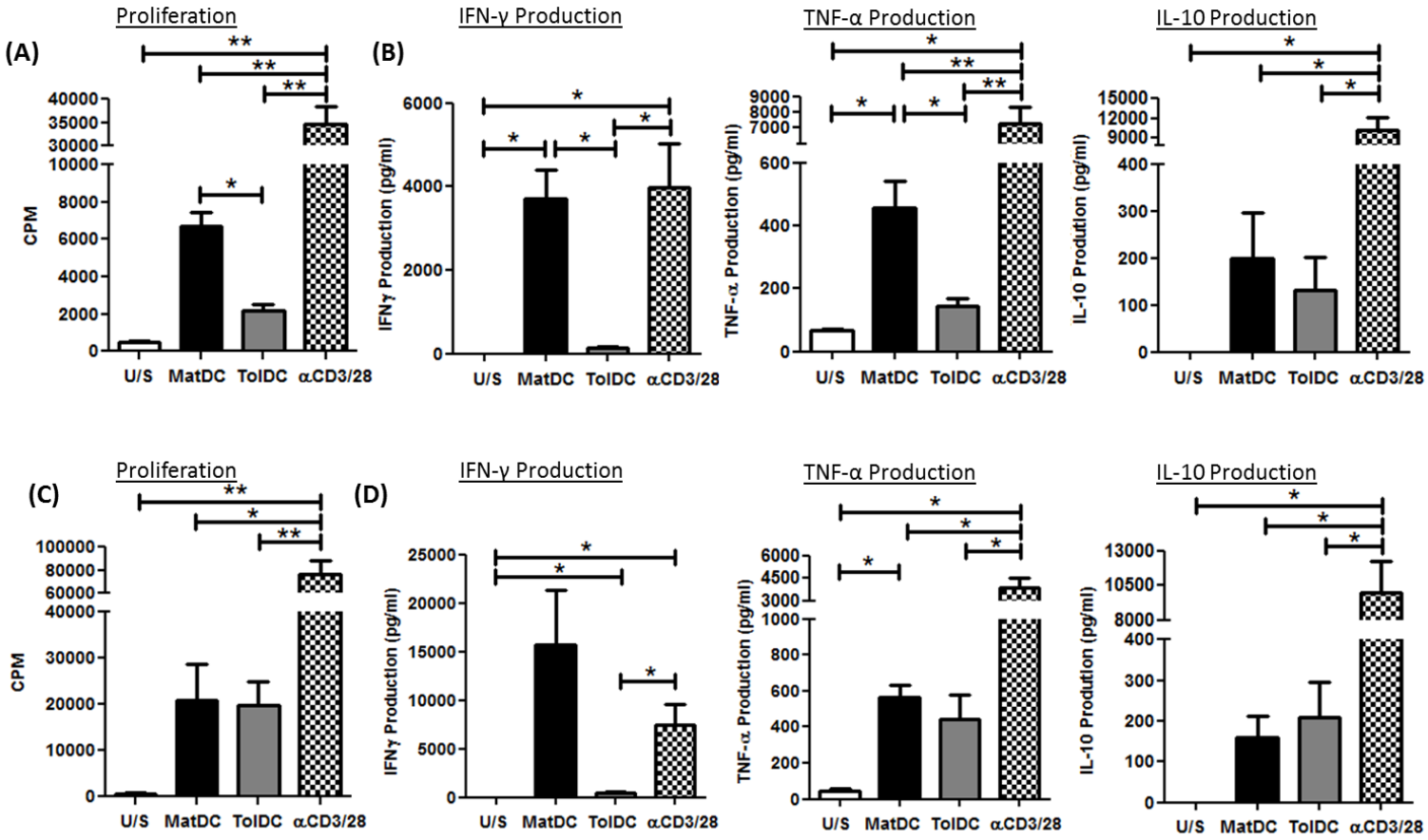

Figure 50. Mat- and tolDC co-cultures with CD4+ T-cells: T-cell activation

Mat- and tolDC were differentiated from CD14+ monocytes. CD4+ T-cells were cultured with DC or α-CD3/CD28 expander beads for (A) 3 days, measuring proliferation by ^{3}HTdR incorporation and (B) IFN-γ, TNF-α and IL-10 secretion by ELISA, or for 6 days (C) measuring proliferation by ^{3}HTdR incorporation and (D) IFN-γ, TNF-α and IL-10 secretion by ELISA. Data illustrate at least four independent experiments. Mean values were plotted with error bars illustrating SEM *p<0.05, **p<0.01, paired Student's t-test.

CLDND1 expression on CD4+ T-cells co-cultured with mat- and tolDC was determined at day 3 and day 6 time-points, looking at both cell surface and total CLDND1 expression (Figure 51). The CLDND1 expression profiles mimicked the proliferation data, with higher CLDND1 cell surface expression at day 3 with matDC compared with tolDC but both T-cell populations having less CLDND1 expression than when stimulated with α-CD3/CD28 expander bead stimulus (Figure 51A). Total CLDND1 expression on DC stimulated T-cells was comparable to unstimulated T-cells, suggesting the total amount of CLDND1 protein did not change (Figure 51B), and differences seen on the surface may be linked to protein trafficking. At day 6, α-CD3/CD28 expander bead stimulus induced CLDND1 cell surface expression was comparable to levels of both the DC stimulated cells (Figure 51C). Again, total CLDND1 expression remained similar between the populations, suggesting no change in the total amount of CLDND1 (Figure 51D). All day 6 values were lower than at day 3, suggesting a transient activation-induced expression of CLDND1.

Based on the findings above, CLDND1 cell surface expression correlated with the intensity of the activation stimulus. α-CD3/CD28 expander bead stimulus resulted in the highest proliferation, cytokine production and CLDND1 cell surface expression, at earlier time-points, followed by matDC. TolDC induced the lowest proliferation and cytokine production and had the lowest CLDND1 cell surface expression, but at a later time-point the profile was similar to the matDC.

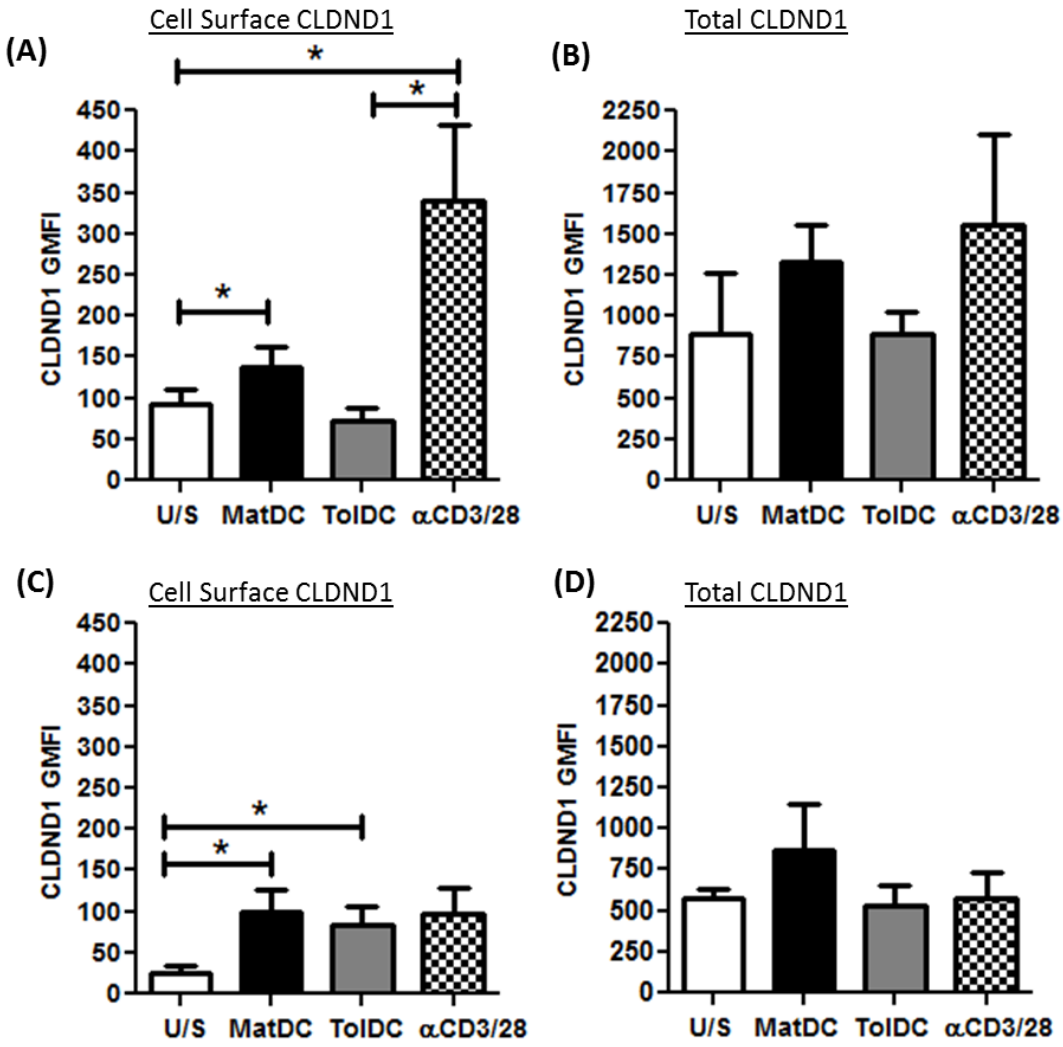

Figure 51. Mat- and tolDC co-cultures with CD4+ T-cells: CLDND1 expression

Mat- and tolDC were differentiated from CD14+ monocytes. CD4+ T-cells were cultured with DC or with α-CD3/CD28 expander beads for 3 or 6 days. Cells were fixed in 4 % formaldehyde before CLDND1 staining. Cell surface CLDND1 protein expression was measured by CLDND1 GMFI. Day 3 CLDND1 expression of (A) cell surface, or (B) total protein. Day 6 CLDND1 expression of (C) cell surface, or (D) total protein. Data illustrate five independent experiments. Mean values were plotted with error bars illustrating SEM. *p<0.05, **p<0.01, paired Student's t-test.

5.3.6 Analysis of CLDND1 expression in Early Arthritis (EA) Patients

Previous studies have shown than RA CD4+ T-cells from synovium adopted a gene expression profile that shares characteristics with an anergic T-cell gene expression profile (Ali et al., 2001). Therefore, CLDND1 cell surface expression was measured in EA patients. EA patients are predominately drug naïve, removing a major confounder that could influence CLDND1 expression. Using a selection of EA patients also allowed for the separation of the arthritides to create control groups. These four groups were: non-inflammatory arthritis (N-IA), osteoarthritis (OA), inflammatory non-RA (INRA) and RA.

Whole blood cells from patients with different diagnoses attending an EA clinic were stained for CLDND1 expression. CLDND1 cell surface expression was measured on CD4+ and CD8+ T-cell subsets, CD14+ monocytes and CD19+ B-cells in whole blood (Figure 52 and Figure 53). A significant increase in the amount of cell surface CLDND1 was detected in RA, compared to N-IA in the CD4+ and CD8+ T-cell subsets. An increase in the median amount of cell surface CLDND1 was also seen in INRA compared to N-IA. These patterns were also seen for the percentage of CLDND1 positive cells, wherein all cell subsets showed significant differences in RA compared to N-IA.

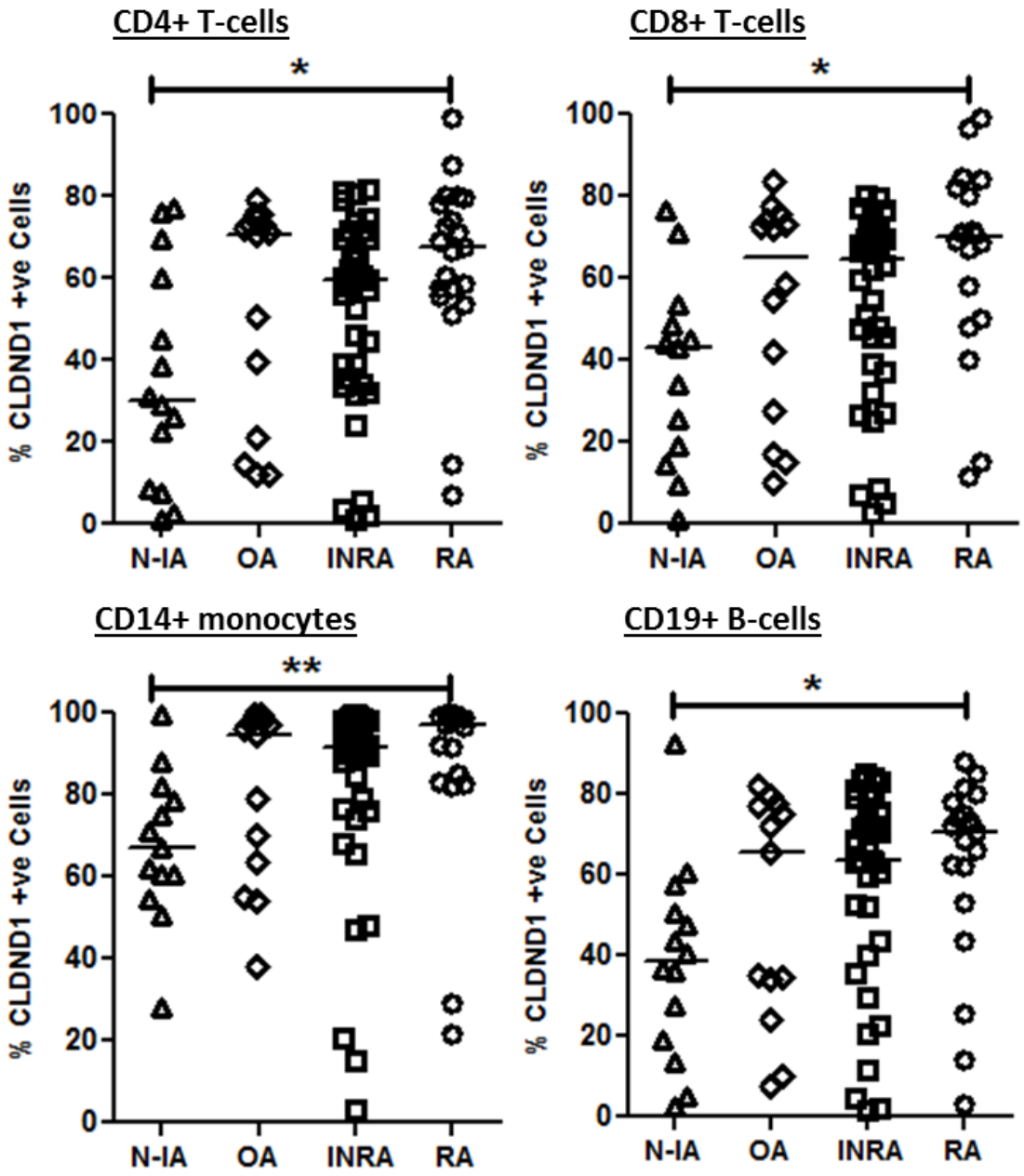

Figure 52. EA patients: disease classification: % CLDND1 positive cells

Whole blood from EA patients was stained for CD3, CD4, CD8, CD14 and CD19 prior to cell fixation in 4 % formaldehyde for CLDND1 staining. Cell surface CLDND1 protein expression was measured by percentage of CLDND1 positive cells, using FMO analysis. EA patients were grouped according to disease classification for each cell subset. Median values are illustrated by the line. *p<0.05, **p<0.01, 1way ANOVA with Dunn's multiple comparison correction.

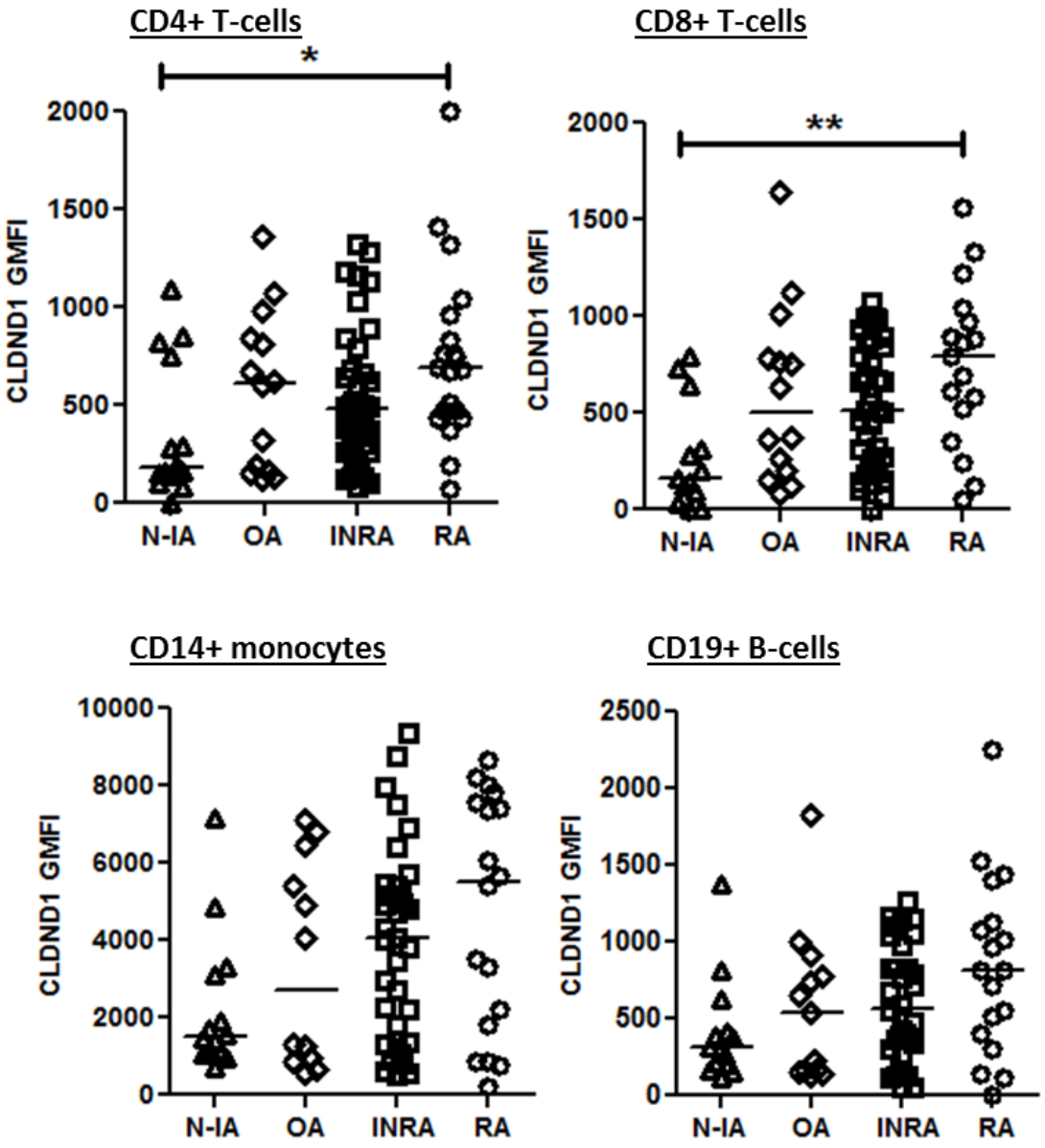

Figure 53. EA patients: disease classification: CLDND1 GMFI

Whole blood from EA patients was stained for CD3, CD4, CD8, CD14 and CD19 prior to cell fixation in 4 % formaldehyde for CLDND1 staining. Cell surface CLDND1 protein expression was measured by CLDND1 GMFI. EA patients were grouped according to disease classification for each cell subset. Median values are illustrated by the line. *p<0.05, **p<0.01, 1way ANOVA with Dunn's multiple comparison correction.

As CLDND1 cell surface levels were increased in RA, CLDND1 expression was correlated to markers of general inflammation or to disease activity to distinguish whether increased CLDND1 levels were due to a general increase in inflammation, or whether CLDND1 expression was associated with disease activity. Inflammation status was measured by the erythrocyte sedimentation rate (ESR) and by levels of C-reactive protein (CRP). No correlation was found between either ESR or CRP and the percentage of CLDND1 positive cells (Figure 54) or the amount of CLDND1 in any of the cell subsets (Figure 55), when comparing all the arthritides, suggesting that CLDND1 levels were not related to systemic inflammation. Analysis of each of the different disease subgroups showed that in non-inflammatory arthritides, the amount of CLDND1 cell surface expression did correlate with CRP in the CD4+ and CD8+ T-cell subsets, but no correlation was found with ESR or in any of the inflammatory arthritides (Table 15). These results raised the possibility of a link between CLDND1 cell surface expression and the inflammatory environment but further investigation is required to test this potential association further. Disease activity was measured using the DAS28 score, which is calculated from severity of joint swelling and tenderness, a global assessment of disease activity and ESR levels. DAS28 score is only validated in RA disease and correlation of the RA subgroup with DAS28 score resulted in a low correlation value and a non-significant P value (r^2=0.02897, p=0.4731), indicating CLDND1 does not correlate with DAS28 score (Data not shown).

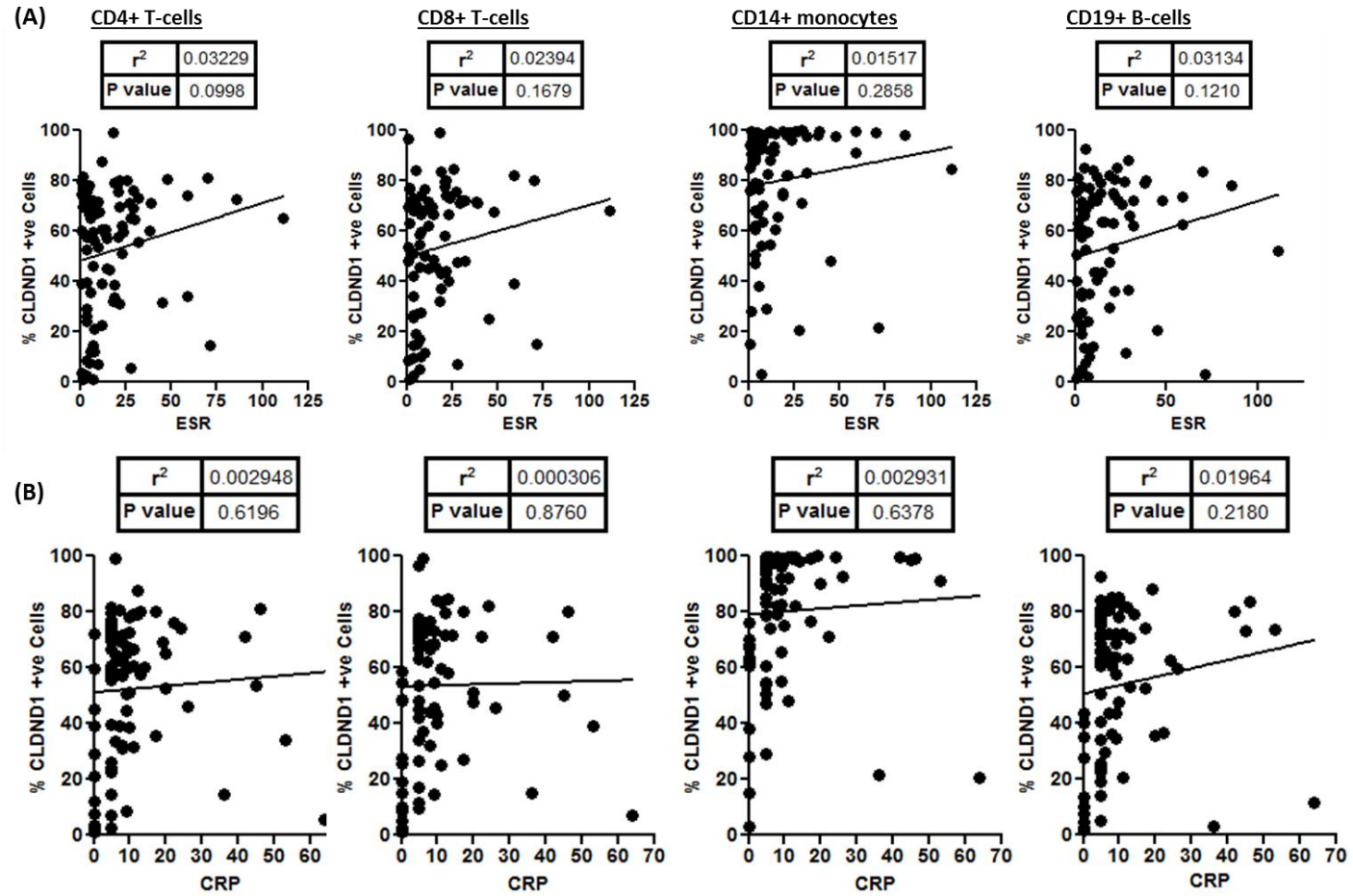

Figure 54. EA samples: correlation between CLDND1 expression and inflammation: % CLDND1 positive cells

Whole blood from EA patients was stained for CD3, CD4, CD8, CD14 and CD19 prior to cell fixation in 4 % formaldehyde for CLDND1 staining. Cell surface CLDND1 protein expression was measured by. percentage of CLDND1 positive cells, using FMO analysis (A) Correlation between ESR and all EA samples (B) Correlation between CRP score and all EA samples.

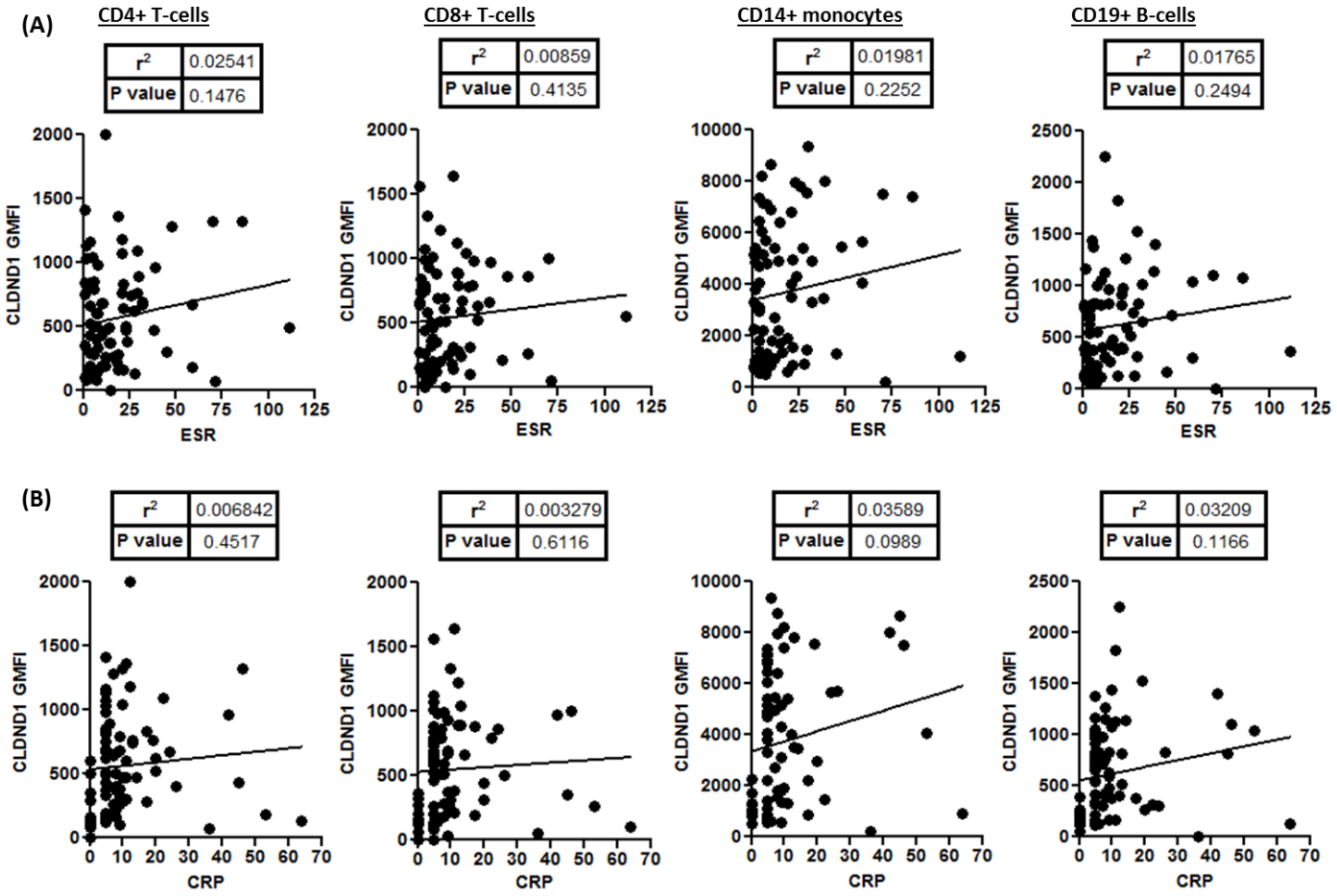

Figure 55. EA samples: correlation between CLDND1 expression and inflammation: CLDND1 GMFI

Whole blood from EA patients was stained for CD3, CD4, CD8, CD14 and CD19 prior to cell fixation in 4 % formaldehyde for CLDND1 staining. Cell surface CLDND1 protein expression was measured by CLDND1 GMFI. (A) Correlation between ESR and all EA samples (B) Correlation between CRP score and all EA samples.

ESR		N-IA	OA	I-NRA	RA
CD4 GMFI	r^2	0.0318	0.1472	0.0161	0.0000
	p value	0.5416	0.1955	0.4542	0.9966
CD8 GMFI	r^2	0.0798	0.1998	0.0124	0.1116
	p value	0.3496	0.1257	0.5112	0.1900
CD14 GMFI	r^2	0.0553	0.1815	0.0046	0.0028
	p value	0.4185	0.1673	0.7070	0.8287
CD19 GMFI	r^2	0.0137	0.1952	0.0304	0.0099
	p value	0.6907	0.1505	0.3322	0.6947
CD4 cells	r^2	0.0961	0.1865	0.0279	0.0203
	p value	0.2808	0.1406	0.3228	0.5377
CD8 cells	r^2	0.2166	0.2302	0.0282	0.0930
	p value	0.1090	0.0971	0.3201	0.2186
CD14 cells	r^2	0.0272	0.2425	0.2143	0.0347
	p value	0.5900	0.1033	0.4163	0.4448
CD19 cells	r^2	0.0061	0.2650	0.0291	0.0074
	p value	0.7916	0.0868	0.3428	0.7270

CRP		N-IA	OA	I-NRA	RA
CD4 GMFI	r^2	0.3169	0.3242	0.0006	0.0200
	p value	0.0316	0.0335	0.8896	0.5517
CD8 GMFI	r^2	0.3288	0.4383	0.0071	0.0423
	p value	0.0405	0.0099	0.6201	0.4283
CD14 GMFI	r^2	0.0034	0.3576	0.0005	0.0256
	p value	0.8443	0.0309	0.8982	0.5133
CD19 GMFI	r^2	0.0170	0.3836	0.0165	0.0008
	p value	0.6574	0.0240	0.4765	0.9102
CD4 cells	r^2	0.1915	0.2784	0.0118	0.0294
	p value	0.1176	0.0525	0.5214	0.4574
CD8 cells	r^2	0.2380	0.3768	0.0213	0.0506
	p value	0.0908	0.0195	0.3887	0.3697
CD14 cells	r^2	0.1362	0.1881	0.0044	0.0024
	p value	0.2147	0.1387	0.7129	0.8416
CD19 cells	r^2	0.0534	0.3322	0.0005	0.0006
	p value	0.4269	0.0392	0.9017	0.9209

Table 15. EA samples: correlation between CLDND1 expression and ESR and CRP

Whole blood from EA patients was stained for CD3, CD4, CD8, CD14 and CD19 prior to cell fixation in 4 % formaldehyde for CLDND1 staining. Cell surface CLDND1 protein expression was measured by CLDND1 GMFI and percentage of CLDND1 positive cells, using FMO analysis. Values were correlated to ESR and CRP values.

As CLDND1 levels were significantly up-regulated in RA cell subsets, CLDND1 expression profiling in RA was examined. RA can be further sub-classified depending on RF and CCP status, so CLDND1 cell surface expression levels were compared between these subclasses (Figure 56 and Figure 57). The percentage of CLDND1 positive cells was similar between the two RF populations in all of the cell types studied (Figure 56A) but the amount of CLDND1 cell surface expression was higher in the RF positive (RF+ve) group in the T-cell population (Figure 57A). Comparison of CCP status revealed no difference in CLDND1 cell surface expression or percentage of CLDND1 positive cells between the CCP subgroups (Figure 56B and Figure 57B).

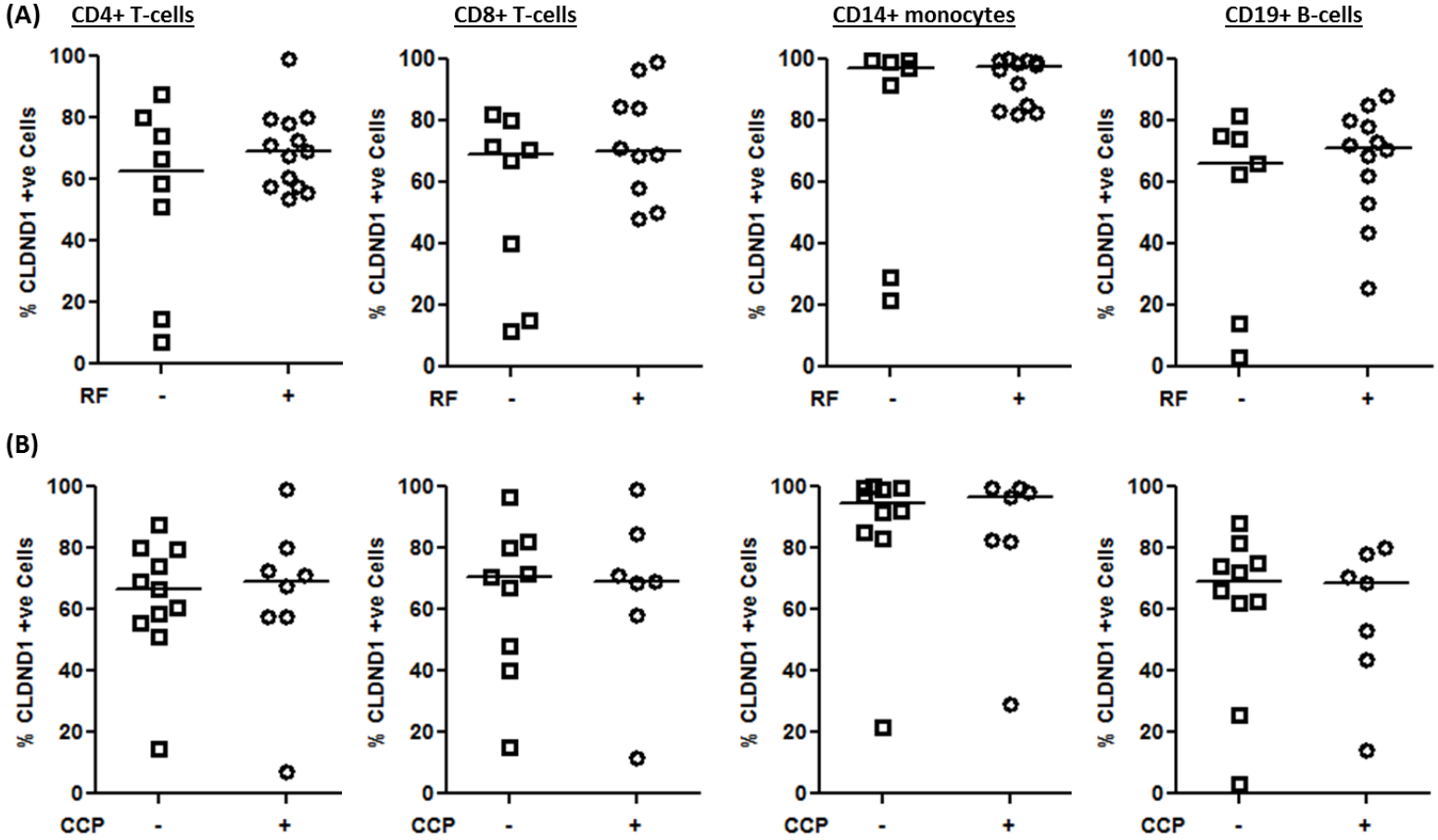

Figure 56. EA samples: CLDND1 expression in early RA according to RF status: % CLDND1 positive cells

Whole blood from early RA patients was stained for CD3, CD4, CD8, CD14 and CD19 prior to cell fixation in 4 % formaldehyde for CLDND1 staining. Cell surface CLDND1 protein expression was measured by percentage of CLDND1 positive cells, using FMO analysis. CLDND1 cell surface expression depending on (A) RF status or, (B) CCP status. Median values are illustrated by the line. Mann Whitney test was performed to determine statistical significance.

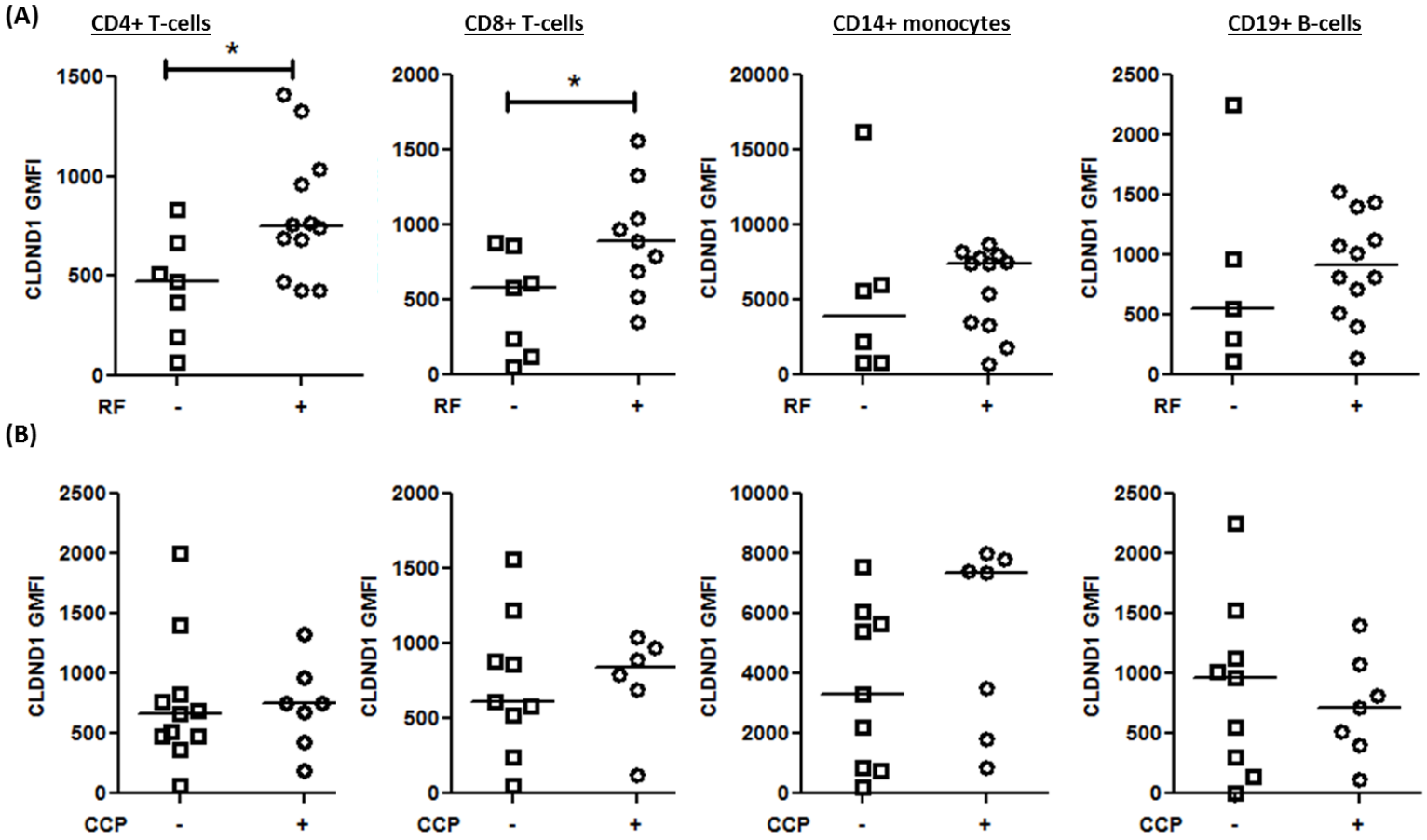

Figure 57. EA samples: CLDND1 expression in early RA according to RF status: CLDND1 GMFI

Whole blood from early RA patients was stained for CD3, CD4, CD8, CD14 and CD19 prior to cell fixation in 4 % formaldehyde for CLDND1 staining. Cell surface CLDND1 protein expression was measured by CLDND1 GMFI. CLDND1 cell surface expression depending on (A) RF status, or (B) CCP status. Median values are illustrated by the line. *p<0.05, Mann Whitney test.

5.3.7 Other factors determining CLDND1 expression

Two independent studies focussing on the effects of smoking status by whole blood or lymphocyte gene microarray identified CLDND1 as one of the two most up-regulated genes in whole blood, and one of the 50 most up-regulated genes in lymphocytes, in the smoking group (Beineke et al., 2012, Charlesworth et al., 2010). It is also worth noting that in seropositive RA, smoking is considered an environmental association with disease susceptibility (Pratt et al., 2009). CLDND1 cell surface protein expression was therefore assessed in the EA samples, to see whether there was also an association with CLDND1 cell surface protein expression and smoking status (Figure 58 and Figure 59). Patients were divided into three groups: never smoked (never), former smoker (former) or current smoker (current). CLDND1 cell surface expression levels were comparable between the three groups, irrespective of cell type. As differences in CLDND1 expression was seen between the different arthritides, smoking status was compared to CLDND1 cell surface levels in each group, but no difference in CLDND1 cell surface expression was observed (Figure 60 and Figure 61).

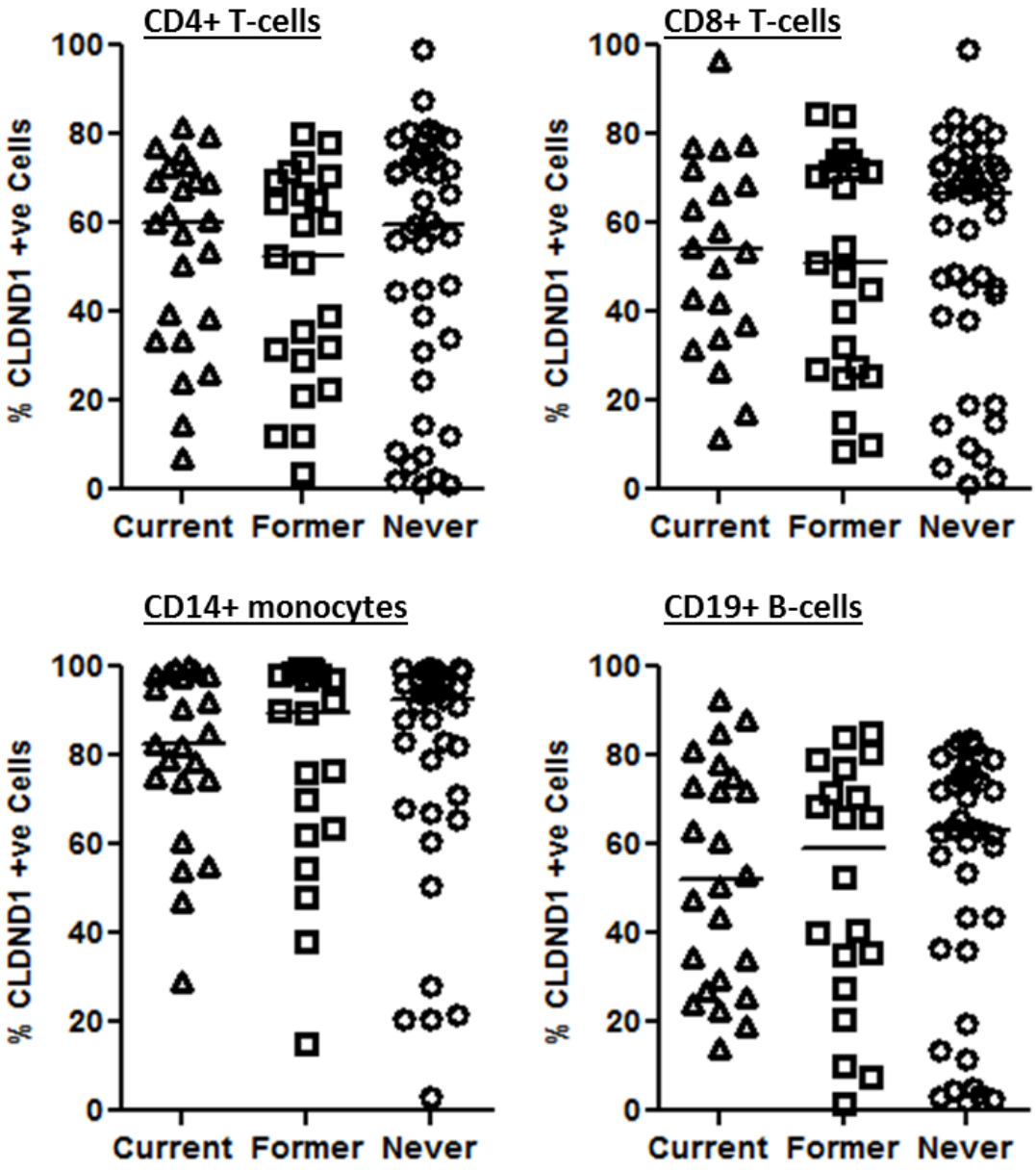

Figure 58. EA samples: CLDND1 cell surface expression according to smoking status: % CLDND1 positive cells

Whole blood from EA patients was stained for CD3, CD4, CD8, CD14 and CD19 prior to cell fixation in 4 % formaldehyde for CLDND1 staining. Cell surface CLDND1 protein expression was measured by percentage of CLDND1 positive cells, using FMO analysis. CLDND1 GMFI was determined in all EA samples depending on smoking status: current smoker (current), former smoker (former), never smoked (never). Median values are illustrated by the line. One way ANOVA with Dunn's multiple Comparison correction was performed to determine statistical significance.

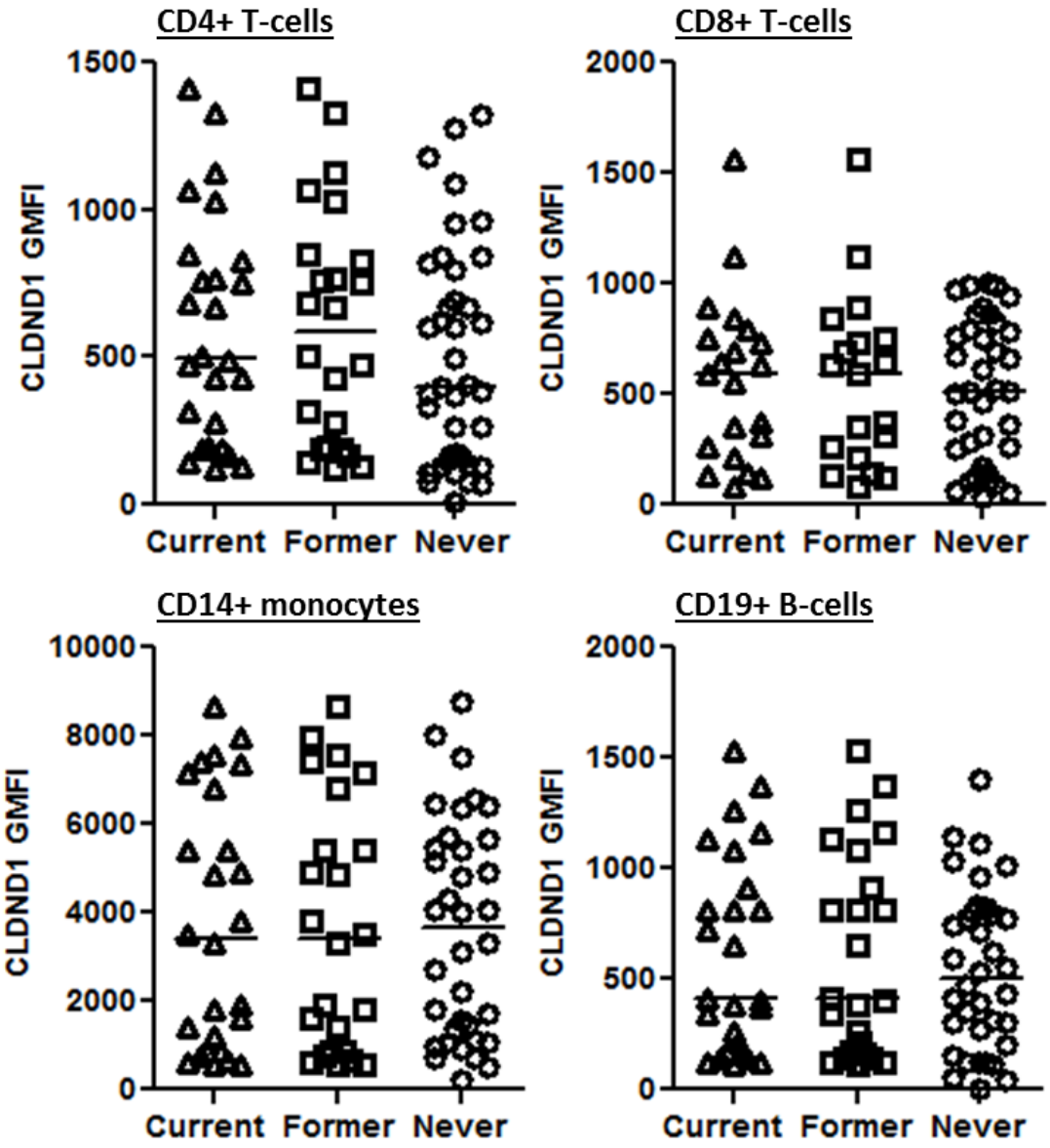

Figure 59. EA samples: CLDND1 cell surface expression according to smoking status: CLDND1 GMFI

Whole blood from EA patients was stained for CD3, CD4, CD8, CD14 and CD19 prior to cell fixation in 4 % formaldehyde for CLDND1 staining. Cell surface CLDND1 protein expression was measured by CLDND1 GMFI in all EA samples depending on smoking status: current smoker (current), former smoker (former), never smoked (never). Median values are illustrated by the line. One way ANOVA with Dunn's multiple Comparison correction was performed to determine statistical significance.

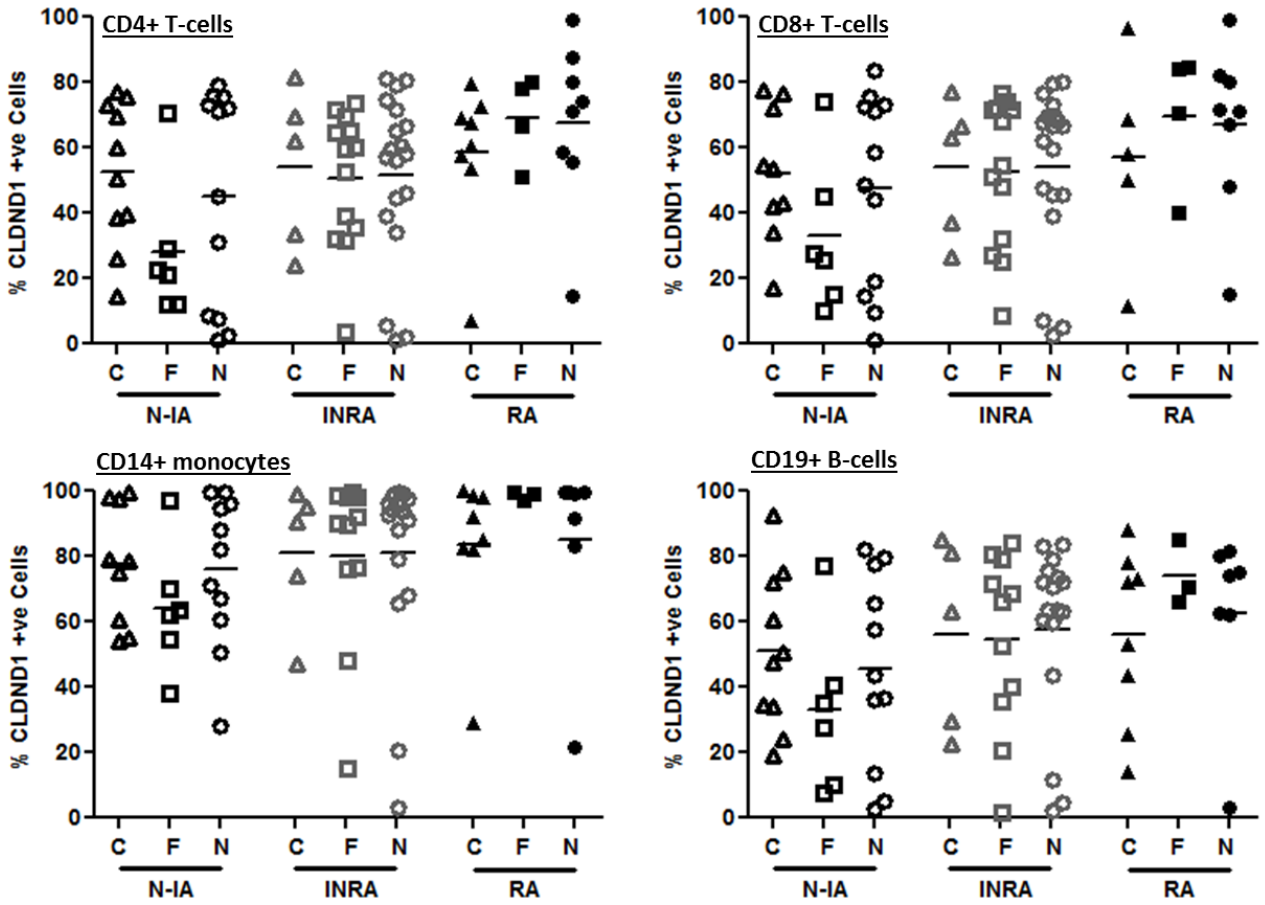

Figure 60. EA samples: CLDND1 cell surface expression according to smoking status: % CLDND1 positive cells

Whole blood from EA patients was stained for CD3, CD4, CD8, CD14 and CD19 prior to cell fixation in 4 % formaldehyde for CLDND1 staining. Cell surface CLDND1 protein expression was measured by percentage of CLDND1 positive cells, using FMO analysis in N-IA, INRA and RA subsets depending on smoking status: current smoker (C), former smoker (F), never smoked (N). Median values are illustrated by the line. One way ANOVA with Dunn's multiple Comparison correction was performed to determine statistical significance.

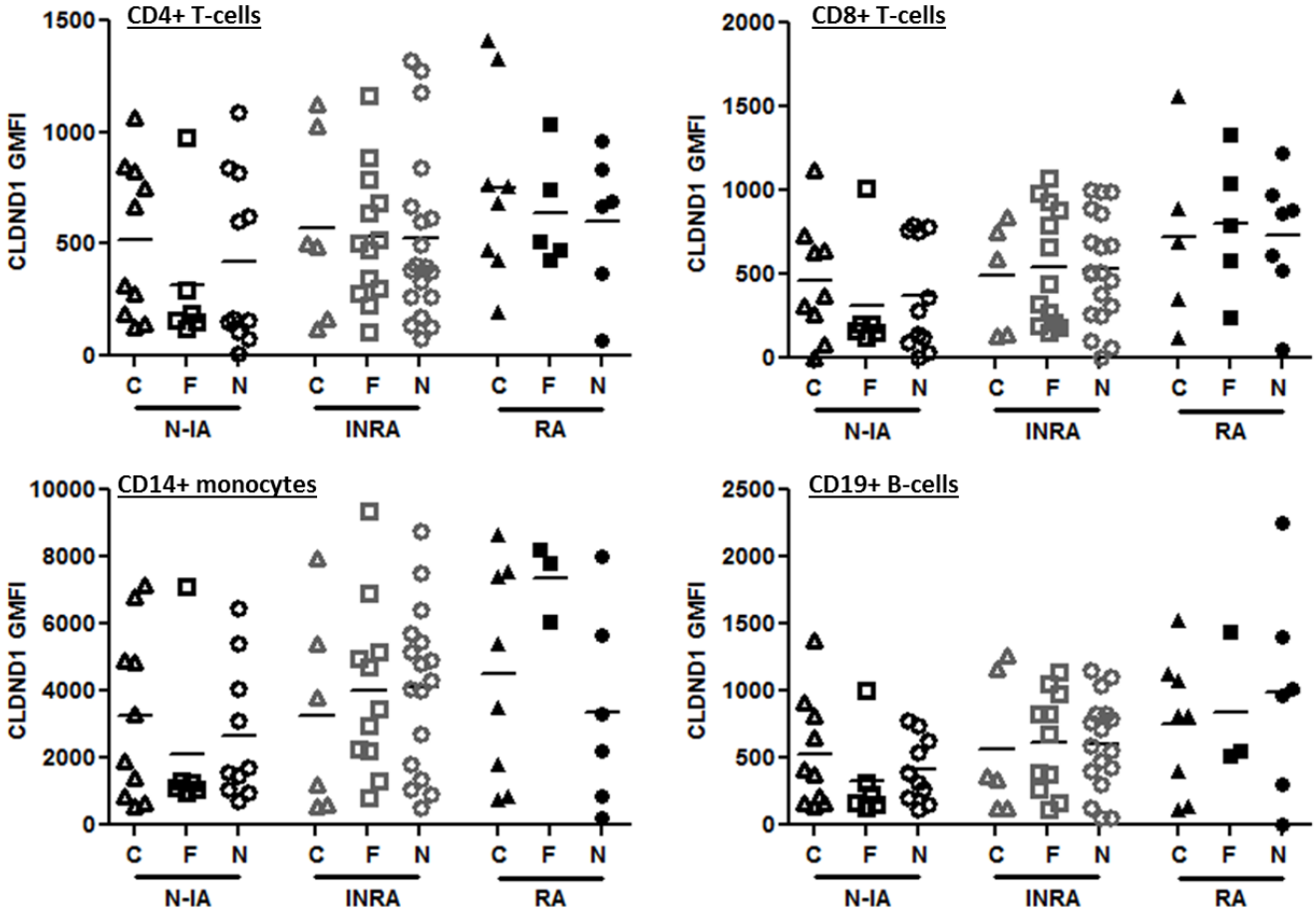

Figure 61. EA samples: CLDND1 cell surface expression according to smoking status: CLDND1 GMFI

Whole blood from EA patients was stained for CD3, CD4, CD8, CD14 and CD19 prior to cell fixation in 4 % formaldehyde for CLDND1 staining. Cell surface CLDND1 protein expression was measured by CLDND1 GMFI in N-IA, INRA and RA subsets depending on smoking status: current smoker (C), former smoker (F), never smoked (N). Median values are illustrated by the line. One way ANOVA with Dunn's multiple Comparison correction was performed to determine statistical significance.

5.4 Discussion

This chapter has identified CLDND1 cell surface expression on a variety of different immune cells. Upon T-cell activation, CLDND1 cell surface levels were shown to be labile, peaking around 48 hours, while the total amount of CLDND1 cell surface expression was dependent on the type of stimulus given. The *in vitro* studies identified a major limitation with CLDND1 expression profiling, as CLDND1 cell surface expression was lost during cell isolation and culture. Cell surface CLDND1 expression profiles were also determined in selected EA patient cell subsets and were shown to be elevated in RA over N-IA, which was independent of RA inflammation status. CLDND1 cell surface levels varied according to RF status in T-cells, but not with CCP status. Overall these experiments have provided insight into CLDND1 expression profiles and potentially suggest a function for CLDND1 within the immune response.

5.4.1 CLDND1 in T-cell activation

CLDND1 cell surface levels increased during both CD4+ and CD8+ T-cell activation. The increase in CLDND1 cell surface expression does not necessarily represent a pro-inflammatory role for CLDND1 as both activatory and regulatory proteins have been shown to be up-regulated at similar time-points, e.g. CD25 and CTLA-4 (Xia et al., 1999), and so these kinetics do not imply a specific role for CLDND1 in T-cells.

CLDND1 protein expression during T-cell activation was transient in nature consistent with a functional process, where protein levels are more likely to fluctuate, as opposed to a more static marker for a specific T-cell subset. CLDND1 cell surface expression was detected on a subpopulation of cells, as determined by the percentage of CLDND1 positive cells seen. The CLDND1 positive cells may express an undiscovered receptor or ligand, which during T-cell activation triggers up-regulation of CLDND1 expression. To date, however, no ligand or receptor for CLDND1 has been identified.

During full TCR triggering, the transcription factors AP-1, NFAT and NFκB complement the transcription of pro-inflammatory mediators that allow for cell cycle progression and the elicitation of an immune response. During a clonal anergy response, a unique set of NFAT-dependent anergy genes are expressed (Paolino and Penninger, 2009). Because CLDND1 is up-regulated

during full TCR activation, this is inconsistent with a role solely in maintenance of the anergic state.

The change in CLDND1 cell surface expression observed during T-cell activation was more pronounced when observing changes in CLDND1 GMFI rather than the percentage of CLDND1 positive cells, possibly suggesting that the amount of CLDND1 displayed on a cell is a more critical factor in CLDND1-mediated T-cell function than the total number of cells expressing CLDND1.

Although CLDND1 cell surface levels were shown to increase during T-cell activation, the relative changes in CLDND1 seen varied depending on whether RNA or protein was measured. Comparison between changes in CLDND1 transcript levels and the changes in CLDND1 cell surface protein showed that during activation, the CLDND1 transcript levels did not increase above 1.9 ± 0.3 SEM fold, whereas the change in CLDND1 protein intensity was 6.0 ± 1.33 SEM fold above resting values. The smaller fold changes in RNA values may indicate post-transcriptional regulation mechanisms for CLDND1. Even though protein and RNA are measured using different techniques and there will be potential noise associated with either technique, a study performed in circulating monocytes identified differences at the cellular level between RNA and protein levels of proteins classified as regulators of cellular function (Guo et al., 2008). A specific example of this is TGF-β, a well-known regulator of T-cell function. The levels of TGF-β protein do not correlate with the amount of RNA due to post-translational regulation of the TGF-β transcript (Kim et al., 1992). My findings indicate that CLDND1 may also be regulated post-translationally.

The strength of the stimulus used for T-cell activation resulted in differences in CLDND1 cell surface and total CLDND1 levels. Higher CLDND1 cell surface expression was seen in CD4+ T-cells activated with a stronger stimulus (α-CD3/CD28 expander bead), than with weaker stimuli (mat- or tolDC) but total CLDND1 protein levels varied less with the strength of stimulus. These data suggest that stimulation strength is an important factor determining the amount of CLDND1 at the cell surface but that this is less dependent on the total amount of protein. In turn these data suggest that CLDND1 function may be regulated through trafficking between distinct cellular locations. Additionally, there could be additional factors present on DC which modulate CLDND1 expression, independently of activation strength.

CLDND1 activation kinetics in CD4+ T-cells share similarities to some of the claudins. Claudin-1 is up-regulated during T-cell activation with a hypothesised tight-junction function due to co-localisation with the integral TJ protein ZO-1 (Mandel et al., 2012). Previous studies with the mouse homologue of CLDND1 showed co-localisation of mouse CLDND1 with ZO-1 in epithelial cells (Mineta et al., 2011) and so co-staining CLDND1 and ZO-1 on human CD4+ T-cells may reveal a TJ-like role of CLDND1. Claudin-1 staining on T-cells showed limited expression on a subpopulation of these cells (Mandel et al., 2012), which was also identified with CLDND1 staining. It was suggested that claudin-1 may be present on a defined T-cell subset, but this was not investigated further.

Given the reduction in CLDND1 expression during cell isolation and culture, *in vitro* cultures may not be the best environment to look at CLDND1 expression. The time-points identified for CLDND1 up-regulation may not reflect similar kinetics *in vivo*. CLDND1 expression profiling between whole blood and PBMC highlighted potential differences between *in vivo* and *in vitro* studies and identifies some limitations with *in vitro* studies, if molecules are artificially down-regulated as part of the cell isolation and culture process.

5.4.2 CLDND1 in EA

Comparisons of EA based on disease classification identified increased CLDND1 cell surface expression on T-cells in RA compared to N-IA, suggesting CLDND1 may be associated with early RA. No correlation between CRP levels and CLDND1 cell surface expression were detected in EA when analysed as a whole, suggesting that CLDND1 was not associated with increased inflammation.

In RA, the disease can be classified further depending on autoantibody status; the two main ones being RF and CCP. No relationship was identified between CLDND1 cell surface levels and CCP status. In the RF positive RA subgroup, CLDND1 cell surface expression was increased on T-cells. Interestingly, the amount of CLDND1 detected on the surface of the cells correlated with RF status, but the percentage of CLDND1 positive cells did not. This observation may suggest that the amount of CLDND1 expressed on a cell may be more important for function than the total number of cells expressing CLDND1. It is known that RF status can fluctuate in early disease (Barra et al., 2013), and so

to accurately determine whether CLDND1 levels correlated with RF titres, additional studies would be required.

RF can be present in several different antibody isoforms; IgM, IgA and IgG, but clinically, levels of IgM RF are measured. The roles of RF in RA disease are not fully understood. Studies have shown that immune complexes are widely found in RA patient joints (Okroj et al., 2007) and polyclonal IgM RF can fix and activate complement (Tanimoto et al., 1975). Along with its well understood role in innate immunity, complement can also activate adaptive immune responses through binding to complement receptors on CD4+ T-cells and DC (Heeger and Kemper, 2012). Fragments of the complement cascade C3a and C5a can bind to these receptors on CD4+ T-cells and DC (C3aR and C5aR, respectively) and induce heightened T-cell activation. The possibility of RF to activate complement and signal through complement receptors to increase T-cell activation may be an explanation for elevated CLDND1 levels in T-cells of RF positive RA patients. As a role for complement in CLDND1 expression was not explored during this thesis, additional studies would need to be performed to ascribe a role for complement in the function of CLDND1.

Chapter 6. Determining a Function for CLDND1 in CD4+ T-cells

6.1 Aims

This chapter documents experiments performed to elucidate a function for CLDND1 in primary human CD4+ T-cells. The main aim was to determine whether CLDND1 plays a role CD4+T-cell activation, by transfecting CLDND1-expressing vectors into these cells. Firstly, optimisations were performed to select for a vector enabling CLDND1 cell surface expression, then these cells were activated with a variety of different stimuli to determine whether CLDND1 played a role in T-cell viability, proliferation, cytokine production and co-stimulation and activation marker expression. Re-stimulation assays were performed with the CLDND1 over-expressed T-cells, as a surrogate model for anergy. Finally, as a result of generating a truncated version of CLDND1 to generate more in-house antibodies, the effect of this mutation on CLDND1 function was assessed.

6.2 Introduction

6.2.1 Proposed CLDND1 function

The CLDND1 gene is differentially expressed during T-cell activation and anergy in the CD4+ T-cell clone, HA1.7, with CLDND1 transcript levels stable in the anergic cells and lower in activated cells, 2 hours into anergy induction (Figure 6) (Ali, M. and Isaacs, J. D., unpublished data). From these data, a role for CLDND1 in T-cell anergy was proposed and a pilot experiment was performed to validate this hypothesis. Silencing and over-expressing the CLDND1 transcript in primary human CD4+ T-cells obtained from one donor identified a potential role for CLDND1 in the regulation of T-cell proliferation (Dixon, C., unpublished data). CLDND1 gene silencing induced more T-cell proliferation in response to stimulation whereas CLDND1 transcript over-expression induced reduced T-cell proliferation (Section 1.11.10, Figure 9). In the absence of an α-CLDND1 antibody at the time of this work, an internal ribosome entry site (IRES) biscistronic system, in which $H2K^k$ is expressed in parallel with CLDND1 (Tahvanainen et al., 2006), was used to estimate CLDND1 expression.

6.2.2 TCR signalling during activation

Two signals are required for full T-cell activation, complemented by the cytokine milieu, which tailors the immune response. TCR ligation constitutes the first signal and is triggered through MHC molecule interaction expressed on APC or direct binding by an α-CD3 antibody. TCR triggering initiates a phosphorylation cascade and subsequent activation of down-stream calcium and ras signalling pathways. Co-stimulatory molecule receptor signalling, for example CD28 interaction with CD80 or CD86 on APC, provides the second signal. The co-operation of these signalling pathways results in the transcription of IL-2, an important cytokine for T-cell proliferation, along with a wide range of other genes involved in pro-inflammatory responses (Figure 1)(Morice et al., 1993, Nourse et al., 1994).

6.2.3 TCR signalling during anergy

Anergy is classified as a hypo-responsive state of a viable T-cell, where T-cell proliferation and IL-2 production is lost. Several models of anergy have been documented, most of which involve TCR triggering in the absence of co-stimulation (Schwartz, 2003) (Figure 3).

6.3 Results

6.3.1 Phylogenetic analysis of the PMP-22/EMP/MP20/claudin superfamily

During the original identification of CLDND1, the predicted protein sequence was assessed for sequence similarities to other proteins. Conserved motifs were shared with PMP-22/EMP/MP20/claudin superfamily members (Fayein et al., 2002) and so CLDND1 has been classified as one if its member. This superfamily contains several proteins with diverse functions.

To gain insight into potential functions for CLDND1, the CLDND1 protein sequence was compared with proteins within the human genome to identify the closest homologies. BLAST analysis of the CLDND1 protein sequence (NP_001035289.1) identified a list of proteins with homology to CLDND1 (Table 16). The majority of the proteins identified were members of the PMP-22/EMP/MP20/claudin superfamily, with the highest homology to the family member, transmembrane protein (TMEM)114.

Description	Accession	Max score	Query coverage	E-value
CLDND1 isoform b	NP_001035272.1	497	100	0.0
CLDND1 isoform a	NP_063948.1	496	100	0.0
TMEM114	NP_001139808.1	43.5	86	$1e^{-7}$
CACNG5	NP_665810.1	38.1	69	$8e^{-6}$
PMP-22	NP_000295.1	34.7	24	$5e^{-5}$
TMEM178b	NP_001182207.1	32.3	28	$5e^{-4}$
EMP-2	NP_001415.1	31.6	24	$7e^{-4}$
EMP	CAA64393.1	31.6	24	$7e^{-4}$
TMEM235 isoform 1	NP_001191139.1	31.2	33	0.001
TMEM235 isoform 2	NP_001191140.1	30.8	33	0.001
Olfactory receptor 11H6	NP_001004480.1	30.4	24	0.001
Claudin-19 isoform b	NP_001116867.1	29.6	32	0.004
Claudin-19 isoform a	NP_683763.2	29.3	32	0.004
CACNG8	EAW72168.1	29.6	39	0.005

Table 16. CLDND1 bioinformatics

BLAST query of CLDND1 protein sequence (NP_001035289.1) identified sequences with greatest similarity. The search parameters were ranked according to max score, query coverage and E-value. Max score relates to sequence alignment with higher scores corresponding to a better alignment. The query coverage identifies the length of the aligned sequence matching the hit within the database. The E-value describes the number of hits expected to be seen by chance when searching the database of a particular size. The lower the E-value, the more significant the alignment.

The TMEM114 transcript is expressed in the developing human eye and central nervous system (Maher et al., 2011) and is linked with normal ocular function (Jamieson et al., 2007). Maher et al., (2011) constructed a phylogenetic tree to determine the evolutionary lineage of TMEM114. The alignment included all members of the PMP-22/EMP/MP20/claudin superfamily, along with the more distantly related CACNG. TMEM114 grouped within the CACNG family and not with the claudins, as was previously suggested (Maher et al., 2011).

Based on these findings, CLDND1 phylogenetic analysis was performed, according to Maher et al., (2011) (Figure 62). A similar phylogenetic profile was achieved, with TMEM114 branching within the CACNG family. CLDND1 also branched within this family, suggesting CLDND1 shared more sequence homology with the CACNG than with the claudins.

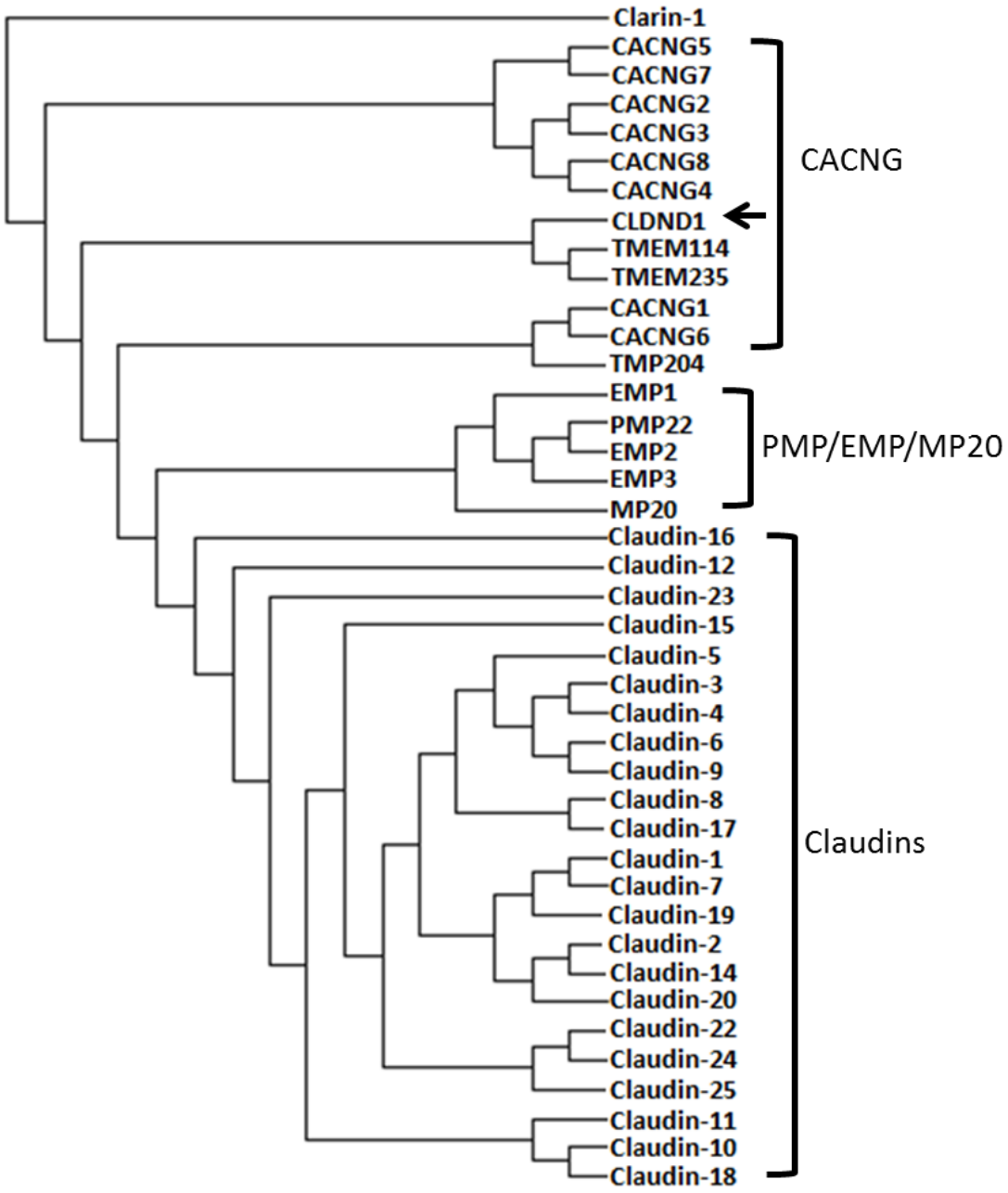

Figure 62. CLDND1 bioinformatics: phylogenetic analysis

Sequences were aligned using clustalW2 before neighbour joining phylogenetic analysis was performed, according to Maher et al., (2011). CLDND1 is indicated by the arrow.

No reference to the CACNG function in immune cell subsets is available, and so no inferences could be made to CLDND1 function from these proteins. To determine a function for CLDND1 in primary human CD4+ T-cells, CLDND1 transfection into primary human CD4+ T-cells was performed, using nucleofection.

6.3.2 Validation of the CLDND1 over-expression pilot study

In the pilot study to determine a function for CLDND1 (Dixon, C., unpublished data), CLDND1 over-expression was performed using the pIRES2-H-2K^k expression system (Tahvanainen et al., 2006). This expression system utilises a biscistronic vector where both CLDND1 and H2K^k are expressed from the same transcript, and translation creates two individual proteins through the use of an IRES. Expression of H2K^k allows for the indirect identification of CLDND1 expressing cells, as during the pilot experiments and the experiments performed in this section, the α-CLDND1 antibody was not yet available. Another advantage of using the CLDND1-H2K vector in the preliminary studies was the ability to separate the transfected population from untransfected cells. The resulting homogenous transfected cell population could then be used to determine the effects of CLDND1 on CD4+ T-cell function. As part of this selection method dead cell removal was required prior to transfected cell isolation due to the possibility of dead cells binding the H2K^k selection beads. The combination of the dead cell removal step and the resulting isolation of H2K^k transfected cells, resulted in a loss of 20 % of H2K^k positive cells from the transfected population (Figure 63A, dead fraction), but did increase H2K^k positivity (40.7 % in alive fraction to 60.3 % in post-isolation fraction) (Figure 63A and B). Two antibodies were used to detect the purity of the selected cells, as during the selection process, the α-H2K^k antibody binding site can be masked by the H2K^k positive selection beads. The MACSelect control antibody binds to the H2K^k positive selection beads and will identify the positively selected cells with masked α-H2K^k antibody epitopes. Transfection of the pIRES2-H-2K^k vector omitting a target gene resulted in high expression of H2K^k, showing that H2K^k can be expressed in the absence of a target protein (Figure 63C, courtesy of Amy Anderson). Therefore, using H2K^k as a marker for CLDND1 protein expression may not have been a reliable read-out. In addition, the presence of the xenogeneic MHC molecule on the T-cell surface, albeit a truncated version, could stimulate T-cell proliferation in its own right, irrespective of a CLDND1-mediated functional phenotype.

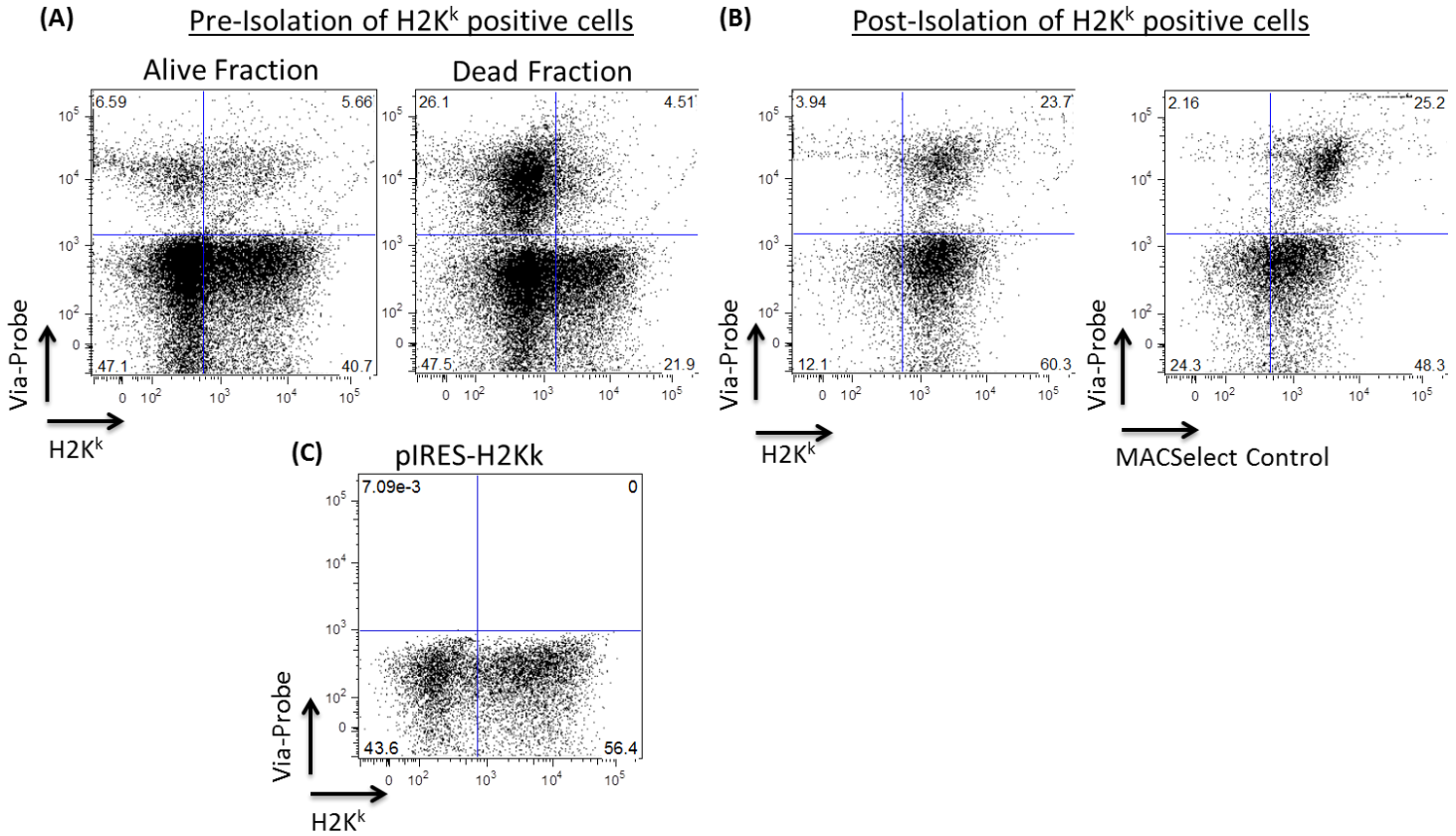

Figure 63. Validation of the CLDND1-H2K vector

CD4+ T-cells were transfected with CLDND1-H2K or pIRES-H2K^k vector. 18 hours after transfection, dead cells were removed from the sample with a dead cell removal kit (Miltenyi) and selection of H2K^k transfected cells was performed. (A) Flow cytometry analysis of CD4+ transfected cells post dead cell removal and before H2K^k positive selection. (B) Flow cytometry analysis of CD4+ transfected cells post H2K^k selection. Transfected cells were stained with either α-H2K^k antibody, or MACSelect control antibody, due to potential H2K^k antibody epitope masking during the positive selection. (C) Transfection of pIRES-H2K^k vector alone. Viable cells were selected based on Via-Probe™ staining (data courtesy of Amy Anderson). Data represent at least two experiments.

6.3.3 Assessing CLDND1 protein over-expression

In light of the concern of the presence of the xenogeneic MHC molecule on the T-cell surface, four different vectors, containing only the CLDND1 (UCB) protein sequence, were generated (see Section 2.2): CLDND1-HCMV, CLDND1-Elf, CLDND1-FerL and CLDND1-PIMMS. These vectors each contain different promoters (Table 7) and so different levels of CLDND1 gene expression could potentially be achieved. CD4+ T-cells were transfected with each of these four vectors or mock transfected and transfection efficiencies were determined (Figure 64).

CLDND1 RNA expression profiling was performed on both endogenous CLDND1 (Figure 64A) and against the transfected CLDND1 sequence (CLDND1(V)) (Figure 64B). The two sequences could be distinguished by different qRT-PCR primer pairs and probes as CLDND1(V) is a codon optimised sequence, so the transcript bases were different. A 81.5 ± 7.0 SEM fold increase in CLDND1(V) mRNA expression was seen with the CLDND1-PIMMS vector, compared to the mock transfected control, while only a minimal fold change in CLDND1(V) mRNA expression was observed with CLDND1-HCMV, CLDND1-Elf or CLDND1-FerL (3.6 ± 0.2 SEM, 5.7 ± 0.8 SEM or 9.8 ± 0.8 SEM, respectively) (Figure 64B). The transfection of DNA into CD4+ T-cells reduced endogenous CLDND1 transcript levels, as vector-transfected samples had lower CLDND1 expression levels than the mock and untransfected control samples (0.3 ± 0.04 SEM, 0.3 ± 0.01 SEM, 0.4 ± 0.02 SEM, 0.1 ± 0.01 SEM, respectively) (Figure 64A).

To determine whether the increase in CLDND1(V) transcript resulted in human CLDND1 (UCB) protein over-expression, CLDND1 protein levels were assessed (Figure 64C). For CLDND1-PIMMS transfections, three bands were detected within the predicted molecular weight range for CLDND1, which corresponded to different CLDND1 glycosylation states (Section 3.3.6, Figure 26). A faint band was also seen for CLDND1-HCMV, CLDND1-Elf and CLDND1-FerL transfections, however this was likely to be endogenous CLDND1 protein, as this band was also present in the mock and untransfected samples. CLDND1-PIMMS was therefore used for all subsequent transfection experiments.

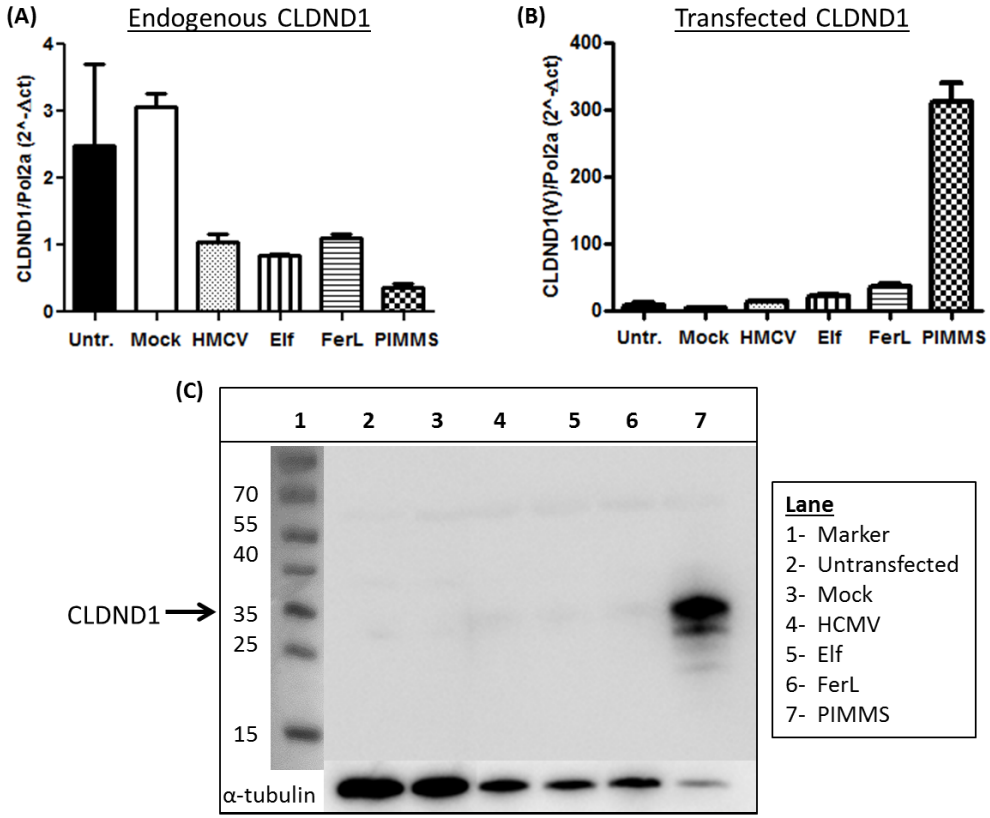

Figure 64. Validation of CLDND1 (UCB)-containing vectors

CD4+ T-cells were transfected with CLDND1-HCMV (HCMV), CLDND1-Elf (Elf), CLDND1-FerL (FerL) or CLDND1-PIMMS (PIMMS), mock transfected or left untransfected. 18 hours after transfection, CLDND1 RNA and protein levels were assessed. RNA was extracted from cell lysates and CLDND1 qRT-PCR values were normalised to pol2a. (A) Endogenous CLDND1 transcript expression. (B) CLDND1(V) transcript expression. (C) Transfected cell lysates were prepared and Western blot analysis was performed with α-CLDND1 antibody. Mean values + SEM are plotted. Data illustrate a single experiment.

6.3.4 CLDND1 transfection into primary human CD4+ T-cells

In the analysis of the above experiments, CLDND1 expression levels were compared to untransfected and mock transfected controls. I found that DNA transfection resulted in a decrease in the endogenous CLDND1 RNA expression (Figure 64A) and so additional controls were required to account for this presence of DNA. Two PIMMS control vectors were therefore generated; one containing a non-coding stuffer fragment (PIMMS-non-coding) and the other containing the coding sequence for the human κ antibody light chain (PIMMS-coding). During data analysis, two methods were adopted to compare CLDND1-PIMMS read-out values to control cells: the two control values were averaged to give one control value, or samples were assessed individually.

6.3.5 CLDND1 transfection efficiency and cell viability

CLDND1-PIMMS, PIMMS-non-coding and PIMMS-coding vectors were transfected into CD4+ T-cells and after 18 hours, CLDND1 cell surface expression and total CLDND1 expression was determined (Figure 65). A significant increase in the amount of both CLDND1 cell surface (Figure 65A) and total protein (Figure 65B) was detected in the CLDND1-PIMMS transfected cells, compared to the PIMMS-non-coding, PIMMS-coding or the averaged control values. The transfection efficiencies in the CLDND1-PIMMS samples averaged 27 ± 3 % SEM for cell surface CLDND1 expression and 44 ± 3 % SEM for total CLDND1 expression and were determined by the percentage of CLDND1 fluorescence greater than mock-transfected control CLDND1 fluorescence. Figure 65C represents the increase in CLDND1 fluorescence identified in the CLDND1-PIMMS transfected samples. The CLDND1 GMFI values were calculated from the whole population.

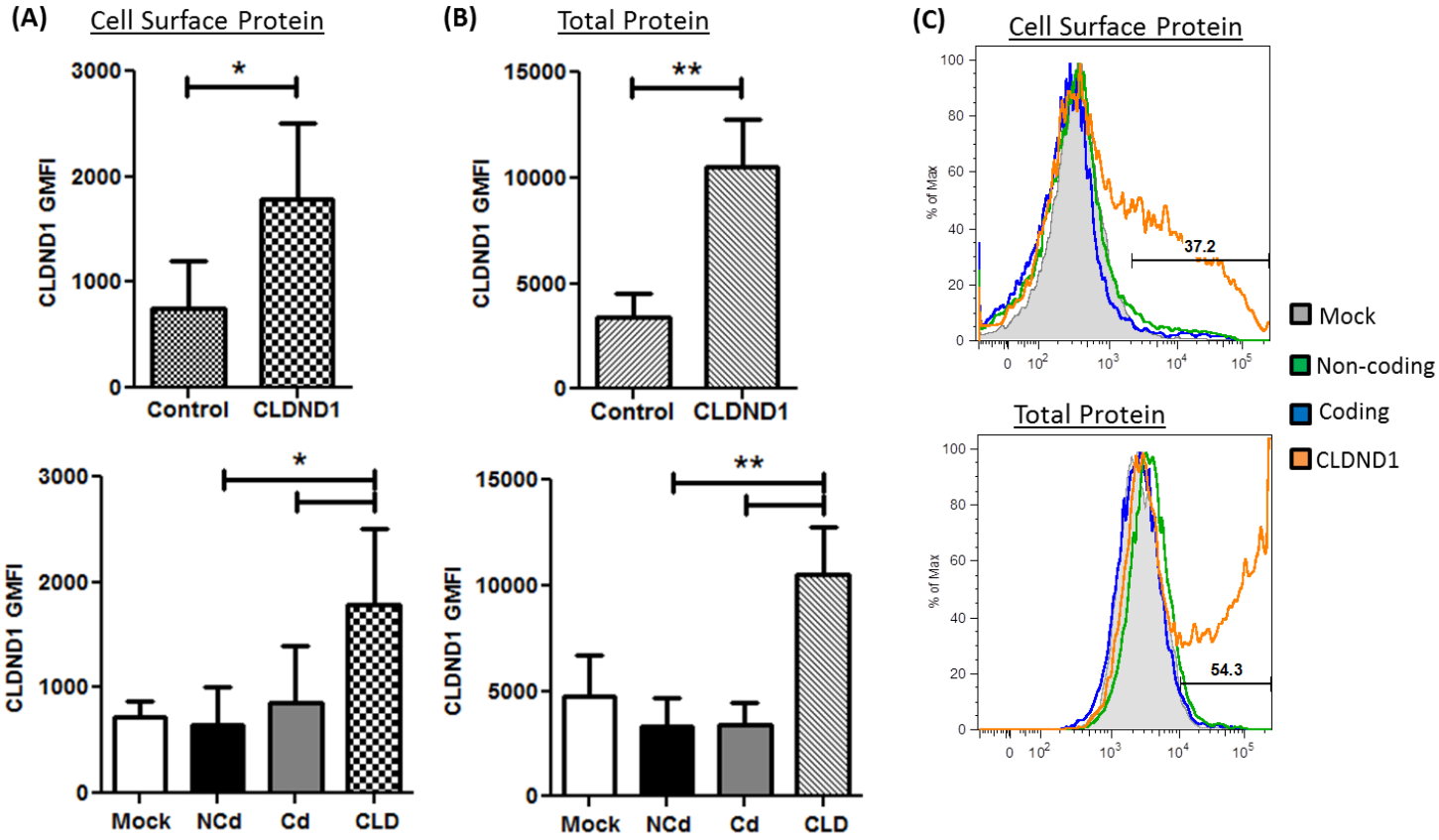

Figure 65. CLDND1 expression during primary human CD4+ T-cell transfection

CD4+ T-cells were transfected with stuffer-PIMMS (NCd) or light-PIMMS (Cd) controls or with CLDND1-PIMMS (CLD). 18 hours post transfection, CLDND1 protein levels were assessed. An average was taken of the control vectors (control, upper panels) or values were plotted independently (lower panels). CLDND1 (A) cell surface expression, or (B) total expression. (C) Representative histogram plot depicting CLDND1 cell surface and total CLDND1 protein levels determined by flow cytometry. Data illustrate four independent experiments. Mean values ± SEM were plotted. Paired Student's t-test analysis was performed *p<0.05, **p<0.01.

A large amount of cell death was discovered in all the PIMMS-transfected samples (Figure 66 “pre values”). Incorporation of a dead cell removal step helped to increase the proportion of viable cells for the resulting functional assays (Figure 66 “post values”). The amount of dead cells present in each sample post dead cell removal reduced on average by 56 %. Only viable cells were counted when determining cell population concentrations for subsequent experiments, so the same number of viable cells was present for each assay.

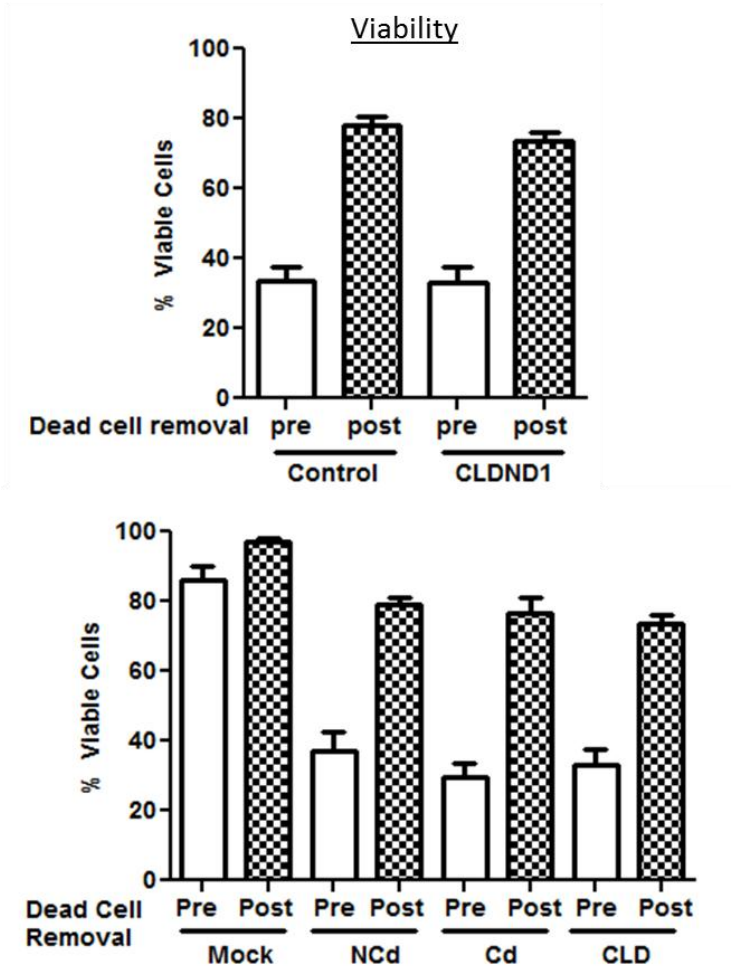

Figure 66. Viability during primary human CD4+ T-cell transfection

CD4+ T-cells were transfected with stuffer-PIMMS (NCd) or light-PIMMS (Cd) control vectors or with the CLDND1-PIMMS (CLD) vector. 18 hours after transfection, CLDND1 protein levels were assessed. An average was taken of the control vectors (control) or values were plotted independently. Annexin V and Via-Probe™ staining were used to determine cell viability 18 hours post transfection or after the dead cell removal step was performed. Data illustrate four independent experiments. Mean values + SEM were plotted. paired Student’s t-test analysis was performed *$p<0.05$, **$p<0.01$.

The experimental protocol for all the functional assays performed in this chapter is depicted in Figure 67.

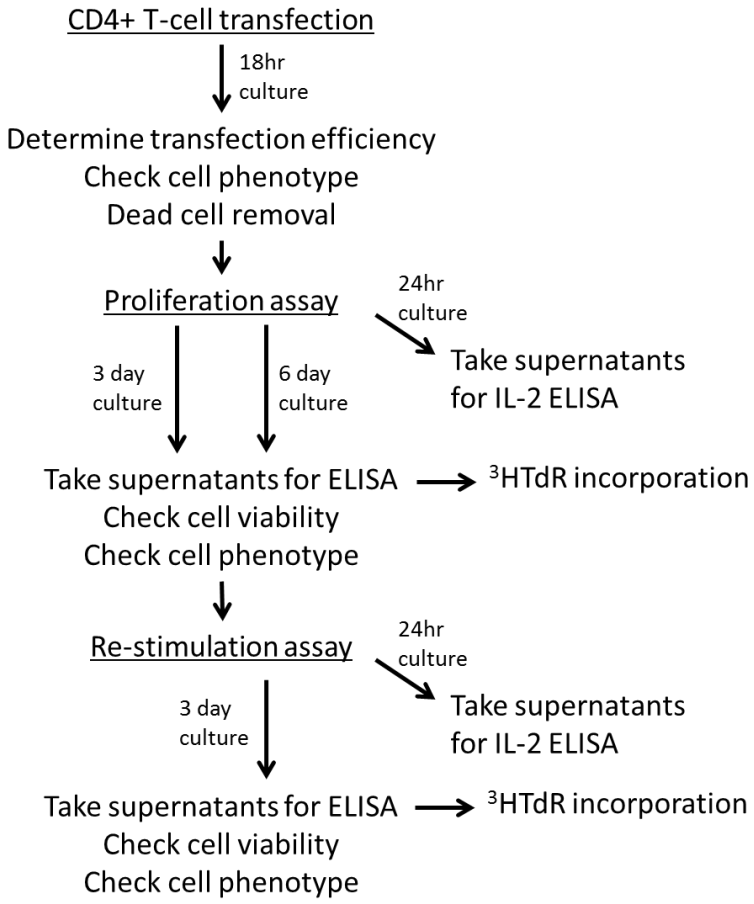

Figure 67. Experimental protocol for CLDND1-transfected T-cell assays

CD4+ T-cells were transfected and cultured for 18 hours. T-cell tranfection efficiency, phenotyping and dead cell removal was performed before T-cell proliferation was assessed by culturing with α-CD3/CD28 expander beads for 3 days, or mat- or tolDC for 3 or 6 days. After 24 hours of co-culture IL-2 production was assessed. After co-culture, T-cell proliferation, cytokine production, cell viability and phenotype were assessed. MatDC stimulated cells were also re-stimulated immediately for 3 days. 24 hours after re-stimulation IL-2 production was assessed. After 3 days of re-stimulation, T-cell proliferation, cytokine production, cell viability and phenotype were assessed.

6.3.6 CLDND1-transfected T-cell proliferation in response to α-CD3/CD28 expander bead stimulation

The transfected CD4+ T-cells were incubated with 10:1 (10 T-cells: 1 bead) ratio of α-CD3/CD28 expander beads for 3 days and T-cell proliferation was measured (Figure 68A). CLDND1 over-expression resulted in a decrease in CD4+ T-cell proliferation in some donors, in keeping with the preliminary

findings (Section 1.11.10, Figure 9), however this was not consistent in all samples. Differences in T-cell proliferation were also observed between the PIMMS-control samples (Figure 68A). The PIMMS-non-coding transfected cells responded less than the PIMMS-coding transfected cells, albeit still with a higher proliferative capacity than the CLDND1-PIMMS transfected cells.

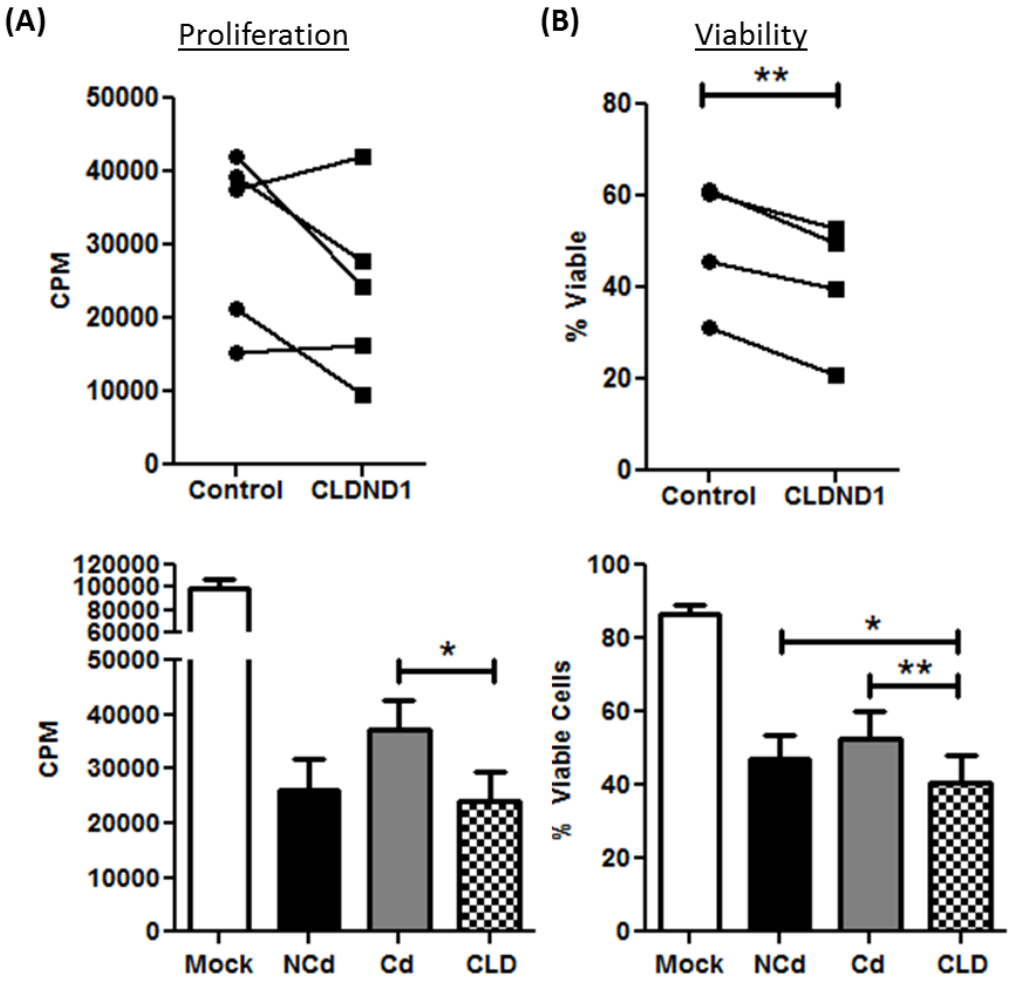

Figure 68. CLDND1-transfected T-cell proliferation in response to α-CD3/CD28 expander bead stimulation

CD4+ T-cells were transfected with stuffer-PIMMS (NCd) or light-PIMMS (Cd) controls or with CLDND1-PIMMS (CLD). 18 hours post transfection cells were harvested and dead cells were removed. Cells were incubated with 10:1 ratio of α-CD3/CD28 expander beads for 3 days. An average was taken of the control vectors (control) or values were plotted independently. (A) Proliferation was measured by ^{3}HTdR incorporation. (B) Annexin V and Via-Probe™ staining was performed to assess cell viability post proliferation. Data illustrate at least four independent experiments. Mean values (+ SEM) were plotted. Paired Student's t-test analysis was performed *p<0.05, **p<0.01.

To determine whether the differences in proliferation were a result of cell death, cell viability was assessed post-proliferation (Figure 68B). A significant reduction in cell viability was seen in the CLDND1-PIMMS transfected samples compared to the averaged PIMMS-control value, suggesting CLDND1 may be involved in cell death pathways. In addition, cell viability was mirrored by the amount of proliferation in each sample and as such, suggested the differences seen in T-cell proliferation between the cell populations may have reflected the viability of those cells. Regression analysis of a limited number of data values identified a significant correlation between CLDND1-transfected T-cell viability and T-cell proliferation (Figure 69).

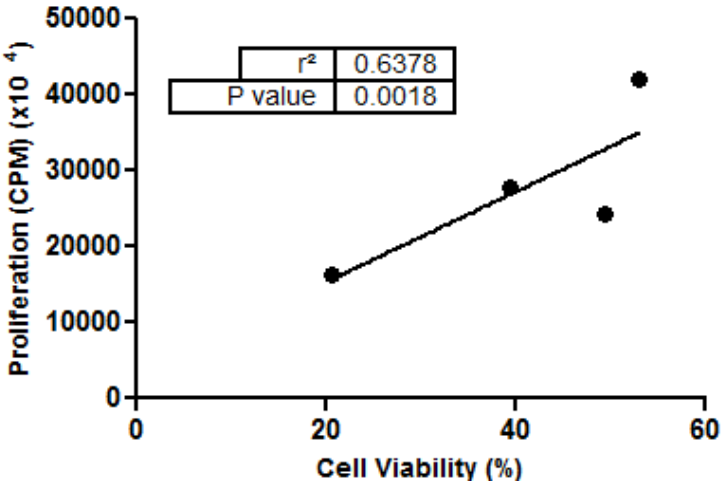

Figure 69. Regression analysis of T-cell proliferation and viability

CD4+ T-cells were transfected with CLDND1-PIMMS. 18 hours post transfection cells were harvested and dead cells were removed. Cells were incubated with 10:1 ratio of α-CD3/CD28 expander beads for 3 days. Proliferation was measured by ^{3}HTdR incorporation and cell viability was determined by Annexin V and Via-Probe™ staining. Data illustrate four independent experiments.

To assess proliferation in the viable T-cells, CFSE staining was performed (Figure 70). No differences were seen between the CFSE dilutions of the PIMMS-transfected T-cells, and proliferation itself was very low. These data may suggest that the introduction of DNA into T-cells by nucleofection affects T-cell proliferation. In addition to T-cell proliferation, cytokine production was also investigated. Over-expressed CLDND1 does not seem to play an important role in the skewing of T-cell responses, as no differences in IFN-γ, IL-10, TNF-α, IL-5 or IL-17 production were seen (Figure 71).

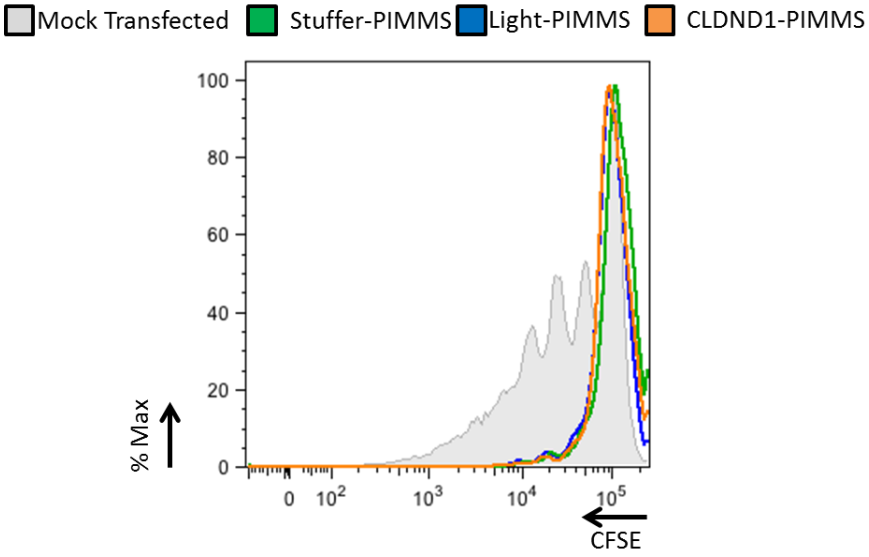

Figure 70. CLDND1-transfected T-cell CFSE staining in response to α-CD3/CD28 expander bead stimulation

CD4+ T-cells were transfected with stuffer-PIMMS or light-PIMMS controls or with CLDND1-PIMMS. 18 hours post transfection cells were harvested and dead cells were removed. Cells were stained with CFSE then incubated with 10:1 ratio of α-CD3/CD28 expander beads for 3 days. CFSE staining was measured by flow cytometry and histograms of CFSE staining are shown. Data represent two independent experiments.

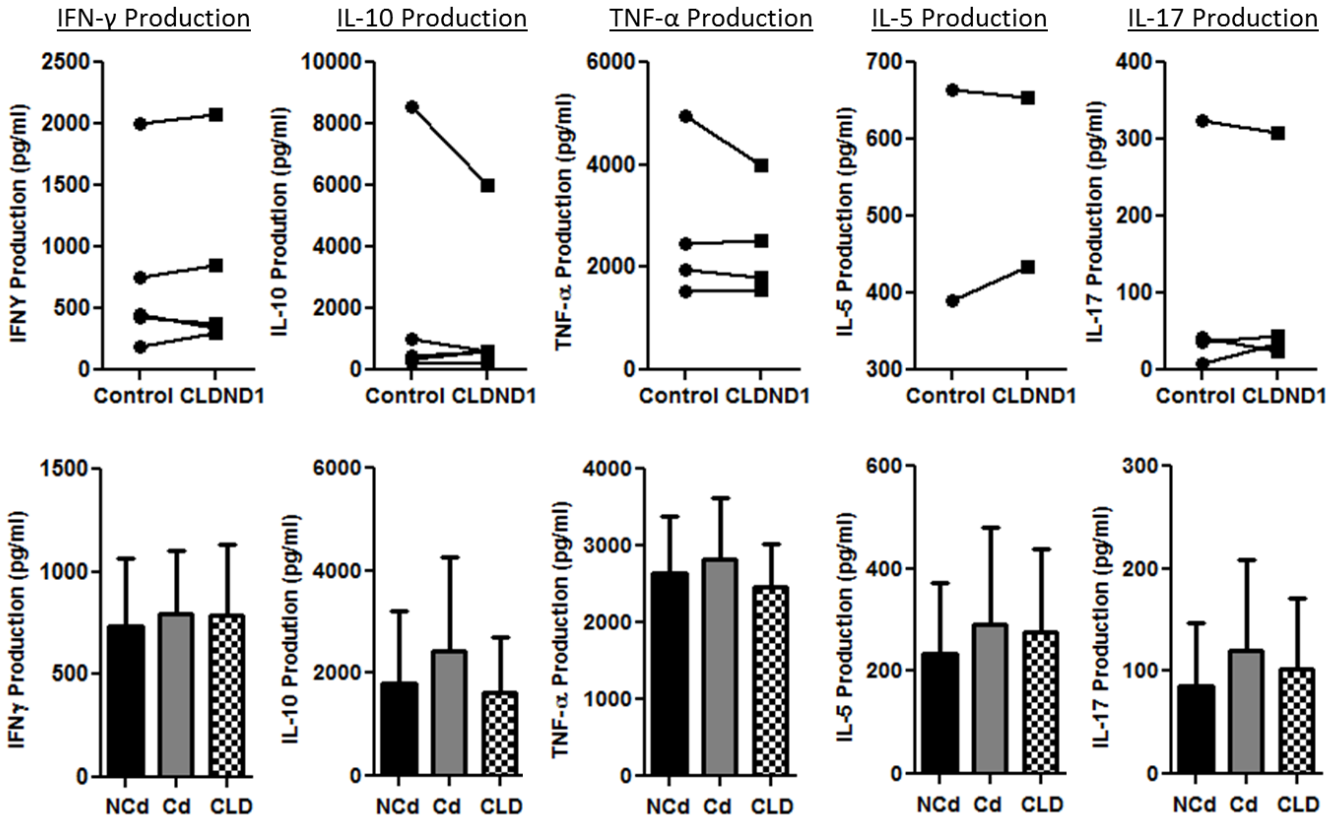

Figure 71. CLDND1-transfected T-cell cytokine production in response to α-CD3/CD28 expander bead stimulation

CD4+ T-cells were transfected with stuffer-PIMMS (NCd) or light-PIMMS (Cd) controls or with the CLDND1-PIMMS (CLD). 18 hours post transfection, cells were harvested and dead cells were removed. Cells were incubated with 10:1 ratio of α-CD3/CD28 expander beads for 3 days. An average was taken of the control vectors (control) or values were plotted independently. Cytokines from supernatants taken at the end of the proliferation were measured by ELISA. Data illustrate four (or two for IL-5) independent experiments. Mean values (+ SEM) were plotted. Paired Student's t-test analysis was performed.

6.3.7 Effect of CLDND1 over-expression on T-cell activation by DC

Previous experiments (Section 5.3.5, Figure 51) have shown that differential CLDND1 expression during T-cell activation was dependent on the type and strength of stimulus, with the highest CLDND1 expression seen during activation with α-CD3/CD28 expander beads, followed by intermediate levels of CLDND1 expression with matDC, and the lowest level of expression with tolDC. As the type and strength of stimulus may be an important factor for CLDND1 function in CD4+ T-cells, the CLDND1-transfected cells were also stimulated with mat- or tolDC. After 3 days or 6 days of co-culture, T-cell proliferation and cytokine production were assessed.

CLDND1-PIMMS transfected cells proliferated significantly less than control cells after 3 day stimulation with either mat- or tolDC (Figure 72). There was also a trend for less IFN-γ production in the matDC stimulated CLDND1-PIMMS cells in three of the four donors (Figure 73). The levels of TNF-α and IL-10 detected at day 3 were low in all samples, close to the limit of detection.

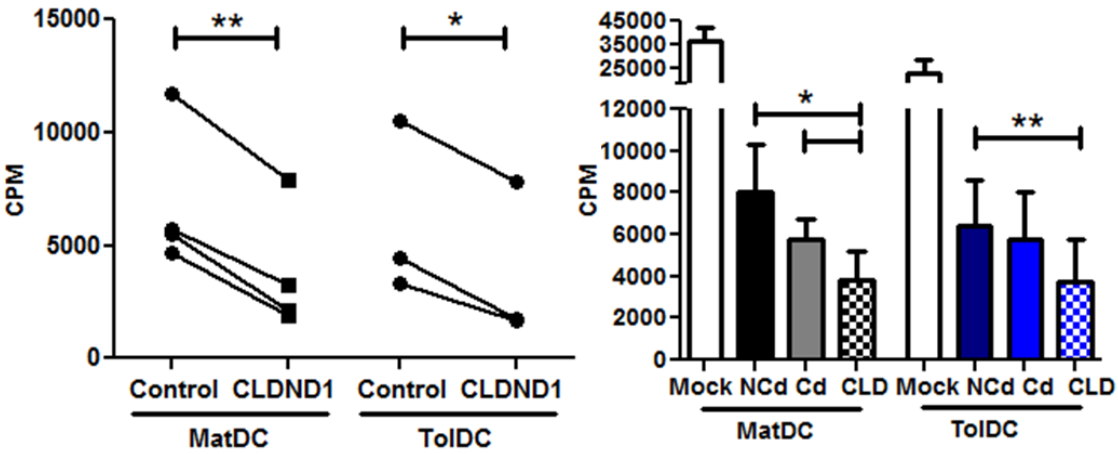

Figure 72. CLDND1-transfected T-cell proliferation in response to 3 day DC stimulation

CD4+ T-cells were transfected with stuffer-PIMMS (Ncd) or light-PIMMS (Cd) controls or with CLDND1-PIMMS (CLD). 18 hours post transfection, cells were harvested and dead cells were removed. Cells were incubated with 10:1 ratio of mat- or tolDC for 3 days. An average was taken of the control vectors (control) or values were plotted independently. Proliferation was measured by ^{3}HTdR incorporation. Data illustrate four or three independent experiments for matDC or tolDC, respectively. Mean values (+ SEM) were plotted. Paired Student's t-test analysis was performed *$p<0.05$, **$p<0.01$.

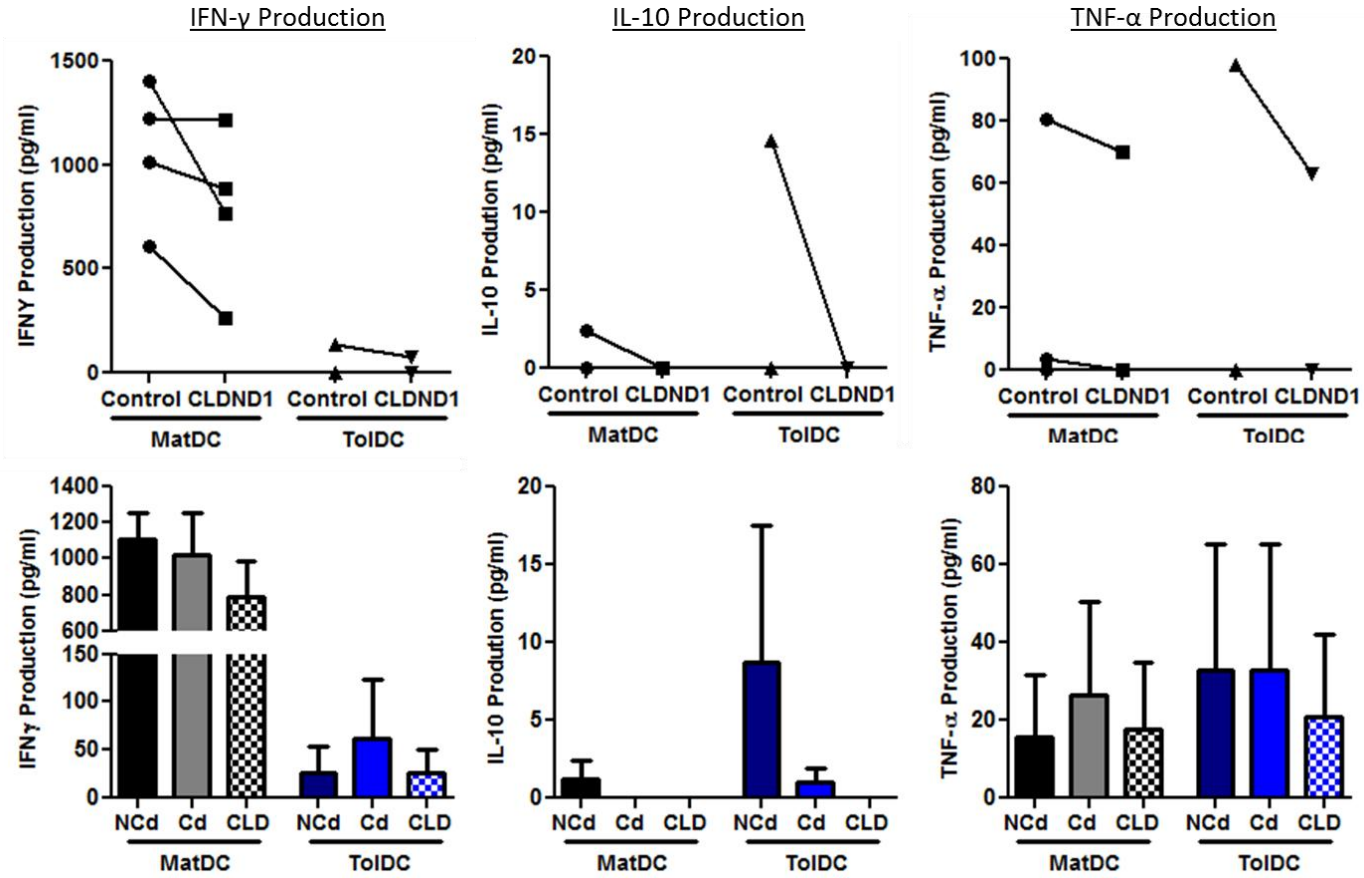

Figure 73. CLDND1-transfected T-cell cytokine production in response to 3 day DC stimulation

CD4+ T-cells were transfected with stuffer-PIMMS (NCd) or light-PIMMS (Cd) controls or with CLDND1-PIMMS (CLD). 18 hours post transfection, cells were harvested and dead cells were removed. Cells were incubated with 10:1 ratio of mat- or tolDC for 3 days. An average was taken of the control vectors (control) or values were plotted independently. Cytokines from supernatants taken at the end of the proliferation were measured by ELISA. Data illustrate four or three independent experiments for the mat- and tolDC, respectively. Mean values (+ SEM) were plotted. Paired Student's t-test analysis was performed *$p<0.05$, **$p<0.01$.

After 6 days of stimulation with either mat- or tolDC, CLDND1-PIMMS transfected T-cell proliferation was also significantly lower (Figure 74), and the difference in proliferation between CLDND1-PIMMS and control transfected T-cells varied between donors. Transfection efficiency correlations to CLDND1 cell surface expression indicated a strong significant correlation between the two values, with more CLDND1 on the cell surface in samples with higher transfection efficiencies (Figure 75A). Comparison of the transfection efficiency against CLDND1-PIMMS transfected T-cell proliferation identified a weak inverse correlation between transfection efficiencies and proliferation in response to matDC stimulus (Figure 75B), although this correlation was not significant.

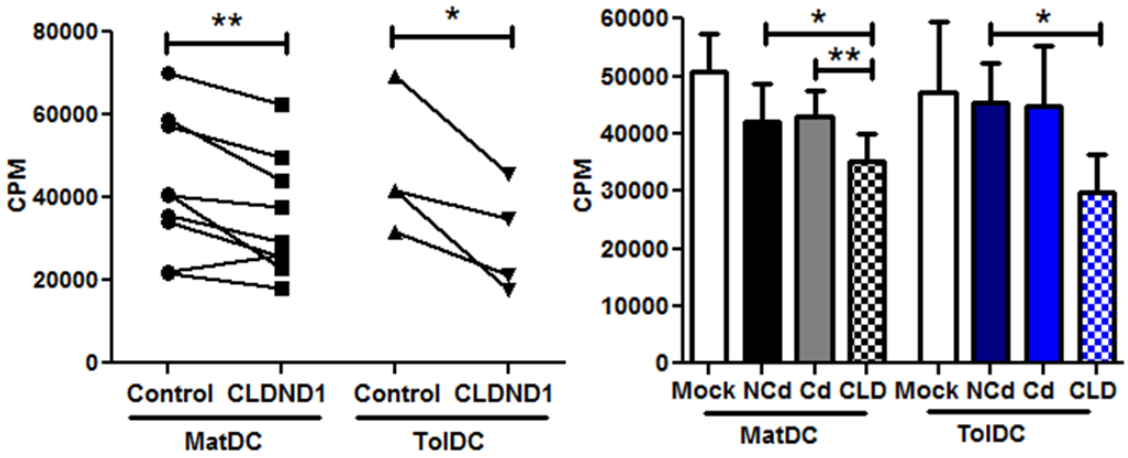

Figure 74. CLDND1-transfected T-cell proliferation in response to 6 day DC stimulation

CD4+ T-cells were transfected with stuffer-PIMMS (NCd) or light-PIMMS (Cd) controls or with CLDND1-PIMMS (CLD). 18 hours after transfection cells were harvested and dead cells were removed. Cells were incubated with 10:1 ratio of mat- or tolDC for 6 days. An average was taken of the control vectors (control) or values were plotted independently. Proliferation was measured by ^{3}HTdR incorporation. Mean values (+ SEM) were plotted. Data illustrate nine or five independent experiments, for mat- or tolDC, respectively. Paired Student's t-test analysis was performed $p<0.05$, $^{**}p<0.01$.

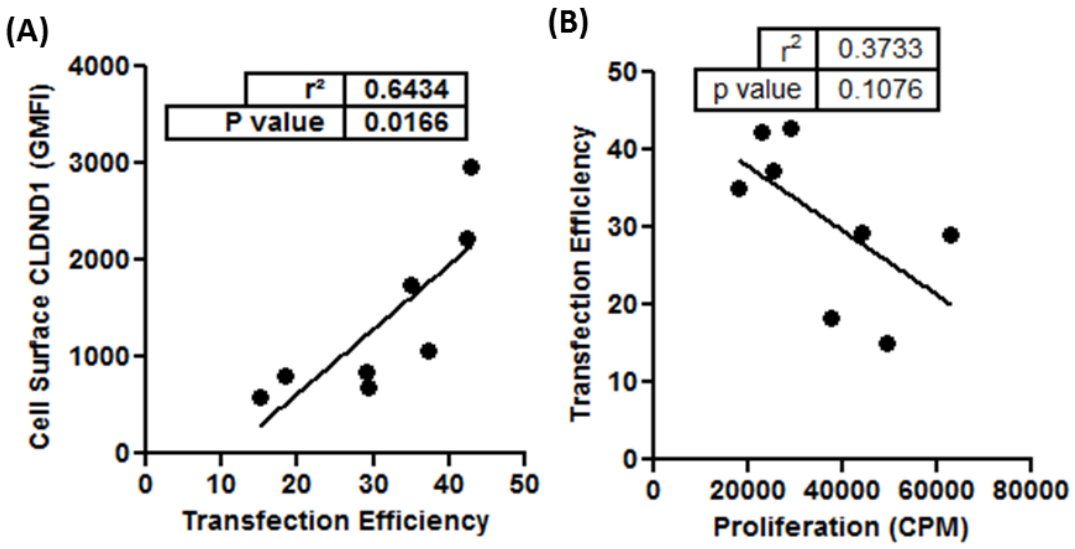

Figure 75. CLDND1-transfected T-cell correlations between transfection efficiency, CLDND1 cell surface GMFI and proliferation

CD4+ T-cells were transfected with CLDND1-PIMMS vector. 18 hours after transfection cells were harvested and dead cells were removed. (A) Transfection efficiency was determined and values were correlated to CLDND1 cell surface GMFI (B) Cells were incubated with 10:1 ratio of matDC for 6 days and proliferation was measured by ^{3}HTdR incorporation and correlated to transfection efficiency. Data illustrate eight independent experiments.

Transfected T-cell viability was also assessed; as differences in this parameter were seen between α-CD3/CD28 expander bead stimulated cells. No significant difference was seen in T-cell viability in the mat- or tolDC stimulated cultures after 6 days of co-culture (Figure 76). Analysis of each donor did show a trend for CLDND1-overexpression to reduce cell viability, albeit not significant, suggesting CLDND1 may still play a role in cell death. A significant difference in proliferation (Figure 74) but no significant difference in cell viability (Figure 76) was identified, suggesting that the differences seen in proliferation were due to additional CLDND1 specific effects rather than solely due to different amounts of live cells within the cultures.

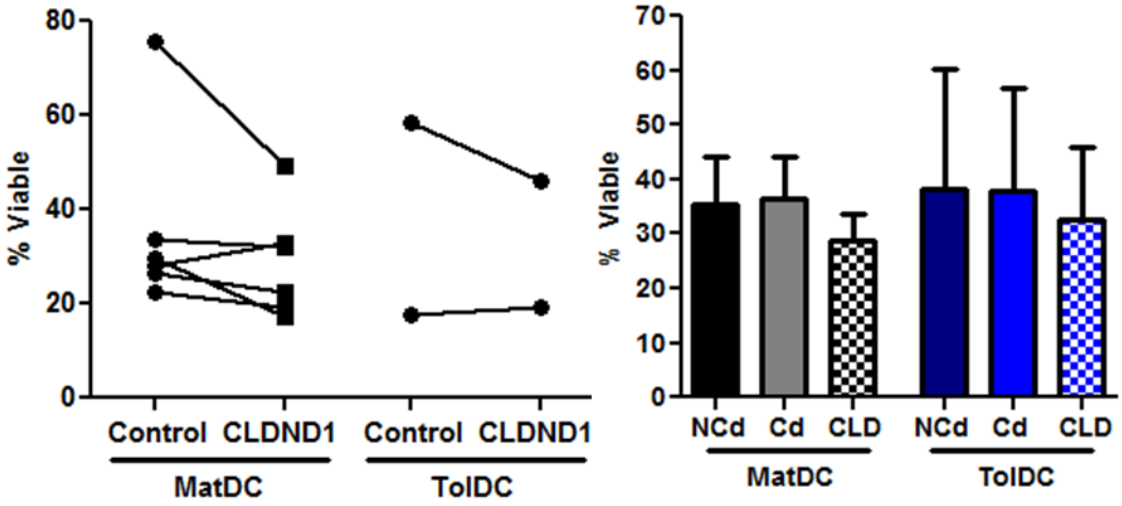

Figure 76. CLDND1-transfected T-cell viability in response to 6 day DC stimulation

CD4+ T-cells were transfected with stuffer-PIMMS (NCd) or light-PIMMS (Cd) controls or with CLDND1-PIMMS (CLD). 18 hours post transfection, cells were harvested and dead cells were removed. Cells were incubated with 10:1 ratio of mat- or tolDC for 6 days. An average was taken of the control vectors (control) or values were plotted independently. Cell viability was determined at the end of the experiment by Annexin V and Via-Probe™ staining by flow cytometry. Mean values (+ SEM) were plotted. Data illustrate six or two independent experiments, for mat- or tolDC, respectively. Paired Student's t-test analysis was performed.

One of the main indicators of an anergic phenotype is the reduction in IL-2 production (Schwartz, 2003) and so IL-2 levels were measured from the supernatants of the transfected co-cultures 24 hours after the initiation of the co-culture (Figure 77). A significant reduction in IL-2 production was observed in the CLDND1-PIMMS transfected samples co-cultured with matDC. This pattern was also mirrored with the IFN-γ levels detected after 6 days of co-culture in the majority of donors, but did not reach significance with all controls (Figure 78). IL-10, TNF-α and IL-5 levels were comparable between PIMMS-controls and CLDND1-PIMMS transfected cells.

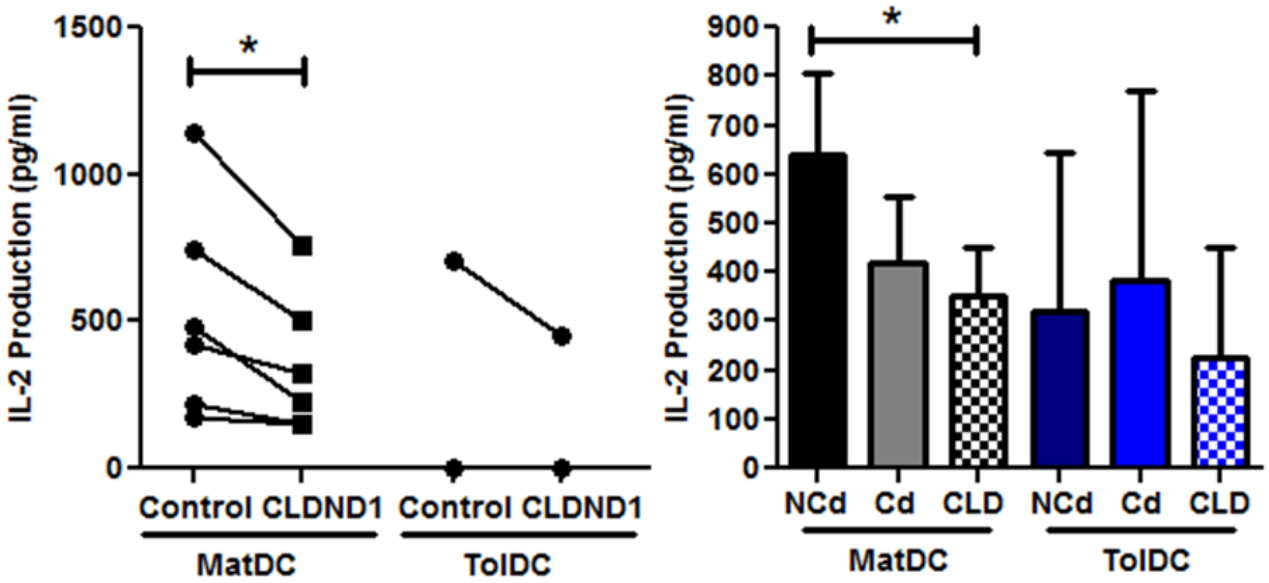

Figure 77. CLDND1-transfected T-cell IL-2 production in response to 6 day DC stimulation

CD4+ T-cells were transfected with stuffer-PIMMS (NCd) or light-PIMMS (Cd) controls or with CLDND1-PIMMS (CLD). 18 hours post transfection cells were harvested and dead cells were removed. Cells were incubated with 10:1 ratio of mat- or tolDC for 6 days. An average was taken of the control vectors (control) or values were plotted independently. IL-2 levels were determined from the supernatants 24 hours after the start of co-culture, by ELISA. Mean values (+ SEM) were plotted. Data illustrate four or two independent experiments for mat- or tolDC, respectively. Paired Student's t-test analysis was performed $p<0.05$.

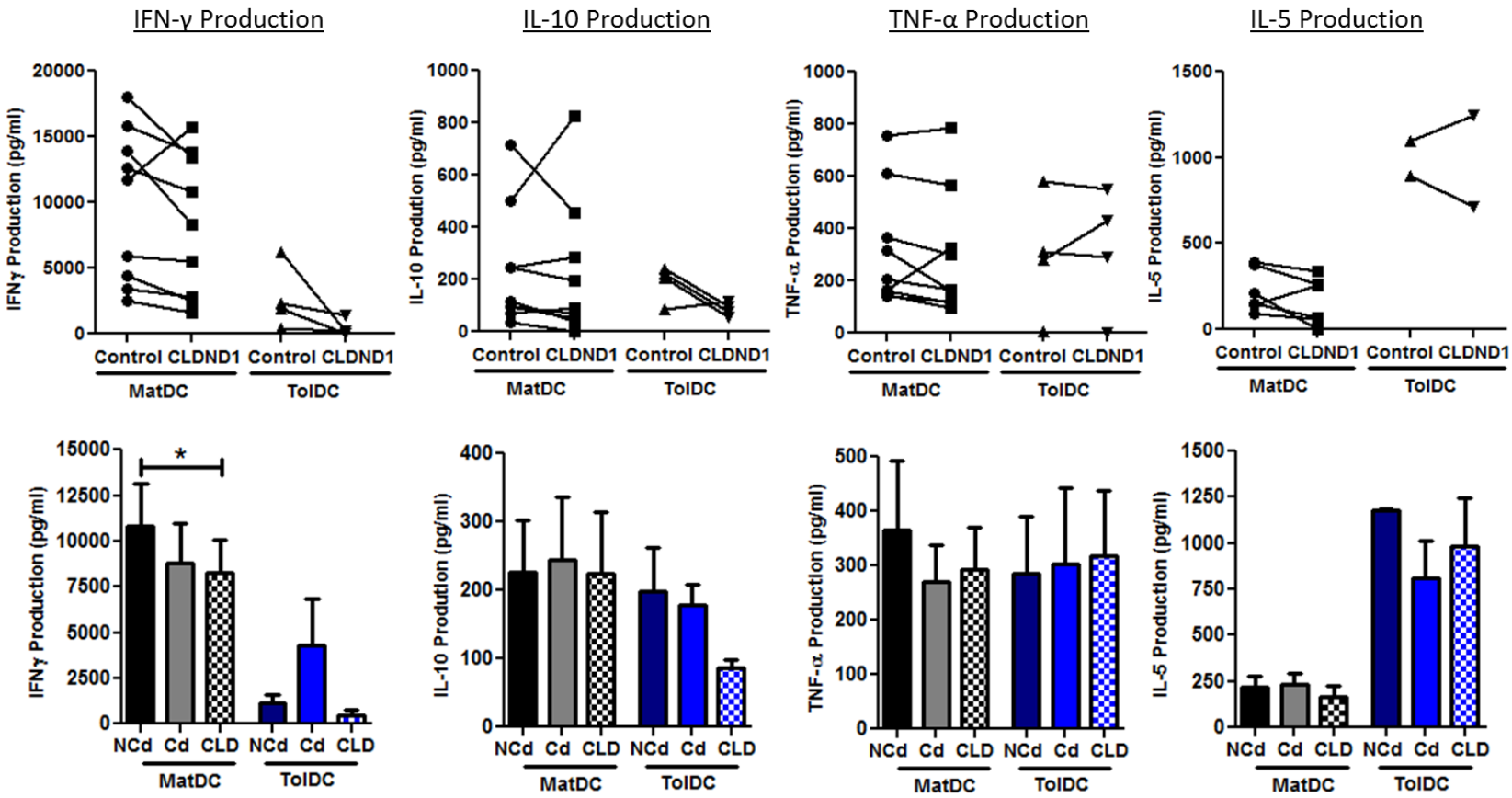

Figure 78. CLDND1-transfected T-cell cytokine production in response to 6 day DC stimulation

CD4+ T-cells were transfected with stuffer-PIMMS (NCd) or light-PIMMS (Cd) controls or with CLDND1-PIMMS (CLD). 18 hours post transfection, cells were harvested and dead cells were removed. Cells were incubated with 10:1 ratio of mat- or tolDC for 6 days. An average was taken of the control vectors (control) or values were plotted independently. Cytokines from supernatants taken at the end of the proliferation were measured by ELISA (for IFN-γ, IL-10 and TNF-α matDC n=9, tolDC n=4; for IL-5 matDC n=6, tolDC n=2). Mean values (+ SEM) were plotted. Paired Student's t-test analysis was performed *$p<0.05$.

6.3.8 Accessory molecule expression during CLDND1-transfected T-cell activation

To determine whether DC stimulation of CLDND1-PIMMS transfected cells resulted in changes in co-stimulatory or accessory molecule expression which in turn was causing the reduction in proliferation, CLDND1, CD4 and CD28 expression on PIMMS-transfected T-cells was assessed. CD25 expression was also assessed. CD25 is the alpha chain of the IL-2 receptor, which forms part of the heterotrimeric receptor structure. Binding of IL-2 to the IL-2 receptor propagates IL-2 signalling and so a reduction in CD25 expression would suggest reduced activation. 18 hours post transfection, but before co-culture, (Figure 79) a significant increase in CLDND1 cell surface and total protein was seen in the CLDND1-PIMMS transfected cells, as expected (Figure 79A). There was a trend in three of the four donors studied for an increase in CD4 expression and a decrease in CD28 expression (Figure 79B). In all four donors studied, there was a subtle increase in CD25 expression on CLDND1-PIMMS transfected T-cells than on control-PIMMS cells (Figure 79B).

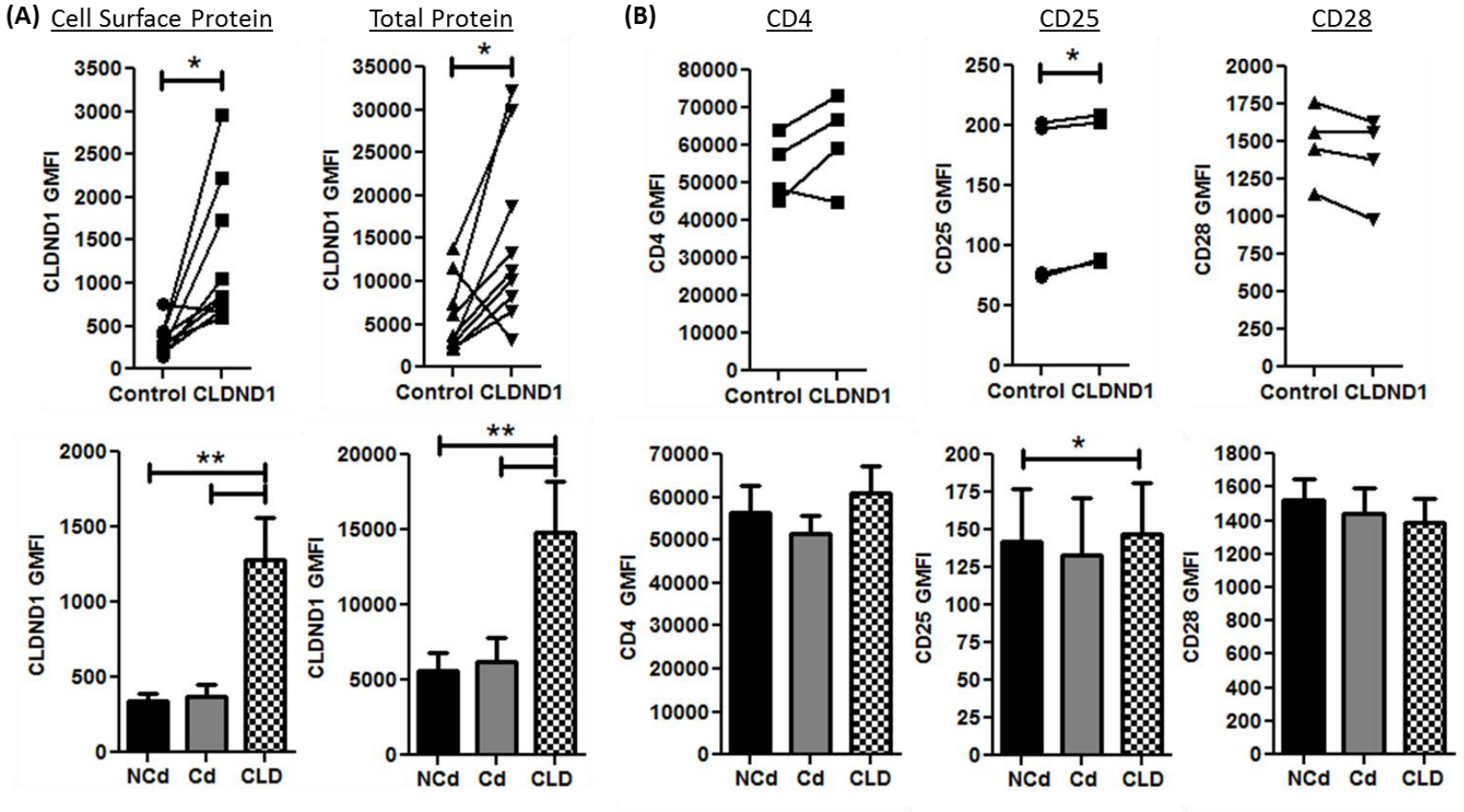

Figure 79. CLDND1-transfected T-cell surface marker expression

CD4+ T-cells were transfected with stuffer-PIMMS (NCd) or light-PIMMS (Cd) controls or with CLDND1-PIMMS (CLD). 18 hours post transfection cells were harvested and dead cells were removed. An average was taken of the control vectors (control) or values were plotted independently. (A) CLDND1 protein expression (n=9) (B) cell surface marker expression (For CD4 and CD28 n=4, for CD25 n=3). Mean values (+ SEM) were plotted. Paired Student's t-test analysis was performed *$p<0.05$, **$p<0.01$.

By day 6 of co-culture (Figure 80), CLDND1 cell surface protein levels were lower than seen post transfection but were still significantly higher compared to the averaged control values. This significance was lost on comparison to each control individually (Figure 80A). CD25 expression had flipped, with the CLDND1-PIMMS transfected cells having a significantly lower cell surface expression of CD25 than the PIMMS-control cells (Figure 80B), which is consistent with the down-regulation in proliferation. The increased CD4 expression in the CLDND1-transfected cells seen at the start of the co-culture was comparable to the control cells by the end of culture and the levels of CD28 varied depending on the donor.

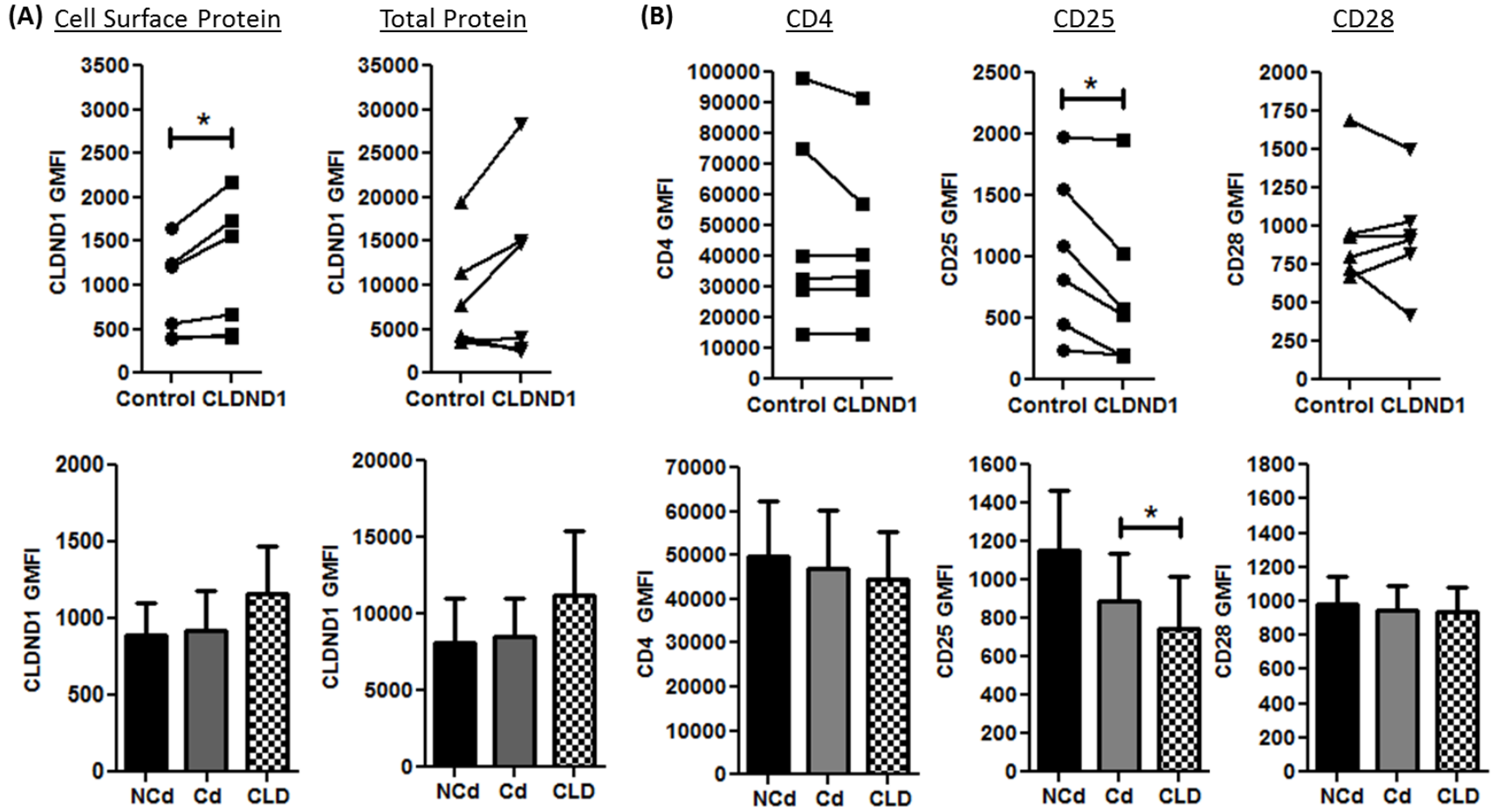

Figure 80. CLDND1-transfected T-cell surface marker expression in response to 6 day DC stimulation

CD4+ T-cells were transfected with stuffer-PIMMS (NCd) or light-PIMMS (Cd) controls or with CLDND1-PIMMS (CLD). 18 hours post transfection cells were harvested and dead cells were removed. Cells were incubated with 10:1 ratio of matDC for 6 days. An average was taken of the control vectors (control) or values were plotted independently. (A) CLDND1 protein expression (n=6). (B) Cell surface marker expression (n=6). Mean values (+ SEM) were plotted. Paired Student's t-test analysis was performed *$p<0.05$.

6.3.9 CLDND1-transfected T- cell re-stimulation: proliferation and cytokine production

Re-stimulation assays were performed to recapitulate an anergy model. As peptide specific responses could not be used, I utilised the recall response to a specific MHC class II mismatch in a MLR. Transfected T-cells were stimulated for 6 days with matDC and then immediately re-stimulated for 3 days in the presence of DC obtained from the same donor as the first round of stimulation (same DC) or with an independent DC donor (diff DC). If CLDND1 is important in the induction or maintenance of anergy, re-stimulation of CLDND1-transfected cells with the same DC donor should result in less T-cell proliferation and IL-2 production, than when stimulated with a MHC mismatched DC donor. It is important to note, that at the stage of re-stimulation, CLDND1 levels were still significantly elevated in the CLDND1-PIMMS transfected cells (Figure 80A).

In two of the three donors studied, CLDND1-PIMMS T-cell proliferation was reduced in response to same DC re-stimulations (Figure 81A), however, this response was mirrored in the diff DC re-stimulations, suggesting a non-specific effect rather than donor-specific anergy induction. Cell viability was also assessed in the re-stimulation cultures and no difference was observed overall in the percentage of viable cells stimulated with either same or diff DC (Figure 81B), but with two experiments, it is difficult to draw robust conclusions from these data.

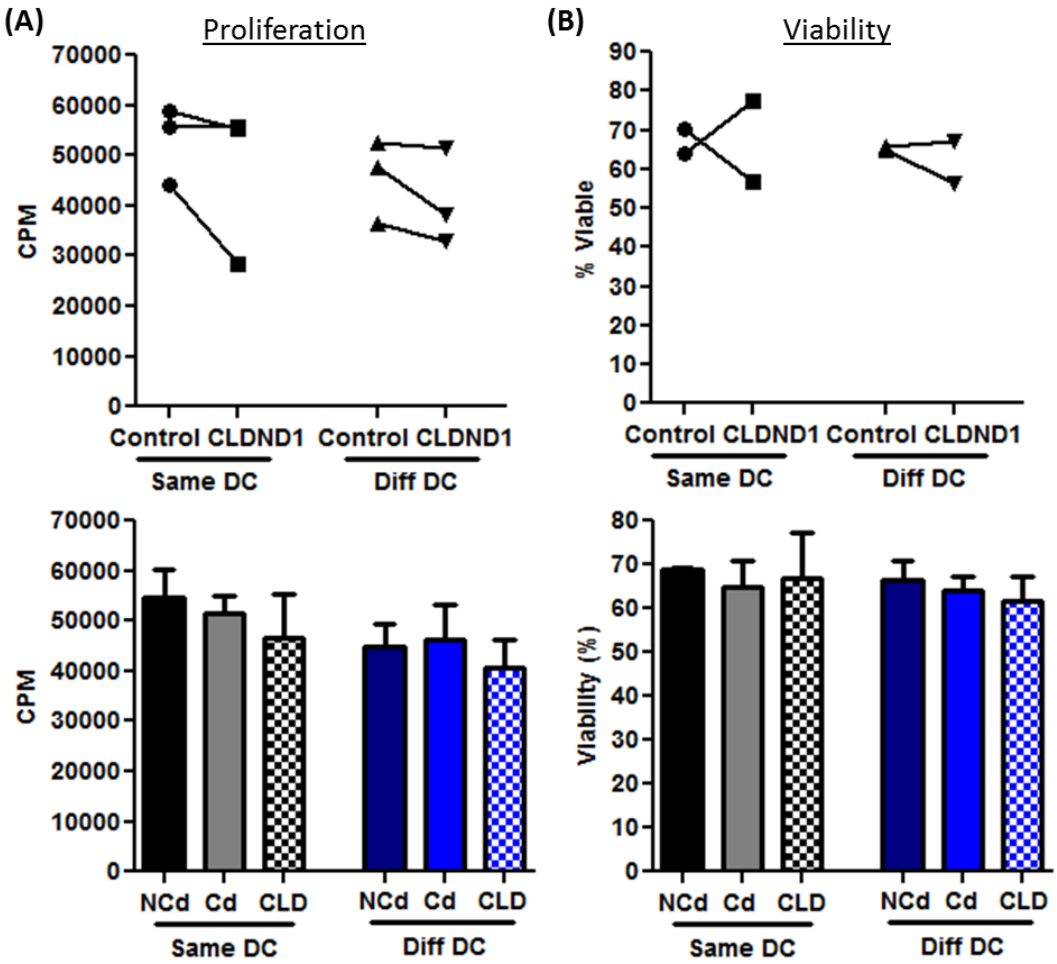

Figure 81. CLDND1-transfected T-cell proliferation and viability in response to DC re-stimulation

CD4+ T-cells were transfected with stuffer-PIMMS (NCd) or light-PIMMS (Cd) controls or with CLDND1-PIMMS (CLD). 18 hours post transfection cells were harvested and dead cells were removed. Cells were incubated with 10:1 ratio of matDC for 6 days. Cells were then re-stimulated with same DC or with diff DC for 3 days. An average was taken of the control vectors (control) or values were plotted independently. (A) Proliferation was measured by ^{3}HTdR incorporation (n=3). (B) Viability of the cells was determined by Annexin V and Via-Probe™ staining by flow cytometry (n=2). Mean values (+ SEM) were plotted. Paired Student's t-test analysis was performed.

Cytokine secretion was also examined (Figure 82). IL-2 was assessed 24 hours after re-stimulation but was below the threshold for detection (data not shown). In two of the three CLDND1-PIMMS transfected donors, IFN-γ and IL-10 levels were decreased and IL-5 production levels were increased, but this was not DC-donor specific. Interestingly, TNF-α production increased in the same DC re-stimulated CLDND1-PIMMS cultures from all three donors, in contrast to a consistent reduction when diff DCs were used for restimulation.

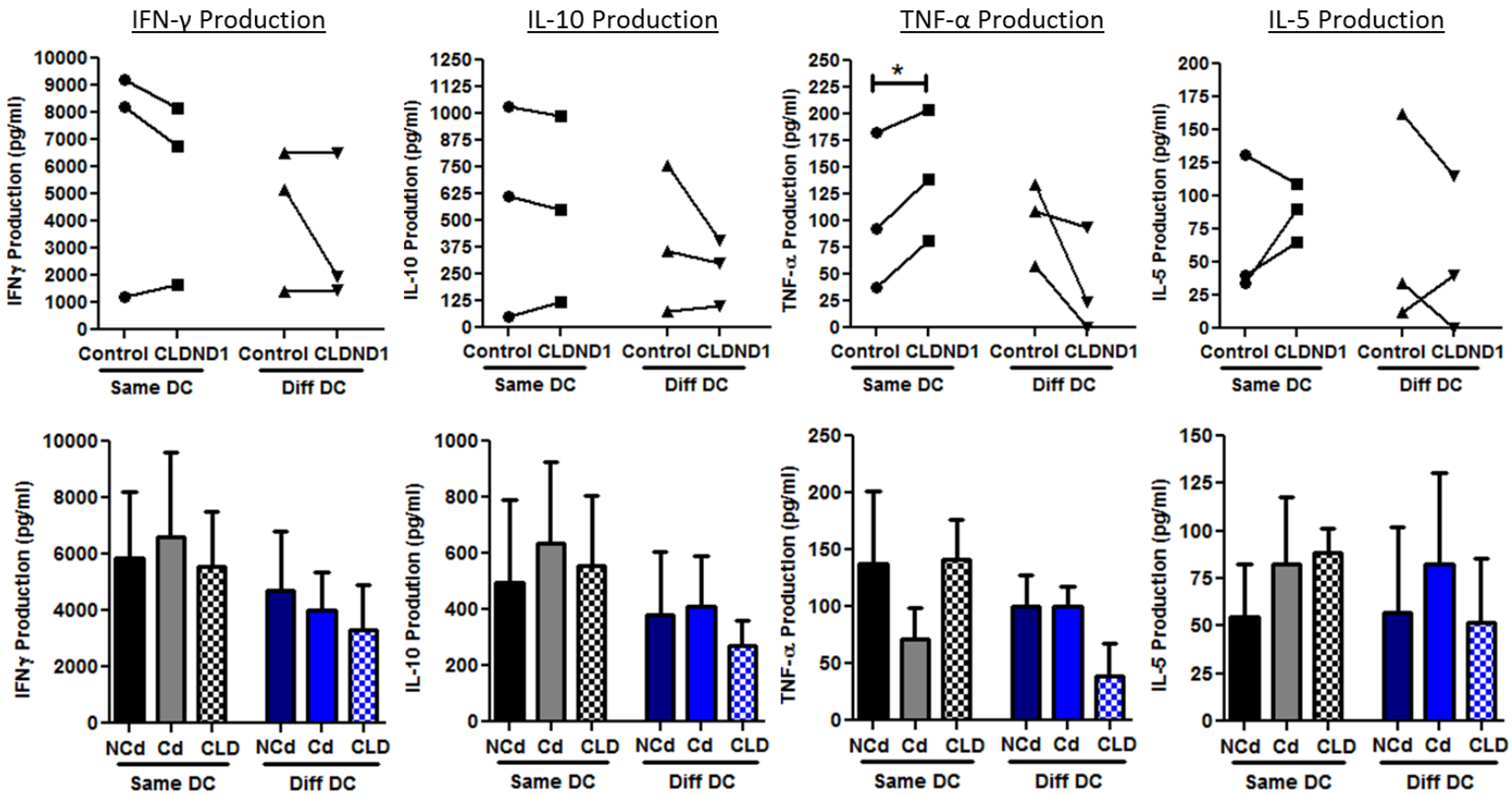

Figure 82. CLDND1-transfected T-cell cytokine production in response to DC re-stimulation

CD4+ T-cells were transfected with stuffer-PIMMS (NCd) or light-PIMMS (Cd) controls or with CLDND1-PIMMS (CLD). 18 hours post transfection cells were harvested and dead cells were removed. Cells were incubated with 10:1 ratio of matDC for 6 days. Cells were then re-stimulated with same DC or diff DC for 3 days. An average was taken of the control vectors (control) or values were plotted independently. Cytokines from supernatants taken at the end of the proliferation were measured by ELISA (n=3). Mean values (+ SEM) were plotted. Paired Student's t-test analysis was performed *$p<0.05$.

6.3.10 CLDND1-transfected T- cell re-stimulations: accessory molecules

As with previous experiments, the levels of cell surface and total CLDND1 were measured (Figure 83) along with CD4, CD25 and CD28 (Figure 84). The levels of cell surface CLDND1 fell dramatically in re-stimulated CLDND1-PIMMS cells, regardless of the re-stimulation signal, while total levels remained similar (Figure 83). CD4, CD25 and CD28 expression was also reduced in CLDND1-PIMMS re-stimulated cells, regardless of the type of restimulation DC (Figure 84). From one or two experimental replicates it is difficult to draw firm conclusions, however.

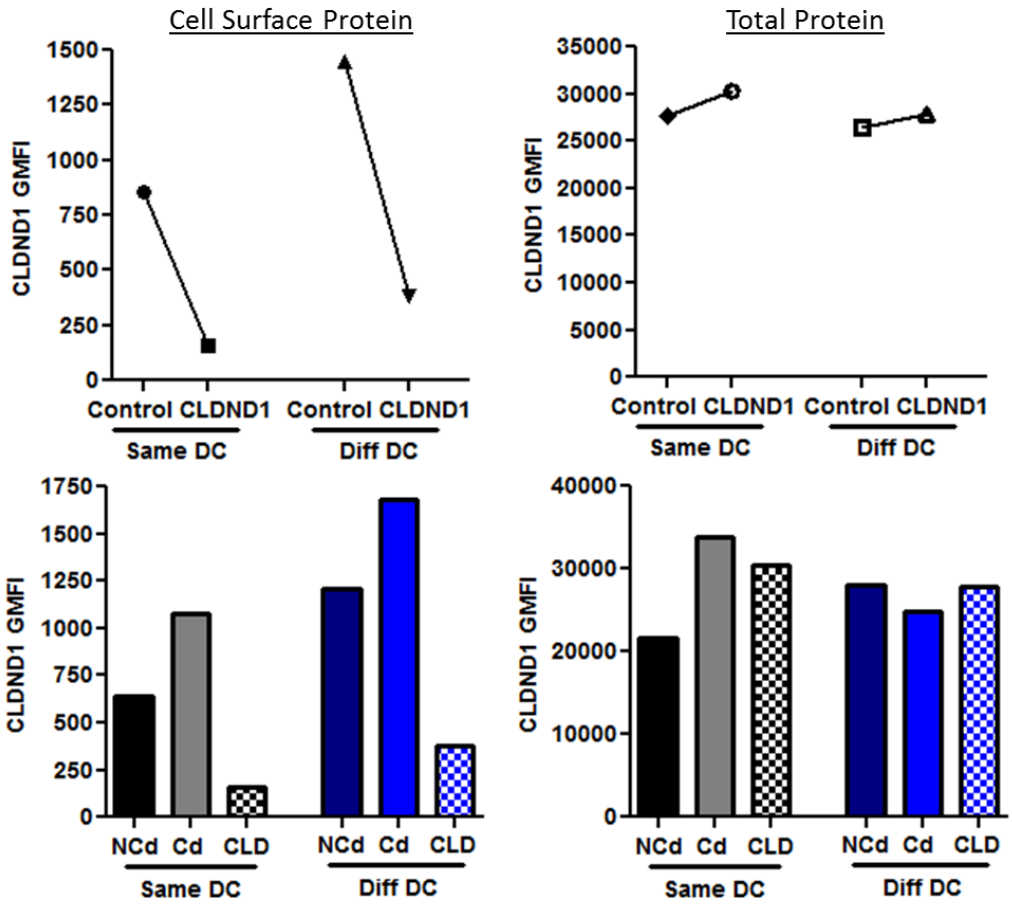

Figure 83. CLDND1-transfected T-cell CLDND1 expression in response to DC re-stimulation

CD4+ T-cells were transfected with stuffer-PIMMS (NCd) or light-PIMMS (Cd) control or with CLDND1-PIMMS (CLD). 18 hours post transfection cells were harvested and dead cells were removed. Cells were incubated with 10:1 ratio of matDC for 6 days. Cells were re-stimulated with same DC or diff DC for 3 days then CLDND1 expression was assessed. An average was taken of the control vectors (control) or values were plotted independently. Mean values were plotted. Data illustrate a single experiment.

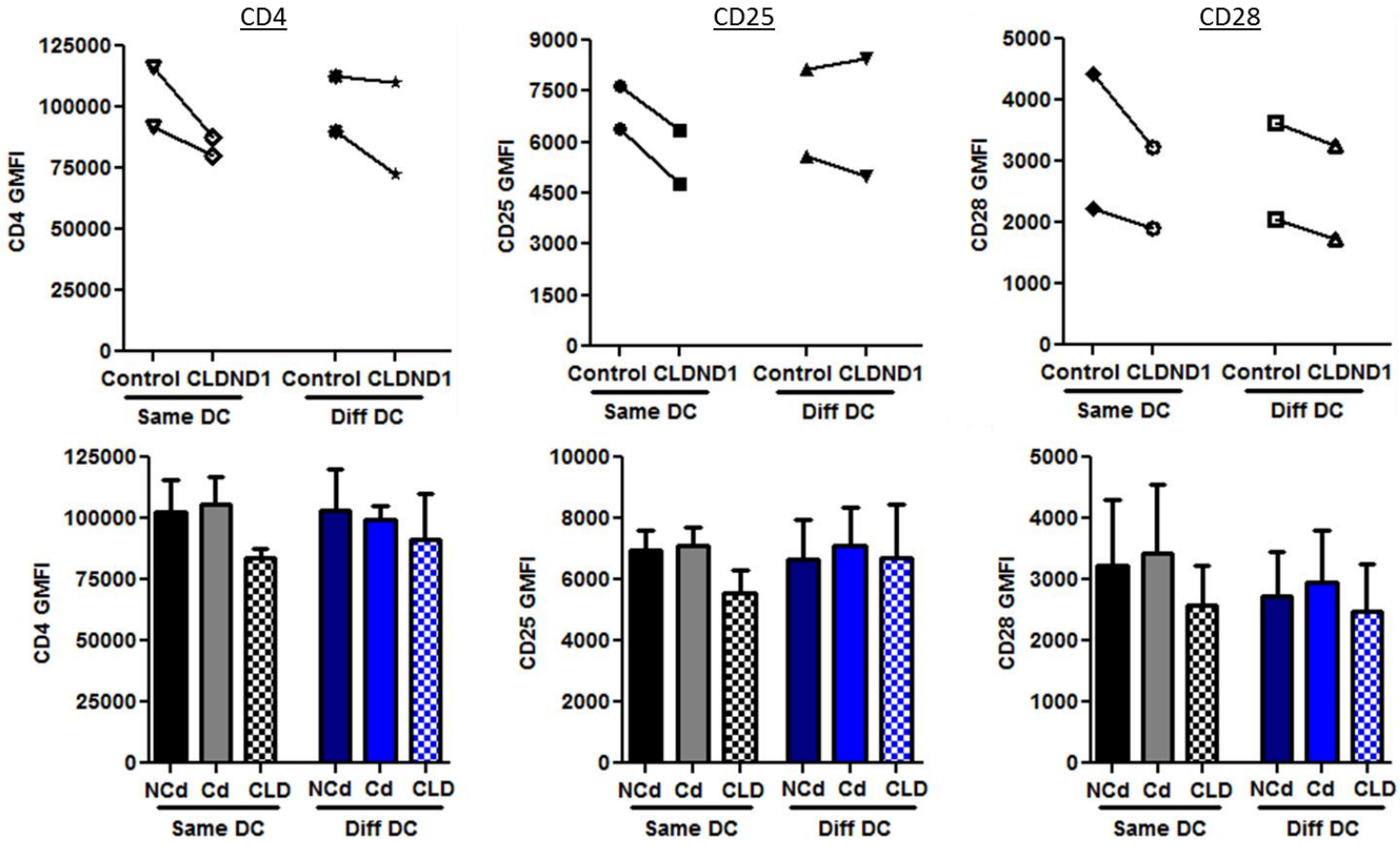

Figure 84. CLDND1-transfected T-cell surface marker expression in response to DC re-stimulation

CD4+ T-cells were transfected with stuffer-PIMMS (NCd) or light-PIMMS (Cd) control or with CLDND1-PIMMS (CLD). 18 hours post transfection cells were harvested and dead cells were removed. Cells were incubated with 10:1 ratio of matDC for 6 days. Cells were then re-stimulated with same DC or with diff DC for 3 days. An average was taken of the control vectors (control) or values were plotted independently. Mean values (+ SEM) were plotted. Data illustrate two independent experiments.

6.3.11 Functional domains of CLDND1

As part of the protocol for generating antibodies against full length CLDND1, vectors expressing truncated versions of CLDND1 were produced (Section 3.3.7, Figure 28). The CLDND1-trunc protein had part of its C-terminal domain removed containing the clathrin endocytosis signal along with two potential tyrosine phosphorylation sites. CLDND1-trunc over-expression into T-cells could either have one of two effects: i) the lack of the clathrin mediated endocytosis signal could potentially increase the effects of CLDND1 seen from the over-expression due to increased cell surface location, as this protein cannot be internalised by clathrin-coated pits; or ii) the lack of phosphorylation sites could prevent the functional effects seen with full length CLDND1. Both CLDND1-PIMMS and CLDND1-trunc-PIMMS were transfected into primary human CD4+ T-cells and 18 hours after transfection, CLDND1 cell surface and total CLDND1 levels were measured (Figure 85). A significant increase in CLDND1 cell surface protein was identified in the CLDND1-trunc-PIMMS transfected cells compared to control cells, yet there was not a trend for increased CLDND1 cell surface location in the CLDND1-trunc-PIMMS transfected samples compared to the full length CLDND1-PIMMS, suggesting that, in this system, clathrin mediated endocytosis may not be important in maintaining cell surface expression. Total levels of CLDND1 were comparable between the CLDND1-PIMMS and CLDND1-trunc-PIMMS transfected samples. Comparison of transfection efficiencies identified that 43.5 ± 3.1 % SEM cells were transfected with CLDND1-PIMMS while only 25.4 ± 3.7 % SEM cells were transfected with CLDND1-trunc-PIMMS.

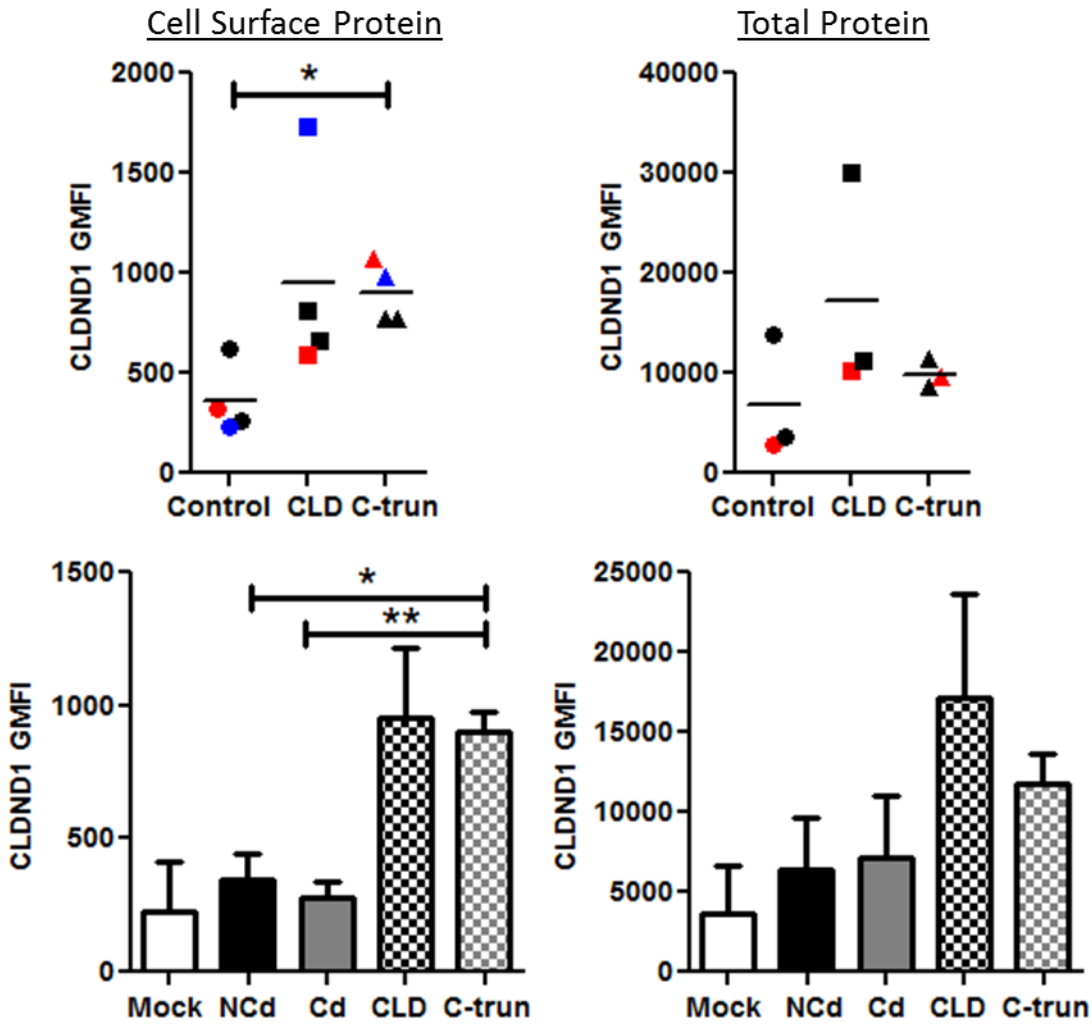

Figure 85. Truncated CLDND1-transfected T-cell CLDND1 expression

CD4+ T-cells were transfected with stuffer-PIMMS (NCd) or light-PIMMS (Cd) controls or with CLDND1-PIMMS (CLD) or CLDND1-trunc-PIMMS (C-trun). 18 hours post transfection, cells were harvested and dead cells were removed. Cells were incubated with 10:1 ratio of matDC for 6 days. An average was taken of the control vectors (control) or values were plotted independently. CLDND1 protein expression 18 hours post transfection. Mean values (+ SEM) were plotted. Data illustrate at least three independent experiments. Red and blue coloured points represent donors where restoration of T-cell proliferation was seen (Figure 86). Paired Student's t-test was performed, *p<0.05, **p<0.01.

The effect of CLDND1 truncation on T-cell proliferation was assessed (Figure 86). A significant reduction in proliferation was seen in the CLDND1-PIMMS transfected cells compared to the PIMMS-non-coding control, as seen previously. In only two of the four donors, (Figure 86, blue and red data points) a difference in proliferation was seen between truncated and full length CLDND1, and proliferation was elevated compared to CLDND1-PIMMS cells. Analysing more individuals may confirm a functional role for CLDND1 C-terminal domain in CLDND1's regulation of T-cell proliferation, however this may also reduce the significance of this observation. Analysis of cytokine secretion in the transfected samples mirrored the proliferation data (Figure 87), with the exception of IL-10 which did not differ greatly in any of the transfected samples.

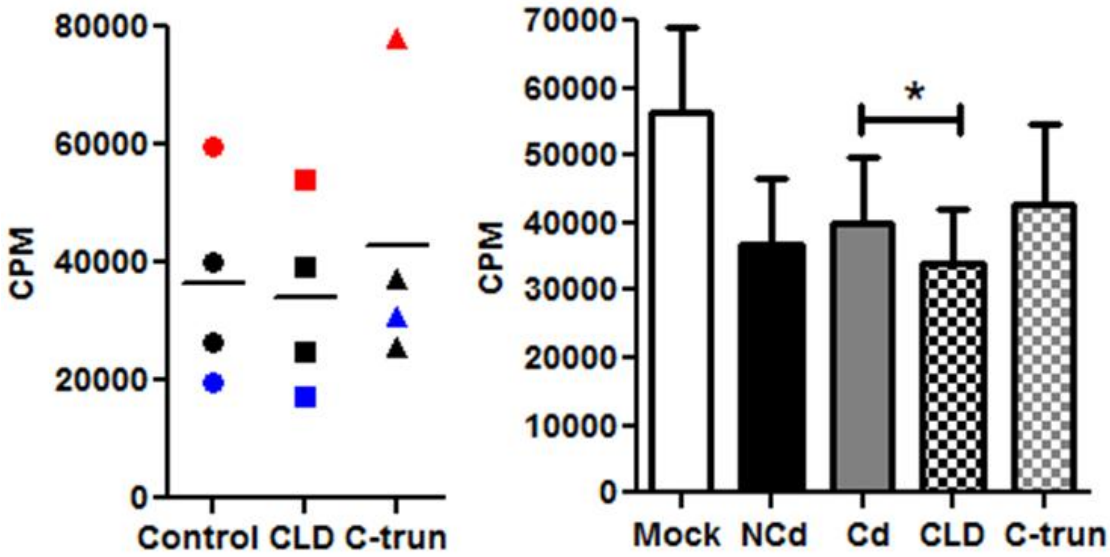

Figure 86. Truncated CLDND1-transfected T-cell proliferation

CD4+ T-cells were transfected with stuffer-PIMMS (NCd) or light-PIMMS (Cd) controls or with CLDND1-PIMMS (CLD) or CLDND1-trunc-PIMMS (C-trun). 18 hours post transfection, cells were harvested and dead cells were removed. Cells were incubated with 10:1 ratio of matDC for 6 days. An average was taken of the control vectors (control) or values were plotted independently. Proliferation was measured by ^{3}HTdR incorporation. Mean values (+ SEM) were plotted. Data illustrate four independent experiments. Red and blue coloured points represent donors where restoration of T-cell proliferation was seen. Paired Student's t-test was performed, *$p<0.05$.

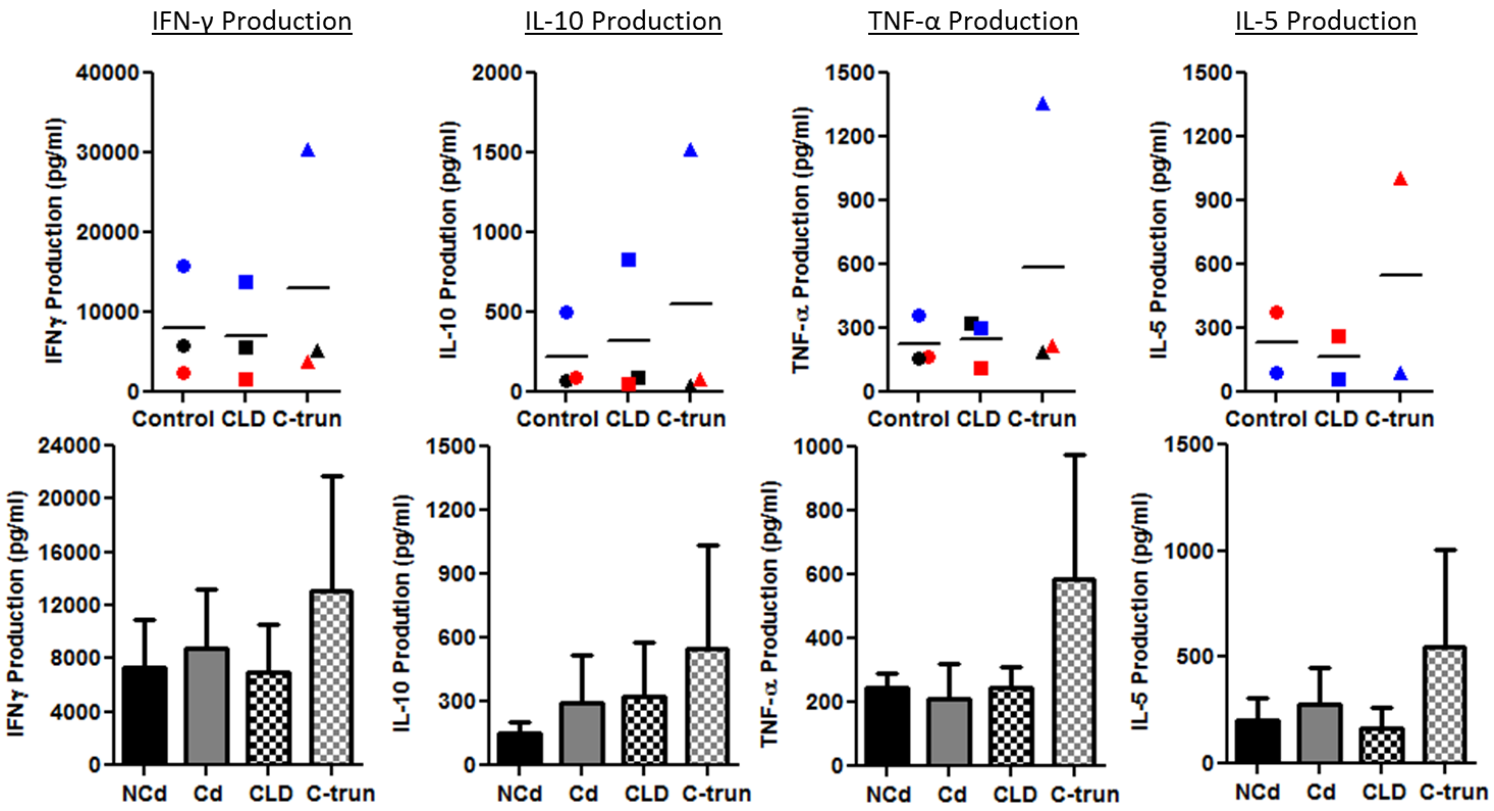

Figure 87. Truncated CLDND1-transfected T-cell cytokine production

CD4+ T-cells were transfected with stuffer-PIMMS (NCd) or light-PIMMS (Cd) controls or with CLDND1-PIMMS (CLD) or CLDND1-trunc-PIMMS (C-trun). 18 hours post transfection cells were harvested and dead cells were removed. Cells were incubated with 10:1 ratio of matDC for 6 days. An average was taken of the control vectors (control) or values were plotted independently. Cytokines from supernatants taken at the end of the proliferation were measured by ELISA. Mean values (+ SEM) were plotted. Data illustrate at least two independent experiments. Red and blue coloured points represent donors where restoration of T-cell proliferation was seen. Paired Student's t-test analysis was performed*$p<0.05$, **$p<0.01$.

6.4 Discussion

Throughout this chapter, a function for CLDND1 in the regulation of CD4+ T-cell proliferation was sought. Based on conserved motifs identified during the discovery of the protein, CLDND1 was categorised as a member of the PMP-22/EMP/MP20/claudin superfamily. Further phylogenetic analysis revealed CLDND1 shared more homology to the more distantly related proteins TMEM114 and CACNG. Over-expression of CLDND1 resulted in significant increases in both cell surface and total CLDND1, which depending on the type of activation stimulus resulted in an increase in cell death, or a reduction in proliferation and pro-inflammatory cytokine production. In order to determine the specific effects of CLDND1 in T-cell recall responses, re-stimulations assays were performed. Minimal differences were observed between different allogeneic stimuli used in the re-stimulation assay, suggesting that CLDND1 may not influence antigen-specific T-cell recall responses. However as MLR provide a particularly strong and heterogeneous immune stimulus, similar studies need to be executed with more subtle T-cell stimuli to define a potential role for CLDND1 in anergy. A reduction in CLDND1-transfected T-cell proliferation during first round stimulations is consistent with the hypothesised role for CLDND1 in the regulation of T-cell responses.

6.4.1 Phylogenetic findings and the implications on CLDND1 function

Sequence analysis of CLDND1 revealed it shares more homology to TMEM114 and the CACNG than to the claudins. Although the former proteins have no identified function in immune cells, differences in protein post-translational modifications and their function in other cells may provide clues to CLDND1 function.

CLDND1 contains N-glycosylation sites (Section 3.3.6, Figure 26), and equivalent sites are important in the plasma-membrane localisation of TMEM114 (Maher et al., 2011). The CACNG family members are also heavily glycosylated (Section 1.11.5, Figure 8), but whether this is important for plasma-membrane localisation or function remains to be determined. Claudins do not have glycosylation sites in their extracellular loops (Koval, 2006). It is worth noting that in primary human CD4+ T-cells, differential glycosylation states were not observed for endogenous CLDND1 by western blot analysis (Section 5.3.2,

Figure 39A). Caution should therefore be applied when linking glycosylation to CLDND1 function in primary human CD4+ T-cells. With claudin-14, palmitoylation plays a similar role to TMEM114 glycosylation as this post translation modification is required for efficient localisation at tight junctions, but is not essential for protein stability or the formation of tight junction strands (Van Itallie et al., 2005). However, no palmitoylation sites have been documented for CLDND1. Similar roles for palmitoylation and glycosylation in the cellular localisation of PMP-22/EMP/MP20/claudin superfamily members may suggest that the location of TMEM114 was dependent on glycosylation and not due to the role glycosylation plays in protein stability, as previously suggested (Section 3.4.2).

Limited studies with truncated CLDND1 suggested a possible functional role for the cytoplasmic C-terminal domain of CLDND1. However, the differences were subtle in a limited number of experiments. Nonetheless, many PMP-22/EMP/MP20/claudin superfamily members are phosphorylated and the phosphorylation is implicated in localisation or function. Phosphorylation of serine or threonine residues within claudins -3, -4, -5 and -16 regulate their localisation as well as the barrier properties of tight junctions (D'Souza et al., 2005, Aono and Hirai, 2008, Ishizaki et al., 2003, Ikari et al., 2006). Additionally, phosphorylation of the C-terminal tail of CACNG2 has been shown to impair interactions with PDZ binding proteins and AMPA receptor synaptic trafficking (Choi et al., 2002). Further experiments are required to confirm or refute a role for the potential phosphorylation sites within the C-terminus sequence of CLDND1.

Some PMP-22/EMP/MP20/claudin superfamily members contain other important motifs within their C-terminal domain. The γ-2, -3, -4 and -8 subunit cluster of the CACNG family are TARP, regulators of AMPA receptor signalling, and possess a PDZ domain, which is the binding domain required for this regulatory function (Tomita et al., 2003). As CLDND1 does not contain this motif, functional characteristics of CLDND1 may be more similar to the non-PDZ possessing family members: TMEM114, γ-1, -5, -6 or -7. Although TMEM114 plays an important role in ocular development in vertebrates, its exact function remains uncertain (Maher et al., 2011) and no inferences to CLDND1 function can be made from this protein. The γ-1 subunit was the first CACNG to be

described and it decreases expression and activity of the pore forming α subunit (Cav1.1) of calcium channels (Sandoval et al., 2007). The γ-6 subunit interacts with and negatively regulates Cav3.1 through a conserved GxxxG motif in the first transmembrane domain of the protein (Hansen et al., 2004, Lin et al., 2008). Although not identical, CLDND1 contains an AxxxA motif, in the first transmembrane region, which has the same proposed functions as the motif in the γ-6 subunit. The γ-5 and -7 subunits have also been classified as a distinct subset of TARP which can positively modulate glutamate-evoked currents via AMPA receptors (Kato et al., 2008, Kato et al., 2007), without altering receptor trafficking, like conventional TARP (Tomita et al., 2003, Kato et al., 2008). As well as their well-known location in neuronal cells, AMPA receptors are also present on human lymphocytes, and can modulate T-cell function through altering calcium flux (Lombardi et al., 2001).

Linking the phylogenetic studies, the role of CACNG in modulating calcium flux in lymphocytes, and the CLDND1 proliferation studies may suggest a role for CLDND1 as a regulator of calcium channels. Calcium signalling is of pivotal importance for both positive and negative regulation of T-cell function (Beyersdorf et al., 2009, Oh-hora and Rao, 2008, Gwack et al., 2008). A proposed model for signalling through store operated calcium channels has been suggested by Qu et al. (2011), where proliferation, apoptosis or tolerance can occur depending on the strength and duration of calcium signalling (Figure 88).

A role for CLDND1 in the regulation of calcium ion channels is also consistent with its expression in glial cells. Oligodendrocytes were originally described as myelin producing cells, important for the modelling of the axons of the nervous system. More recently, a lot of interest has been generated in the function of these cells due to their pivotal role in multiple sclerosis (Prineas and Parratt, 2012). One aspect has focussed on the role of calcium signalling within these cells. Several experiments indicate that cells of oligodendroglial lineage exhibit remarkable plasticity with regard to the expression of ion channels and receptors linked to calcium signalling and that perturbation of calcium homeostasis contributes to the pathogenesis of demyelinating diseases, primarily though the induction of apoptosis in these cells (Alberdi et al., 2005).

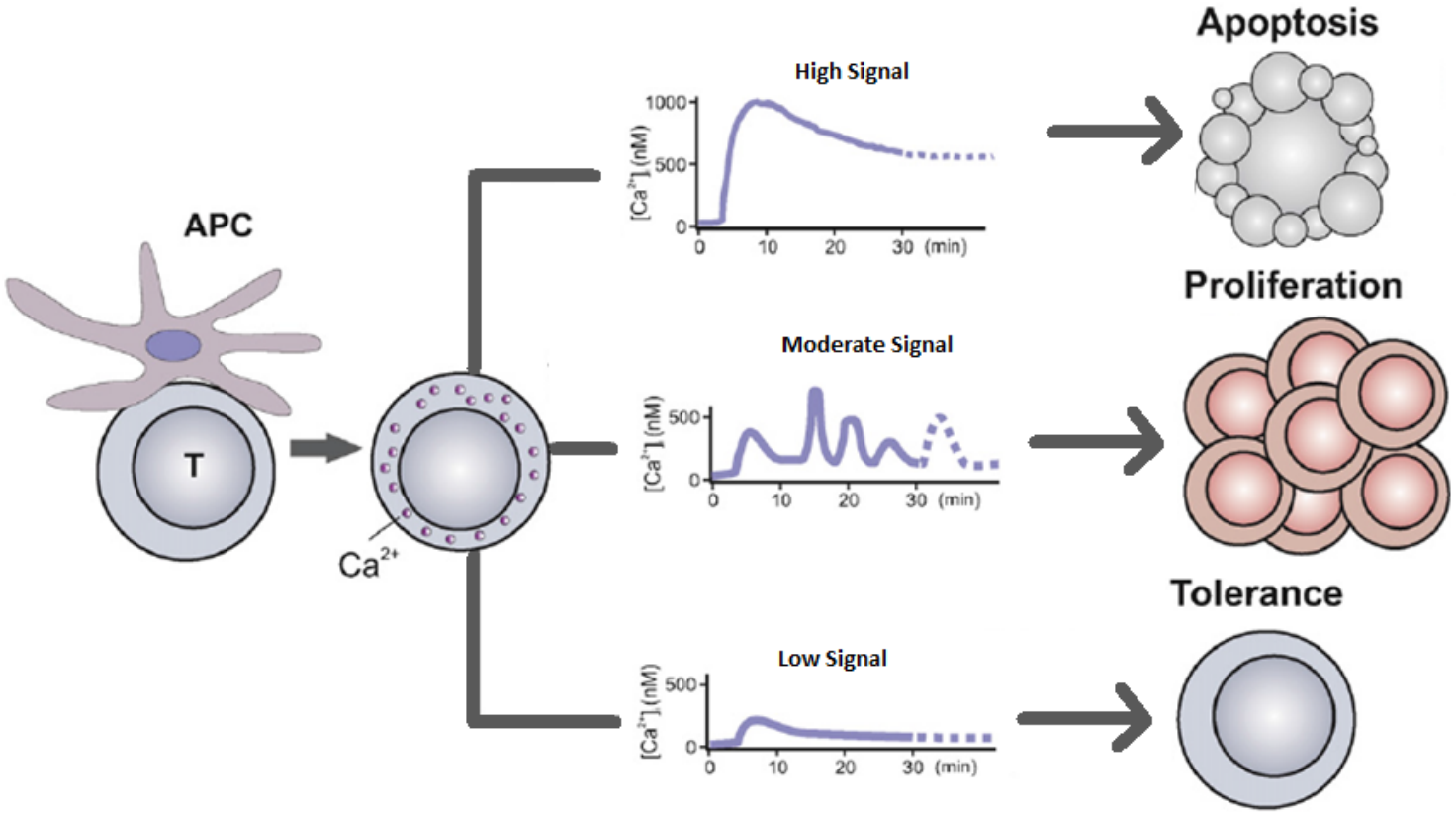

Figure 88. [Ca]i signalling and T-cell proliferation, apoptosis and tolerance

The strength of [Ca]i signalling within a T-cell dictates its response. High [Ca]i signalling can induce T-cell apoptosis, moderate strength signalling can induce T-cell proliferation and low signal strength can induce T-cell tolerance. Adapted from Qu et al. (2011).

6.4.2 CLDND1 function during primary T-cell responses

The effect of CLDND1 transfection on CD4+ T-cell proliferation was dependent on the type of stimulus. Activation of CLDND1-transfected T-cells with α-CD3/CD28 expander beads resulted in a decrease in cell viability and no consistent effect on proliferation, whereas stimulation with either mat- or tolDC resulted in a reduction in proliferation, CD25 expression and IL-2 and IFN-γ production, which was independent of cell death. One hypothesis for the differences observed between the two stimuli relates to the differences in strength of activating signal, as illustrated by the proliferation and IFN-γ production of non-transfected cells (Section 5.3.5, Figure 50), and a selection of examples have been chosen to represent this hypothesis.

Firstly, I have already shown that higher cell surface expression of endogenous CLDND1 was observed in samples stimulated with α-CD3/CD28 expander beads compared to DC (Figure 51). Therefore a certain threshold of CLDND1 cell surface expression, reached during stimulation with α-CD3/CD28 expander beads but not with DC, may have promoted the initiation of cell death pathways. In contrast, regulatory pathways could be induced in DC stimulated cells. Although proposed CLDND1 function is distinct from Foxp3, it serves as an example of altered T-cell phenotypes as a result of different expression patterns of this gene. In scurfy mice, which lack CD4+CD25+ Treg due to absent Foxp3 expression, CD4+ T-cells are hyper-responsive to TCR stimulation (Brunkow et al., 2001) and induction of Foxp3 expression in CD4+CD25- T-cells results in the acquisition of a Treg-like phenotype (Hori et al., 2003, Fontenot et al., 2003). On the other hand, elevating Foxp3 beyond a certain threshold leads to increased susceptibility to apoptosis following T-cell activation, through activation induced cell death (AICD) (Kasprowicz et al., 2005).

Another example in which protein function is modulated by the amount of protein expressed is mTOR. In this case higher levels of mTOR are associated with T-cell activation and not cell death, like Foxp3, and inhibition results in anergy. The function of mTOR is also dependent on the cell type in which it is expressed. In CD4+ CD25+ Treg, mTOR signalling can induce AICD under stimulatory conditions whereas the same activation through mTOR in CD4+CD25- T-cells promotes cell survival (Strauss et al., 2009). In addition, inhibition of mTOR signalling in whole CD4+ T-cell populations induces anergy

under stimulatory conditions (Zheng et al., 2007). Determining the effects of CLDND1 in specific cell subsets may depict specific effects for CLDND1 in these subsets, which may not be evident in whole CD4+ T-cell populations.

If the strength of stimulus influenced a threshold level of cell surface CLDND1 and subsequent T-cell function, then functional differences might also have been observed between the mat- and tolDC stimulated CLDND1-transfected cells, because mat- and tolDC promote different strengths of T-cell responses (Section 5.3.5, Figure 50). However, similar effects were identified between the mat- and tolDC stimulated CLDND1-transfected cells. By definition mat- and tolDC impart major differences on T-cells which could have over-ridden any influences of CLDND1 per se. Furthermore, any quantitative relationship between CLDND1 expression and function has not been defined by my work; this would require titrations of both α-CD3/CD28 expander bead and DC stimulus to determine whether CLDND1 function is regulated in a dose dependent manner.

The fact that DC themselves express CLDND1 (Section 5.3.5, Figure 49) is another key difference between experiments studying bead or DC stimulation. It is well accepted that claudin family members mediate homotypic interactions (Findley and Koval, 2009), which could have a profound influence on interactions between DC and CLDND1-transfected T-cells if CLDND1 behaved similarly.

Other regulatory interactions between DC and T-cells include CD40/CD154 and 1-IBB/4-IBBL receptor interactions. Through the use of CD154-knock-out mice, an interaction between CD40 and CD154 has proved important in the efficient priming of T-cell responses *in vivo* (Grewal et al., 1995). Similarly, interactions between 4-IBB/4-IBBL are important in the priming of some T-cell responses in the absence of CD28 (DeBenedette et al., 1997). Although these receptors aid the priming of T-cell responses, they serve as an example of the complex signalling pathways between T-cell and DC, not present with α-CD3/CD28 expander beads, which CLDND1 could directly or indirectly influence.

Post CLDND1 transfection, T-cells had increased CD4 and CD25 and reduced CD28 expression. Independently, $CD4^{high}$ and $CD25^{high}$ T-cells have been linked to an enhanced susceptibility to activation in a number of diseases (Li et al., 2007, Stanzani et al., 2004). In contrast, it is well established that Treg cells

also have high CD25 expression, and are characteristically anergic, which is consistent with the subsequent fall in CD25 expression in the CLDND1-transfected cells and a reduced level of activation. Based on contradictory examples, the relevance of CLDND1 induced changes in CD4 and CD25 expression remains uncertain.

6.4.3 CLDND1 function during secondary immune responses

I also attempted to examine the role of CLDND1 in the regulation of T-cell anergy. Owing to the lack of a peptide-reactive T-cell clone, a surrogate system was adopted, where CLDND1-transfectants were re-stimulated with the same allogeneic DC, or with third party DC. No apparent differences were observed between the two different models suggesting CLDND1 may not influence recall responses. Nonetheless, MLR provide a particularly strong and heterogeneous immune stimulus and similar studies need to be executed with alternative modes of T-cell activation. Although no difference in proliferation was observed between the stimulated CLDND1-transfected cell populations, there was an increase in TNF-α production in the recall CLDND1-transfected cultures in contrast to a fall in third party DC-stimulated cultures. The source of TNF-α in these cultures is uncertain as both T-cells and DC can express this cytokine. TNF-α is linked to the induction of apoptosis (Chu, 2013), the attenuation of TCR signalling, T-cell proliferation and cytokine production (Cope et al., 1997) and the effective priming and maturation of DC in response to infection (Trevejo et al., 2001), and so the role of TNF- α in this system remains to be determined. Future work could also focus on the DC populations within these cultures, to determine whether the effects of CLDND1-overexpression were affecting DC phenotype.

6.4.4 Mechanisms of CLDND1 function

The limited CLDND1 truncation studies raised the possibility that part of the C-terminal domain of CLDND1 may be important for transduction of intracellular signals, through its clathrin mediated endocytosis motif and phosphorylation sites. CTLA-4, a negative regulator of T-cell proliferation, has a clathrin mediated endocytosis motif in its C-terminal tail that provides an interaction point for the src family tyrosine kinases, fyn, lyn and lck and acts as a site for phosphorylation for CTLA-4 function (Miyatake et al., 1998). Claudin-4 also

associates with lck in human CD4+ T-cells (Kawai et al., 2011) and so the CLDND1 clathrin mediated endocytosis motif may indicate a potential signalling function.

In summary, studies to determine a function for CLDND1 in primary human CD4+ T-cell have pointed towards an inhibitory role for CLDND1 in the induction of T-cell pro-inflammatory responses, although different effects were observed depending on the type of stimulus. This finding is common within the T-cell biology field, where several proteins have different functions depending on the context of the experiment; the findings also fit with current knowledge of other PMP-22/EMP/MP20/claudin superfamily members' roles in different cell systems. These studies have not provided evidence to suggest that CLDND1 plays a role in anergy induction, although different models need to be studied. The function of CLDND1 may be modulated through C-terminal sequence motifs, which also fits with other PMP-22/EMP/MP20/claudin superfamily members and other proteins involved in the regulation of T-cell responses. In all, my experiments have suggested many further avenues for research on CLDND1 in order to determine its role in T-cell proliferation or homeostasis.

Chapter 7. General Discussion

Preliminary work had suggested a potential role for CLDND1 in the regulation of T-cell proliferation and the aims of this project were to recapitulate these findings and provide further evidence of a role for CLDND1 in the regulation of T-cell responses. Using a number of approaches I have added to these original findings. I have investigated how CLDND1 may modulate T-cell function, how the protein itself is organised within cellular membranes, the way in which the protein is expressed, which proteins or signalling systems may modulate CLDND1 function and postulated a potential role for CLDND1 in autoimmune disease. Some findings identify similarities between CLDND1 and other members of the PMP-22/EMP/MP20/claudin superfamily, providing potential links for functional pathways.

7.1 CLDND1 RNA and Protein Levels

Based on differences identified between CLDND1 RNA and protein levels, a hypothesis was generated whereby CLDND1 may be regulated through post-translational mechanisms rather than at the level of gene transcription. The idea builds further with the concept that CLDND1 function is also regulated through its cellular location, the amount of protein available and associations with other proteins.

7.1.1 CLDND1 RNA versus protein levels

The CLDND1 gene could be effectively silenced at the transcript level; however no reduction in cell surface or total CLDND1 protein was seen. The siRNA method used has since been successfully used to silence the tyrosine kinase Jak3, at both the mRNA and protein level in primary human T-cells (Gomez-Valades et al., 2012), suggesting a CLDND1 specific observation. It was established that the techniques used to detect CLDND1 RNA or protein during the silencing experiments were effective, which therefore suggested CLDND1 RNA and protein were independently regulated.

The tracking of CLDND1 RNA and protein expression levels during T-cell activation further supported a disconnect between CLDND1 RNA and protein levels. In either CD4+ or CD8+ T-cells, the increase in CLDND1 RNA levels seen during T-cell activation was consistently smaller than the increase in

CLDND1 protein levels, with CLDND1 transcript levels showing 1.9 ± 0.3 SEM fold change and CLDND1 cell surface protein levels 6.0 ± 1.33 SEM fold change above the resting values. Additionally, during CLDND1 over-expression experiments, a large fold change in CLDND1 RNA was identified (81.5 ± 7 SEM) in the CLDND1-transfected samples, yet the fold change in CLDND1 protein levels was much lower (3.9 ± 0.6 SEM or 3.3 ± 0.4 SEM, depending on cell surface or total CLDND1 protein expression, respectively). Although in this instance, the changes in CLDND1 RNA levels were greater than the protein levels, a discrepancy between the RNA and protein levels was still observed. As the Central Dogma of molecular biology states that "DNA makes RNA makes protein" this would suggest a linear relationship between these entities. This linear relationship underpins the basis for a number of transcript-profiling experiments to identify genes that are up- and down-regulated under normal or disease conditions, with the underlying assumption that differences in mRNA levels in different phenotypes will result in differences of protein levels. As such, the correlations between differential expression of mRNA and proteins have been the centre of a number of studies. A comprehensive study correlating yeast mRNA and proteins identified greater than 70 % of proteins levels were regulated by the abundance of their mRNA (Lu et al., 2007). Similarly, in circulating monocytes, Guo et al., (2008) identified at a cellular level, the amount of total protein detected was reflected by the amount of that transcript, again supporting the Central Dogma. There are at least four reasons for poor correlations between transcript and protein levels: firstly, many post-transcriptional mechanisms exist which are involved in turning mRNA into protein which may prevent the direct computation of protein expression from mRNA; secondly, protein half-lives are likely to differ substantially and so skew a linear relationship between mRNA and protein; thirdly, there will be a significant amount of error and noise in both protein and mRNA experiments (Greenbaum et al., 2003); and fourthly, post-translational modifications may account for the regulation of protein function and therefore mRNA abundance does not relate to the total amount of protein and its function. In some instances, discrepancies in certain mRNA and protein levels have been described, which occur as a result of post-translational mechanisms. The protein BiP, involved in the sensing of ER stress, has been shown to have independently regulated protein and RNA levels, as an artificial increase in

cellular BiP mRNA did not result in an increase in BiP synthesis. However, under ER stress, the translational efficiency of BiP was enhanced and cellular protein levels increased, independently of the abundance of transcript. These events were independent of the 5' and 3' UTR of the transcript, which instead suggested translational control mechanisms (Gulow et al., 2002). Additionally, TGF-β mRNA and protein levels are also not correlated, as a result of many regulatory post-translational mechanisms that influence the protein (Kim et al., 1992). These examples demonstrate non-proportionate quantitative changes in mRNA and protein, and my data suggest the same may be true for CLDND1.

7.1.2 CLDND1 protein localisation

In conjunction with the concept that CLDND1 protein is regulated independently of RNA levels, the location of CLDND1 within the cell may also act as a regulating mechanism. During DC-mediated CD4+ T-cell activation, a significant increase in cell surface CLDND1 was detected whereas no significant change in total CLDND1 protein was seen. This finding suggests CLDND1 traffics to the cell surface upon activation. An example of where cell surface location is imperative for protein function is CTLA-4. CTLA-4 is a potent negative regulator of CD4+ T-cell proliferation and functions at the cell surface where it binds and prevents interactions between the co-stimulatory molecule CD28 and the B7 molecules, CD80 and CD86, on DC. The cell surface location of CTLA-4 is tightly regulated where CLTA-4 is located in cytoplasmic vesicles in resting T-cells and these traffic to the cell surface during T-cell activation (McCoy and Le Gros, 1999).

7.1.3 CLDND1 protein quantity

The quantity of T-cell surface CLDND1 may be an important factor in CLDND1-mediated regulation of T-cell proliferation. Transfected CLDND1 cell surface expression levels weakly correlated with a reduction in T-cell proliferation, suggesting higher levels of CLDND1 at the cell surface result in lower T-cell activation. Significant changes in the quantity of cell surface CLDND1 were seen during T-cell activation but not for the total number of CLDND1-expressing cells. Similarly, in the EA patient study, the quantity of cell surface CLDND1 correlated with RA RF status but not the total number of CLDND1-expressing cells. In conjunction with the observation that CLDND1 cell surface expression

is identified on a proportion of T-cells, these findings are consistent with the hypothesis that the quantity of CLDND1 expressed relates to the functional role of CLDND1.

7.1.4 Potential CLDND1-protein interactions

CLDND1 function may be governed through interactions with other proteins. The presence of CLDND1 on a subpopulation of cells may indicate a possible protein interaction with a yet to be identified receptor or ligand expressed on these cells. In addition, it is well accepted that claudin family members can mediate homotypic interactions (Findley and Koval, 2009) and as CLDND1 is expressed on T-cells as well as DC, CLDND1 homotypic interactions may provide a generic mechanism of action for CLDND1. Western blot analysis on CD4+ T-cell CLDND1-transfected cell lysates revealed a band with a molecular weight approximately double the size of CLDND1, which according to independent studies on two other PMP-22/EMP/MP20/claudin superfamily members (Suzuki et al., 2013, Mobley et al., 2007), could indicate the presence of a CLDND1 homodimer.

Interactions between CLDND1 and other proteins may also be mediated from the intracellular portion of the protein. Limited studies to determine a function for the C-terminal tail of CLDND1 suggested CLDND1 regulatory function could be mediated through this region. Similar motifs identified in the C-terminal tail of CTLA-4 have been shown to provide an interaction point for the src family tyrosine kinases, fyn, lyn and lck and act as a site for phosphorylation (Miyatake et al., 1998). Claudin-4 can also associate with lck in human CD4+ T-cells (Kawai et al., 2011) and so this motif in the C-terminal tail of CLDND1 may indicate potential signalling functions for CLDND1 via lck.

Studies using the highly homologous mouse CLDND1 protein, claudin-25, showed this protein interacted with the integral tight junction protein ZO-1 in epithelial cells (Mineta et al., 2011). In addition, staining of claudin-1 on human CD4+ T-cells identified co-localisation of this protein with ZO-1 and so it was suggested that in lymphocytes, claudins can form TJ complexes with similar structure or composition as reported in endothelial or epithelial TJ complexes (Mandel et al., 2012). Co-staining of ZO-1 with CLDND1 on CD4+ T-cells may indicate a role for CLDND1 in cell-cell interactions through TJ- like structures. A role for claudin-1 in T-cell motility was also postulated in that study, based on

similar claudin-1 kinetics in melanoma cells (Mandel et al., 2012). CLDND1 may therefore also play a role in T-cell motility or similar mechanisms such as T-cell diapedesis.

The presence of TGF-β may in part be responsible for modulating CLDND1 cell surface expression, yet as the results obtained from these experiments were variable and not consistently reproducible, a role for TGF-β in the modulation of CLDND1 cell surface expression cannot currently be defined. One notion to explain the effects of TGF-β-mediated modulation of CLDND1 expression was through down-regulating T-cell activation (Delisle et al., 2013) and so lowering CLDND1 cell surface levels indirectly. Given the variability and inconsistency of my data, any role for TGF-β in modulating CLDND1 expression in CD4+ T-cells may be minor.

7.2 CLDND1 during T-cell Activation

CLDND1 cell surface protein levels were transiently increased during T-cell activation and so initial thoughts reflected on an inflammatory role for CLDND1 during the T-cell response. However, both positive and negative regulators of T-cell activation are also up-regulated at similar time-points, such as CD25 and CTLA-4 (Xia et al., 1999). CLDND1 cell surface levels were transiently increased in both CD4+ and CD8+ T-cells, suggesting CLDND1 function during T-cell activation is not restricted to the CD4+ T-cell subset.

7.3 CLDND1 during Anergy

A role for CLDND1 in the induction and maintenance of anergy was sought as part of this project, yet the lack of a sufficiently sensitive anergy model has limited the ability to collect this information. Based on the lack of a peptide specific model, a surrogate system was adopted to determine a role for CLDND1 in anergy induction. CLDND1-transfected cells were re-stimulated with the same allogeneic stimulus or with an alternative allogeneic stimulus, to determine any effect CLDND1 may impart on T-cell recall responses. Based on the data collected, there were no obvious differences identified between the differentially stimulated CLDND1-transfected populations, suggesting that CLDND1 may not be a major factor in recall responses in this model. Until a more sensitive model is used to prove or disprove this suggestion, a potential role for CLDND1 in anergy remains to be determined.

7.4 CLDND1 structure

A confounding and limiting finding during this thesis was the inability of the α-CLDND1 antibody to recognise CLDND1 in its native conformation. This resulted in a non-functional antibody that could only recognise fixed CLDND1, nonetheless it was still a useful tool for investigating CLDND1. The antibody binding characteristics also provided insight into the structure of the CLDND1 molecule.

The antibody was raised against a linear epitope and so the lack of antibody binding could suggest this epitope is hidden within folds of the extracellular loop under native conditions, but can be accessed after formaldehyde treatment. The role of formaldehyde cross-linking with primary amines and thiol groups to open up the CLDND1 structure (Metz et al., 2004, Fowler et al., 2011) was suggested, yet this phenomenon usually results in epitope masking (Fritschy, 2008). An additional theory where formaldehyde fixation unmasked the epitope was through disrupting the binding of an interacting partner. Although there is little evidence of unmasking epitopes via formaldehyde fixation in the literature, the potential for CLDND1 to interact with binding partners, such as homotypic interactions between CLDND1 molecules, have been suggested and this interaction may explain a lack of antibody binding to CLDND1 in its native conformation.

CLDND1 exists in different glycosylation states, potentially on residues in the first extracellular loop. Based on homology to the superfamily member TMEM114, in which glycosylation was required for the cell surface location of the protein (Maher et al., 2011), it may be that glycosylation plays a role in regulating cell surface expression of CLDND1. It is worth noting that in primary human CD4+ T-cells differential glycosylation states were not observed for endogenous CLDND1 and therefore caution should be applied in relating the importance of glycosylation to CLDND1 function in these cells.

Other post-translational modifications may also play a role in CLDND1 cell signalling. The cytoplasmic C-terminal domain of CLDND1 has been implicated in mediating interactions, possibly with lck, as similar interactions are found on other PMP-22/EMP/MP20/claudin superfamily members (Kawai et al., 2011). Many of the PMP-22/EMP/MP20/claudin superfamily members are phosphorylated and these phosphorylation motifs are implicated in cell location

or functional attributes of the proteins (D'Souza et al., 2005, Aono and Hirai, 2008, Ishizaki et al., 2003, Ikari et al., 2006, Choi et al., 2002). Therefore, potential phosphorylation sites within the CLDND1 C-terminal sequence may be important for its function.

7.5 Proposed Functional Model for CLDND1

Combining all the data for CLDND1, a model for the role for CLDND1 in CD4+ T-cells can start to be developed. The effect of CLDND1 on T-cell proliferation was dependent on the type of stimulus given to the cells, where a strong stimulus (α-CD3/CD28 expander beads) induced cell death and a weaker stimulus (mat- or tolDC) resulted in the reduction in T-cell proliferation. As the types of stimuli were different, two hypotheses were developed to explain the functions observed: firstly, that the strength of stimulation governs CLDND1 responses; and secondly, that unique factors present on the DC mediate unique signalling interactions.

The first hypothesis was generated from combining CLDND1 expression profiles with differences in CLDND1 function. T-cell stimulation with α-CD3/CD28 expander beads increased cell surface CLDND1 over mat- or tolDC stimulated cells. CLDND1-transfected α-CD3/CD28 expander bead stimulated T-cell viability was low, whereas CLDND1-transfected mat- or tolDC stimulated T-cells had a less activated phenotype and sustained viability. Therefore, during CLDND1-transfected T-cell stimulation, α-CD3/CD28 expander bead stimulus may have elevated CLDND1 cell surface levels beyond those in the DC stimulated cells which surmounted cellular mechanisms to regulate cell death and so cell death pathways were initiated. Failure to initiate cell death pathways due to a weaker stimulus (mat- or tolDC) instead led to a hypo-responsive phenotype. Similar protein expression kinetics and functions are seen with the Foxp3 protein, where high Foxp3 levels induce cell death, induced expression of Foxp3 induces a regulatory T-cell phenotype, in particular Treg, and loss of Foxp3 expression results in a hyperproliferative phenotype (Brunkow et al., 2001, Hori et al., 2003, Fontenot et al., 2003, Kasprowicz et al., 2005).

The second hypothesis promotes DC-specific interactions with CLDND1 to support the differences in CLDND1 function with the two types of stimuli. Potential CLDND1-interacting partners on the DC which are not present with the α-CD3/CD28 expander bead stimulus may include homotypic interactions

between CLDND1 molecules on T-cells and DC; interactions between CLDND1 and a yet to be identified ligand; or CLDND1 may be modulated indirectly as a consequence of other activatory or inhibitory binding partners present on DC and T-cells. Examples of this include: OX40 on T-cells interacting with OX40L on DC which enhances T-cell proliferation and activation through NFAT transcription factor activation (Yan et al., 2013); or PD-1 expression on T-cells interacting with PD-L1 molecule expression on DC which results in the inhibition of T-cell receptor-mediated lymphocyte proliferation through inhibition of TCR proximal phosphorylation events (Gianchecchi et al., 2013).

Some members of the PMP-22/EMP/MP20/claudin superfamily have been shown to regulate the activity of calcium channels through interactions with the channel subunit responsible for calcium permeability (Sandoval et al., 2007, Hansen et al., 2004, Lin et al., 2008). CLDND1, therefore, may have a role as a regulator of calcium channels. Calcium signalling in T-cells is of pivotal importance for T-cell physiology, as determined by a number of knock-out mice studies (Beyersdorf et al., 2009, Oh-hora and Rao, 2008, Gwack et al., 2008). A model for signalling through store operated calcium channels has been proposed by Qu et al., (2011), where tolerance, proliferation or apoptosis can occur with increasing strength and duration of calcium signalling. Additionally, the correlation of genes from RA patients and the anergic T-cell clone HA1.7, from which this work stemmed, also identified genes involved in calcium signalling, such as calmodulin, which was downregulated in both sets of samples (Ali et al., 2001). From the results generated in my thesis, it may be postulated that the calcium load induced by the weaker DC stimulus may be counteracted by CLDND1 regulating calcium signalling, resulting in a suppressed phenotype, whereas a higher calcium load through a stronger α-CD3/CD28 expander bead stimulus may surpass the regulatory effect of CLDND1 and result in cell death.

A potential role for CLDND1 in the regulation of calcium ion channels could provide a link to its expression and original identification in glial cells (Fayein et al., 2002). Oligodendrocytes were originally described as myelin producing cells and so were important cells in the modelling of the axons of the nervous system. One aspect of oligodendrocyte function has focussed on the role of calcium signalling within these cells. Several pieces of experimental evidence

indicate that cells of oligodendroglial lineage exhibit remarkable plasticity with regard to the expression of ion channels and receptors linked to calcium signalling and that perturbation of calcium homeostasis contributes to the pathogenesis of demyelinating diseases, primarily though the induction of apoptosis in these cells (Alberdi et al., 2005, Orrenius et al., 2003, Stirling and Stys, 2010, Paez et al., 2009).

In summary, a functional model for CLDND1 in CD4+ T-cell activation is proposed (Figure 89), where the functional outcomes vary depending on the system used, but indicate a suppressive role for CLDND1 in the regulation of T-cell proliferation. Suggested internal pathways and interactions are also highlighted, yet further experimentation would be required to reinforce these claims.

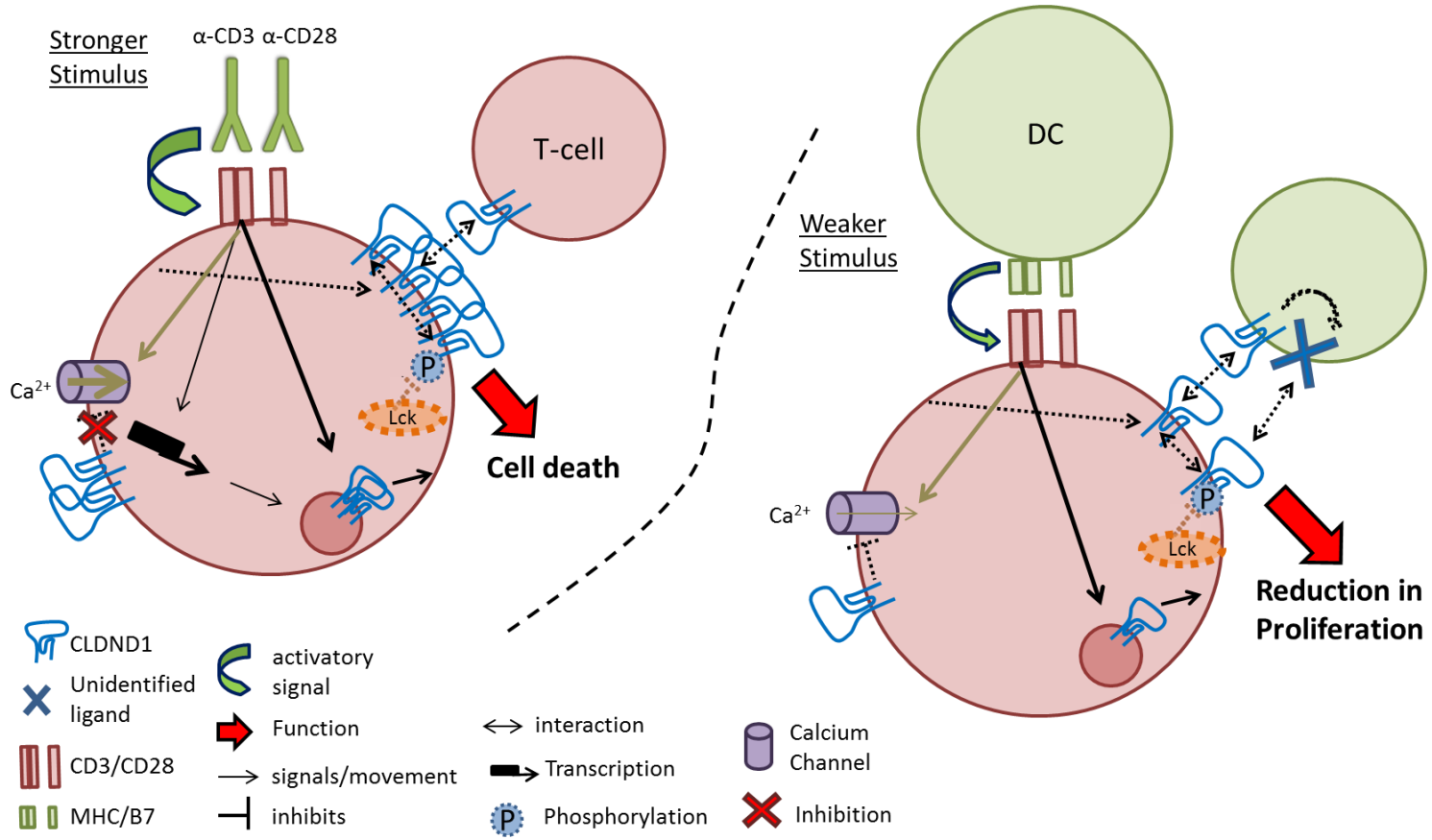

Figure 89. Proposed functional model for CLDND1 in primary human CD4+ T-cells

Depending on the type of stimulation events that occur, CLDND1 induces CD4+ T-cell death or imparts a regulatory function on the T-cell. Pathways that have been established during this thesis (shown in black) or documented in the literature (shown in brown) are indicated by solid lines. Hypothesised functions and interactions are indicated by dashed lines. Arrows of differing thicknesses identify strength of signal, with thicker bands representing a stronger signal.

Chapter 8. Future Work

8.1 Similarities to PMP-22/EMP/MP20/Claudin Superfamily Members

The homology of CLDND1 to the PMP-22/EMP/MP20/claudin superfamily has linked some potentially important findings for CLDND1 to similar findings in this group of proteins. The observation that over-expressed CLDND1 was differentially glycosylated identified similarities to TMEM114 (Maher et al., 2011), where glycosylation was important for cellular location, and to the CACNG family. Mutational analysis of the glycosylation sites in the extracellular loops of CLDND1 could be performed in conjunction with immunofluorescence microscopy, to determine whether glycosylation is also required for CLDND1 cellular localisation.

Similar cell surface expression kinetics were seen in my work with CLDND1 and with claudin-1 (Mandel et al., 2012), during T-cell activation. Although it has been suggested that CLDND1 may share more functional characteristics to the CACNG rather than the claudins, the following experiments are still worth pursuing to either strengthen this statement or to give more insight into how CLDND1 may function during T-cell signalling. Claudin-1 co-localised with the integral TJ protein ZO-1 (Mandel et al., 2012). Similarly, the mouse homologue of CLDND1 was also shown to co-localise with ZO-1 in epithelial cells (Mineta et al., 2011) so confocal microscopy of ZO-1 and CLDND1 could also indicate a TJ- like role for CLDND1 in T-cells, which may be important in cell-cell contacts, at the IS or during cell migration.

CLDND1 truncation studies suggest that the cytoplasmic C-terminal domain of CLDND1 may be important for CLDND1 function, yet these studies were limited and require further clarification. Two potential phosphorylation sites lie within this region and may be important for function, based on other PMP-22/EMP/MP20/claudin superfamily members (D'Souza et al., 2005, Aono and Hirai, 2008, Ishizaki et al., 2003, Ikari et al., 2006, Choi et al., 2002). Therefore mutational analysis of the potential phosphorylation sites could be performed to clarify whether CLDND1's function in T-cell proliferation is affected and whether CLDND1 can signal or be modulated through these potential phosphorylation sites.

Part of the C-terminal sequence of CTLA-4 provides an interaction point for the src family tyrosine kinases fyn, lyn and lck, and act as a site for phosphorylation (Miyatake et al., 1998). In addition, claudin-4 can associate with lck in human CD4+ T-cells (Kawai et al 2011) and so the potential for CLDND1 to interact with these T-cell signalling molecules could be explored. Potential interactions could be determined by co-localisation studies using confocal immunofluorescence microscopy, or through IP studies.

CLDND1 functional characteristics may be similar to the non-PDZ possessing CACNG family members, where functions range from regulating the activity of calcium channels (Sandoval et al., 2007, Hansen et al., 2004, Lin et al., 2008) to modulating AMPA receptors (Kato et al., 2008, Kato et al., 2007, Tomita et al., 2003). As AMPA receptors and calcium channels are present in human lymphocytes and can modulate T-cell function (Lombardi et al., 2001, Beyersdorf et al., 2009, Oh-hora and Rao, 2008, Gwack et al., 2008), determining whether CLDND1 also co-localises with these or similar proteins, through confocal immunofluorescence microscopy or IP studies, will help determine whether CLDND1 may play a role in calcium signalling. As a similar functional profile to CLDND1 has been seen with differential signalling through store-operated calcium channels (Qu et al., 2011), studies determining the effect of calcium signalling on CLDND1 expression and vice versa could be performed. These studies could include experiments working with calcium signalling agonists (e.g. ionomycin) or inhibitors (e.g. the non-selective Ca^{2+} channel inhibitor bepridil hydrochloride) to determine whether CLDND1 expression level changes. CLDND1-transfected cells could also be stained with Fura-2, which stains [Ca]i (Grynkiewicz et al., 1985), to determine whether calcium signalling is altered during T-cell activation.

8.2 Determining the Relationship between mRNA and Protein

An outstanding question throughout this thesis lies in whether CLDND1 RNA is a good predictor of protein expression. Replication of an ingenious experiment performed by Gulow et al., (2002) may indicate whether CLDND1 RNA and protein levels are distinct. Transfecting heterologous CLDND1 RNA into a cell line of a different species and monitoring CLDND1 RNA and protein from the host and recipient species can determine CLDND1 RNA and protein kinetics, provided each species contained unique regions in which to target for protein or

RNA analysis. There are distinct regions within the human and mouse CLDND1 transcript variant 1 sequence to allow for different probe and primer pairs to be designed, and while the mouse and human homologues of CLDND1 share 92 % sequence identity, there is a unique region in the first extracellular loop, providing a species-specific epitope.

8.3 Kinetics and Dynamics of CLDND1 Protein Expression

The potency of CLDND1 in reducing T-cell proliferation varied between experiments. This finding may indicate the importance of sorting the transfected cells into pure populations, for example using a system such as the IRES-H2K^k dual expression system (Tahvanainen et al., 2006). The percentage of CLDND1-transfected cells could also be increased by performing antibiotic resistance selection of stable transfectants or generation of CLDND1-transfected T-cell clones through viral transfection (Stevenson et al., 1986, Dardalhon et al., 2001). Generating stable transfectants by incorporating this gene into the T-cell genome followed by appropriate selection would ensure CLDND1 expression in all cells. Additionally, stable transfectants could be made using vectors expressing CLDND1 siRNA sequences to see whether CLDND1 protein could be silenced by sustained siRNA expression, in contrast to transient siRNA transfection.

8.4 Depicting Protein-Protein Interactions

In light of the differences in CLDND1 function on T-cell proliferation in response to α-CD3/CD28 expander beads or DC stimulation, DC-T-cell protein interactions could be explored. Two protein-protein interaction techniques have already been discussed (see Section 4.4.2): yeast-two hybrid screening and co-IP. Given that attempts to perform co-IP were unsuccessful with the α-CLDND1 antibody, additional native α-CLDND1-binding antibodies would need to be generated to use this technique. The yeast-two hybrid screening could still be attempted using a genomic expression system or limiting expression to potential interacting partners on the DC. Another method reliant on robust functional antibodies is antibody blocking experiments to disrupt potential interaction sites on CLDND1 acting in an agonistic or antagonistic fashion. This also requires the generation of more antibodies (see Section below). Alternatively, if interaction sites on CLDND1 were identified, blocking peptides could also be used.

8.5 Future Immunisations

I originally intended to utilise antibodies to manipulate the function of CLDND1. A function for CLDND1 in the modulation of T-cell proliferation has been suggested and so further immunisation using full length protein (see Section 3.3.7) may create an array of antibodies, which impart agonistic, neutral or antagonist effects on CLDND1 function. Subsequently, an antibody that recognises native CLDND1 can be used for live cell imaging to determine trafficking patterns and CLDND1 interactions. Additionally, this antibody could be utilised for co-IP experiments (see Section 8.4) to find potential binding partners for CLDND1.

8.6 Stimulation Strength and CLDND1 Expression

I have postulated that CLDND1 may dictate T-cell responses during activation in relation to the strength of the stimulus, in comparison to similar effects seen with Foxp3 (Brunkow et al., 2001, Hori et al., 2003, Fontenot et al., 2003, Kasprowicz et al., 2005). In order to determine whether the protein expression patterns for CLDND1 are similar to Foxp3, CLDND1-knockout mice studies could be developed, imitating the Foxp3 experiments. A CLDND1 null mouse, or if this proved embryonic lethal, a conditional knockout could be generated. Similarly, in order to depict the role of stimulation strength further, titrations of both the quantities of α-CD3/CD28 expander bead and DC stimulus would determine whether CLDND1 function is regulated in a dose dependent manner. The execution of these experiments with the potential effects from calcium signalling pathways in mind may link stimulation strength and calcium signalling to similarities to PMP-22/EMP/MP20/claudin superfamily members.

8.7 Further Work from EA Patient Samples

CLDND1 expression was shown to associate with RF status in early RA patients; however RF titres could not be correlated with CLDND1 levels. Performing *in vitro* experiments titrating RF in PBMC cultures and then assessing changes in CLDND1 protein expression would indicate a direct connection between RF and CLDND1. Developing from this hypothesised link between RF and CLDND1 cell surface expression, it was further hypothesised that complement may form the basis of this connection. Immune complexes are widely found in RA patient joints (Okroj et al., 2007) and polyclonal IgM RF can

fix and activate complement (Tanimoto et al., 1975). Complement also binds to receptors on CD4+ T-cells and DC and heightens T-cell activation (Heeger and Kemper, 2012). I have shown that CLDND1 cell surface expression is up-regulated during T-cell activation (Section 5.3.2, Figure 38), therefore elevated CLDND1 cell surface levels in RF positive early RA patients may be linked through complement, although in reality this link is likely to be more complex due to the heterogenous attributes of RF positive and negative RA disease. In order to generate a basic link between CLDND1 expression levels and complement activation, co-staining of CLDND1 and complement receptors by flow cytometry could be performed, followed by complement receptor activation studies, using complement receptor agonists (Asgari et al., 2013), to assess changes in CLDND1 expression levels.

8.8 Further Functional Studies

Ultimately, in order to study a physiological function for CLDND1 *in vivo*, an appropriate mouse model would need to be generated. The translation of CLDND1 function in a mouse model to a human system however, is dependent on a number of factors. Firstly, low mouse and human CLDND1 homology may indicate species-unique function, but the human and mouse CLDND1 proteins share high (92 %) homology (Figure 90). The sequence variations do however occur within the two extracellular loop regions, which may indicate differences in protein interactions or alternatively, may be a consequence of complementary modifications in the same potential mouse interacting partners.

```
H 1   MDNRFATAFVIACVLSLISTIYMAASIGTDFWYEYRSPVQENSSDLNKSIWDEFISDEAD 60
Hom.  MDNRFATAFVIACVLSLISTIYMAASIGTDFWYEYRSP-QENSSD-NK--W--F--DEAD
M 1   MDNRFATAFVIACVLSLISTIYMAASIGTDFWYEYRSPIQENSSDSNKIAWEDFLGDEAD 60

H 61  EKTYNDALFRYNGTVGLWRRCITIPKNMHWYSPPERTESFDVVTKCVSFTLTEQFMEKFV 120
Hom.  EKTYND-LFRYNG--GLWRRCITIPKN-HWY-PPERTESFDVVTKC-SFTL-EQFMEK-V
M 61  EKTYNDVLFRYNGSLGLWRRCITIPKNTHWYAPPERTESFDVVTKCMSFTLNEQFMEKYV 120

H 121 DPGNHNSGIDLLRTYLWRCQFLLPFVSLGLMCFGALIGLCACICRSLYPTIATGILHLLA 180
Hom.  DPGNHNSGIDLLRTYLWRCQFLLPFVSLGLMCFGALIGLCACICRSLYPT+ATGILHLLA
M 121 DPGNHNSGIDLLRTYLWRCQFLLPFVSLGLMCFGALIGLCACICRSLYPTLATGILHLLA 180

H 181 GLCTLGSVSCYVAGIELLHQKLELPDNVSGEFGWSFCLACVSAPLQFMASALFIWAAHTN 240
Hom.  GLCTLGSVSCYVAGIELLHQK-ELP--VSGEFGWSFCLACVSAPLQFMA-ALFIWAAHTN
M 181 GLCTLGSVSCYVAGIELLHQKVELPKDVSGEFGWSFCLACVSAPLQFMAAALFIWAAHTN 240

H 241 RKEYTLMKAYRVA 253
Hom.  RKEYTLMKAYRVA
M 241 RKEYTLMKAYRVA 253
```

Figure 90. Human and mouse homology of the CLDND1 protein

Human (H) and mouse (M) CLDND1 isoform A were aligned using the basic local alignment tool, with the blasp alogarithm. Underlined regions indicate transmembrane regions. The “hom.” sequence identifies identical amino acids. Mismatches are indicated by “-”.

Additionally, the type of mouse model generated must reflect the predicted consequences of CLDND1 function. If a CLDND1 null mouse proved embryonically lethal, this would suggest CLDND1 expression was essential in foetal development. A conditional or selective knockout may therefore be more suitable. There are numerous possible approaches and one example is the cre/loxP recombinase system to excise the CLDND1 gene. Two mice stains are utilised: one expresses an inducible cre recombinase and the other expresses the transgene of interest (in this case CLDND1) flanked by loxP sequences. Mating the two strains of mice allows for selective control of CLDND1 expression by inducing cre recombinase expression (Jaisser, 2000). Depending on the type of cre recombinase induction, this technique can ablate all CLDND1, or alternatively can selectively inhibit CLDND1 expression in a lymphocyte-specific manner, using a T-cell specific inducible promoter (Zhang et al., 2005) and would provide a model for determining a physiological role for CLDND1 in the immune system.

Appendix

Protein	NCBI Label
TMEM114	NP_001139808.1
TMEM235	NP_001191139.1
CLARIN-1	NP_777367.1
Claudin-1	NP_066924.1
Claudin-2	NP_065117.1
Claudin-3	NP_001297.1
Claudin-4	NP_001296.1
Claudin-5	NP_001124333.1
Claudin-6	NP_067018.2
Claudin-7	NP_001298.3
Claudin-8	NP_955360.1
Claudin-9	NP_066192.1
Claudin-10	NP_878268.1
Claudin-11	NP_005593.2
Claudin-12	NP_001172001.1
Claudin-14	NP_652763.1
Claudin-15	NP_001172009.1
Claudin-16	NP_006571.1
Claudin-17	NP_036263.1
Claudin-18	NP_057453.1
Claudin-19	NP_683763.2
Claudin-20	NP_001001346.1
Claudin-21	NP_001094859
Claudin-22	NP_001104789.1
Claudin-23	NP_919260.2
Claudin-24	NP_001172078.1
EMP-1	NP_001414.1
EMP-2	NP_001415.1
EMP-3	NP_001416.1
PMP-22	NP_000295.1

Protein	NCBI Label
MP20	NP_001155220.1
CLP24	NP_078876.2
CACNG1	NP_000718.1
CACNG2	NP_006069.1
CACNG3	NP_006530.1
CACNG4	NP_055220.1
CACNG5a	NP_665810.1
CACNG6	NP_665813.1
CACNG7	NP_114102.2
CACNG8	NP_114101.4
CLDND1 isoform A	NP_001035289.1
CLDND1 isoform B	NP_001035272
CLDND1 isoform D	NP_001035290.1
Mouse CLDND1 isoform A	NP_741968.1

Appendix Table 1. Accession numbers for all the protein sequences used through the thesis

```
v6 TATCGCCGCCTCAGACAGCTTTCAGTCTGTCCCTCCTACAACTCCCACAAGGCCCCTCGG 60
v7 TATCGCCGCCTCAGACAGCTTTCAGTCTGTCCCTCCTACAACTCCCACAAGGCCCCTCGG 60
v3 TATCGCCGCCTCAGACAGCTTTCAGTCTGTCCCTCCTACAACTCCCACAAGGCCCCTCGG 60
v1 TATCGCCGCCTCAGACAGCTTTCAGTCTGTCCCTCCTACAACTCCCACAAGGCCCCTCGG 60
v2 TATCGCCGCCTCAGACAGCTTTCAGTCTGTCCCTCCTACAACTCCCACAAGGCCCCTCGG 60
v4 TATCGCCGCCTCAGACAGCTTTCAGTCTGTCCCTCCTACAACTCCCACAAGGCCCCTCGG 60
   ************************************************************

v6 CCCCGGGCCGCGGCCCGGCCCGGAGTGGGGGCGGGCGGAGGCGCGGGAGTTATGGAGGGG 120
v7 CCCCGGGCCGCGGCCCGGCCCGGAGTGGGGGCGGGCGGAGGCGCGGGAGTTATGGAGGGG 120
v3 CCCCGGGCCGCGGCCCGGCCCGGAGTGGGGGCGGGCGGAGGCGCGGGAGTTATGGAGGGG 120
v1 CCCCGGGCCGCGGCCCGGCCCGGAGTGGGGGCGGGCGGAGGCGCGGGAGTTATGGAGGGG 120
v2 CCCCGGGCCGCGGCCCGGCCCGGAGTGGGGGCGGGCGGAGGCGCGGGAGTTATGGAGGGG 120
v4 CCCCGGGCCGCGGCCCGGCCCGGAGTGGGGGCGGGCGGAGGCGCGGGAGTTATGGAGGGG 120
   ************************************************************

v6 GCGGGCTCTGCAGGGAAGTGCGTCAGAGGAGGCGCGGGGAGAGTAGGGTGCTGTGGTCTG 180
v7 GCGGGCTCTGCAGGGAAGTGCGTCAGAGGAGGCGCGGGGAGAGTAGGGTGCTGTGGTCTG 180
v3 GCGGGCTCTGCAGGGAAGTGCGTCAGAGGAGGCGCGGGGAGAGTAGGGTGCTGTGGTCTG 180
v1 GCGGGCTCTGCAGGGAAGTGCGTCAGAGGAGGCGCGGGGAGAGTAGGGTGCTGTGGTCTG 180
v2 GCGGGCTCTGCAGGGAAGTGCGTCAGAGGAGGCGCGGGGAGAGTAGGGTGCTGTGGTCTG 180
v4 GCGGGCTCTGCAGGGAAGTGCGTCAGAGGAGGCGCGGGGAGAGTAGGGTGCTGTGGTCTG 180
   ************************************************************

v6 AGCTAGAGGGTGAAGCTGGCGGAGCAGGAGGATGGGCGGTGAGTGAGCGGGACCTGCGTC 240
v7 AGCTAGAGGGTGAAGCTGGCGGAGCAGGAGGATGGGCG---------------------- 218
v3 AGCTAGAGGGTGAAGCTGGCGGAGCAGGAGGATGGGCG---------------------- 218
v1 AGCTAGAGGGTGAAGCTGGCGGAGCAGGAGGATGGGCG---------------------- 218
v2 AGCTAGAGGGTGAAGCTGGCGGAGCAGGAGGATGGGCGTATGCAGGTGATAGACTAGAGA 240
v4 AGCTAGAGGGTGAAGCTGGCGGAGCAGGAGGATGGGCG-------GTGATAGACTAGAGA 233
   ************************************

v6 GCCGGGCAGGGGTCGCGTCGCGGTTCCATGTTCCCGGCGGTTTGAAGAGGGGCCCCCTTC 300
v7 ------------------------------------------------------------
v3 ------------------------------------------------------------
v1 ------------------------------------------------------------
v2 ACAAG-------------------------------------------------------- 245
v4 ACAAG-------------------------------------------------------- 238

v6 CCGGGCGTGGTCGGGCTGGGCGGGTTCCGAGCGGCGGATTTGTCCCAGGGCCGAGCCCTC 360
v7 ------------------------------------------------------------
v3 ------------------------------------------------------------
v1 ------------------------------------------------------------
v2 ------------------------------------------------------------
v4 ------------------------------------------------------------

v6 TAGGGCGGGGCCTGGTCGGGTACCGGGGGACCCTGGCCCGGGGCCGAGCACGGCTGCCCC 420
v7 ------------------------------------------------------------
v3 ------------------------------------------------------------
v1 ------------------------------------------------------------
v2 ------------------------------------------------------------
v4 ------------------------------------------------------------

v6 GCCCCAGCCCTGGCCTTCTCCGGCCCCGCCGTGAGGCCCAGGAGGTGGCTGCTGCAGGCG 480
v7 ------------------------------------------------------------
v3 ------------------------------------------------------------
v1 ------------------------------------------------------------
v2 ------------------------------------------------------------
v4 ------------------------------------------------------------
```

```
v6 TCCGGCTTGGACGAACCGCCGTTCCCAGTGCTGGGACCCTTTAAGAGCAGTCTGAATGCC 540
v7 ------------------------------------------------------------
v3 ----------------------------------------------TCTGAATGCC 228
v1 -------------------------------------------AGCAGTCTGAATGCC 233
v2 --------------------ACCTCTGTCTCCGTAGCATCCTGGAGCAGTCTGAATGCC 284
v4 --------------------ACCTCTGTCTCCGTAGCATCCTGGAGCAGTCTGAATGCC 277

v6 AGAATGGATAACCGTTTTGCTACAGCATTTGTAATTGCTTGTGTGCTTAGCCTCATTTCC 600
v7 ------------------------------------------------------------
v3 AGAATGGATAACCGTTTTGCTACAGCATTTGTAATTGCTTGTGTGCTTAGCCTCATTTCC 288
v1 AGAATGGATAACCGTTTTGCTACAGCATTTGTAATTGCTTGTGTGCTTAGCCTCATTTCC 293
v2 AGAATGGATAACCGTTTTGCTACAGCATTTGTAATTGCTTGTGTGCTTAGCCTCATTTCC 344
v4 AGAATGGATAACCGTTTTGCTACAGCATTTGTAATTGCTTGTGTGCTTAGCCTCATTTCC 337

v6 ACCATCTACATGGCAGCCTCCATTGGCACAGACTTCTGGTATGAATATCGAAGTCCAGTT 660
v7 ------------------------------------------------------------
v3 ACCATCTACATGGCAGCCTCCATTGGCACAGACTTCTGGTATGAATATCGAAGTCCAGTT 348
v1 ACCATCTACATGGCAGCCTCCATTGGCACAGACTTCTGGTATGAATATCGAAGTCCAGTT 353
v2 ACCATCTACATGGCAGCCTCCATTGGCACAGACTTCTGGTATGAATATCGAAGTCCAGTT 404
v4 ACCATCTACATGGCAGCCTCCATTGGCACAGACTTCTGGTATGAATATCGAAGTCCAGTT 397

v6 CAAGAAAATTCCAGTGATTTGAATAAAAGCATCTGGGATGAATTCATTAGTGATGAGGCA 720
v7 ------------------------------------------------------------
v3 CAAGAAAATTCCAGTGATTTGAATAAAAGCATCTGGGATGAATTCATTAGTGATGAGGCA 408
v1 CAAGAAAATTCCAGTGATTTGAATAAAAGCATCTGGGATGAATTCATTAGTGATGAGGCA 413
v2 CAAGAAAATTCCAGTGATTTGAATAAAAGCATCTGGGATGAATTCATTAGTGATGAGGCA 464
v4 CAAGAAAATTCCAGTGATTTGAATAAAAGCATCTGGGATGAATTCATTAGTGATGAGGCA 457

v6 GATGAAAAGACTTATAATGATGCACTTTTTCGATACAATGGCACAGTGGGATTGTGGAGA 780
v7 ------------------------------------------------------------
v3 GATGAAAAGACTTATAATGATGCACTTTTTCGATACAATGGCACAGTGGGATTGTGGAGA 468
v1 GATGAAAAGACTTATAATGATGCACTTTTTCGATACAATGGCACAGTGGGATTGTGGAGA 473
v2 GATGAAAAGACTTATAATGATGCACTTTTTCGATACAATGGCACAGTGGGATTGTGGAGA 524
v4 GATGAAAAGACTTATAATGATGCACTTTTTCGATACAATGGCACAGTGGGATTGTGGAGA 517

v6 CGGTGTATCACCATACCCAAAAACATGCATTGGTATAGCCCACCAGAAAGGACAGAGTCA  840
v7 ----------------------------------------------------AGTCA  223
v3 CGGTGTATCACCATACCCAAAAACATGCATTGGTATAGCCCACCAGAAAG**gacagagtca** 528
v1 CGGTGTATCACCATACCCAAAAACATGCATTGGTATAGCCCACCAGAAA**ggacagagtca** 533
v2 CGGTGTATCACCATACCCAAAAACATGCATTGGTATAGCCCACCAGAAAGGACAGAGTCA  584
v4 CGGTGTATCACCATACCCAAAAACATGCATTGGTATAGCCCACCAGAAAGGACAGAGTCA  577
                                                     *****

v6 TTTGATGTGGTCACAAAATGTGTGAGTTTCACACTAACTGAGCAGTTCATGGAGAAATTT 900
v7 TTTGATGTGGTCACAAAATGTGTGAGTTTCACACTAACTGAGCAGTTCATGGAGAAATTT 283
v3 TTTGATGTGGTCACAAAATGTGTGAGTTTCACACTAACTGAGCAGTTCATGGAGAAATTT 588
v1 TTTGATGTGGTCACAAAATGTGTGAGTTTCACACTAACTGAGCAGTTCATGGAGAAATTT 593
v2 TTTGATGTGGTCACAAAATGTGTGAGTTTCACACTAACTGAGCAGTTCATGGAGAAATTT 644
v4 TTTGATGTGGTCACAAAATGTGTGAGTTTCACACTAACTGAGCAGTTCATGGAGAAATTT 637
   ************************************************************
```

```
v6 GTTGATCCCGGAAACCACAATAGCGGGATTGATCTCCTTAGgacctatctttGGCGTTGC 960
v7 GTTGATCCCGGAAACCACAATAGCGGGATTGATCTCCTTAGGacctatctttgGCGTTGC 343
v3 GTTGATCCCGGAAACCACAATAGCGGGATTGATCTCCTTAGGACCTATCTTTGGCGTTGC  648
v1 GTTGATCCCGGAAACCACAATAGCGGGATTGATCTCCTTAGGACCTATCTTTGGCGTTGC  653
v2 GTTGATCCCGGAAACCACAATAGCGGGATTGATCTCCTTAGGacctatctttGGCGTTGC 704
v4 GTTGATCCCGGAAACCACAATAGCGGGATTGATCTCCTTAGGacctatctttGGCGTTGC 697
   ************************************************************

v6 CAGTTCCTTTTACCTTTTGTGAGTTTAGGTTTGATGTGCTTTGGGGCTTTGATCGGACTT 1020
v7 CAGTTCCTTTTACCTTTTGTGAGTTTAGGTTTGATGTGCTTTGGGGCTTTGATCGGACTT 403
v3 CAGTTCCTTTTACCTTTTGTGAGTTTAGGTTTGATGTGCTTTGGGGCTTTGATCGGACTT 708
v1 CAGTTCCTTTTACCTTTTGTGAGTTTAGGTTTGATGTGCTTTGGGGCTTTGATCGGACTT 713
v2 CAGTTCCTTTTACCTTTTGTGAGTTTAGGTTTGATGTGCTTTGGGGCTTTGATCGGACTT 764
v4 CAGTTCCTTTTACCTTTTGTGAGTTTAGGTTTGATGTGCTTTGGGGCTTTGATCGGACTT 757
   ************************************************************

v6 TGTGCTTGCATTTGCCGAAGCTTATATCCCACCATTGCCACGGGCATTCTCCATCTCCTT 1080
v7 TGTGCTTGCATTTGCCGAAGCTTATATCCCACCATTGCCACGGGCATTCTCCATCTCCTT 463
v3 TGTGCTTGCATTTGCCGAAGCTTATATCCCACCATTGCCACGGGCATTCTCCATCTCCTT 768
v1 TGTGCTTGCATTTGCCGAAGCTTATATCCCACCATTGCCACGGGCATTCTCCATCTCCTT 773
v2 TGTGCTTGCATTTGCCGAAGCTTATATCCCACCATTGCCACGGGCATTCTCCATCTCCTT 824
v4 TGTGCTTGCATTTGCCGAAGCTTATATCCCACCATTGCCACGGGCATTCTCCATCTCCTT 817
   ************************************************************

v6 GCAGGTCTGTGTACACTGGGCTCAGTAAGTTGTTATGTTGCTGGAATTGAACTACTCCAC 1140
v7 GCAGGTCTGTGTACACTGGGCTCAGTAAGTTGTTATGTTGCTGGAATTGAACTACTCCAC 523
v3 GCAGGTCTGTGTACACTGGGCTCAGTAAGTTGTTATGTTGCTGGAATTGAACTACTCCAC 828
v1 GCAGGTCTGTGTACACTGGGCTCAGTAAGTTGTTATGTTGCTGGAATTGAACTACTCCAC 833
v2 GCAGGTCTGTGTACACTGGGCTCAGTAAGTTGTTATGTTGCTGGAATTGAACTACTCCAC 884
v4 GCAGGTCTGTGTACACTGGGCTCAGTAAGTTGTTATGTTGCTGGAATTGAACTACTCCAC 877
   ************************************************************
                                          CLDND1 siRNA 1

v6 CAGAAACTAGAGCTCCCTGACAATGTATCCGGTGAATTTGGATGGTCCTTCTGCCTGGCT 1200
v7 CAGAAACTAGAGCTCCCTGACAATGTATCCGGTGAATTTGGATGGTCCTTCTGCCTGGCT 583
v3 CAGAAACTAGAGCTCCCTGACAATGTATCCGGTGAATTTGGATGGTCCTTCTGCCTGGCT 888
v1 CAGAAACTAGAGCTCCCTGACAATGTATCCGGTGAATTTGGATGGTCCTTCTGCCTGGCT 893
v2 CAGAAACTAGAGCTCCCTGACAATGTATCCGGTGAATTTGGATGGTCCTTCTGCCTGGCT 944
v4 CAGAAACTAGAGCTCCCTGACAATGTATCCGGTGAATTTGGATGGTCCTTCTGCCTGGCT 937
   ************************************************************
                                           CLDND1 siRNA 2

v6 TGTGTCTCTGCTCCCTTACAGTTCATGGCTTCTGCTCTCTTCATCTGGGCTGCTCACACC 1260
v7 TGTGTCTCTGCTCCCTTACAGTTCATGGCTTCTGCTCTCTTCATCTGGGCTGCTCACACC 643
v3 TGTGTCTCTGCTCCCTTACAGTTCATGGCTTCTGCTCTCTTCATCTGGGCTGCTCACACC 948
v1 TGTGTCTCTGCTCCCTTACAGTTCATGGCTTCTGCTCTCTTCATCTGGGCTGCTCACACC 953
v2 TGTGTCTCTGCTCCCTTACAGTTCATGGCTTCTGCTCTCTTCATCTGGGCTGCTCACACC 1004
v4 TGTGTCTCTGCTCCCTTACAGTTCATGGCTTCTGCTCTCTTCATCTGGGCTGCTCACACC 997
   ************************************************************

v6 AACCGGAAAGAGTACACCTTAATGAAGGCATATCGTGTGGCATGAGCAAGAAACTGCCTG 1320
v7 AACCGGAAAGAGTACACCTTAATGAAGGCATATCGTGTGGCATGAGCAAGAAACTGCCTG 703
v3 AACCGGAAAGAGTACACCTTAATGAAGGCATATCGTGTGGCATGAGCAAGAAACTGCCTG 1008
v1 AACCGGAAAGAGTACACCTTAATGAAGGCATATCGTGTGGCATGAGCAAGAAACTGCCTG 1013
v2 AACCGGAAAGAGTACACCTTAATGAAGGCATATCGTGTGGCATGAGCAAGAAACTGCCTG 1064
v4 AACCGGAAAGAGTACACCTTAATGAAGGCATATCGTGTGGCATGAGCAAGAAACTGCCTG 1057
   ************************************************************
```

```
v6 CTTTACAATTGCCATTTTTATTTTTTTAAAATAATACTGATATTTTCCCCACCTCTCAAT 1380
v7 CTTTACAATTGCCATTTTTATTTTTTTAAAATAATACTGATATTTTCCCCACCTCTCAAT 763
v3 CTTTACAATTGCCATTTTTATTTTTTTAAAATAATACTGATATTTTCCCCACCTCTCAAT 1068
v1 CTTTACAATTGCCATTTTTATTTTTTTAAAATAATACTGATATTTTCCCCACCTCTCAAT 1073
v2 CTTTACAATTGCCATTTTTATTTTTTTAAAATAATACTGATATTTTCCCCACCTCTCAAT 1124
v4 CTTTACAATTGCCATTTTTATTTTTTTAAAATAATACTGATATTTTCCCCACCTCTCAAT 1117
   ************************************************************
v6 TGTTTTTAATTTTTATTTGTGGATATACCATTTTATTATGAAAATCTATTTTATTTATAC 1440
v7 TGTTTTTAATTTTTATTTGTGGATATACCATTTTATTATGAAAATCTATTTTATTTATAC 823
v3 TGTTTTTAATTTTTATTTGTGGATATACCATTTTATTATGAAAATCTATTTTATTTATAC 1128
v1 TGTTTTTAATTTTTATTTGTGGATATACCATTTTATTATGAAAATCTATTTTATTTATAC 1133
v2 TGTTTTTAATTTTTATTTGTGGATATACCATTTTATTATGAAAATCTATTTTATTTATAC 1184
v4 TGTTTTTAATTTTTATTTGTGGATATACCATTTTATTATGAAAATCTATTTTATTTATAC 1177
   ************************************************************
v6 ACATTCACCACTAAATACACACTTAATACCACTAAAATTTATGTGGTTTACTTTAAGCGA 1500
v7 ACATTCACCACTAAATACACACTTAATACCACTAAAATTTATGTGGTTTACTTTAAGCGA 883
v3 ACATTCACCACTAAATACACACTTAATACCACTAAAATTTATGTGGTTTACTTTAAGCGA 1188
v1 ACATTCACCACTAAATACACACTTAATACCACTAAAATTTATGTGGTTTACTTTAAGCGA 1193
v2 ACATTCACCACTAAATACACACTTAATACCACTAAAATTTATGTGGTTTACTTTAAGCGA 1244
v4 ACATTCACCACTAAATACACACTTAATACCACTAAAATTTATGTGGTTTACTTTAAGCGA 1237
   ************************************************************
v6 TGCCATCTTTCAAATAAACTAATCTAGGTCTAGACAGAAAGAAATGGATAGAGACTTGAC 1560
v7 TGCCATCTTTCAAATAAACTAATCTAGGTCTAGACAGAAAGAAATGGATAGAGACTTGAC 943
v3 TGCCATCTTTCAAATAAACTAATCTAGGTCTAGACAGAAAGAAATGGATAGAGACTTGAC 1248
v1 TGCCATCTTTCAAATAAACTAATCTAGGTCTAGACAGAAAGAAATGGATAGAGACTTGAC 1253
v2 TGCCATCTTTCAAATAAACTAATCTAGGTCTAGACAGAAAGAAATGGATAGAGACTTGAC 1304
v4 TGCCATCTTTCAAATAAACTAATCTAGGTCTAGACAGAAAGAAATGGATAGAGACTTGAC 1297
   ************************************************************
v6 ACAAATTTATGAAAGAAAATTGGGAGTAGGAATGTGACCGAAAACAAGTTGTGCTAATGT 1620
v7 ACAAATTTATGAAAGAAAATTGGGAGTAGGAATGTGACCGAAAACAAGTTGTGCTAATGT 1003
v3 ACAAATTTATGAAAGAAAATTGGGAGTAGGAATGTGACCGAAAACAAGTTGTGCTAATGT 1308
v1 ACAAATTTATGAAAGAAAATTGGGAGTAGGAATGTGACCGAAAACAAGTTGTGCTAATGT 1313
v2 ACAAATTTATGAAAGAAAATTGGGAGTAGGAATGTGACCGAAAACAAGTTGTGCTAATGT 1364
v4 ACAAATTTATGAAAGAAAATTGGGAGTAGGAATGTGACCGAAAACAAGTTGTGCTAATGT 1357
   ************************************************************
v6 CTGTTAGACTTTTCAGTAAAACTAAAGTAACTGTATCTGTTCAACTAAAAACTCTATATT 1680
v7 CTGTTAGACTTTTCAGTAAAACTAAAGTAACTGTATCTGTTCAACTAAAAACTCTATATT 1063
v3 CTGTTAGACTTTTCAGTAAAACTAAAGTAACTGTATCTGTTCAACTAAAAACTCTATATT 1368
v1 CTGTTAGACTTTTCAGTAAAACTAAAGTAACTGTATCTGTTCAACTAAAAACTCTATATT 1373
v2 CTGTTAGACTTTTCAGTAAAACTAAAGTAACTGTATCTGTTCAACTAAAAACTCTATATT 1424
v4 CTGTTAGACTTTTCAGTAAAACTAAAGTAACTGTATCTGTTCAACTAAAAACTCTATATT 1417
   ************************************************************
v6 AGTTTCTTTGGGAAACCTCTCATCGTCAAAACTTTATGTTCACTTTGCTGTTGTAGATAG 1740
v7 AGTTTCTTTGGGAAACCTCTCATCGTCAAAACTTTATGTTCACTTTGCTGTTGTAGATAG 1123
v3 AGTTTCTTTGGGAAACCTCTCATCGTCAAAACTTTATGTTCACTTTGCTGTTGTAGATAG 1428
v1 AGTTTCTTTGGGAAACCTCTCATCGTCAAAACTTTATGTTCACTTTGCTGTTGTAGATAG 1433
v2 AGTTTCTTTGGGAAACCTCTCATCGTCAAAACTTTATGTTCACTTTGCTGTTGTAGATAG 1484
v4 AGTTTCTTTGGGAAACCTCTCATCGTCAAAACTTTATGTTCACTTTGCTGTTGTAGATAG 1477
   ************************************************************
v6 CCAGTCAACCAGCAGTATTAGTGCTGTTTTCAAAGATTTAAGCTCTATAAAATTGGGAAA 1800
v7 CCAGTCAACCAGCAGTATTAGTGCTGTTTTCAAAGATTTAAGCTCTATAAAATTGGGAAA 1183
v3 CCAGTCAACCAGCAGTATTAGTGCTGTTTTCAAAGATTTAAGCTCTATAAAATTGGGAAA 1488
v1 CCAGTCAACCAGCAGTATTAGTGCTGTTTTCAAAGATTTAAGCTCTATAAAATTGGGAAA 1493
v2 CCAGTCAACCAGCAGTATTAGTGCTGTTTTCAAAGATTTAAGCTCTATAAAATTGGGAAA 1544
v4 CCAGTCAACCAGCAGTATTAGTGCTGTTTTCAAAGATTTAAGCTCTATAAAATTGGGAAA 1537
   ************************************************************
```

```
v6 TTATCTAAGATCATTTTCCCTAAGCATTGACACATAGCTTCATCTGAGGTGAGATATGGC 1860
v7 TTATCTAAGATCATTTTCCCTAAGCATTGACACATAGCTTCATCTGAGGTGAGATATGGC 1243
v3 TTATCTAAGATCATTTTCCCTAAGCATTGACACATAGCTTCATCTGAGGTGAGATATGGC 1548
v1 TTATCTAAGATCATTTTCCCTAAGCATTGACACATAGCTTCATCTGAGGTGAGATATGGC 1553
v2 TTATCTAAGATCATTTTCCCTAAGCATTGACACATAGCTTCATCTGAGGTGAGATATGGC 1604
v4 TTATCTAAGATCATTTTCCCTAAGCATTGACACATAGCTTCATCTGAGGTGAGATATGGC 1597
   ************************************************************
v6 AGCTGTTTGTATCTGCACTGTGTCTGTCTACAAAAAGTGAAAAATACAGTGTTTACTTGA 1920
v7 AGCTGTTTGTATCTGCACTGTGTCTGTCTACAAAAAGTGAAAAATACAGTGTTTACTTGA 1303
v3 AGCTGTTTGTATCTGCACTGTGTCTGTCTACAAAAAGTGAAAAATACAGTGTTTACTTGA 1608
v1 AGCTGTTTGTATCTGCACTGTGTCTGTCTACAAAAAGTGAAAAATACAGTGTTTACTTGA 1613
v2 AGCTGTTTGTATCTGCACTGTGTCTGTCTACAAAAAGTGAAAAATACAGTGTTTACTTGA 1664
v4 AGCTGTTTGTATCTGCACTGTGTCTGTCTACAAAAAGTGAAAAATACAGTGTTTACTTGA 1657
   ************************************************************
v6 AATTTTAACTTTGTAACTGCAAGAATTCCAGTTCAGCCGGGCGAGGATTAGTATTATTTT 1980
v7 AATTTTAACTTTGTAACTGCAAGAATTCCAGTTCAGCCGGGCGAGGATTAGTATTATTTT 1363
v3 AATTTTAACTTTGTAACTGCAAGAATTCCAGTTCAGCCGGGCGAGGATTAGTATTATTTT 1668
v1 AATTTTAACTTTGTAACTGCAAGAATTCCAGTTCAGCCGGGCGAGGATTAGTATTATTTT 1673
v2 AATTTTAACTTTGTAACTGCAAGAATTCCAGTTCAGCCGGGCGAGGATTAGTATTATTTT 1724
v4 AATTTTAACTTTGTAACTGCAAGAATTCCAGTTCAGCCGGGCGAGGATTAGTATTATTTT 1717
   ************************************************************
v6 TAACTCTCCGTAAGATTTTCAGTACCACCAAATTGTTTTGGATTTTTTTTCTTTCCTCTT 2040
v7 TAACTCTCCGTAAGATTTTCAGTACCACCAAATTGTTTTGGATTTTTTTTCTTTCCTCTT 1423
v3 TAACTCTCCGTAAGATTTTCAGTACCACCAAATTGTTTTGGATTTTTTTTCTTTCCTCTT 1728
v1 TAACTCTCCGTAAGATTTTCAGTACCACCAAATTGTTTTGGATTTTTTTTCTTTCCTCTT 1733
v2 TAACTCTCCGTAAGATTTTCAGTACCACCAAATTGTTTTGGATTTTTTTTCTTTCCTCTT 1784
v4 TAACTCTCCGTAAGATTTTCAGTACCACCAAATTGTTTTGGATTTTTTTTCTTTCCTCTT 1777
   ************************************************************
v6 CACATACCAGGGTTATTAAAAGTGTGCTTTCTTTTTACATTATATTACAGTTACAAGGTA 2100
v7 CACATACCAGGGTTATTAAAAGTGTGCTTTCTTTTTACATTATATTACAGTTACAAGGTA 1483
v3 CACATACCAGGGTTATTAAAAGTGTGCTTTCTTTTTACATTATATTACAGTTACAAGGTA 1788
v1 CACATACCAGGGTTATTAAAAGTGTGCTTTCTTTTTACATTATATTACAGTTACAAGGTA 1793
v2 CACATACCAGGGTTATTAAAAGTGTGCTTTCTTTTTACATTATATTACAGTTACAAGGTA 1844
v4 CACATACCAGGGTTATTAAAAGTGTGCTTTCTTTTTACATTATATTACAGTTACAAGGTA 1837
   ******************************************************************
                    CLDND1 siRNA 3
v6 AAATTCCTCAACTGCTATTTATTTATTCCAGCCCAGTACTATAAAGAACGTTTCACCATA 2160
v7 AAATTCCTCAACTGCTATTTATTTATTCCAGCCCAGTACTATAAAGAACGTTTCACCATA 1543
v3 AAATTCCTCAACTGCTATTTATTTATTCCAGCCCAGTACTATAAAGAACGTTTCACCATA 1848
v1 AAATTCCTCAACTGCTATTTATTTATTCCAGCCCAGTACTATAAAGAACGTTTCACCATA 1853
v2 AAATTCCTCAACTGCTATTTATTTATTCCAGCCCAGTACTATAAAGAACGTTTCACCATA 1904
v4 AAATTCCTCAACTGCTATTTATTTATTCCAGCCCAGTACTATAAAGAACGTTTCACCATA 1897
   ************************************************************
v6 ATGACCCTCCAGAGCTGGGAAACCTACCACAAGATCTAAAGTTCTGGCTGTCCATTAACC 2220
v7 ATGACCCTCCAGAGCTGGGAAACCTACCACAAGATCTAAAGTTCTGGCTGTCCATTAACC 1603
v3 ATGACCCTCCAGAGCTGGGAAACCTACCACAAGATCTAAAGTTCTGGCTGTCCATTAACC 1908
v1 ATGACCCTCCAGAGCTGGGAAACCTACCACAAGATCTAAAGTTCTGGCTGTCCATTAACC 1913
v2 ATGACCCTCCAGAGCTGGGAAACCTACCACAAGATCTAAAGTTCTGGCTGTCCATTAACC 1964
v4 ATGACCCTCCAGAGCTGGGAAACCTACCACAAGATCTAAAGTTCTGGCTGTCCATTAACC 1957
   ************************************************************
```

```
v6 TCCAACTATGGTCTTTATTTCTTGTGGTAATATGATGTGCCTTTCCTTGCCTAAATCCCT 2280
v7 TCCAACTATGGTCTTTATTTCTTGTGGTAATATGATGTGCCTTTCCTTGCCTAAATCCCT 1663
v3 TCCAACTATGGTCTTTATTTCTTGTGGTAATATGATGTGCCTTTCCTTGCCTAAATCCCT 1968
v1 TCCAACTATGGTCTTTATTTCTTGTGGTAATATGATGTGCCTTTCCTTGCCTAAATCCCT 1973
v2 TCCAACTATGGTCTTTATTTCTTGTGGTAATATGATGTGCCTTTCCTTGCCTAAATCCCT 2024
v4 TCCAACTATGGTCTTTATTTCTTGTGGTAATATGATGTGCCTTTCCTTGCCTAAATCCCT 2017
   ************************************************************

v6 TCCTGGTGTGTATCAACATTATTTAATGTCTTCTAATTCAGTCATTTTTTTATAAGTATG 2340
v7 TCCTGGTGTGTATCAACATTATTTAATGTCTTCTAATTCAGTCATTTTTTTATAAGTATG 1723
v3 TCCTGGTGTGTATCAACATTATTTAATGTCTTCTAATTCAGTCATTTTTTTATAAGTATG 2028
v1 TCCTGGTGTGTATCAACATTATTTAATGTCTTCTAATTCAGTCATTTTTTTATAAGTATG 2033
v2 TCCTGGTGTGTATCAACATTATTTAATGTCTTCTAATTCAGTCATTTTTTTATAAGTATG 2084
v4 TCCTGGTGTGTATCAACATTATTTAATGTCTTCTAATTCAGTCATTTTTTTATAAGTATG 2077
   **********************************************************

               CLDND1 siRNA 4

v6 TCTATAAACATTGAACTTTAAAAAACTTATTTATTTATTCCACTACTGTAGCAATTGACA 2400
v7 TCTATAAACATTGAACTTTAAAAAACTTATTTATTTATTCCACTACTGTAGCAATTGACA 1783
v3 TCTATAAACATTGAACTTTAAAAAACTTATTTATTTATTCCACTACTGTAGCAATTGACA 2088
v1 TCTATAAACATTGAACTTTAAAAAACTTATTTATTTATTCCACTACTGTAGCAATTGACA 2093
v2 TCTATAAACATTGAACTTTAAAAAACTTATTTATTTATTCCACTACTGTAGCAATTGACA 2144
v4 TCTATAAACATTGAACTTTAAAAAACTTATTTATTTATTCCACTACTGTAGCAATTGACA 2137
   ************************************************************

v6 GATTAAAAAAATGTAACTTCATAATTTCTTACCATAACCTCAATGTCTTTTTTAAAAAAT 2460
v7 GATTAAAAAAATGTAACTTCATAATTTCTTACCATAACCTCAATGTCTTTTTTAAAAAAT 1843
v3 GATTAAAAAAATGTAACTTCATAATTTCTTACCATAACCTCAATGTCTTTTTTAAAAAAT 2148
v1 GATTAAAAAAATGTAACTTCATAATTTCTTACCATAACCTCAATGTCTTTTTTAAAAAAT 2153
v2 GATTAAAAAAATGTAACTTCATAATTTCTTACCATAACCTCAATGTCTTTTTTAAAAAAT 2204
v4 GATTAAAAAAATGTAACTTCATAATTTCTTACCATAACCTCAATGTCTTTTTTAAAAAAT 2197
         ************************************************************

v6 AAAATTAAAAATGAAAAGAGACTCAATTGTAAAAAAAAAA 2500
v7 AAAATTAAAAATGAAAAGAGACTCAATTGTAAAAAAAAAA 1883
v3 AAAATTAAAAATGAAAAGAGACTCAATTGTAAAAAAAAAA 2188
v1 AAAATTAAAAATGAAAAGAGACTCAATTGTAAAAAAAAAA 2193
v2 AAAATTAAAAATGAAAAGAGACTCAATTGTAAAAAAAAAA 2244
v4 AAAATTAAAAATGAAAAGAGACTCAATTGTAAAAAAAAAA 2237
```

Appendix Figure 1. Accell CLDND1 siRNA and CLDND1 Taqman assay binding

The 6 CLDND1 transcripts were aligned using clustalW2 (EBI). CLDND1 ORF are highlighted with the boxed regions. Underlined regions represent where each CLDND1 siRNA binds. Lower-case bold letters indicate the exon junction where the CLDND1 taqman assay for qRT-PCR binds.

References

ALBERDI, E., SANCHEZ-GOMEZ, M. V. & MATUTE, C. 2005. Calcium and glial cell death. *Cell Calcium,* 38**,** 417-25.

ALI, M., PONCHEL, F., WILSON, K. E., FRANCIS, M. J., WU, X., VERHOEF, A., BOYLSTON, A. W., VEALE, D. J., EMERY, P., MARKHAM, A. F., LAMB, J. R. & ISAACS, J. D. 2001. Rheumatoid arthritis synovial T cells regulate transcription of several genes associated with antigen-induced anergy. *J Clin Invest,* 107**,** 519-28.

ALLER, E., JAIJO, T., OLTRA, S., ALIO, J., GALAN, F., NAJERA, C., BENEYTO, M. & MILLAN, J. M. 2004. Mutation screening of USH3 gene (clarin-1) in Spanish patients with Usher syndrome: low prevalence and phenotypic variability. *Clin Genet,* 66**,** 525-9.

ANDERSON, A. E., SAYERS, B. L., HANIFFA, M. A., SWAN, D. J., DIBOLL, J., WANG, X. N., ISAACS, J. D. & HILKENS, C. M. 2008. Differential regulation of naive and memory CD4+ T cells by alternatively activated dendritic cells. *J Leukoc Biol,* 84**,** 124-33.

ANGELOW, S., AHLSTROM, R. & YU, A. S. 2008. Biology of claudins. *Am J Physiol Renal Physiol,* 295**,** F867-76.

ANGELOW, S., EL-HUSSEINI, R., KANZAWA, S. A. & YU, A. S. 2007. Renal localization and function of the tight junction protein, claudin-19. *Am J Physiol Renal Physiol,* 293**,** F166-77.

AONO, S. & HIRAI, Y. 2008. Phosphorylation of claudin-4 is required for tight junction formation in a human keratinocyte cell line. *Exp Cell Res,* 314**,** 3326-39.

APETOH, L., QUINTANA, F. J., POT, C., JOLLER, N., XIAO, S., KUMAR, D., BURNS, E. J., SHERR, D. H., WEINER, H. L. & KUCHROO, V. K. 2010. The aryl hydrocarbon receptor interacts with c-Maf to promote the differentiation of type 1 regulatory T cells induced by IL-27. *Nat Immunol,* 11**,** 854-61.

ASGARI, E., LE FRIEC, G., YAMAMOTO, H., PERUCHA, E., SACKS, S. S., KOHL, J., COOK, H. T. & KEMPER, C. 2013. C3a modulates IL-1beta secretion in human monocytes by regulating ATP efflux and subsequent NLRP3 inflammasome activation. *Blood*.

AYACHE, S., PANELLI, M. C., BYRNE, K. M., SLEZAK, S., LEITMAN, S. F., MARINCOLA, F. M. & STRONCEK, D. F. 2006. Comparison of proteomic profiles of serum, plasma, and modified media supplements used for cell culture and expansion. *J Transl Med,* 4**,** 40.

BARRA, L., BYKERK, V., POPE, J. E., HARAOUI, B. P., HITCHON, C. A., THORNE, J. C., KEYSTONE, E. C. & BOIRE, G. 2013. Anticitrullinated Protein Antibodies and Rheumatoid Factor Fluctuate in Early Inflammatory Arthritis and Do Not Predict Clinical Outcomes. *J Rheumatol,* 40**,** 1259-1267.

BEENHOUWER, D. O., YOO, E. M., LAI, C. W., ROCHA, M. A. & MORRISON, S. L. 2007. Human immunoglobulin G2 (IgG2) and IgG4, but not IgG1 or IgG3, protect mice against Cryptococcus neoformans infection. *Infect Immun,* 75**,** 1424-35.

BEINEKE, P., FITCH, K., TAO, H., ELASHOFF, M. R., ROSENBERG, S., KRAUS, W. E. & WINGROVE, J. A. 2012. A whole blood gene expression-based signature for smoking status. *BMC Med Genomics,* 5**,** 58.

BEN-PORATH, I. & BENVENISTY, N. 1996. Characterization of a tumor-associated gene, a member of a novel family of genes encoding membrane glycoproteins. *Gene,* 183**,** 69-75.

BEYERSDORF, N., BRAUN, A., VOGTLE, T., VARGA-SZABO, D., GALDOS, R. R., KISSLER, S., KERKAU, T. & NIESWANDT, B. 2009. STIM1-independent T cell development and effector function in vivo. *J Immunol,* 182**,** 3390-7.

BIROUK, N., GOUIDER, R., LE GUERN, E., GUGENHEIM, M., TARDIEU, S., MAISONOBE, T., LE FORESTIER, N., AGID, Y., BRICE, A. & BOUCHE, P. 1997. Charcot-Marie-Tooth disease type 1A with 17p11.2 duplication. Clinical and electrophysiological phenotype study and factors influencing disease severity in 119 cases. *Brain,* 120 (Pt 5)**,** 813-23.

BRANCOLINI, C., EDOMI, P., MARZINOTTO, S. & SCHNEIDER, C. 2000. Exposure at the cell surface is required for gas3/PMP-22 To regulate both cell death and cell spreading: implication for the Charcot-Marie-Tooth type 1A and Dejerine-Sottas diseases. *Mol Biol Cell,* 11**,** 2901-14.

BREEDVELD, F. C. & VERWEIJ, C. L. 1997. T cells in rheumatoid arthritis. *Br J Rheumatol,* 36**,** 617-9.

BRUNKOW, M. E., JEFFERY, E. W., HJERRILD, K. A., PAEPER, B., CLARK, L. B., YASAYKO, S. A., WILKINSON, J. E., GALAS, D., ZIEGLER, S. F. & RAMSDELL, F. 2001. Disruption of a new forkhead/winged-helix protein, scurfin, results in the fatal lymphoproliferative disorder of the scurfy mouse. *Nat Genet,* 27**,** 68-73.

CARRUTHERS, D. M., NAYLOR, W. G., ALLEN, M. E., KITAS, G. D., BACON, P. A. & YOUNG, S. P. 1996. Characterization of altered calcium signalling in T lymphocytes from patients with rheumatoid arthritis (RA). *Clin Exp Immunol,* 105**,** 291-6.

CATTERALL, W. A., STRIESSNIG, J., SNUTCH, T. P., PEREZ-REYES, E. & INTERNATIONAL UNION OF, P. 2003. International Union of Pharmacology. XL. Compendium of voltage-gated ion channels: calcium channels. *Pharmacol Rev,* 55**,** 579-81.

CHAMORRO, S., GARCIA-VALLEJO, J. J., UNGER, W. W., FERNANDES, R. J., BRUIJNS, S. C., LABAN, S., ROEP, B. O., T HART, B. A. & VAN KOOYK, Y. 2009. TLR triggering on tolerogenic dendritic cells results in TLR2 up-regulation and a reduced proinflammatory immune program. *J Immunol,* 183**,** 2984-94.

CHARLESWORTH, J. C., CURRAN, J. E., JOHNSON, M. P., GORING, H. H., DYER, T. D., DIEGO, V. P., KENT, J. W., JR., MAHANEY, M. C., ALMASY, L., MACCLUER, J. W., MOSES, E. K. & BLANGERO, J. 2010. Transcriptomic epidemiology of smoking: the effect of smoking on gene expression in lymphocytes. *BMC Med Genomics,* 3**,** 29.

CHEN, R. S., DENG, T. C., GARCIA, T., SELLERS, Z. M. & BEST, P. M. 2007. Calcium channel gamma subunits: a functionally diverse protein family. *Cell Biochem Biophys,* 47**,** 178-86.

CHEN, Y., MEDVEDEV, A., RUZANOV, P., MARVIN, K. W. & JETTEN, A. M. 1997. cDNA cloning, genomic structure, and chromosome mapping of the human epithelial membrane protein CL-20 gene (EMP1), a member of the PMP-22 family. *Genomics,* 41**,** 40-8.

CHENG, C., BHARDWAJ, N. & GERSTEIN, M. 2009. The relationship between the evolution of microRNA targets and the length of their UTRs. *BMC Genomics,* 10**,** 431.

CHIODETTI, L., CHOI, S., BARBER, D. L. & SCHWARTZ, R. H. 2006. Adaptive tolerance and clonal anergy are distinct biochemical states. *J Immunol,* 176**,** 2279-91.

CHOI, J., KO, J., PARK, E., LEE, J. R., YOON, J., LIM, S. & KIM, E. 2002. Phosphorylation of stargazin by protein kinase A regulates its interaction with PSD-95. *J Biol Chem,* 277**,** 12359-63.

CHOI, J. M., KIM, H. J., LEE, K. Y., CHOI, H. J., LEE, I. S. & KANG, B. Y. 2009. Increased IL-2 production in T cells by xanthohumol through enhanced NF-AT and AP-1 activity. *Int Immunopharmacol,* 9**,** 103-7.

CHOI, S. & SCHWARTZ, R. H. 2007. Molecular mechanisms for adaptive tolerance and other T cell anergy models. *Semin Immunol,* 19**,** 140-52.

CHOY, E. 2012. Understanding the dynamics: pathways involved in the pathogenesis of rheumatoid arthritis. *Rheumatology (Oxford),* 51 Suppl 5**,** v3-11.

CHU, W. M. 2013. Tumor necrosis factor. *Cancer Lett,* 328**,** 222-5.

COOLES, F. A., ISAACS, J. D. & ANDERSON, A. E. 2013. Treg cells in rheumatoid arthritis: an update. *Curr Rheumatol Rep,* 15**,** 352.

COPE, A. P., LIBLAU, R. S., YANG, X. D., CONGIA, M., LAUDANNA, C., SCHREIBER, R. D., PROBERT, L., KOLLIAS, G. & MCDEVITT, H. O. 1997. Chronic tumor necrosis factor alters T cell responses by attenuating T cell receptor signaling. *J Exp Med,* 185**,** 1573-84.

CURTSINGER, J. M. & MESCHER, M. F. 2010. Inflammatory cytokines as a third signal for T cell activation. *Curr Opin Immunol,* 22**,** 333-40.

CUSH, J. J. & LIPSKY, P. E. 1988. Phenotypic analysis of synovial tissue and peripheral blood lymphocytes isolated from patients with rheumatoid arthritis. *Arthritis Rheum,* 31**,** 1230-8.

D'SOUZA, T., AGARWAL, R. & MORIN, P. J. 2005. Phosphorylation of claudin-3 at threonine 192 by cAMP-dependent protein kinase regulates tight junction barrier function in ovarian cancer cells. *J Biol Chem,* 280**,** 26233-40.

DACOSTA BYFIELD, S., MAJOR, C., LAPING, N. J. & ROBERTS, A. B. 2004. SB-505124 is a selective inhibitor of transforming growth factor-beta type I receptors ALK4, ALK5, and ALK7. *Mol Pharmacol,* 65**,** 744-52.

DANIELSEN, J. M., SYLVESTERSEN, K. B., BEKKER-JENSEN, S., SZKLARCZYK, D., POULSEN, J. W., HORN, H., JENSEN, L. J.,

MAILAND, N. & NIELSEN, M. L. 2011. Mass spectrometric analysis of lysine ubiquitylation reveals promiscuity at site level. *Mol Cell Proteomics,* 10**,** M110 003590.

DARDALHON, V., HERPERS, B., NORAZ, N., PFLUMIO, F., GUETARD, D., LEVEAU, C., DUBART-KUPPERSCHMITT, A., CHARNEAU, P. & TAYLOR, N. 2001. Lentivirus-mediated gene transfer in primary T cells is enhanced by a central DNA flap. *Gene Ther,* 8**,** 190-8.

DATTA, H. K., NG, W. F., WALKER, J. A., TUCK, S. P. & VARANASI, S. S. 2008. The cell biology of bone metabolism. *J Clin Pathol,* 61**,** 577-87.

DAVIES, J. K., BARBON, C. M., VOSKERTCHIAN, A. R., NADLER, L. M. & GUINAN, E. C. 2011. Induction of alloantigen-specific anergy in human peripheral blood mononuclear cells by alloantigen stimulation with co-stimulatory signal blockade. *J Vis Exp*.

DEBENEDETTE, M. A., SHAHINIAN, A., MAK, T. W. & WATTS, T. H. 1997. Costimulation of CD28- T lymphocytes by 4-1BB ligand. *J Immunol,* 158**,** 551-9.

DELISLE, J. S., GIROUX, M., BOUCHER, G., LANDRY, J. R., HARDY, M. P., LEMIEUX, S., JONES, R. G., WILHELM, B. T. & PERREAULT, C. 2013. The TGF-beta-Smad3 pathway inhibits CD28-dependent cell growth and proliferation of CD4 T cells. *Genes Immun,* 14**,** 115-26.

DESILVA, D. R., FEESER, W. S., TANCULA, E. J. & SCHERLE, P. A. 1996. Anergic T cells are defective in both jun NH2-terminal kinase and mitogen-activated protein kinase signaling pathways. *J Exp Med,* 183**,** 2017-23.

DUSTIN, M. L., CHAKRABORTY, A. K. & SHAW, A. S. 2010. Understanding the structure and function of the immunological synapse. *Cold Spring Harb Perspect Biol,* 2**,** a002311.

EBERST, R., DAI, S., KLUGBAUER, N. & HOFMANN, F. 1997. Identification and functional characterization of a calcium channel gamma subunit. *Pflugers Arch,* 433**,** 633-7.

EBINU, J. O., BOTTORFF, D. A., CHAN, E. Y., STANG, S. L., DUNN, R. J. & STONE, J. C. 1998. RasGRP, a Ras guanyl nucleotide- releasing protein with calcium- and diacylglycerol-binding motifs. *Science,* 280**,** 1082-6.

EDWARDS, J. C. & CAMBRIDGE, G. 2006. B-cell targeting in rheumatoid arthritis and other autoimmune diseases. *Nat Rev Immunol,* 6**,** 394-403.

ELBASHIR, S. M., HARBORTH, J., LENDECKEL, W., YALCIN, A., WEBER, K. & TUSCHL, T. 2001. Duplexes of 21-nucleotide RNAs mediate RNA interference in cultured mammalian cells. *Nature,* 411**,** 494-8.

EMERY, P. 1994. The Roche Rheumatology Prize Lecture. The optimal management of early rheumatoid disease: the key to preventing disability. *Br J Rheumatol,* 33**,** 765-8.

FABBRETTI, E., EDOMI, P., BRANCOLINI, C. & SCHNEIDER, C. 1995. Apoptotic phenotype induced by overexpression of wild-type gas3/PMP-22: its relation to the demyelinating peripheral neuropathy CMT1A. *Genes Dev,* 9**,** 1846-56.

FAYEIN, N. A., STANKOFF, B., AUFFRAY, C. & DEVIGNES, M. D. 2002. Characterization of tissue expression and full-length coding sequence of a novel human gene mapping at 3q12.1 and transcribed in oligodendrocytes. *Gene,* 289**,** 119-29.

FIELDS, P. E., GAJEWSKI, T. F. & FITCH, F. W. 1996. Blocked Ras activation in anergic CD4+ T cells. *Science,* 271**,** 1276-8.

FIFE, B. T., PAUKEN, K. E., EAGAR, T. N., OBU, T., WU, J., TANG, Q., AZUMA, M., KRUMMEL, M. F. & BLUESTONE, J. A. 2009. Interactions between PD-1 and PD-L1 promote tolerance by blocking the TCR-induced stop signal. *Nat Immunol,* 10**,** 1185-92.

FINDLEY, M. K. & KOVAL, M. 2009. Regulation and roles for claudin-family tight junction proteins. *IUBMB Life,* 61**,** 431-7.

FONTENOT, J. D., GAVIN, M. A. & RUDENSKY, A. Y. 2003. Foxp3 programs the development and function of CD4+CD25+ regulatory T cells. *Nat Immunol,* 4**,** 330-6.

FOWLER, C. B., EVERS, D. L., O'LEARY, T. J. & MASON, J. T. 2011. Antigen retrieval causes protein unfolding: evidence for a linear epitope model of recovered immunoreactivity. *J Histochem Cytochem,* 59**,** 366-81.

FOX, D. A. 1997. The role of T cells in the immunopathogenesis of rheumatoid arthritis: new perspectives. *Arthritis Rheum,* 40**,** 598-609.

FREEMAN, G. J., LONG, A. J., IWAI, Y., BOURQUE, K., CHERNOVA, T., NISHIMURA, H., FITZ, L. J., MALENKOVICH, N., OKAZAKI, T., BYRNE, M. C., HORTON, H. F., FOUSER, L., CARTER, L., LING, V., BOWMAN, M. R., CARRENO, B. M., COLLINS, M., WOOD, C. R. & HONJO, T. 2000. Engagement of the PD-1 immunoinhibitory receptor by a novel B7

family member leads to negative regulation of lymphocyte activation. *J Exp Med,* 192**,** 1027-34.

FREISE, D., HELD, B., WISSENBACH, U., PFEIFER, A., TROST, C., HIMMERKUS, N., SCHWEIG, U., FREICHEL, M., BIEL, M., HOFMANN, F., HOTH, M. & FLOCKERZI, V. 2000. Absence of the gamma subunit of the skeletal muscle dihydropyridine receptor increases L-type Ca2+ currents and alters channel inactivation properties. *J Biol Chem,* 275**,** 14476-81.

FRITSCHY, J. M. 2008. Is my antibody-staining specific? How to deal with pitfalls of immunohistochemistry. *Eur J Neurosci,* 28**,** 2365-70.

FURUSE, M., FUJITA, K., HIIRAGI, T., FUJIMOTO, K. & TSUKITA, S. 1998. Claudin-1 and -2: novel integral membrane proteins localizing at tight junctions with no sequence similarity to occludin. *J Cell Biol,* 141**,** 1539-50.

GALVAN, A., LAMPE, P. D., HUR, K. C., HOWARD, J. B., ECCLESTON, E. D., ARNESON, M. & LOUIS, C. F. 1989. Structural organization of the lens fiber cell plasma membrane protein MP18. *J Biol Chem,* 264**,** 19974-8.

GIANCHECCHI, E., DELFINO, D. V. & FIERABRACCI, A. 2013. Recent insights into the role of the PD-1/PD-L1 pathway in immunological tolerance and autoimmunity. *Autoimmun Rev,* 12**,** 1091-100.

GOLDRING, M. B. & MARCU, K. B. 2009. Cartilage homeostasis in health and rheumatic diseases. *Arthritis Res Ther,* 11**,** 224.

GOMEZ-VALADES, A. G., LLAMAS, M., BLANCH, S., PERALES, J. C., ROMAN, J., GOMEZ-CASAJUS, L. & MASCARO, C. 2012. Specific Jak3 Downregulation in Lymphocytes Impairs gammac Cytokine Signal Transduction and Alleviates Antigen-driven Inflammation In Vivo. *Mol Ther Nucleic Acids,* 1**,** e42.

GORELIK, L. & FLAVELL, R. A. 2002. Transforming growth factor-beta in T-cell biology. *Nat Rev Immunol,* 2**,** 46-53.

GORENTLA, B. K., WAN, C. K. & ZHONG, X. P. 2011. Negative regulation of mTOR activation by diacylglycerol kinases. *Blood,* 117**,** 4022-31.

GREENBAUM, D., COLANGELO, C., WILLIAMS, K. & GERSTEIN, M. 2003. Comparing protein abundance and mRNA expression levels on a genomic scale. *Genome Biol,* 4**,** 117.

GREENWALD, R. J., BOUSSIOTIS, V. A., LORSBACH, R. B., ABBAS, A. K. & SHARPE, A. H. 2001. CTLA-4 regulates induction of anergy in vivo. *Immunity,* 14**,** 145-55.

GREWAL, I. S., XU, J. & FLAVELL, R. A. 1995. Impairment of antigen-specific T-cell priming in mice lacking CD40 ligand. *Nature,* 378**,** 617-20.

GREY, A. C., JACOBS, M. D., GONEN, T., KISTLER, J. & DONALDSON, P. J. 2003. Insertion of MP20 into lens fibre cell plasma membranes correlates with the formation of an extracellular diffusion barrier. *Exp Eye Res,* 77**,** 567-74.

GRYNKIEWICZ, G., POENIE, M. & TSIEN, R. Y. 1985. A new generation of Ca2+ indicators with greatly improved fluorescence properties. *J Biol Chem,* 260**,** 3440-50.

GULOW, K., BIENERT, D. & HAAS, I. G. 2002. BiP is feed-back regulated by control of protein translation efficiency. *J Cell Sci,* 115**,** 2443-52.

GUO, Y., XIAO, P., LEI, S., DENG, F., XIAO, G. G., LIU, Y., CHEN, X., LI, L., WU, S., CHEN, Y., JIANG, H., TAN, L., XIE, J., ZHU, X., LIANG, S. & DENG, H. 2008. How is mRNA expression predictive for protein expression? A correlation study on human circulating monocytes. *Acta Biochim Biophys Sin (Shanghai),* 40**,** 426-36.

GWACK, Y., SRIKANTH, S., OH-HORA, M., HOGAN, P. G., LAMPERTI, E. D., YAMASHITA, M., GELINAS, C., NEEMS, D. S., SASAKI, Y., FESKE, S., PRAKRIYA, M., RAJEWSKY, K. & RAO, A. 2008. Hair loss and defective T- and B-cell function in mice lacking ORAI1. *Mol Cell Biol,* 28**,** 5209-22.

HANSEN, J. P., CHEN, R. S., LARSEN, J. K., CHU, P. J., JANES, D. M., WEIS, K. E. & BEST, P. M. 2004. Calcium channel gamma6 subunits are unique modulators of low voltage-activated (Cav3.1) calcium current. *J Mol Cell Cardiol,* 37**,** 1147-58.

HAO, N., LEE, K. L., FURNESS, S. G., BOSDOTTER, C., POELLINGER, L. & WHITELAW, M. L. 2012. Xenobiotics and loss of cell adhesion drive distinct transcriptional outcomes by aryl hydrocarbon receptor signaling. *Mol Pharmacol,* 82**,** 1082-93.

HARRY, R. A., ANDERSON, A. E., ISAACS, J. D. & HILKENS, C. M. 2010. Generation and characterisation of therapeutic tolerogenic dendritic cells for rheumatoid arthritis. *Ann Rheum Dis,* 69**,** 2042-50.

HATACHI, S., IWAI, Y., KAWANO, S., MORINOBU, S., KOBAYASHI, M., KOSHIBA, M., SAURA, R., KUROSAKA, M., HONJO, T. & KUMAGAI, S. 2003. CD4+ PD-1+ T cells accumulate as unique anergic cells in rheumatoid arthritis synovial fluid. *J Rheumatol,* 30**,** 1410-9.

HEEGER, P. S. & KEMPER, C. 2012. Novel roles of complement in T effector cell regulation. *Immunobiology,* 217**,** 216-24.

HEIBER, J. F. & GEIGER, T. L. 2012. Context and location dependence of adaptive Foxp3(+) regulatory T cell formation during immunopathological conditions. *Cell Immunol,* 279**,** 60-5.

HEISSMEYER, V., MACIAN, F., IM, S. H., VARMA, R., FESKE, S., VENUPRASAD, K., GU, H., LIU, Y. C., DUSTIN, M. L. & RAO, A. 2004. Calcineurin imposes T cell unresponsiveness through targeted proteolysis of signaling proteins. *Nat Immunol,* 5**,** 255-65.

HERBERT, M., COPPIETERS, N., LASHAM, A., CAO, H. & REID, G. 2011. The importance of RT-qPCR primer design for the detection of siRNA-mediated mRNA silencing. *BMC Res Notes,* 4**,** 148.

HIRAHARA, K., POHOLEK, A., VAHEDI, G., LAURENCE, A., KANNO, Y., MILNER, J. D. & O'SHEA, J. J. 2013. Mechanisms underlying helper T-cell plasticity: implications for immune-mediated disease. *J Allergy Clin Immunol,* 131**,** 1276-87.

HOLMES, K., WILLIAMS, C. M., CHAPMAN, E. A. & CROSS, M. J. 2010. Detection of siRNA induced mRNA silencing by RT-qPCR: considerations for experimental design. *BMC Res Notes,* 3**,** 53.

HORI, S., NOMURA, T. & SAKAGUCHI, S. 2003. Control of regulatory T cell development by the transcription factor Foxp3. *Science,* 299**,** 1057-61.

HOVES, S., KRAUSE, S. W., SCHUTZ, C., HALBRITTER, D., SCHOLMERICH, J., HERFARTH, H. & FLECK, M. 2006. Monocyte-derived human macrophages mediate anergy in allogeneic T cells and induce regulatory T cells. *J Immunol,* 177**,** 2691-8.

HTTP://WWW.SYSTEMSIMMUNOLOGY.ORG/. no date. *Human Correlation Data* [Online]. Institute for Systems Biology. Available: http://www.systemsimmunology.org/cores/human_correlation_data.html [Accessed 04/09 2013].

HUI, A. Y., MCCARTY, W. J., MASUDA, K., FIRESTEIN, G. S. & SAH, R. L. 2012. A systems biology approach to synovial joint lubrication in health, injury, and disease. *Wiley Interdiscip Rev Syst Biol Med,* 4**,** 15-37.

IANNONE, F., CORRIGALL, V. M., KINGSLEY, G. H. & PANAYI, G. S. 1994. Evidence for the continuous recruitment and activation of T cells into the joints of patients with rheumatoid arthritis. *Eur J Immunol,* 24**,** 2706-13.

IKARI, A., MATSUMOTO, S., HARADA, H., TAKAGI, K., HAYASHI, H., SUZUKI, Y., DEGAWA, M. & MIWA, M. 2006. Phosphorylation of paracellin-1 at Ser217 by protein kinase A is essential for localization in tight junctions. *J Cell Sci,* 119**,** 1781-9.

ISHIZAKI, T., CHIBA, H., KOJIMA, T., FUJIBE, M., SOMA, T., MIYAJIMA, H., NAGASAWA, K., WADA, I. & SAWADA, N. 2003. Cyclic AMP induces phosphorylation of claudin-5 immunoprecipitates and expression of claudin-5 gene in blood-brain-barrier endothelial cells via protein kinase A-dependent and -independent pathways. *Exp Cell Res,* 290**,** 275-88.

ITOH, M., FURUSE, M., MORITA, K., KUBOTA, K., SAITOU, M. & TSUKITA, S. 1999. Direct binding of three tight junction-associated MAGUKs, ZO-1, ZO-2, and ZO-3, with the COOH termini of claudins. *J Cell Biol,* 147**,** 1351-63.

JAISSER, F. 2000. Inducible gene expression and gene modification in transgenic mice. *J Am Soc Nephrol,* 11 Suppl 16**,** S95-S100.

JAMIESON, R. V., FARRAR, N., STEWART, K., PERVEEN, R., MIHELEC, M., CARETTE, M., GRIGG, J. R., MCAVOY, J. W., LOVICU, F. J., TAM, P. P., SCAMBLER, P., LLOYD, I. C., DONNAI, D. & BLACK, G. C. 2007. Characterization of a familial t(16;22) balanced translocation associated with congenital cataract leads to identification of a novel gene, TMEM114, expressed in the lens and disrupted by the translocation. *Hum Mutat,* 28**,** 968-77.

JANEWAY, C. A., TRAVERS, P., WALPORT, M. & SHLOMCHIK, M. J. 2001. *Immunobiology: The Immune System in Health and Disease* New York: Garland Science.

JONK, L. J., ITOH, S., HELDIN, C. H., TEN DIJKE, P. & KRUIJER, W. 1998. Identification and functional characterization of a Smad binding element (SBE) in the JunB promoter that acts as a transforming growth factor-

beta, activin, and bone morphogenetic protein-inducible enhancer. *J Biol Chem,* 273**,** 21145-52.

JONULEIT, H., SCHMITT, E., STEINBRINK, K. & ENK, A. H. 2001. Dendritic cells as a tool to induce anergic and regulatory T cells. *Trends Immunol,* 22**,** 394-400.

KALERGIS, A. M. 2003. Modulation of T cell immunity by TCR/pMHC dwell time and activating/inhibitory receptor pairs on the antigen-presenting cell. *Curr Pharm Des,* 9**,** 233-44.

KANG, S. M., BEVERLY, B., TRAN, A. C., BRORSON, K., SCHWARTZ, R. H. & LENARDO, M. J. 1992. Transactivation by AP-1 is a molecular target of T cell clonal anergy. *Science,* 257**,** 1134-8.

KASPROWICZ, D. J., DROIN, N., SOPER, D. M., RAMSDELL, F., GREEN, D. R. & ZIEGLER, S. F. 2005. Dynamic regulation of FoxP3 expression controls the balance between CD4+ T cell activation and cell death. *Eur J Immunol,* 35**,** 3424-32.

KATO, A. S., SIUDA, E. R., NISENBAUM, E. S. & BREDT, D. S. 2008. AMPA receptor subunit-specific regulation by a distinct family of type II TARPs. *Neuron,* 59**,** 986-96.

KATO, A. S., ZHOU, W., MILSTEIN, A. D., KNIERMAN, M. D., SIUDA, E. R., DOTZLAF, J. E., YU, H., HALE, J. E., NISENBAUM, E. S., NICOLL, R. A. & BREDT, D. S. 2007. New transmembrane AMPA receptor regulatory protein isoform, gamma-7, differentially regulates AMPA receptors. *J Neurosci,* 27**,** 4969-77.

KAWAI, Y., HAMAZAKI, Y., FUJITA, H., FUJITA, A., SATO, T., FURUSE, M., FUJIMOTO, T., JETTEN, A. M., AGATA, Y. & MINATO, N. 2011. Claudin-4 induction by E-protein activity in later stages of CD4/8 double-positive thymocytes to increase positive selection efficiency. *Proc Natl Acad Sci U S A,* 108**,** 4075-80.

KEARNEY, E. R., WALUNAS, T. L., KARR, R. W., MORTON, P. A., LOH, D. Y., BLUESTONE, J. A. & JENKINS, M. K. 1995. Antigen-dependent clonal expansion of a trace population of antigen-specific CD4+ T cells in vivo is dependent on CD28 costimulation and inhibited by CTLA-4. *J Immunol,* 155**,** 1032-6.

KIM, S. J., PARK, K., KOELLER, D., KIM, K. Y., WAKEFIELD, L. M., SPORN, M. B. & ROBERTS, A. B. 1992. Post-transcriptional regulation of the

human transforming growth factor-beta 1 gene. *J Biol Chem,* 267**,** 13702-7.

KIM, W., BENNETT, E. J., HUTTLIN, E. L., GUO, A., LI, J., POSSEMATO, A., SOWA, M. E., RAD, R., RUSH, J., COMB, M. J., HARPER, J. W. & GYGI, S. P. 2011. Systematic and quantitative assessment of the ubiquitin-modified proteome. *Mol Cell,* 44**,** 325-40.

KIRKHAM, B. W., KAVANAUGH, A. & REICH, K. 2013. IL-17A: A Unique Pathway in Immune-Mediated Diseases: Psoriasis, Psoriatic Arthritis, and Rheumatoid Arthritis. *Immunology*.

KIRKHAM, B. W., LASSERE, M. N., EDMONDS, J. P., JUHASZ, K. M., BIRD, P. A., LEE, C. S., SHNIER, R. & PORTEK, I. J. 2006. Synovial membrane cytokine expression is predictive of joint damage progression in rheumatoid arthritis: a two-year prospective study (the DAMAGE study cohort). *Arthritis Rheum,* 54**,** 1122-31.

KOHLER, G. & MILSTEIN, C. 1975. Continuous cultures of fused cells secreting antibody of predefined specificity. *Nature,* 256**,** 495-7.

KONRAD, M., SCHALLER, A., SEELOW, D., PANDEY, A. V., WALDEGGER, S., LESSLAUER, A., VITZTHUM, H., SUZUKI, Y., LUK, J. M., BECKER, C., SCHLINGMANN, K. P., SCHMID, M., RODRIGUEZ-SORIANO, J., ARICETA, G., CANO, F., ENRIQUEZ, R., JUPPNER, H., BAKKALOGLU, S. A., HEDIGER, M. A., GALLATI, S., NEUHAUSS, S. C., NURNBERG, P. & WEBER, S. 2006. Mutations in the tight-junction gene claudin 19 (CLDN19) are associated with renal magnesium wasting, renal failure, and severe ocular involvement. *Am J Hum Genet,* 79**,** 949-57.

KOVAL, M. 2006. Claudins--key pieces in the tight junction puzzle. *Cell Commun Adhes,* 13**,** 127-38.

KRAMER, F., WHITE, K., KUBBIES, M., SWISSHELM, K. & WEBER, B. H. 2000. Genomic organization of claudin-1 and its assessment in hereditary and sporadic breast cancer. *Hum Genet,* 107**,** 249-56.

KURRECK, J. 2009. RNA interference: from basic research to therapeutic applications. *Angew Chem Int Ed Engl,* 48**,** 1378-98.

LAL-NAG, M. & MORIN, P. J. 2009. The claudins. *Genome Biol,* 10**,** 235.

LAMB, J. R., SKIDMORE, B. J., GREEN, N., CHILLER, J. M. & FELDMANN, M. 1983. Induction of tolerance in influenza virus-immune T lymphocyte

clones with synthetic peptides of influenza hemagglutinin. *J Exp Med,* 157**,** 1434-47.

LECHLER, R., CHAI, J. G., MARELLI-BERG, F. & LOMBARDI, G. 2001. The contributions of T-cell anergy to peripheral T-cell tolerance. *Immunology,* 103**,** 262-9.

LEECH, M. T. & MORAND, E. F. 2013. Fibroblasts and synovial immunity. *Curr Opin Pharmacol,* 13**,** 565-9.

LETTS, V. A., FELIX, R., BIDDLECOME, G. H., ARIKKATH, J., MAHAFFEY, C. L., VALENZUELA, A., BARTLETT, F. S., 2ND, MORI, Y., CAMPBELL, K. P. & FRANKEL, W. N. 1998. The mouse stargazer gene encodes a neuronal Ca2+-channel gamma subunit. *Nat Genet,* 19**,** 340-7.

LEWIS, M. J., WAGNER, B. & WOOF, J. M. 2008. The different effector function capabilities of the seven equine IgG subclasses have implications for vaccine strategies. *Mol Immunol,* 45**,** 818-27.

LI, J., RIDGWAY, W., FATHMAN, C. G., TSE, H. Y. & SHAW, M. K. 2007. High cell surface expression of CD4 allows distinction of CD4(+)CD25(+) antigen-specific effector T cells from CD4(+)CD25(+) regulatory T cells in murine experimental autoimmune encephalomyelitis. *J Neuroimmunol,* 192**,** 57-67.

LIN, Z., WITSCHAS, K., GARCIA, T., CHEN, R. S., HANSEN, J. P., SELLERS, Z. M., KUZMENKINA, E., HERZIG, S. & BEST, P. M. 2008. A critical GxxxA motif in the gamma6 calcium channel subunit mediates its inhibitory effect on Cav3.1 calcium current. *J Physiol,* 586**,** 5349-66.

LIU, Y., SUN, W., ZHANG, K., ZHENG, H., MA, Y., LIN, D., ZHANG, X., FENG, L., LEI, W., ZHANG, Z., GUO, S., HAN, N., TONG, W., FENG, X., GAO, Y. & CHENG, S. 2007. Identification of genes differentially expressed in human primary lung squamous cell carcinoma. *Lung Cancer,* 56**,** 307-17.

LODISH, H., BERK, A. & ZIPURSKY, S. L. 2000a. Molecular Cell Biology. *Section 17.7, Protein Glycosylation in the ER and Golgi Complex.* 5th ed.: New York: W. H. Freeman.

LODISH, H., BERK, A. & ZIPURSKY, S. L. 2000b. Molecular Cell Biology. *Section 17.9, Receptor-Mediated Endocytosis and the Sorting of Internalized Proteins.* 5th ed.: New York: W. H. Freeman.

LOMBARDI, G., DIANZANI, C., MIGLIO, G., CANONICO, P. L. & FANTOZZI, R. 2001. Characterization of ionotropic glutamate receptors in human lymphocytes. *Br J Pharmacol,* 133**,** 936-44.

LORETO, M. P., BERRY, D. M. & MCGLADE, C. J. 2002. Functional cooperation between c-Cbl and Src-like adaptor protein 2 in the negative regulation of T-cell receptor signaling. *Mol Cell Biol,* 22**,** 4241-55.

LU, P., VOGEL, C., WANG, R., YAO, X. & MARCOTTE, E. M. 2007. Absolute protein expression profiling estimates the relative contributions of transcriptional and translational regulation. *Nat Biotechnol,* 25**,** 117-24.

LYONS, P. A., KOUKOULAKI, M., HATTON, A., DOGGETT, K., WOFFENDIN, H. B., CHAUDHRY, A. N. & SMITH, K. G. 2007. Microarray analysis of human leucocyte subsets: the advantages of positive selection and rapid purification. *BMC Genomics,* 8**,** 64.

MAGGI, E., COSMI, L., LIOTTA, F., ROMAGNANI, P., ROMAGNANI, S. & ANNUNZIATO, F. 2005. Thymic regulatory T cells. *Autoimmun Rev,* 4**,** 579-86.

MAHER, G. J., HILTON, E. N., URQUHART, J. E., DAVIDSON, A. E., SPENCER, H. L., BLACK, G. C. & MANSON, F. D. 2011. The cataract-associated protein TMEM114, and TMEM235, are glycosylated transmembrane proteins that are distinct from claudin family members. *FEBS Lett,* 585**,** 2187-92.

MALEY, F., TRIMBLE, R. B., TARENTINO, A. L. & PLUMMER, T. H., JR. 1989. Characterization of glycoproteins and their associated oligosaccharides through the use of endoglycosidases. *Anal Biochem,* 180**,** 195-204.

MANDEL, I., PAPERNA, T., GLASS-MARMOR, L., VOLKOWICH, A., BADARNY, S., SCHWARTZ, I., VARDI, P., KOREN, I. & MILLER, A. 2012. Tight junction proteins expression and modulation in immune cells and multiple sclerosis. *J Cell Mol Med,* 16**,** 765-75.

MANTEI, A., RUTZ, S., JANKE, M., KIRCHHOFF, D., JUNG, U., PATZEL, V., VOGEL, U., RUDEL, T., ANDREOU, I., WEBER, M. & SCHEFFOLD, A. 2008. siRNA stabilization prolongs gene knockdown in primary T lymphocytes. *Eur J Immunol,* 38**,** 2616-25.

MATTHEWS, N., EMERY, P., PILLING, D., AKBAR, A. & SALMON, M. 1993. Subpopulations of primed T helper cells in rheumatoid arthritis. *Arthritis Rheum,* 36**,** 603-7.

MCCOY, K. D. & LE GROS, G. 1999. The role of CTLA-4 in the regulation of T cell immune responses. *Immunol Cell Biol,* 77**,** 1-10.

MCGONAGLE, D., CONAGHAN, P. G., O'CONNOR, P., GIBBON, W., GREEN, M., WAKEFIELD, R., RIDGWAY, J. & EMERY, P. 1999. The relationship between synovitis and bone changes in early untreated rheumatoid arthritis: a controlled magnetic resonance imaging study. *Arthritis Rheum,* 42**,** 1706-11.

MCMANUS, M. T., HAINES, B. B., DILLON, C. P., WHITEHURST, C. E., VAN PARIJS, L., CHEN, J. & SHARP, P. A. 2002. Small interfering RNA-mediated gene silencing in T lymphocytes. *J Immunol,* 169**,** 5754-60.

MCQUEEN, F. M., BENTON, N., CRABBE, J., ROBINSON, E., YEOMAN, S., MCLEAN, L. & STEWART, N. 2001. What is the fate of erosions in early rheumatoid arthritis? Tracking individual lesions using x rays and magnetic resonance imaging over the first two years of disease. *Ann Rheum Dis,* 60**,** 859-68.

METZ, B., KERSTEN, G. F., HOOGERHOUT, P., BRUGGHE, H. F., TIMMERMANS, H. A., DE JONG, A., MEIRING, H., TEN HOVE, J., HENNINK, W. E., CROMMELIN, D. J. & JISKOOT, W. 2004. Identification of formaldehyde-induced modifications in proteins: reactions with model peptides. *J Biol Chem,* 279**,** 6235-43.

MINETA, K., YAMAMOTO, Y., YAMAZAKI, Y., TANAKA, H., TADA, Y., SAITO, K., TAMURA, A., IGARASHI, M., ENDO, T., TAKEUCHI, K. & TSUKITA, S. 2011. Predicted expansion of the claudin multigene family. *FEBS Lett,* 585**,** 606-12.

MIYATAKE, S., NAKASEKO, C., UMEMORI, H., YAMAMOTO, T. & SAITO, T. 1998. Src family tyrosine kinases associate with and phosphorylate CTLA-4 (CD152). *Biochem Biophys Res Commun,* 249**,** 444-8.

MOBLEY, C. K., MYERS, J. K., HADZISELIMOVIC, A., ELLIS, C. D. & SANDERS, C. R. 2007. Purification and initiation of structural characterization of human peripheral myelin protein 22, an integral membrane protein linked to peripheral neuropathies. *Biochemistry,* 46**,** 11185-95.

MONTGOMERY, M. K., XU, S. & FIRE, A. 1998. RNA as a target of double-stranded RNA-mediated genetic interference in Caenorhabditis elegans. *Proc Natl Acad Sci U S A,* 95**,** 15502-7.

MORICE, W. G., BRUNN, G. J., WIEDERRECHT, G., SIEKIERKA, J. J. & ABRAHAM, R. T. 1993. Rapamycin-induced inhibition of p34cdc2 kinase activation is associated with G1/S-phase growth arrest in T lymphocytes. *J Biol Chem,* 268**,** 3734-8.

MOUTON, P., TARDIEU, S., GOUIDER, R., BIROUK, N., MAISONOBE, T., DUBOURG, O., BRICE, A., LEGUERN, E. & BOUCHE, P. 1999. Spectrum of clinical and electrophysiologic features in HNPP patients with the 17p11.2 deletion. *Neurology,* 52**,** 1440-6.

MUELLER, D. L. 2010. Mechanisms maintaining peripheral tolerance. *Nat Immunol,* 11**,** 21-7.

MYERS, M. D., SOSINOWSKI, T., DRAGONE, L. L., WHITE, C., BAND, H., GU, H. & WEISS, A. 2006. Src-like adaptor protein regulates TCR expression on thymocytes by linking the ubiquitin ligase c-Cbl to the TCR complex. *Nat Immunol,* 7**,** 57-66.

NAKAYAMADA, S., TAKAHASHI, H., KANNO, Y. & O'SHEA, J. J. 2012. Helper T cell diversity and plasticity. *Curr Opin Immunol,* 24**,** 297-302.

NIETO, J. C., CANTO, E., ZAMORA, C., ORTIZ, M. A., JUAREZ, C. & VIDAL, S. 2012. Selective loss of chemokine receptor expression on leukocytes after cell isolation. *PLoS One,* 7**,** e31297.

NOURSE, J., FIRPO, E., FLANAGAN, W. M., COATS, S., POLYAK, K., LEE, M. H., MASSAGUE, J., CRABTREE, G. R. & ROBERTS, J. M. 1994. Interleukin-2-mediated elimination of the p27Kip1 cyclin-dependent kinase inhibitor prevented by rapamycin. *Nature,* 372**,** 570-3.

OH-HORA, M. & RAO, A. 2008. Calcium signaling in lymphocytes. *Curr Opin Immunol,* 20**,** 250-8.

OKROJ, M., HEINEGARD, D., HOLMDAHL, R. & BLOM, A. M. 2007. Rheumatoid arthritis and the complement system. *Ann Med,* 39**,** 517-30.

OLENCHOCK, B. A., GUO, R., CARPENTER, J. H., JORDAN, M., TOPHAM, M. K., KORETZKY, G. A. & ZHONG, X. P. 2006. Disruption of diacylglycerol metabolism impairs the induction of T cell anergy. *Nat Immunol,* 7**,** 1174-81.

OMILUSIK, K. D., NOHARA, L. L., STANWOOD, S. & JEFFERIES, W. A. 2013. Weft, Warp, and Weave: The Intricate Tapestry of Calcium Channels Regulating T Lymphocyte Function. *Front Immunol,* 4**,** 164.

ORBAN, T. I. & IZAURRALDE, E. 2005. Decay of mRNAs targeted by RISC requires XRN1, the Ski complex, and the exosome. *RNA,* 11**,** 459-69.

ORRENIUS, S., ZHIVOTOVSKY, B. & NICOTERA, P. 2003. Regulation of cell death: the calcium-apoptosis link. *Nat Rev Mol Cell Biol,* 4**,** 552-65.

OSTEN, P. & STERN-BACH, Y. 2006. Learning from stargazin: the mouse, the phenotype and the unexpected. *Curr Opin Neurobiol,* 16**,** 275-80.

PAEZ, P. M., FULTON, D., COLWELL, C. S. & CAMPAGNONI, A. T. 2009. Voltage-operated Ca(2+) and Na(+) channels in the oligodendrocyte lineage. *J Neurosci Res,* 87**,** 3259-66.

PALACIOS, E. H. & WEISS, A. 2004. Function of the Src-family kinases, Lck and Fyn, in T-cell development and activation. *Oncogene,* 23**,** 7990-8000.

PAOLINO, M. & PENNINGER, J. M. 2009. E3 ubiquitin ligases in T-cell tolerance. *Eur J Immunol,* 39**,** 2337-44.

PEREZ, V. L., VAN PARIJS, L., BIUCKIANS, A., ZHENG, X. X., STROM, T. B. & ABBAS, A. K. 1997. Induction of peripheral T cell tolerance in vivo requires CTLA-4 engagement. *Immunity,* 6**,** 411-7.

PERNEGER, T. V. 1998. What's wrong with Bonferroni adjustments. *BMJ,* 316**,** 1236-8.

PRATT, A. G., ISAACS, J. D. & MATTEY, D. L. 2009. Current concepts in the pathogenesis of early rheumatoid arthritis. *Best Pract Res Clin Rheumatol,* 23**,** 37-48.

PRINEAS, J. W. & PARRATT, J. D. 2012. Oligodendrocytes and the early multiple sclerosis lesion. *Ann Neurol,* 72**,** 18-31.

QU, B., AL-ANSARY, D., KUMMEROW, C., HOTH, M. & SCHWARZ, E. C. 2011. ORAI-mediated calcium influx in T cell proliferation, apoptosis and tolerance. *Cell Calcium,* 50**,** 261-9.

QUINN, M. A. & EMERY, P. 2003. Window of opportunity in early rheumatoid arthritis: possibility of altering the disease process with early intervention. *Clin Exp Rheumatol,* 21**,** S154-7.

RANTAPAA-DAHLQVIST, S. 2009. What happens before the onset of rheumatoid arthritis? *Curr Opin Rheumatol,* 21**,** 272-8.

RATH, A. & DEBER, C. M. 2013. Correction factors for membrane protein molecular weight readouts on sodium dodecyl sulfate-polyacrylamide gel electrophoresis. *Anal Biochem,* 434**,** 67-72.

RATUSHNY, V. & GOLEMIS, E. 2008. Resolving the network of cell signaling pathways using the evolving yeast two-hybrid system. *Biotechniques,* 44**,** 655-62.

RESNICK, M. B., KONKIN, T., ROUTHIER, J., SABO, E. & PRICOLO, V. E. 2005. Claudin-1 is a strong prognostic indicator in stage II colonic cancer: a tissue microarray study. *Mod Pathol,* 18**,** 511-8.

ROBERT, V., TRIFFAUX, E., SAVIGNAC, M. & PELLETIER, L. 2011. Calcium signalling in T-lymphocytes. *Biochimie,* 93**,** 2087-94.

ROONEY, J. W., SUN, Y. L., GLIMCHER, L. H. & HOEY, T. 1995. Novel NFAT sites that mediate activation of the interleukin-2 promoter in response to T-cell receptor stimulation. *Mol Cell Biol,* 15**,** 6299-310.

ROUX, K. J., AMICI, S. A., FLETCHER, B. S. & NOTTERPEK, L. 2005. Modulation of epithelial morphology, monolayer permeability, and cell migration by growth arrest specific 3/peripheral myelin protein 22. *Mol Biol Cell,* 16**,** 1142-51.

RUBTSOV, Y. P. & RUDENSKY, A. Y. 2007. TGFbeta signalling in control of T-cell-mediated self-reactivity. *Nat Rev Immunol,* 7**,** 443-53.

SAFFORD, M., COLLINS, S., LUTZ, M. A., ALLEN, A., HUANG, C. T., KOWALSKI, J., BLACKFORD, A., HORTON, M. R., DRAKE, C., SCHWARTZ, R. H. & POWELL, J. D. 2005. Egr-2 and Egr-3 are negative regulators of T cell activation. *Nat Immunol,* 6**,** 472-80.

SANDOVAL, A., ARIKKATH, J., MONJARAZ, E., CAMPBELL, K. P. & FELIX, R. 2007. gamma1-dependent down-regulation of recombinant voltage-gated Ca2+ channels. *Cell Mol Neurobiol,* 27**,** 901-8.

SCHWARTZ, R. H. 1990. A cell culture model for T lymphocyte clonal anergy. *Science,* 248**,** 1349-56.

SCHWARTZ, R. H. 2003. T cell anergy. *Annu Rev Immunol,* 21**,** 305-34.

SHAPIRO, V. S., TRUITT, K. E., IMBODEN, J. B. & WEISS, A. 1997. CD28 mediates transcriptional upregulation of the interleukin-2 (IL-2) promoter through a composite element containing the CD28RE and NF-IL-2B AP-1 sites. *Mol Cell Biol,* 17**,** 4051-8.

SIMON, D. B., LU, Y., CHOATE, K. A., VELAZQUEZ, H., AL-SABBAN, E., PRAGA, M., CASARI, G., BETTINELLI, A., COLUSSI, G., RODRIGUEZ-SORIANO, J., MCCREDIE, D., MILFORD, D., SANJAD, S. & LIFTON, R.

P. 1999. Paracellin-1, a renal tight junction protein required for paracellular Mg2+ resorption. *Science,* 285**,** 103-6.

SIMONE, R., FLORIANI, A. & SAVERINO, D. 2009. Stimulation of human CD4(+) T lymphocytes via TLR3, TLR5 and TLR7/8 up-regulates expression of costimulatory and modulates proliferation. *Open Microbiol J,* 3**,** 1-8.

SIOUD, M. 2010. Recent advances in small interfering RNA sensing by the immune system. *N Biotechnol,* 27**,** 236-42.

SMIDA, M., POSEVITZ-FEJFAR, A., HOREJSI, V., SCHRAVEN, B. & LINDQUIST, J. A. 2007. A novel negative regulatory function of the phosphoprotein associated with glycosphingolipid-enriched microdomains: blocking Ras activation. *Blood,* 110**,** 596-615.

STANZANI, M., MARTINS, S. L., SALIBA, R. M., ST JOHN, L. S., BRYAN, S., COURIEL, D., MCMANNIS, J., CHAMPLIN, R. E., MOLLDREM, J. J. & KOMANDURI, K. V. 2004. CD25 expression on donor CD4+ or CD8+ T cells is associated with an increased risk for graft-versus-host disease after HLA-identical stem cell transplantation in humans. *Blood,* 103**,** 1140-6.

STEIN, P. L., LEE, H. M., RICH, S. & SORIANO, P. 1992. pp59fyn mutant mice display differential signaling in thymocytes and peripheral T cells. *Cell,* 70**,** 741-50.

STEVENSON, M., VOLSKY, B., HEDENSKOG, M. & VOLSKY, D. J. 1986. Immortalization of human T lymphocytes after transfection of Epstein-Barr virus DNA. *Science,* 233**,** 980-4.

STIRLING, D. P. & STYS, P. K. 2010. Mechanisms of axonal injury: internodal nanocomplexes and calcium deregulation. *Trends Mol Med,* 16**,** 160-70.

STRAUSS, L., CZYSTOWSKA, M., SZAJNIK, M., MANDAPATHIL, M. & WHITESIDE, T. L. 2009. Differential responses of human regulatory T cells (Treg) and effector T cells to rapamycin. *PLoS One,* 4**,** e5994.

SUZUKI, H., ITO, Y., YAMAZAKI, Y., MINETA, K., UJI, M., ABE, K., TANI, K., FUJIYOSHI, Y. & TSUKITA, S. 2013. The four-transmembrane protein IP39 of Euglena forms strands by a trimeric unit repeat. *Nat Commun,* 4**,** 1766.

TAHVANAINEN, J., PYKALAINEN, M., KALLONEN, T., LAHTEENMAKI, H., RASOOL, O. & LAHESMAA, R. 2006. Enrichment of nucleofected

primary human CD4+ T cells: a novel and efficient method for studying gene function and role in human primary T helper cell differentiation. *J Immunol Methods,* 310**,** 30-9.

TANIMOTO, K., COOPER, N. R., JOHNSON, J. S. & VAUGHAN, J. H. 1975. Complement fixation by rheumatoid factor. *J Clin Invest,* 55**,** 437-45.

TAYLOR, V. & SUTER, U. 1996. Epithelial membrane protein-2 and epithelial membrane protein-3: two novel members of the peripheral myelin protein 22 gene family. *Gene,* 175**,** 115-20.

THAMINY, S., MILLER, J. & STAGLJAR, I. 2004. The split-ubiquitin membrane-based yeast two-hybrid system. *Methods Mol Biol,* 261**,** 297-312.

THOMAS, R., TURNER, M. & COPE, A. P. 2008. High avidity autoreactive T cells with a low signalling capacity through the T-cell receptor: central to rheumatoid arthritis pathogenesis? *Arthritis Res Ther,* 10**,** 210.

THOMSON, A. W. & ROBBINS, P. D. 2008. Tolerogenic dendritic cells for autoimmune disease and transplantation. *Ann Rheum Dis,* 67 Suppl 3**,** iii90-6.

TOMITA, S., CHEN, L., KAWASAKI, Y., PETRALIA, R. S., WENTHOLD, R. J., NICOLL, R. A. & BREDT, D. S. 2003. Functional studies and distribution define a family of transmembrane AMPA receptor regulatory proteins. *J Cell Biol,* 161**,** 805-16.

TREVEJO, J. M., MARINO, M. W., PHILPOTT, N., JOSIEN, R., RICHARDS, E. C., ELKON, K. B. & FALCK-PEDERSEN, E. 2001. TNF-alpha - dependent maturation of local dendritic cells is critical for activating the adaptive immune response to virus infection. *Proc Natl Acad Sci U S A,* 98**,** 12162-7.

TROUW, L. A., HUIZINGA, T. W. & TOES, R. E. 2013. Autoimmunity in rheumatoid arthritis: different antigens--common principles. *Ann Rheum Dis,* 72 Suppl 2**,** ii132-6.

TSUKITA, S. & FURUSE, M. 2000. Pores in the wall: claudins constitute tight junction strands containing aqueous pores. *J Cell Biol,* 149**,** 13-6.

TUOSTO, L. 2011. NF-kappaB family of transcription factors: biochemical players of CD28 co-stimulation. *Immunol Lett,* 135**,** 1-9.

UHLEN, M. & PONTEN, F. 2005. Antibody-based proteomics for human tissue profiling. *Mol Cell Proteomics,* 4**,** 384-93.

UPCHURCH, K. S. & KAY, J. 2012. Evolution of treatment for rheumatoid arthritis. *Rheumatology (Oxford),* 51 Suppl 6**,** vi28-36.

VALENCIA-SANCHEZ, M. A., LIU, J., HANNON, G. J. & PARKER, R. 2006. Control of translation and mRNA degradation by miRNAs and siRNAs. *Genes Dev,* 20**,** 515-24.

VAN ITALLIE, C. M., GAMBLING, T. M., CARSON, J. L. & ANDERSON, J. M. 2005. Palmitoylation of claudins is required for efficient tight-junction localization. *J Cell Sci,* 118**,** 1427-36.

VISCO, C., MAGISTRELLI, G., BOSOTTI, R., PEREGO, R., RUSCONI, L., TOMA, S., ZAMAI, M., ACUTO, O. & ISACCHI, A. 2000. Activation of Zap-70 tyrosine kinase due to a structural rearrangement induced by tyrosine phosphorylation and/or ITAM binding. *Biochemistry,* 39**,** 2784-91.

VON KEMPIS, J., DUDLER, J., HASLER, P., KYBURZ, D., TYNDALL, A., ZUFFEREY, P. & VILLIGER, P. M. 2012. Use of abatacept in rheumatoid arthritis. *Swiss Med Wkly,* 142**,** w13581.

VON MERING, C., KRAUSE, R., SNEL, B., CORNELL, M., OLIVER, S. G., FIELDS, S. & BORK, P. 2002. Comparative assessment of large-scale data sets of protein-protein interactions. *Nature,* 417**,** 399-403.

WADEHRA, M., IYER, R., GOODGLICK, L. & BRAUN, J. 2002. The tetraspan protein epithelial membrane protein-2 interacts with beta1 integrins and regulates adhesion. *J Biol Chem,* 277**,** 41094-100.

WAGNER, S. A., BELI, P., WEINERT, B. T., NIELSEN, M. L., COX, J., MANN, M. & CHOUDHARY, C. 2011. A proteome-wide, quantitative survey of in vivo ubiquitylation sites reveals widespread regulatory roles. *Mol Cell Proteomics,* 10**,** M111 013284.

WEAVER, J. C. 1995. Electroporation theory. Concepts and mechanisms. *Methods Mol Biol,* 55**,** 3-28.

WEBER, K. S., MILLER, M. J. & ALLEN, P. M. 2008. Th17 cells exhibit a distinct calcium profile from Th1 and Th2 cells and have Th1-like motility and NF-AT nuclear localization. *J Immunol,* 180**,** 1442-50.

WEN, H., WATRY, D. D., MARCONDES, M. C. & FOX, H. S. 2004. Selective decrease in paracellular conductance of tight junctions: role of the first extracellular domain of claudin-5. *Mol Cell Biol,* 24**,** 8408-17.

WILSON, H. L., WILSON, S. A., SURPRENANT, A. & NORTH, R. A. 2002. Epithelial membrane proteins induce membrane blebbing and interact with the P2X7 receptor C terminus. *J Biol Chem,* 277**,** 34017-23.

WOLLSCHEID, B., BAUSCH-FLUCK, D., HENDERSON, C., O'BRIEN, R., BIBEL, M., SCHIESS, R., AEBERSOLD, R. & WATTS, J. D. 2009. Mass-spectrometric identification and relative quantification of N-linked cell surface glycoproteins. *Nat Biotechnol,* 27**,** 378-86.

WONEROW, P. & WATSON, S. P. 2001. The transmembrane adapter LAT plays a central role in immune receptor signalling. *Oncogene,* 20**,** 6273-83.

XIA, M., GASSER, J. & FEIGE, U. 1999. Dexamethasone enhances CTLA-4 expression during T cell activation. *Cell Mol Life Sci,* 55**,** 1649-56.

YAN, J., SU, H., XU, L. & WANG, C. 2013. OX40-OX40L interaction promotes proliferation and activation of lymphocytes via NFATc1 in ApoE-deficient mice. *PLoS One,* 8**,** e60854.

ZHA, Y., MARKS, R., HO, A. W., PETERSON, A. C., JANARDHAN, S., BROWN, I., PRAVEEN, K., STANG, S., STONE, J. C. & GAJEWSKI, T. F. 2006. T cell anergy is reversed by active Ras and is regulated by diacylglycerol kinase-alpha. *Nat Immunol,* 7**,** 1166-73.

ZHANG, D. J., WANG, Q., WEI, J., BAIMUKANOVA, G., BUCHHOLZ, F., STEWART, A. F., MAO, X. & KILLEEN, N. 2005. Selective expression of the Cre recombinase in late-stage thymocytes using the distal promoter of the Lck gene. *J Immunol,* 174**,** 6725-31.

ZHENG, Y., COLLINS, S. L., LUTZ, M. A., ALLEN, A. N., KOLE, T. P., ZAREK, P. E. & POWELL, J. D. 2007. A role for mammalian target of rapamycin in regulating T cell activation versus anergy. *J Immunol,* 178**,** 2163-70.

ZHONG, X. P., GUO, R., ZHOU, H., LIU, C. & WAN, C. K. 2008. Diacylglycerol kinases in immune cell function and self-tolerance. *Immunol Rev,* 224**,** 249-64.

ZOIDL, G., BLASS-KAMPMANN, S., D'URSO, D., SCHMALENBACH, C. & MULLER, H. W. 1995. Retroviral-mediated gene transfer of the peripheral myelin protein PMP-22 in Schwann cells: modulation of cell growth. *EMBO J,* 14**,** 1122-8.

ZVAIFLER, N. J., BOYLE, D. & FIRESTEIN, G. S. 1994. Early synovitis--synoviocytes and mononuclear cells. *Semin Arthritis Rheum,* 23**,** 11-6.